
Politecnico di Torino

Politecnico di Torino

Master of Science Program in Civil Engineering

Academic year 2022/2023

Graduation session July 2023

# Preliminary analysis for the structural retrofitting of the Church of Santo Stefano in Frassino

Supervisor:

Prof. Engr. Gabriele Bertagnoli

Co-supervisor:

Engr. Dario Granatiero

Candidate:

Milagros Soteras

# Acknowledgements

*I am deeply grateful to Engineer Gabriele Bertagnoli for his invaluable guidance, expertise, and unwavering support as my thesis supervisor. His supervision and insightful feedback significantly contributed to the completion of this thesis.*

*I would also like to extend my heartfelt appreciation to Engineer Dario Granatiero, my thesis co-supervisor, for his meticulous attention to detail and continuous guidance. His expertise and dedication played a crucial role in shaping and refining my work.*

*I am grateful to Politecnico di Torino and Universidad Nacional de Cordoba for providing the necessary resources for my university degree. Their support and commitment to excellence have been instrumental in my educational journey.*

*I want to express my sincere gratitude to my friends, university peers, and colleagues for their companionship and support. Their presence during both the good and challenging times has been a source of encouragement and motivation.*

*Lastly, my deepest appreciation goes to my family. Without their unwavering love, encouragement, and sacrifices, none of this would have been possible. Their constant support and belief in me have been my greatest strength throughout this academic endeavor.*

*Thank you all sincerely.*

# Contents

# Abstract

The purpose of this thesis is to conduct a comprehensive structural evaluation of the Church of Santo Stefano. The research is conducted in accordance with the "Norme Techniche per le Costruzioni 2018", Eurocodes, and Guidelines for Seismic Risk Assessment and Mitigation in Cultural Heritage.

The theoretical framework of the study is primarily based on the aforementioned standards and guidelines. The research methodology begins with an extensive data collection process, including the examination of historical records, documentation of modifications over time, and analysis of past extreme events. Additionally, a thorough investigation of the structural materials is conducted, yielding valuable mechanical parameter data.

Following the research phase, two calculation models are developed: a global model to comprehend the overall structural behavior, and a local model to analyze potential kinematic mechanisms. Advanced calculation software is employed to facilitate these modeling processes.

The outcomes of the research provide a comprehensive understanding of the current structural condition of the church, highlighting areas that require intervention to ensure structural stability. The findings contribute to the preservation and conservation efforts of the church, assisting in the formulation of effective strategies for the safeguarding of this cultural heritage.

# 1

# Knowledge of the building

In order to assess the current seismic safety of a historic masonry building and to choose an effective improvement intervention, knowledge of the building is fundamental. Although the problems are common to all existing buildings, it is even more important to know the original characteristics, the changes that have occurred over time due to damage caused by human activity, ageing of materials and calamitous events. However, in relation to the need to prevent irreparable losses, carrying out a complete investigation campaign may be too invasive on the building itself.

Knowledge can in fact be achieved at different levels of investigation, depending on the accuracy of the survey operations, historical research, and experimental investigations. As a result, the operations will be based on the objectives and may affect an entire building or only a part of it. By examining the characteristics of the building, it is intended to establish an interpretative model that permits both a qualitative interpretation of the structural functioning as well as a structural analysis for quantitative evaluation during the various phases of the calibration process. The degree of reliability of the model will be closely linked to the level of in-depth and the data available. [1]

## 1.1 Identification of the building

A proper and complete identification of the body and its location on the territory is the first step in determining the sensitivity of the construction to various risks, particularly seismic ones. [1]

The Church of Santo Stefano is located in the south-eastern portion of the village of Frassino, slightly detached from the historical core of the village. [2] The aforementioned village is located in the Varaita Valley in the province of Cuneo in Piedmont, Italy, it has a number of inhabitants equal to 271. This church is the only one in the town and therefore has a very important historical and patrimonial value for the Frassino's community. The building under examination is located at Via Vittorio Veneto 10, where it occupies a sub-flat lot underlying the roadway "Strada Provinciale 8" (SP8). Due to its direct connection to this route, accessibility to the church is easy. In addition, two other secondary streets "Val Varaita" delimit the church. It is also important to note that the church property has a front garden and a parking zone, which are directly accessible from the route.

As far as the neighboring buildings are concerned, there is one in correspondence with the east façade, but it is not directly connected to the church. The Figure 1-1 shows how the church looks nowadays. But as will be discussed in the next part of this chapter, the church has been modified several times in order to have its current appearance.

Figure 1-1. Church of Santo Stefano.

The Figure 1-2 represents a planimetric scheme of the church structure, which was obtained from a survey of the current state. The Figure 1-3 is a functional scheme of the building under analysis. This scheme is fundamental to understanding in a general way the composition of the building and the different dimensions of the elements that compose it. The following parts can be identified from this scheme: 1) Apse: that in this case is a polygonal termination of the main building, in this space the altar is situated, 2) Presbytery: space around the high altar of a church, 3) Central Nave, 4) Lateral Nave, 5) Sacristy: it is defined as a room in Christian churches that is destinated to keep vestments and church furnishings, 6) Bell tower base, 7) Warehouse: is used to store goods.

It was also possible to reconstruct a frontal and longitudinal view of the church from images and from the inspections carried out. The Figure 1-4 represents a front view, particularly the western façade, the east façade is represented by the Figure 1-5, the north longitudinal view of the church is represented by the Figure 1-7, while the south longitudinal view can be seen in the Figure 1-6.

The Figure 1-2 it can be seen that the layout is longitudinal, rectangular in shape with the exception of the polygonal apse. The main entrance to the building is located to the west and the access to the presbytery to the east.

As far as the structure of the building under analysis is concerned, it is composed by a central nave, two lateral naves and a bell tower. This bell tower stands on the north side of the presbytery from which it is accessed, it is on the upstream side. Regarding its façade it is simple in form and with few decorations. Situated in a symmetrical position to the bell tower is the sacristy, this is located on the valley side.

As can be seen in the Figure 1-1 and in the Figure 1-7 the structure of the bell tower is higher than the church. The entrance to the bell tower is located at the level of the SP8, in contiguity with the parking area, which is between the apse and the roadway.

Regarding the church and its aisles, the corridor in the middle is the longest and widest of all, considered as the main corridor, while the other two on the sides have a smaller length and width. The aforementioned can be seen in the Figure 1-2.

It is possible to note from the Figure 1-1 that the church is at a different level from the street. The building is at a lower level than the road, which from the point of view of flooding can be a drawback because the water does not find a way out. This feature can be seen in the Figure 1-8, that represents a section where it is possible to notice the difference of levels that exist in the building, the left nave is located at -0.16 m from the central nave that is consider in a level of 0.00 m, while the right nave is at +0.44 m from the central one. Also, it can be seen that the street that borders the church on the north side is at +2.86 m from the main entrance. Below the aforementioned street, there is an intracavity.

The load-bearing structure consists mainly of walls and columns, of considerable thickness, as there is no evidence at the time that they have been calculated and verified. As will be seen and discussed in more detail in the following chapters, the core material of the church is masonry. Therefore, it is possible to intuit that a purely expeditious and experimental method has been used for its construction, resulting in considerable dimensions that is also linked with the material used.

Regarding the ceiling of the church, as a wide space was needed to cover, an optimal solution for that time was a groin vault. The surface of this kind of structure consists of a framework of four perimeter arches and two diagonal arches. Located in the center of the vault, the latter are larger than the perimeter arches. In the center, there is a wedge-shaped stone known as the keystone, which is placed. Once the keystone is in place, the structure supports itself, unloading its weight onto the supports. Spaces between diagonal arches and perimeter arches are called segments or sails,

and they are sometimes separated by ribs that highlight architectural surfaces. When the arches of the vault are round, the projection will usually be square, when the arches are pointed, the projection will usually be rectangular. From a static point of view, the cross vault offers considerable comfort and structural freedom due to its resistance to bearing loads. However, it is a pushing structure that therefore requires buttresses or tie rods to remain standing.

In the case of the church under analysis, in the Figure 1-2, can be seen that the projections of the vaults are rectangular, so in line with the above mentioned the arches are pointed. In addition, the green lines represent the chains introduced as a structural intervention in order to give it strength to the vaults.

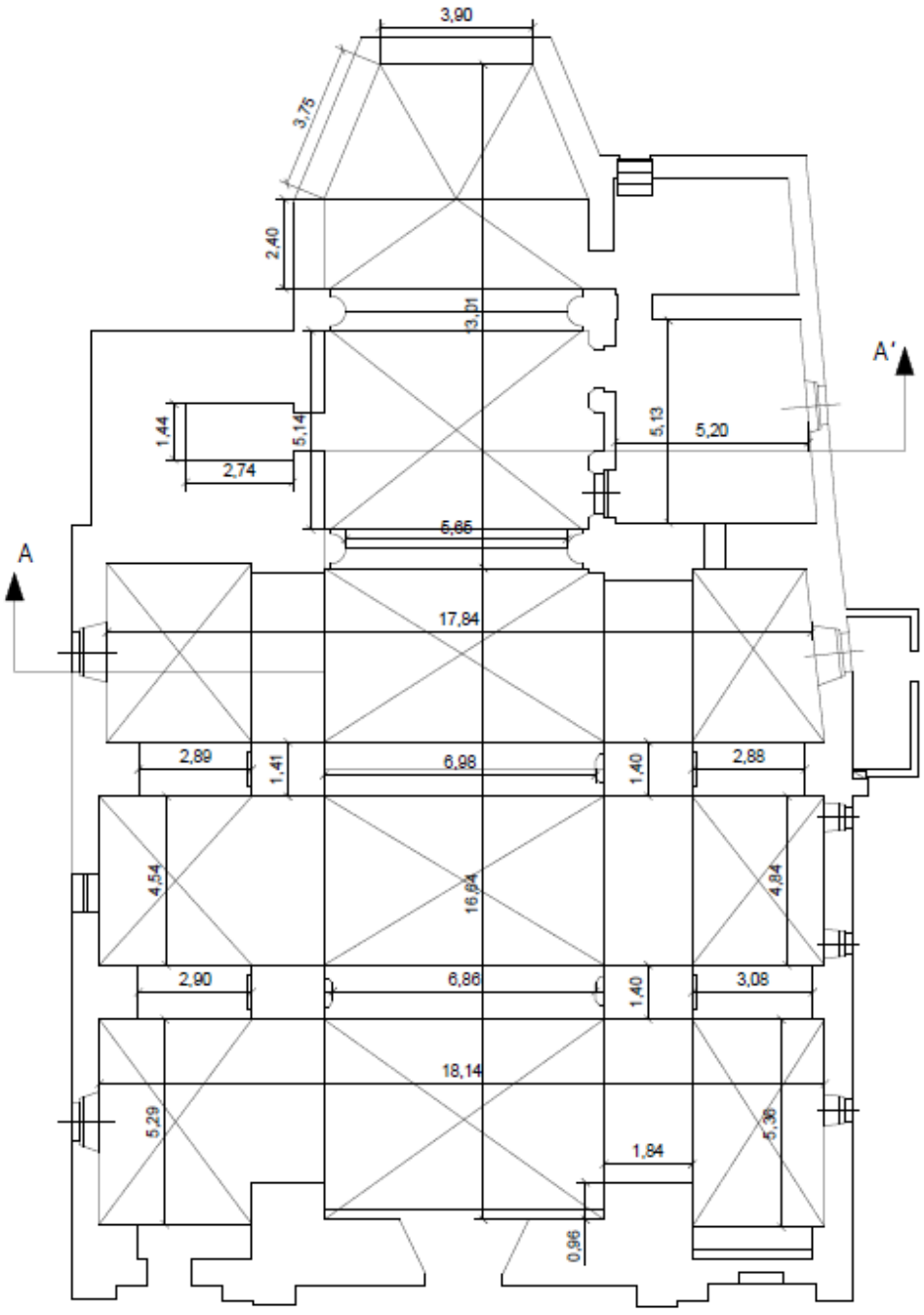


Figure 1-2. Planimetric diagram of Santo Stefano Church

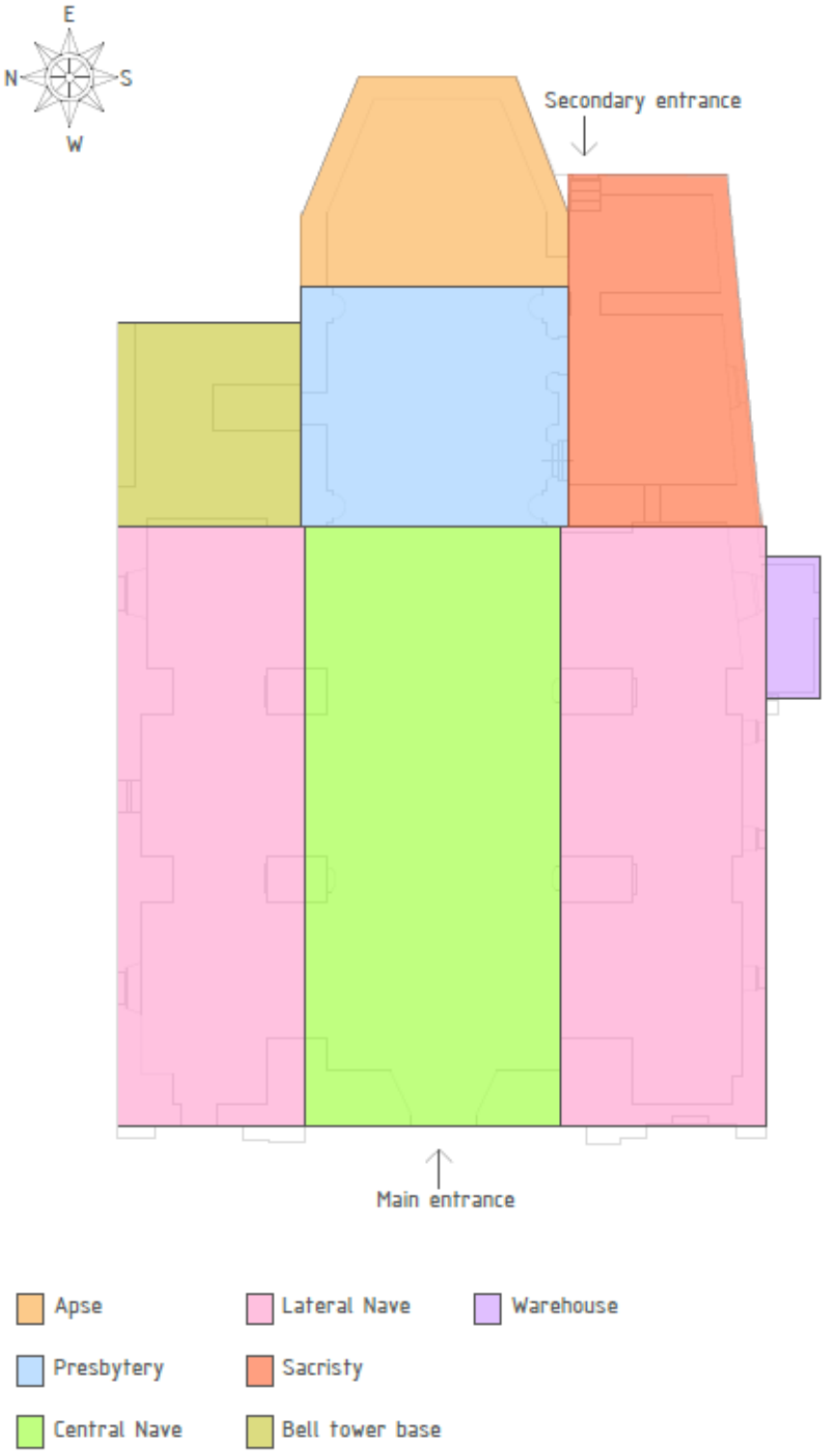


Figure 1-3. Functional scheme

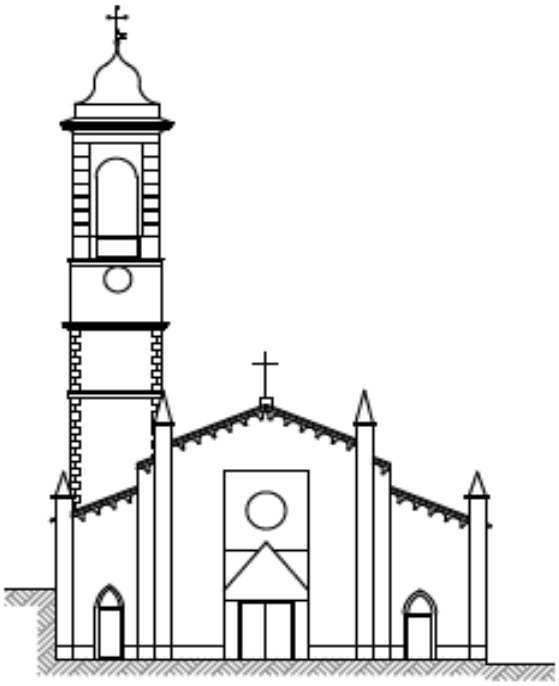

Figure 1-4.Front view- Western façade of the Church.

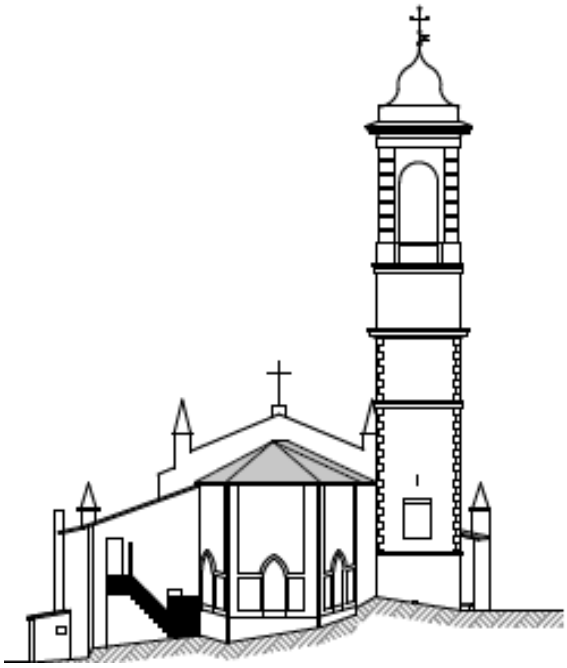

Figure 1-5 - Front view- Est façade of the Church.

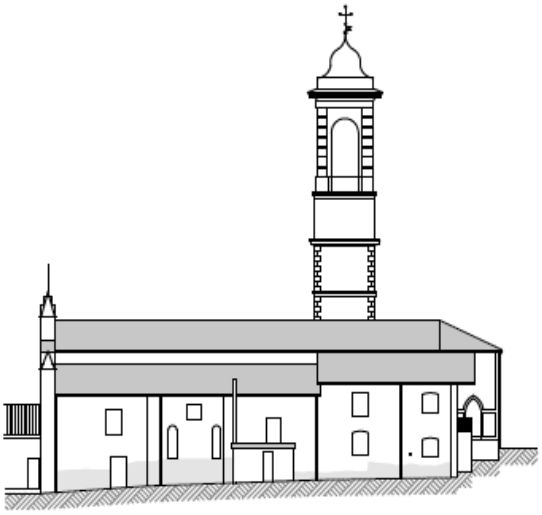

Figure 1-7. Longitudinal view of the Church (south view).

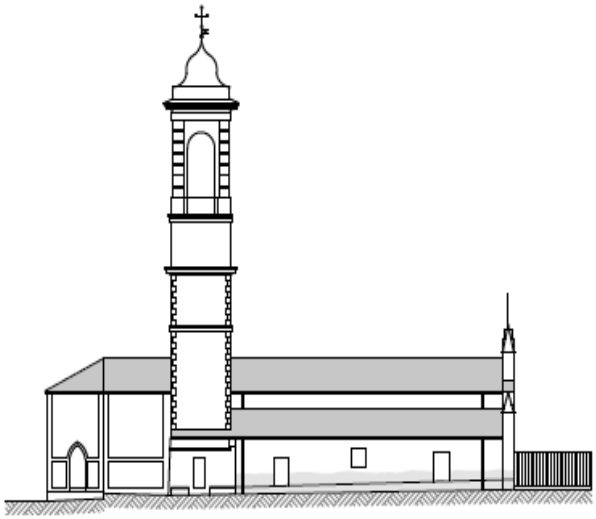

Figure 1-6. Longitudinal view of the Church (north view).

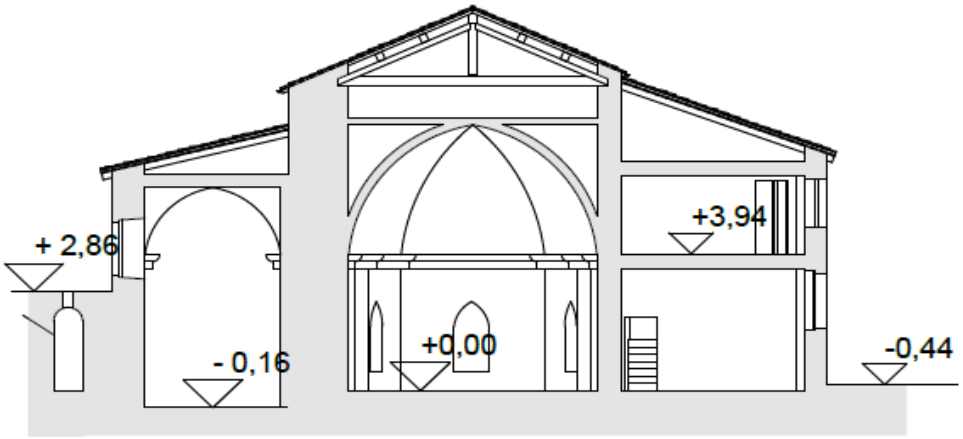


Figure 1-8. Section A-A' of the church.

The Figure 1-9 shows one of the domes corresponding to the side aisle, through this figure is possible to confirm that the arches are pointed. Also, it is possible to confirm what was said before regarding the chains, these kinds of elements are introduced to counteract the thrust from pushing elements, in this case the vaults that make up the roof.

Figure 1-9. Groin vault located in one of the lateral aisles.

Figure 1-10. Central hall.

The Figure 1-10 shows a part of the central hall of the church, where at the end it is possible to distinguish the presbyterium. Also, in this figure the vaults corresponding with the central nave are noticed and is possible to see the two chains, which have the above-mentioned function.

As already mentioned above, the church is fitted with ribbed vaults. However, by analysing the external coverage, it is of two pitched types for the main nave and of the single-pitched type for the side aisles. The loading frame is made of wood and the roof covering is made of stone slabs.

## 1.2 Historical critical analysis

In order to correctly identify the resistant system and its state of stress, the construction history and subsequent modifications of the protected cultural property must be reconstructed. It is also possible to use the building history as a tool for monitoring and verifying how the building responded to specific natural events or man-made transformations. Therefore, significant, and traumatic events must be identified, as well as the corresponding effects, through a direct analytical survey of the building or through documentary sources (written or iconographic sources). [1]

Regarding church history, the earliest evidence dates back to 1304, when the church reflected the typical Romanesque of the oldest structures in the Varaita Valley. In 1821 the parish priest and the community decide to repair the parish church and rebuild the rectory house. On the 30th of June 1823 a survey was carried out in the church, which revealed that *"disarrayed vault threatening ruin and that the west corner of the façade wall be out of level and in danger of being ruined".*

In 1824 the community of Frassino deliberates about repairs and a project completed on 11 July 1822 by the architect "Giuseppe Negro" is reported. But after few months of work parish priest "Antonio Allione" notices that the entire church roof is bearing down on the vault because the ridge beam is missing, the work was suspended, and a new survey was performed. In September 1824 started the project of refitting of the roof and façade.

Initially the building comprised a single east-west oriented nave and the presbytery. On 19 January 1835, a project for the extension of the church was started, the two side naves were added and a bell tower was inserted upstream, at the corner of the left nave and presbytery. In the Figure 1-11 and Figure 1-12 the project for the extension of the church is detailed. The second drawing on the right represents a plan of the church at that time, where it is possible to identify with the red color the part that was added. The other drawings represent cuts in different sections of the construction, where the bell tower project was already being considered.

In the Figure 1-12 it is possible to appreciate the plan of the church and the enlargement project in greater detail. At the same time, a particularity can be

observed in the scale used. At that time, units of measurement of the international system were not used, the units taken as a reference were the “trabucco piemontese”.

The value of the trabucco changed from region to region, for example in area of Asti, Cuneo, Biella, Vercelli, Torino, Ivrea, Pinerolo e Susa 1 trabbuco piemontese was equivalent to 3.086 m. [2]

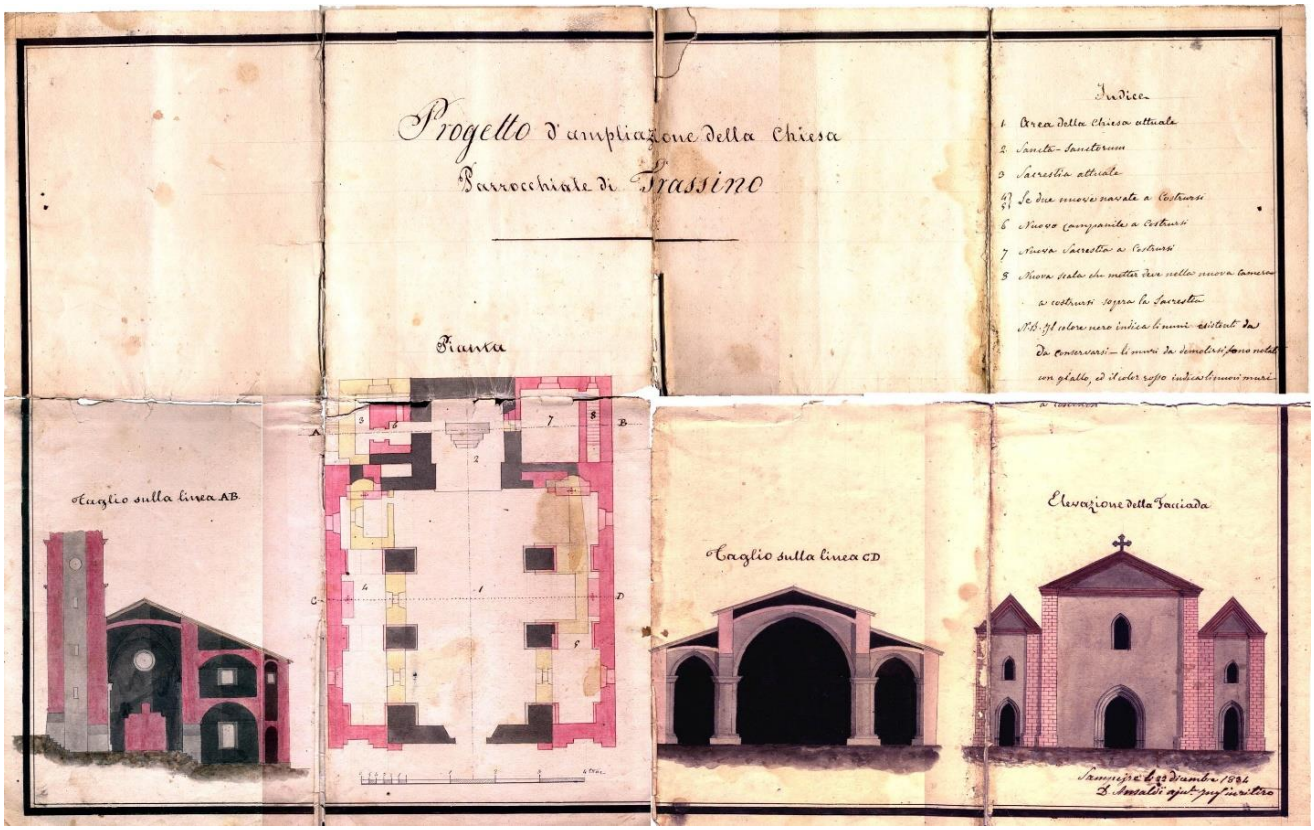


Figure 1-11. Source: Archivio storico Comune di Frassino.

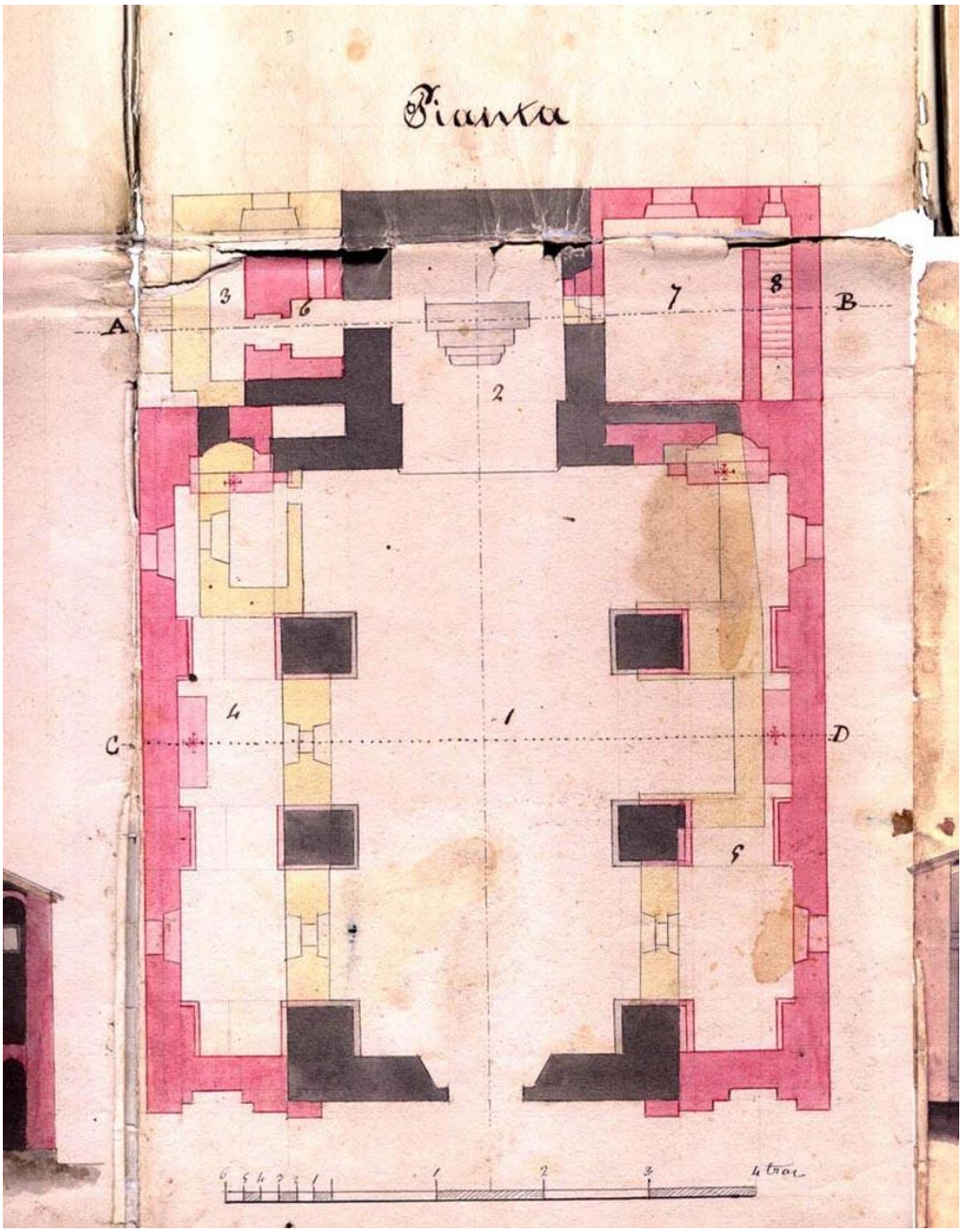


Figure 1-12. Source: (Archivio storico Comune di Frassino)

In the historical archive of Frassino, the project for the elevation of the bell tower was found, which is dated 28th May 1846. The Figure 1-13 details the project, with the colour red the part that has already been built was represented and in black the part to be built. Again, the units of measurement are the “trabucco piemontese”, where the scale is represented in the lower left corner. So, knowing that 1 trabucco is

equal to 3.086 m is possible to deduce that the total heigh projected to the campanile was of 24.80m. [3]

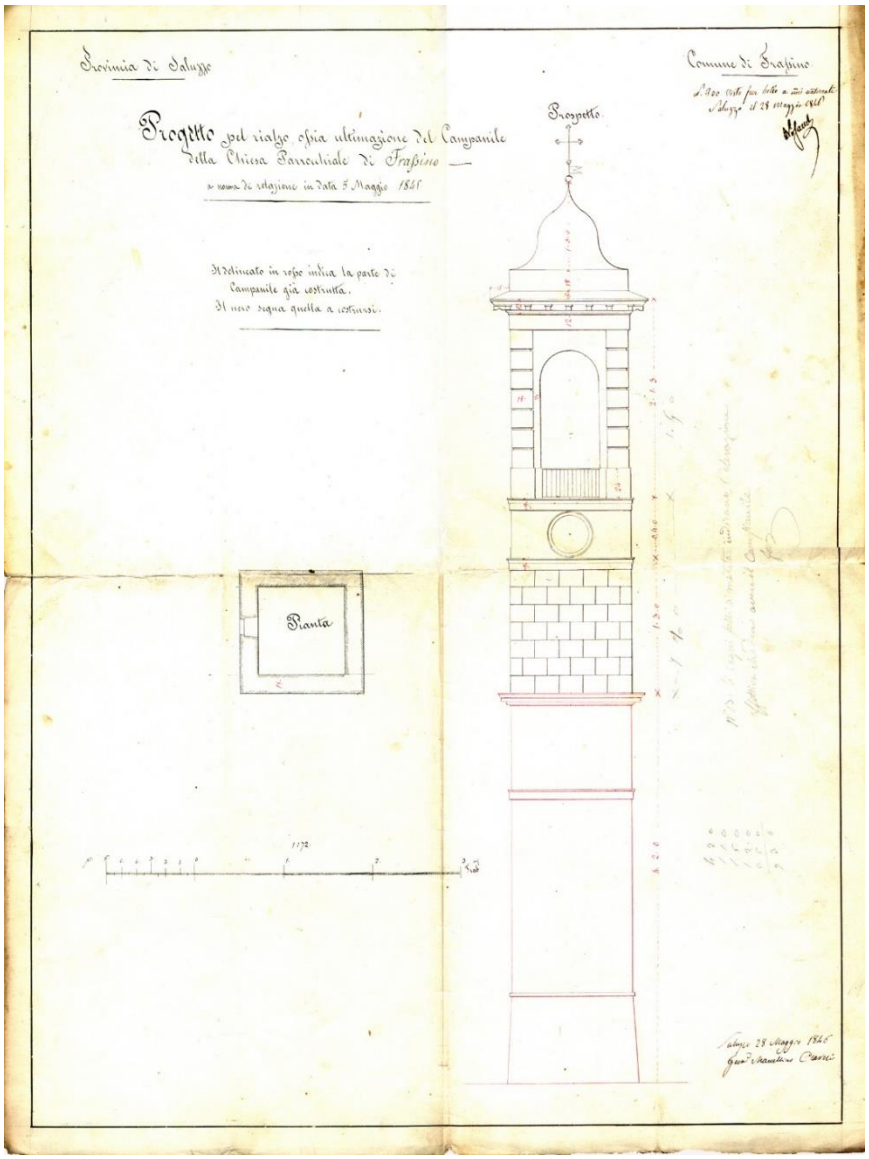


Figure 1-13. Source: Archivio storico Comune di Frassino.

On 23 February 1887, the "Diano Marina" earthquake hit Western Liguria hard. The event had a magnitude between 6.4 and 7, the main shock was felt throughout northern Italy, southern and central France, and Switzerland. [4]

This event, which affected northern Italy, resulted in extensive damage to the church, which was closed for public use. The parish priest at that time, "Giacomo Bonetti", stated that *"There is damage to the entire face of the main nave that poses a critical risk of*

*collapse in conjunction with the façade wall".* For that reason, subsidies were requested for repair works.

In 1903, a letter from the parish priest to the local syndic formally requested the repair of the wall of the church garden to prevent the overflowing of the water course known as "Bedale della Villa". This watercourse was considered dangerous, and it was feared that it could damage the building.

In 1936 the need to resurface the pavement of the municipal road arises. Also, the section of the vault above the altar of the Blessed Virgin Mary, whose decoration is badly damaged by water seepage due to the poor maintenance of the bell tower cornice. In 1941 the municipality gave a grant for the restoration of the perimeter walls against the ground. [3]

More recently, in 2003, the building was subjected to the "Conservative renovation project, consolidation and retrofitting of the church of S. Stefano in Frassino". In this project, the main cracks in the building were identified and repaired, as well as the resurfacing of the entire roof with the related arrangement of downpipes. [3]

According to the design drawings, that are represented by the Figure 1-14, there were cracks in the side aisles and apse as well as moisture problems on the walls. However, the original 14$^{th}$ century core appears to be less damaged. Particularly, the central vaulting area of the right nave is cracked. For the aforementioned reason, the central nave was reinforced in remote times with three chains, of which two were inserted at the external supporting counter- forts, while a fourth chain crosses the sacristy. The tension of these chains was also controlled and two more of the same dimensions were added inside the left aisle. In addition to the above-mentioned procedures, the plaster on the walls was also removed up to one meter above the level of moisture found. These plasters were redone. [2]

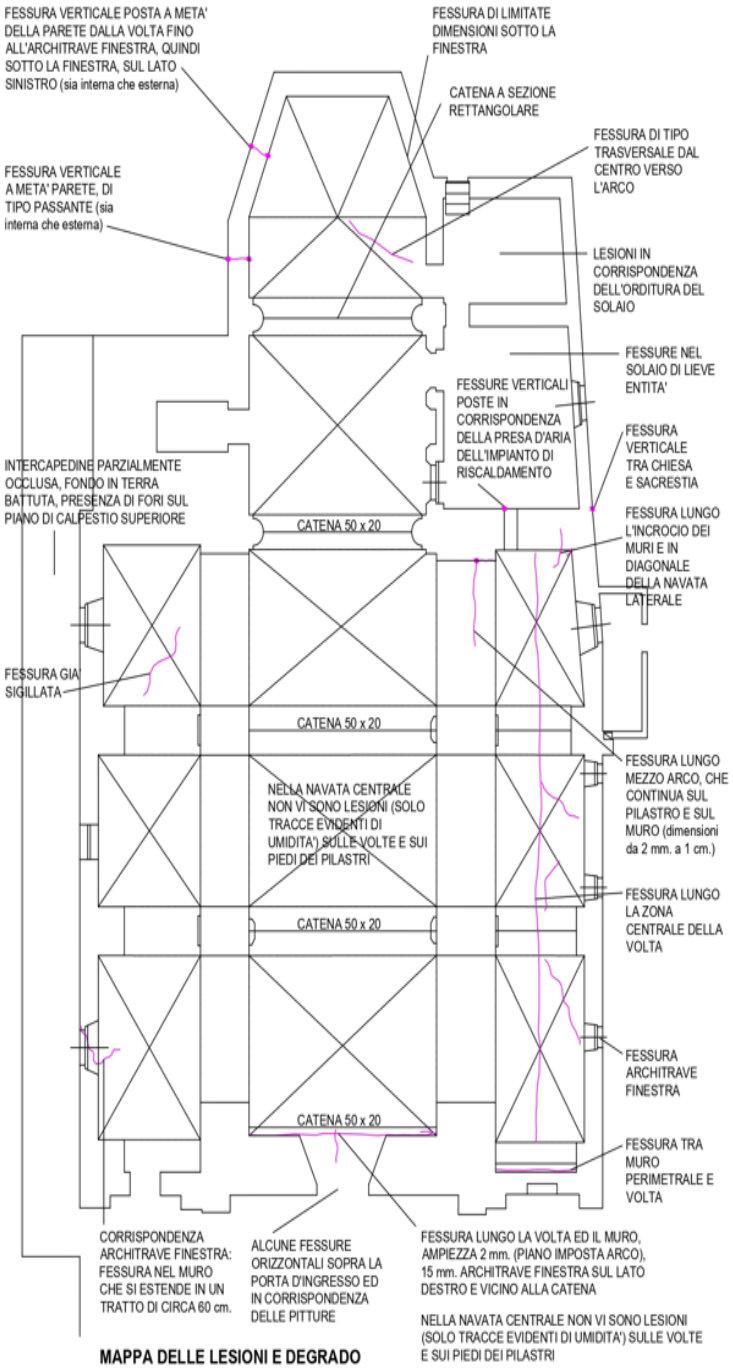


Figure 1-14. Map of lesions and degradation.

Regarding the roof replacement project, an inspection was carried out that year in order to determine the condition of the existing ceiling. The Figure 1-15 represents the state of the roof in 2003. The structure is made of wooden trusses, still in good condition, while *"le terzere"* and the floorboard were not in optimal condition. The former can be defined as a half-beam supporting the main structure of the pitched roofs, its task is to carry the warp of the beams and to determine the slope of the roof.

The latter element is used to support the roof slabs. Both elements were replaced. In addition to these elements, the upper beam was also replaced, this part in the Italian language is named “colmo”.

As previously stated, the roof covering of the church of “Santo Stefano” is entirely made of slabs. The decking for the slabs was entirely removed and substituted, the material used was larch wood, also on this structure was placed an insulating sheathing. All the aforementioned modifications were made to the roof of the central nave. While in the case of the lateral roofs, the main structure remained unchanged and only the decking was substituted, using the same material that was mentioned before and with the incorporation of an insulating sheathing for the slabs.

Figure 1-15. Condition of the roof.

The Figure 1-16 provides a general understanding of how the roof of the structure under analysis was built. The red circles represent different details that were individuated in the construction, these were mentioned with the name Detail 1 and Detail 2. In the figures that are related to detail 1 it is possible to understand how the trussing elements were inserted into the masonry. On the other hand, in the figure Figure 1-19 that corresponds with the detail 2, the center of the truss element was shown.

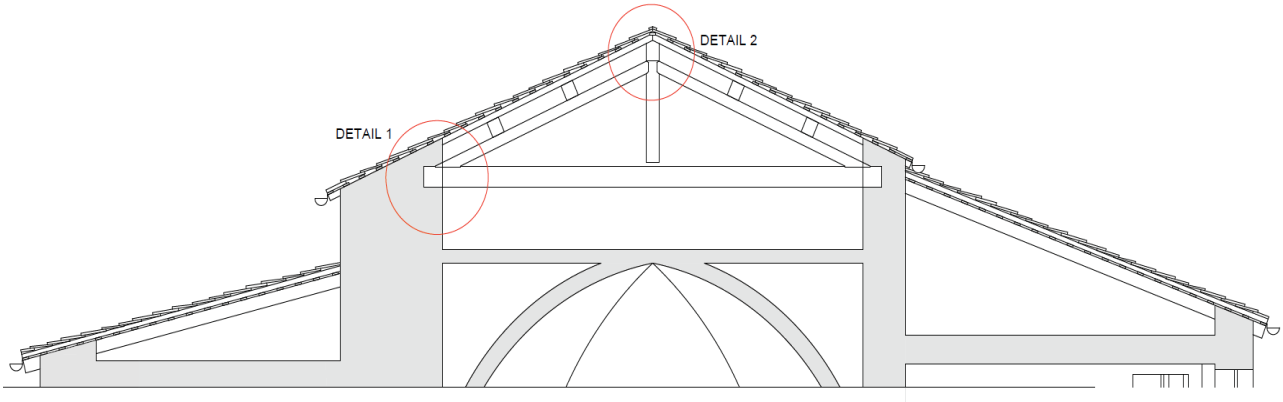


Figure 1-16. Cross section of roofing.

In the case of the detail 1 it is possible to analyze two states, the Figure 1-17 represents the state before the intervention, while the Figure 1-18 represents the state after the intervention, where the replacement of the elements mentioned before can be seen.

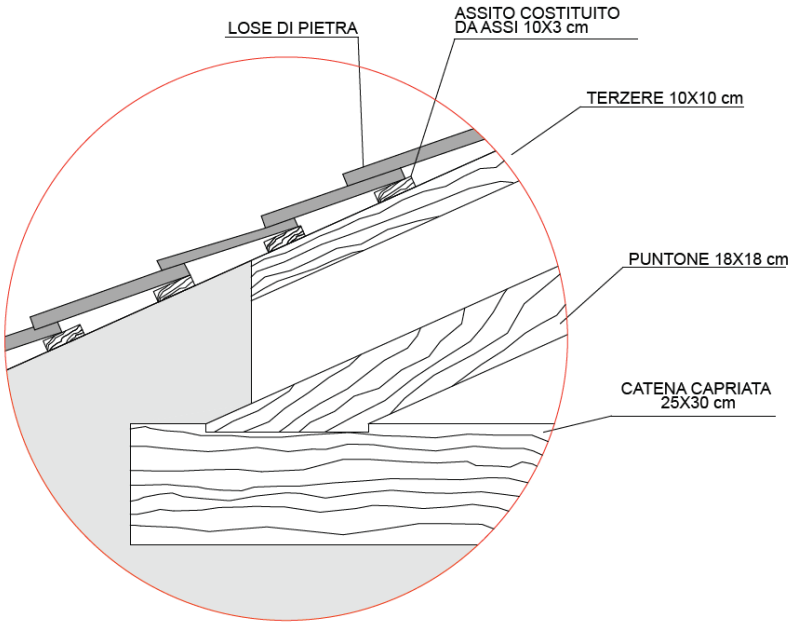


Figure 1-17. Insertion of the truss into the masonry before the intervention.

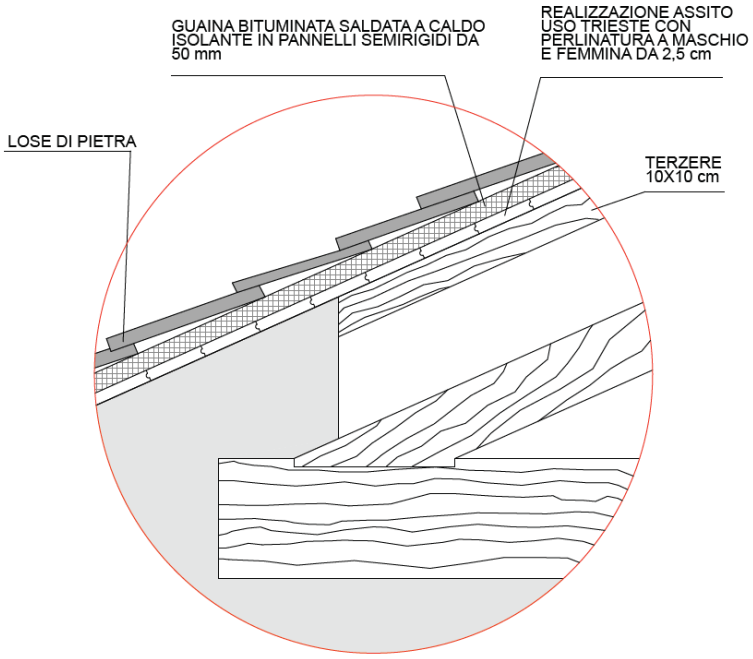


Figure 1-18. Insertion of the truss into the masonry after the intervention.

In the Figure 1-19, it is evidence with an orange circle the “colmo”, that means the upper part of the truss system that was changed.

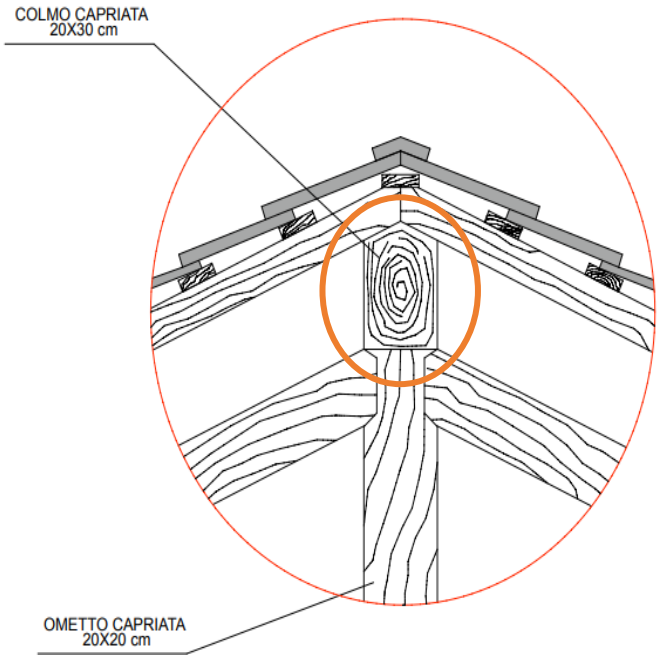


Figure 1-19. Centre of the truss element.

In 2020/2021 a new inspection of the structure was carried out and the humidity marks on the perimeter walls of the building were found again. It can therefore be concluded that this trouble is already part of the building. [2]

## 1.3 Geological and Geotechnical analysis

In order to identify geotechnical models that are appropriate for analyzing local earthquake response and dynamic soil-structure interactions, geotechnical investigations must allow physical-mechanical characterization of foundation soils, both in situ and in the laboratory. [1]

The country of Frassino lies on the slopes of the middle valley of Val Varaita. As it is located in a valley, it is strongly linked to the erosion and dispositional action of the Varaita torrent and its minor tributaries. The above-mentioned torrent is a watercourse located in the province of Cuneo, is the first tributary on the right of the Po river and it has an extension of 92.4 km with a catchment area of 604.9 $km^2$. [5]

In turn, the village of Frassino is crossed by the river Vermenagna, which is 27.1 km long and has a catchment area of 166.17 $km^2$. This river is channeled between the meeting of “Curtil” and “Bernardo” streets up to the eastern part of the camping area and then meets again with the Varaita river. At the same time, it can be said that the river crosses provincial street 8 (Strada Provinciale 8), where it deviates slightly to the south-west to avoid the church, and then continues its way to the south to meet its confluence with the Varita river.

In order to reconstruct the stratigraphy in detail and to parameterize geomechanically the ground on which the construction to be intervened is located, 3 continuous dynamic penetrometer tests (DPSH) were carried out on the day 12/02/2021. [2]

In dynamic penetrometer tests, a metal cone at the end of a steel rod is driven vertically into the ground as part of a geotechnical point test. A mallet weighing 73.0 kg is used to deliver penetration energy, which falls from a height of 75.0 cm by an automatic release device and performs a specific work of 234 kj/sq.m per stroke.

During the test, the number of blows required to penetrate 30 cm of drill bit and alternate coating is measured, it is indicated with the term $N_{30}$, that as it was said before represents the number of beats required to penetrate 30 cm, the test is stopped when 50 strokes for the advancement of a single 30 cm section are required, it is indicated with “refusal to penetrate”.

The physical-mechanical properties of soil play a pivotal role in determining its strength. In the case of non-cohesive soil, the strength is primarily influenced by the consolidation of granules, whereas cohesive soils' strength relies on the moisture content. Considering that penetration resistance measurements are conducted throughout the entire penetration process, the dynamic penetrometer tests conducted by DPSH yield continuous and valuable information. [6]

As mentioned above, 3 tests were carried out at the site under examination. The tests were carried out at the following locations:

- DPSH1: adjacent to the fracture observed in the north wall of the apse. Depth from the ground level: 8.10 m.
- DPSH2: in front of the church's main entrance. Depth from the ground level: 7.20 m.

- DPSH3: adjacent to the cistern at the southern end of the façade. Depth from the ground level: 7.20 m.

In the Figure 1-20 a distribution of the tests is given.

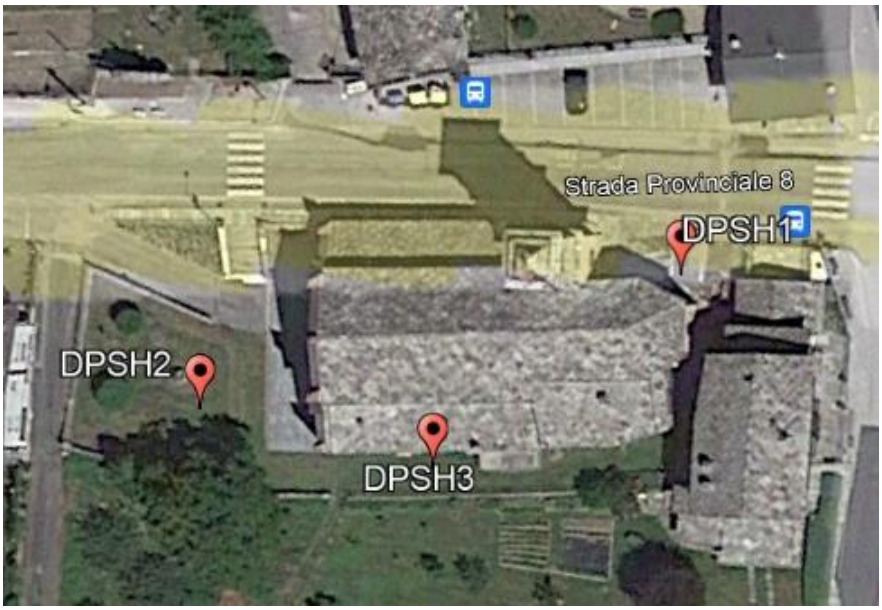


Figure 1-20. Localization of the tests. Source: GoogleEarthPro.

A dynamic heavy-duty penetrometer was used to carry out the investigation, the ones used is the type Pagani, model TG 63/100. In the Table *1-1* is possible to see the main characteristics.

| | |
|---|---|
| Weight of the hammer mass | 73 kg |
| Free fall height | 0.75 m |
| Tapered tip diameter | 51.00 mm |
| Base area of the tip | 20.43 $cm^2$ |
| Angle of tip opening | 60° |
| Rod length | 1.00 m |
| Weight of 1 rod | 6.31 Kg/m |
| Tip advancement | 0.30 m |
| Number of strokes | $N_{30}$ |
| Specific work per stroke | 265 $KJ/m^2$ |
| Reference standard | A.G.I. 1977 |

Table 1-1. Technical Characteristics Pagani 63/100.

The figures Figure 1-21 Figure 1-22 and Figure 1-23 show the results of the tests carried out.

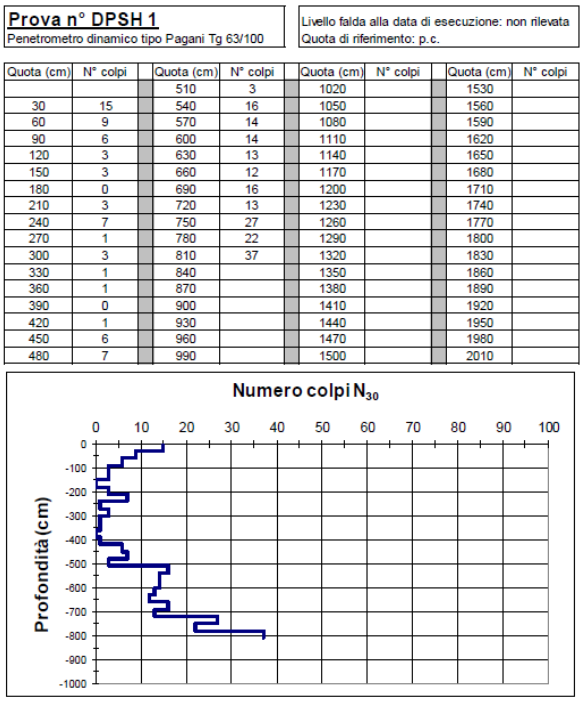

**Prova n° DPSH 1**
Penetrometro dinamico tipo Pagani Tg 63/100

Livello falda alla data di esecuzione: non rilevata
Quota di riferimento: p.c.

| Quota (cm) | N° colpi | Quota (cm) | N° colpi | Quota (cm) | N° colpi | Quota (cm) | N° colpi |
|---|---|---|---|---|---|---|---|
| | | 510 | 3 | 1020 | | 1530 | |
| 30 | 15 | 540 | 16 | 1050 | | 1560 | |
| 60 | 9 | 570 | 14 | 1080 | | 1590 | |
| 90 | 6 | 600 | 14 | 1110 | | 1620 | |
| 120 | 3 | 630 | 13 | 1140 | | 1650 | |
| 150 | 3 | 660 | 12 | 1170 | | 1680 | |
| 180 | 0 | 690 | 16 | 1200 | | 1710 | |
| 210 | 3 | 720 | 13 | 1230 | | 1740 | |
| 240 | 7 | 750 | 27 | 1260 | | 1770 | |
| 270 | 1 | 780 | 22 | 1290 | | 1800 | |
| 300 | 3 | 810 | 37 | 1320 | | 1830 | |
| 330 | 1 | 840 | | 1350 | | 1860 | |
| 360 | 1 | 870 | | 1380 | | 1890 | |
| 390 | 0 | 900 | | 1410 | | 1920 | |
| 420 | 1 | 930 | | 1440 | | 1950 | |
| 450 | 6 | 960 | | 1470 | | 1980 | |
| 480 | 7 | 990 | | 1500 | | 2010 | |



Figure 1-21. Results of DPSH 1.Source: Studio Architetti Fissore Ghione e Associati.

**Prova n° DPSH 2**
Penetrometro dinamico tipo Pagani Tg 63/100

Livello falda alla data di esecuzione: non rilevata
Quota di riferimento: p.c.

| Quota (cm) | N° colpi | Quota (cm) | N° colpi | Quota (cm) | N° colpi | Quota (cm) | N° colpi |
|---|---|---|---|---|---|---|---|
| | | 510 | 13 | 1020 | | 1530 | |
| 30 | 3 | 540 | 14 | 1050 | | 1560 | |
| 60 | 1 | 570 | 17 | 1080 | | 1590 | |
| 90 | 2 | 600 | 21 | 1110 | | 1620 | |
| 120 | 0 | 630 | 18 | 1140 | | 1650 | |
| 150 | 1 | 660 | 16 | 1170 | | 1680 | |
| 180 | 2 | 690 | 20 | 1200 | | 1710 | |
| 210 | 2 | 720 | 26 | 1230 | | 1740 | |
| 240 | 0 | 750 | | 1260 | | 1770 | |
| 270 | 1 | 780 | | 1290 | | 1800 | |
| 300 | 2 | 810 | | 1320 | | 1830 | |
| 330 | 5 | 840 | | 1350 | | 1860 | |
| 360 | 10 | 870 | | 1380 | | 1890 | |
| 390 | 10 | 900 | | 1410 | | 1920 | |
| 420 | 15 | 930 | | 1440 | | 1950 | |
| 450 | 19 | 960 | | 1470 | | 1980 | |
| 480 | 13 | 990 | | 1500 | | 2010 | |

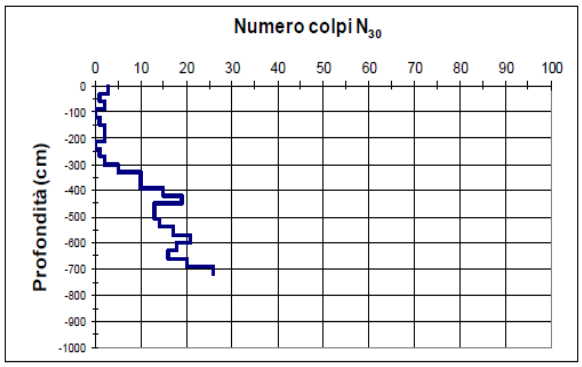


Figure 1-22. Results of DPSH2. Source: Studio Architetti Fissore Ghione e Associati.

**Prova n° DPSH 3**
Penetrometro dinamico tipo Pagani Tg 63/100

Livello falda alla data di esecuzione: non rilevata
Quota di riferimento: p.c.

| Quota (cm) | N° colpi | Quota (cm) | N° colpi | Quota (cm) | N° colpi | Quota (cm) | N° colpi |
|---|---|---|---|---|---|---|---|
| | | 510 | 9 | 1020 | | 1530 | |
| 30 | 3 | 540 | 5 | 1050 | | 1560 | |
| 60 | 1 | 570 | 11 | 1080 | | 1590 | |
| 90 | 1 | 600 | 17 | 1110 | | 1620 | |
| 120 | 1 | 630 | 20 | 1140 | | 1650 | |
| 150 | 1 | 660 | 28 | 1170 | | 1680 | |
| 180 | 4 | 690 | 35 | 1200 | | 1710 | |
| 210 | 1 | 720 | 27 | 1230 | | 1740 | |
| 240 | 2 | 750 | | 1260 | | 1770 | |
| 270 | 5 | 780 | | 1290 | | 1800 | |
| 300 | 3 | 810 | | 1320 | | 1830 | |
| 330 | 4 | 840 | | 1350 | | 1860 | |
| 360 | 2 | 870 | | 1380 | | 1890 | |
| 390 | 3 | 900 | | 1410 | | 1920 | |
| 420 | 1 | 930 | | 1440 | | 1950 | |
| 450 | 1 | 960 | | 1470 | | 1980 | |
| 480 | 7 | 990 | | 1500 | | 2010 | |

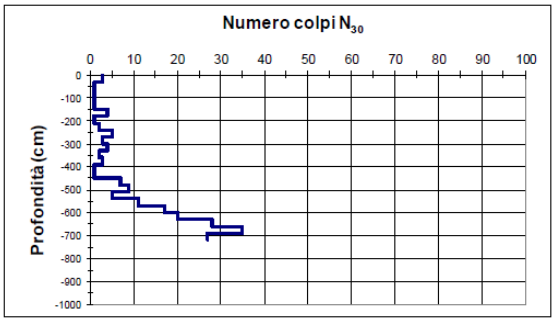


Figure 1-23. Results of DPSH3. Source: Studio Architetti Fissore Ghione e Associati.

As a result of the penetrometer tests, three main stratigraphic horizons were superimposed on each other, resulting in comparable and homogeneous values. On the side of the hill, Nord, in correspondence with DPSH1, it has yielded up to about 3 metres from the street plane a sandy-loamy terrain that goes from loose to little dense. In fact, the depth of 3m roughly coincides with the floor level of the hollow space and the floor level of the of the church itself, this horizon is called “Horizon 1”. Continuing in depth, natural deposits due to an eluvial-colluvial layer were found up to 5.4 m (“Horizon 2”), from this level there is distinguished improvement in granulometric and geomechanically characteristic with the emergence of a rocky-sandy-loamy terrain, “Horizon 3”. On the other hand, on the side of the valley in correspondence with the sample DPSH2, the Horizon 2 was found up to 3.6m, after this level the Horizon 3 was also defined. Test DPSH3, performed in the square in front of the main façade, substantially confirms what was found in test DPSH1, up to a depth of approximately 3.0 m Horizon 1 is found, below which is the natural debris mat and at 5.7 m outcrops the glacial deposits of Horizon 3. [7]

Based on the description above, it can be stated that the soil is granular or non-cohesive. They are characterized by high hydraulic conductivity (permeability), so that the interstitial overpressures resulting from changes in total limit stresses are dissipated almost instantly. Additionally, the microscopic mechanical behaviour is largely determined by the forces of gravity and friction between granules, while chemical interactions between solid particles and liquid phases appear to be secondary and negligible. [8]

Table 1-2 summarises the characteristics of the above-mentioned horizons.

| | Facies | Top Level (m) | Lower Level (m) |
|---|---|---|---|
| **Horizon 1** | Surface fill soil consisting of silty sands and sandy silts, loose to slightly thickened, with a scattered clastic skeleton minute. | Ground level | 3 |
| **Horizon 2** | Eluvial-colluvial column consisting of sands and silts, with scattered minute clastic skeleton. | Ground level - 3 | 3.6 - 5.4 |
| **Horizon 3** | Deposits of probable glacial origin: pebbles and subordinate blocks immersed in an abundant matrix of fine sands and loams. | 3.6 - 5.4 | |

Table 1-2. Geological Section.

As far as the hydrological model is concerned, the tests carried out do not reveal the presence of the groundwater level. Nevertheless, the moisture problems found on the perimeter walls of the church suggest a seasonal underground water circulation in the interior of the eluvial· colluvial column.

Once the geological model was characterised, different lithotechnical units were defined. Based on the characteristic values of geotechnical parameters, lithotechnical units can be separated from adjacent bodies based on their mechanical behaviour: these units are defined based on the homogeneity of these parameters, and a variation in these parameters defines a new unit, horizontally and vertically. For soils, the lithotechnical unit name is based on the granulometric classification performed on representative samples and for rock masses and weak rocks, the name of the rock. [8]

Therefore, 2 geotechnical units were identified, geometrically coinciding with the stratigraphic bodies described above. The unit A is defined by horizon 1 and horizon 2, while unit B is related with horizon 3. For all the units, in correspondence with the values of the $N_{30}$ brought back to NSPT, the values of the Young's Modulus and the effective angle of friction were calculated. For the former there have been correlations established by Schmertmann (1978), Schultze & Menzebach (1961), D'Apollonia et al. (1970) and Bowles (1982), while for the latter the correlations of Peck et al. (1956), Sowers (1961), Shioi & Fukuni (1982), Owasaki & Iwasaki (1959), Meyerhof (1965) and Road Bridge Specification. As previously mentioned, the type of soil under consideration is non cohesive as result the effective cohesion value (c') is equal to zero. [2]

The Table 1-3 provides information about the mechanical parameters of the soil under examination.

| | Φ' | γ | E | c' | Top level | Lower level |
|---|---|---|---|---|---|---|
| | ° | kg/cm2 | kg/cm2 | kg/cm2 | m | m |
| Unit A | 27 | 1800 | 140 | 0 | Ground Level | 3.6-5.4 |
| Unit B | 36 | 1900 | 440 | 0 | 3.6-5.4 | - |

Table 1-3. Soil's parameters. Source: Genovese&Associati.

## 1.4 Seismic characterization of the ground

Design seismic actions, which determine whether or not compliance with various limit states is achieved, are derived from the 'basic seismic hazard' of the construction site and are determined by its morphological and stratigraphic characteristics that determine the local seismic response.

From a dynamic point of view, soil characterization requires knowledge of the shear wave velocity profile Vs of the soil layers present at the site. Knowledge is especially required up to 30 meters above the ground level, indicated with the acronym $Vs_{30}$.

To obtain this velocity profile a non-invasive seismic method "MASW" (Multichannel analysis of surface waves) was implemented. The above-mentioned method measures the shear-wave speed dispersion and can be used to determine the composition of overburden and bedrock. [9] Surface waves, usually Rayleigh, are analyzed using this method. Rayleigh waves travel along an elastic surface, like the Earth, combining longitudinal compression and dilation to cause elliptical motions of points. These waves spread out most over time among seismic waves. [10]

An array of geophones measures seismic signals, just as in other seismic techniques. Active sources, such as sledgehammers, or ambient sources, such as vehicles and heavy machinery, can generate surface waves for MASW. [9]

MASW analysis can be carried out in four stages:

1. The first phase is the transformation of the time series in the frequency f-wavenumber K domain.
2. The second phase consists of identifying the f-k pairs whose spectral energy maxima (spectral density) allow the Rayleigh wave scattering curve to be plotted in the V plane phase (m/sec) - frequency (slowness (s/m) - frequency (Hz).
3. The third phase consists of calculating the theoretical dispersion curve by formulating the vertical shear wave velocity profile Vs, modifying the thickness h, the shear wave velocities Vs and compressional velocities Vp, the mass density ρ of the layers forming the soil model.
4. The final step consists of modifying the theoretical curve until the optimal overlap between the experimental phase velocity (or dispersion curve) and the numerical phase velocity (or dispersion curve) corresponding to the model is achieved.

After all the above steps have been performed, the forecast information reveals that the equivalent wave velocity $Vs_{30}$ is equal to 355 m/s, from the ground level.

Once the wave velocity profile has been determined, the seismic soil type may be defined (A, B, C, D, E) according to the NTC 2018 (Norme tecniche per le Costruzioni). [11]

It gives the main characteristics of the different soil types in correspondence to the thickness of the layers and the wave velocity.

**Tab. 3.2.II** – *Categorie di sottosuolo che permettono l'utilizzo dell'approccio semplificato.*

| Categoria | Caratteristiche della superficie topografica |
|---|---|
| A | *Ammassi rocciosi affioranti o terreni molto rigidi* caratterizzati da valori di velocità delle onde di taglio superiori a 800 m/s, eventualmente comprendenti in superficie terreni di caratteristiche meccaniche più scadenti con spessore massimo pari a 3 m. |
| B | *Rocce tenere e depositi di terreni a grana grossa molto addensati o terreni a grana fina molto consistenti*, caratterizzati da un miglioramento delle proprietà meccaniche con la profondità e da valori di velocità equivalente compresi tra 360 m/s e 800 m/s. |
| C | *Depositi di terreni a grana grossa mediamente addensati o terreni a grana fina mediamente consistenti* con profondità del substrato superiori a 30 m, caratterizzati da un miglioramento delle proprietà meccaniche con la profondità e da valori di velocità equivalente compresi tra 180 m/s e 360 m/s. |
| D | *Depositi di terreni a grana grossa scarsamente addensati o di terreni a grana fina scarsamente consistenti*, con profondità del substrato superiori a 30 m, caratterizzati da un miglioramento delle proprietà meccaniche con la profondità e da valori di velocità equivalente compresi tra 100 e 180 m/s. |
| E | *Terreni con caratteristiche e valori di velocità equivalente riconducibili a quelle definite per le categorie C o D*, con profondità del substrato non superiore a 30 m. |

Table 1-4. Category of Subsoil. Source: NTC2018.

The Figure 1-24 represents a flow chart showing how to determine the soil category.

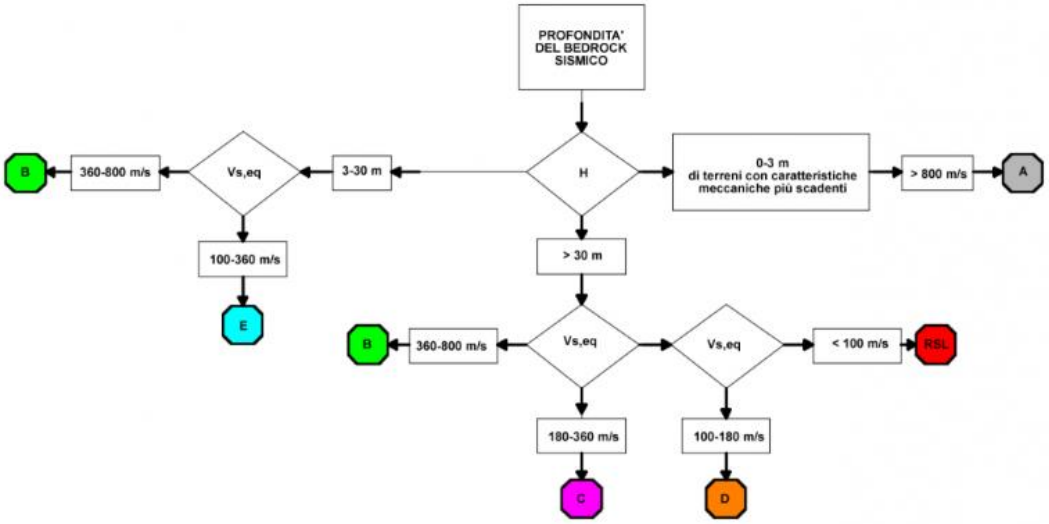


Figure 1-24 Flow chart for soil category determination (NTC 2018). Source: Web page GeoStru.

Then, from the above- mentioned graph, knowing that the depth of the seismic bed rock is greater than 30 m, and with the wave velocity equal to 355 m/s is possible to assume that the soil category is C, which is characterized in the following way, "Deposits of moderately thickened coarse-grained soils or moderately consistent fine-grained soils with substrate depths greater than 30 m, characterized by an improvement in mechanical properties with depth and equivalent velocity values between 180 m/s to 360 m/s". [12]

According to the "Deliberazione della Giunta Regionale 30 dicembre 2019, n. 6-887" the site under consideration is categorized as seismic zone 3s (medium- low seismicity).

## 1.5 Mechanical characterisation of materials

In masonry construction, in view of the great variety of materials and construction techniques used, knowledge of the composition of the construction elements and the characteristics of the connections is of primary importance, beginning with the type and arrangement of materials and the presence of discontinuities.

The masonry in an existing building is the result of the assembly of different materials, in which the construction technique, the laying methods, the mechanical characteristics of the constituent materials and their state of preservation, determine the mechanical behaviour of the whole.

As a preliminary theory of the behaviour of this material it is known that the elements that compose the masonry generally exhibit elastic fragility, with lower tensile strength than compressive strength, but still significant.

While the grout exhibits elastic brittleness in tension with a much lower resistance than the elements, in absolute value it has a very low resistance but under compression and shear, it exhibits plasticity and non-linear behaviour. In summary, masonry has the following characteristics:

- The non-homogeneity of behaviour at different points, due to different mechanical characteristics of the elements.
- Anisotropy behaviour in different directions due to the arrangement of the elements.
- The strength of the masonry is strongly influenced by the thickness of the joints, as the thickness increases the strength decreases.
- Asymmetric behaviour in compression and traction. This can be seen in the Figure 1-25, where all the components have a better mechanical behaviour in compression rather than in traction (superior part of the y axis).
- The non-linearity of the stress-strain bond.

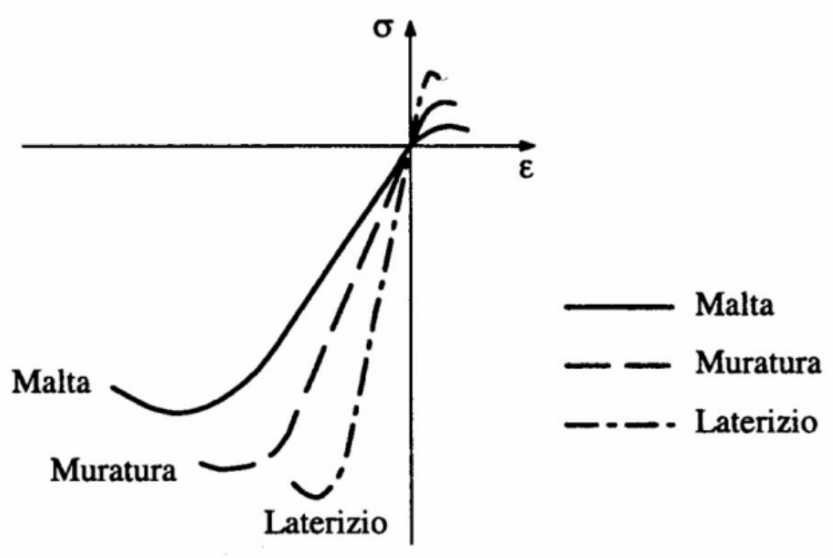


Figure 1-25. Tension-strain diagram of brick ("laterizio"), mortar ("malta") and masonry ("muratura").

The direct measurement of the mechanical characteristics of masonry is carried out by performing in-situ tests on portions of masonry, or laboratory tests on undisturbed elements taken in-situ, where this is possible. The tests may be of compression and shear tests, chosen in relation to the type of masonry and the resistance criterion adopted for the analysis. It is also important to remark that the test methods and the interpretation of the results must follow procedures of recognised validity.

In the mechanical characterisation of materials, three levels can be distinguished, depending on their degree of depth of testing.

**- Limited tests:** These surveys are not detailed and not extensive, based mainly on visual examinations of surfaces, which involve limited inspections of the masonry elements. Local plaster removals are planned to identify the materials of which the building is composed. Using historical-critical analysis, it is possible to subdivide the walls into areas that can be considered homogeneous. The purpose of the investigations is to allow the identification of the types of masonry to which to refer to determine the mechanical properties. This involves surveying the masonry texture of the facing and an estimate of the masonry section.

**-Extensive tests:** These are visual, diffuse, and systematic investigations, accompanied by local in-depth studies. Extensive assays are envisaged, both on the surface and in the thickness of the masonry (including with endoscopies), aimed at gaining knowledge of the materials and internal morphology of the masonry, the

identification of homogeneous zones in terms of materials and masonry texture, transversal connection devices, as well as degradation phenomena.

It is also planned to carry out analyses of the mortars and, if significant, of the constituent elements, accompanied by non-destructive diagnostic techniques (penetrometer, sclerometer, sonic, thermographic, radar, etc.) and, if necessary, supplemented by moderately destructive techniques (e.g. flat jacks), aimed at classifying the type of masonry and its quality more accurately. This type of tests were carried out in the building under consideration.

**-Exhaustive tests:** In addition to the requirements of the previous category, direct testing of materials to determine their mechanical parameters. The engineer determines the type and quantity according to the knowledge requirements of the structure. The tests must be performed either in situ or in the laboratory on undisturbed elements taken in situ. They may include, if significant: compression tests (e.g. on panels or using double flat jacks), shear tests (e.g: compression and shear, diagonal compression, direct shear on the joint), selected according to the type of wall and the resistance criterion adopted for the analysis. [12]

From the information obtained from the history of the church it is described that the masonry that compose the walls is “pietre frammiste a calce”. Research confirm that this material was also used to build other churches of the past.

One of the first invasive tests carried out on the structure under examination was the penetrometer test, which is essential in existing building diagnosis operations to investigate the mechanical properties of materials, aimed at identifying present deficiencies and anomalies. This test was carried out on 11 February 2021 by the company 4 EMME Service S.p.A., specialised in performing experimental tests on in-situ structures. Before performing this test, samples were taken, for that reason the removal of the plaster layers on 8 samples inside the church and 12 outside was performed. The aim was to get the level of the masonry to take samples of the mortar connecting the bricks or stones. The purpose of this type of sampling is to determine the bonding strength of the mortar and the level of seismic vulnerability of the building. A total of 20 samples were collected at an elevation of roughly 1.5 meters above the ground, to a size of approximately 20 square centimetres each.

A mortar penetrometer model RSM15 serial number. 15G00Z1L was used to perform the tests. The RSM penetrometer allows to obtain information regarding the

conditions of preservation and homogeneity of mortar on-site. This instrument is based on driving depth measurements of a needle in a mortar joint subjected to a series of strikes generated by a known mass. The penetration resistance of a mortar course is determined by penetrating a steel drill bit, four millimetres in diameter and 80 millimetres in length, through a course of mortar using a special beating mass. Through an experimental curve, penetration resistance is correlated with compressive strength.

The procedure was as follows, once a measuring section has been identified, three separate points are operated with a distance between them generally not exceeding 10 cm. Each survey point is followed by 10 beats, a specific micrometre is then used to measure the depth of penetration of the needle. With the help of a specific experimental correlation curve, the compressive strength can be estimated.

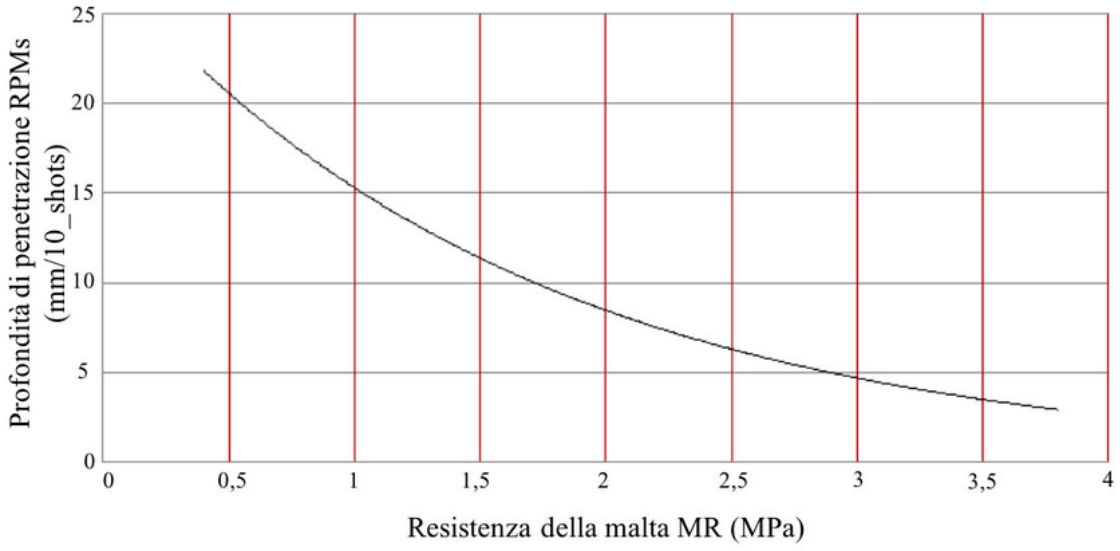


Figure 1-26. Correlation graph for estimating the strength of mortars.

The church was investigated in 20 areas as outlined in the Figure 1-27, 8 samples inside the church and 12 outsides were taken. The subindex PIN is correlated to the penetrometer tests that were performed, while the subindex M is related to the laboratory tests that consisted in the collection of mortar samples. The latter will be explained in the following paragraphs.

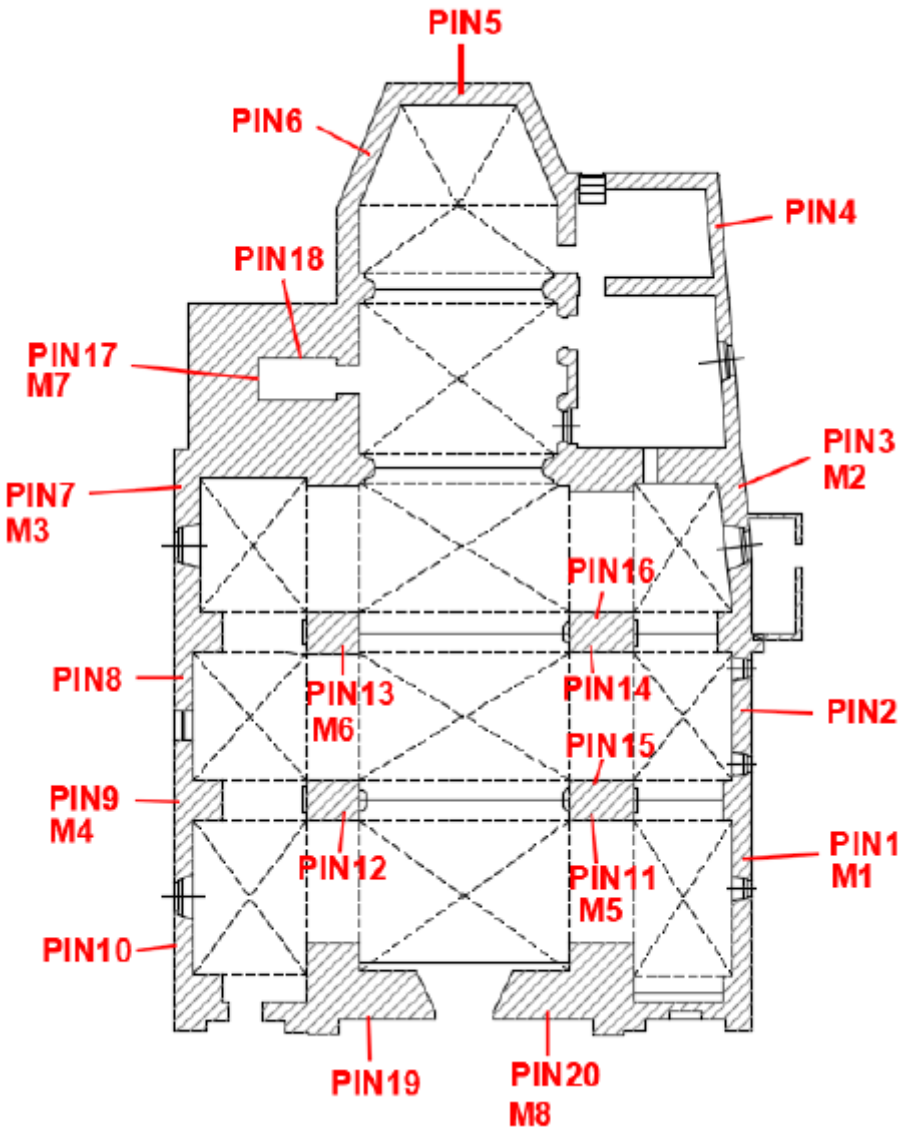


Figure 1-27. Locations of the tests.

Results of the penetrometer tests are given in the Table 1-5, where it is possible to see that the first measure is correlated to the 10 strokes that was given to each point, the second measure is related to the mm of penetration that each point suffered, then trough the correlation curve that was introduce by the Figure 1-26, was possible to make a correlation between the mm of penetration and the strength. Finally, the average of the strength was calculated, obtaining a finally result. The average strength with very low values were not considered, for that reason these values were indicated with f.s.

A mortar with very low resistance is found in zones 17 and 18 based on the distribution of the tests. These zones are located to the right of the presbyterium. Then, the zone 20 also individuates a low average strength, this zone is related with the entrance to the church.

| | | Reading 10 strokes | | | Penetration | | | Estimated strenght | | | Estimated average strength |
|---|---|---|---|---|---|---|---|---|---|---|---|
| Section | Type of survey | Point 1 | Point 2 | Point 3 | Point 1 | Point 2 | Point 3 | Point 1 | Point 2 | Point 3 | |
| Zone 1 | Sup. | 60 | 67 | 57 | 20 | 13 | 23 | 0.6 | 1.0 | 0.5 | 0.7 |
| Zone 2 | Sup. | 56 | 60 | 55 | 24 | 20 | 25 | 0.5 | 0.6 | 0.4 | 0.5 |
| Zone 3 | Sup. | 58 | 61 | 17 | 32 | 19 | 0.7 | 0.3 | 0.6 | 0.8 | 0.6 |
| Zone 4 | Sup. | 63 | 48 | 61 | 17 | 32 | 19 | 0.7 | 0.3 | 0.6 | 0.5 |
| Zone 5 | Sup. | 65 | 64 | 55 | 15 | 16 | 25 | 0.8 | 0.8 | 0.4 | 0.7 |
| Zone 6 | Sup. | 65 | 63 | 64 | 15 | 17 | 16 | 0.8 | 0.7 | 0.8 | 0.8 |
| Zone 7 | Sup. | 57 | 44 | 49 | 23 | 36 | 31 | 0.5 | 0.3 | 0.3 | 0.4 |
| Zone 8 | Sup. | 58 | 44 | 42 | 22 | 36 | 38 | 0.5 | 0.3 | 0.3 | 0.4 |
| Zone 9 | Sup. | 60 | 57 | 54 | 20 | 23 | 26 | 0.6 | 0.5 | 0.4 | 0.5 |
| Zone 10 | Sup. | 55 | 62 | 62 | 25 | 18 | 18 | 0.4 | 0.7 | 0.7 | 0.6 |
| Zone 11 | Sup. | 50 | 43 | 55 | 30 | 37 | 25 | 0.4 | 0.3 | 0.4 | 0.4 |
| Zone 12 | Sup. | 56 | 57 | 43 | 24 | 23 | 37 | 0.5 | 0.5 | 0.3 | 0.4 |
| Zone 13 | Sup. | 64 | 62 | 58 | 16 | 18 | 22 | 0.8 | 0.7 | 0.5 | 0.7 |
| Zone 14 | Sup. | 57 | 65 | 62 | 23 | 15 | 18 | 0.5 | 0.8 | 0.7 | 0.7 |
| Zone 15 | Sup. | 58 | 69 | 68 | 22 | 11 | 12 | 0.5 | 1.2 | 1.1 | 0.9 |
| Zone 16 | Sup. | 63 | 62 | 65 | 17 | 18 | 15 | 0.7 | 0.7 | 0.8 | 0.7 |
| Zone 17 | Sup. | 52 | 39 | 54 | 28 | 41 | 26 | 0.4 | 0.2 | 0.4 | fs |
| Zone 18 | Sup. | 47 | 52 | 46 | 33 | 28 | 34 | 0.3 | 0.4 | 0.3 | fs |
| Zone 19 | Sup. | 61 | 65 | 56 | 19 | 15 | 24 | 0.6 | 0.8 | 0.5 | 0.6 |
| Zone 20 | Sup. | 51 | 49 | 45 | 29 | 31 | 35 | 0.4 | 0.3 | 0.3 | fs |

Table 1-5· Results of the penetrometer test.

As mentioned above, laboratory tests on the mortar were also carried out. Mortar samples were taken at 8 locations on the wall elements of the church. The following figures show the analysed masonry in different sections of the building. For instance, the Figure 1-28 represents the masonry corresponding to the southern perimeter wall. From this picture is understandable that the masonry does not have a regular shape.

Figure 1-28. View of the test area – M1.

The Figure 1-29 represents the masonry corresponding also with the southern perimeter wall. The haphazard masonry pattern is also repeated in this area. On the other hand, the Figure 1-30 and Figure 1-31, represent the external masonry of the north side wall. In this case it is not easy to determine the type of masonry with the simple eye, but as will be seen later, once the tests have been carried out, it is also revealed to be made of irregular stone.

Figure 1-29. View of the test area - M2.

Figure 1-30. View of the test area - M3

Figure 1-31. View of the test area - M4

The Figure 1-32 represents the view of the test area M5 and M6, these areas are in correspondence with the interior part of the church, more precisely with the columns that are responsible to support all the bearing load that is coming from the vaults. As this picture shows, the type of masonry is not of disordered stone, but the presence of brickwork is noticed. The discovery of a different material could be related to the enlargement project that the church has undergone.

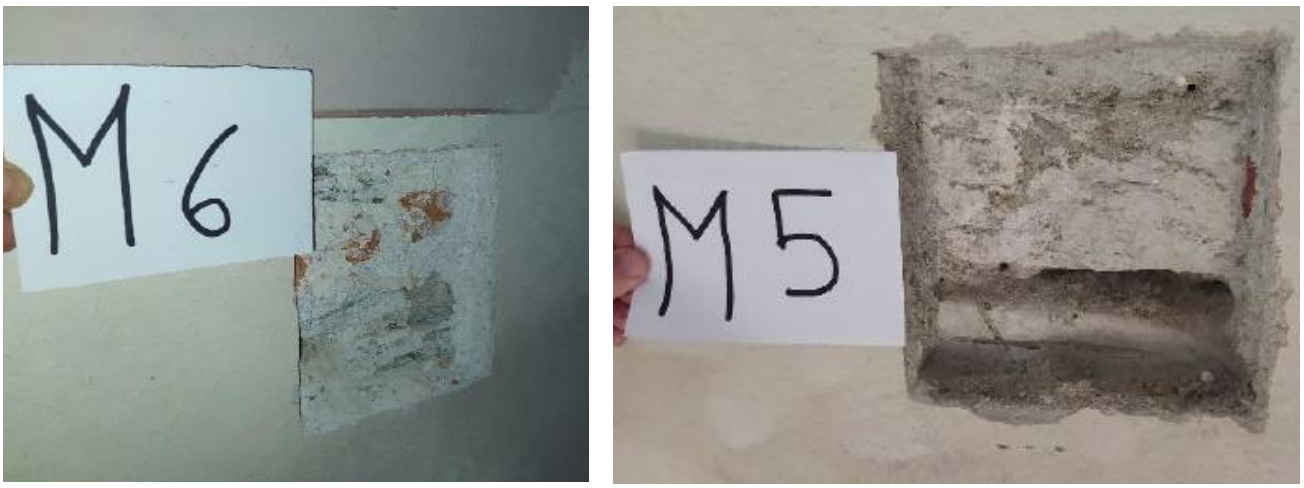


Figure 1-32. View of the test area - M5 and M6.

The Figure 1-33 represents the test point which is in correspondence with the base of the bell tower. From this image it can be seen at a quick glance that the masonry is made of stones in disarray.


Figure 1-33. View of the test area -M7.

Lastly, Figure 1-34 shows the masonry in correspondence with the western part of the building, it means the main façade that is in correspondence with the entrance.


Figure 1-34. View of the test area -M8.

Samples taken from different areas mentioned above were taken to the laboratory and analysed. The result of this analysis was that in all the cases the type of mortar detected was M 2,5 (hydraulic type) according to D.M 17/01/2018, that is the Italian Technical Standard for Construction. The following Table 1-6, taken from the above-mentioned standard, represents the correlation between the strength grade and the volume composition of the mortar.

| Classe | Tipo di malta | Composizione | | | | |
|---|---|---|---|---|---|---|
| | | Cemento | Calce aerea | Calce idraulica | Sabbia | Pozzolana |
| M 2,5 | Idraulica | – | – | 1 | 3 | – |
| M 2,5 | Pozzolanica | – | 1 | – | – | 3 |
| M 2,5 | Bastarda | 1 | – | 2 | 9 | – |
| M 5 | Bastarda | 1 | – | 1 | 5 | – |
| M 8 | Cementizia | 2 | – | 1 | 8 | – |
| M 12 | Cementizia | 1 | – | – | 3 | – |

Table 1-6. Extracted from the "Italian Technical Standard for Construction" (NTC 2018) Tab. 11.10.V – Chapter 11.

Table 1-5 shows the results of the test. In turn, the results of these tests could be related to common masonry typologies, thus making it possible to obtain numerical values for the different mechanical parameters. On the outside part of the church the kind of masonry used was mostly “Stone masonry”, while in the interior in correspondence with the zones 7 and 8 , as was mentioned before, part the type of mortar is “Brickwork”, also is possible to say that this kind of mortar is related with the columns of the church.

So, from the Figure 1-35 a correlation between the materials was made by assigning “muratura in pietra disordinate” that means "messy stone masonry" to the parts corresponding to “Stone masonry”. For parties related to brickwork the equivalent assigned was “muratura in mattoni pieni e malta di calce” that means “solid brick and cement mortar masonry”. As it is possible to see in the Figure 1-35 each typology has its specific mechanical parameters which are within a certain range, the value to be adopted within this range will then be pre-set in the next chapter according to the level of knowledge of the construction.

| Tipologia di muratura | f (N/mm²) | $\tau_0$ (N/mm²) | $f_{V0}$ (N/mm²) | E (N/mm²) | G (N/mm²) | w (kN/m³) |
|---|---|---|---|---|---|---|
| | min-max | min-max | | min-max | min-max | |
| Muratura in pietrame disordinata (ciottoli, pietre erratiche e irregolari) | 1,0-2,0 | 0,018-0,032 | - - | 690-1050 | 230-350 | 19 |
| Muratura a conci sbozzati, con paramenti di spessore disomogeneo (*) | 2,0 | 0,035-0,051 | - - | 1020-1440 | 340-480 | 20 |
| Muratura in pietre a spacco con buona tessitura | 2,6-3,8 | 0,056-0,074 | - - | 1500-1980 | 500-660 | 21 |
| Muratura irregolare di pietra tenera (tufo, calcarenite, ecc.,) | 1,4-2,2 | 0,028-0,042 | - - | 900-1260 | 300-420 | 13 ÷ 16(**) |
| Muratura a conci regolari di pietra tenera (tufo, calcarenite, ecc.,) (**) | 2,0-3,2 | 0,04-0,08 | 0,10-0,19 | 1200-1620 | 400-500 | |
| Muratura a blocchi lapidei squadrati | 5,8-8,2 | 0,09-0,12 | 0,18-0,28 | 2400-3300 | 800-1100 | 22 |
| Muratura in mattoni pieni e malta di calce (***) | 2,6-4,3 | 0,05-0,13 | 0,13-0,27 | 1200-1800 | 400-600 | 18 |
| Muratura in mattoni semipieni con malta cementizia (es,: doppio UNI foratura ≤40%) | 5,0-8,0 | 0,08-0,17 | 0,20-0,36 | 3500-5600 | 875-1400 | 15 |

Figure 1-35. Reference values of mechanical parameters of masonry. NTC2018.

| | | | | | f(N/mm2) | | tau0 (N/mm2) | | fv0 (N/mm2) | | E | | G | | weight (kN/m3) |
|---|---|---|---|---|---|---|---|---|---|---|---|---|---|---|---|
| POINT | SIDE | OUTSIDE / INSIDE | MORTAR TAKEN | TYPE OF MASONRY | min | max | min | max | min | max | min | max | min | max | |
| M1 | SOUTH | OUTSIDE | MURATURA IN PIETRA | *muratura in pietrame disordinata | 1.0 | 2.0 | 0.0 | 0.0 | - | - | 690.0 | 1050.0 | 230.0 | 350.0 | 19.0 |
| M2 | SOUTH | OUTSIDE | MURATURA IN PIETRA | *muratura in pietrame disordinata | 1.0 | 2.0 | 0.0 | 0.0 | - | - | 690.0 | 1050.0 | 230.0 | 350.0 | 19.0 |
| M3 | SOUTH | OUTSIDE | MURATURA IN PIETRA | *muratura in pietrame disordinata | 1.0 | 2.0 | 0.0 | 0.0 | - | - | 690.0 | 1050.0 | 230.0 | 350.0 | 19.0 |
| M4 | SOUTH | OUTSIDE | MURATURA IN PIETRA | *muratura in pietrame disordinata | 1.0 | 2.0 | 0.0 | 0.0 | - | - | 690.0 | 1050.0 | 230.0 | 350.0 | 19.0 |
| M5 | SOUTH | INSIDE | MURATURA IN LATERIZIO | *muratura in mattoni pieni e malta di calce | 2.6 | 4.3 | 0.1 | 0.1 | 0.1 | 0.3 | 1200.0 | 1800.0 | 400.0 | 600.0 | 18.0 |
| M6 | NORTH | INSIDE | MURATURA IN LATERIZIO | | 2.6 | 4.3 | 0.1 | 0.1 | 0.1 | 0.3 | 1200.0 | 1800.0 | 400.0 | 600.0 | 18.0 |
| M7 | NORTH | OUTSIDE | MURATURA IN PIETRA | *muratura in pietrame disordinata | 1.0 | 2.0 | 0.0 | 0.0 | - | - | 690.0 | 1050.0 | 230.0 | 350.0 | 19.0 |
| M8 | NORTH | OUTSIDE | MURATURA IN PIETRA | *muratura in pietrame disordinata | 1.0 | 2.0 | 0.0 | 0.0 | - | - | 690.0 | 1050.0 | 230.0 | 350.0 | 19.0 |

Table 1-7. Reference values of mechanical parameters of masonry. NTC2018

Regarding non-destructive tests, an infrared thermography test was carried out. It consists in an investigation that captures the heat energy emitted from the surface of a material. Images are recorded using an infrared camera, in which the intensity of the infrared radiation is converted to a colour or black and white palette, the patterns of which are an indicator of temperature. Infrared radiation is invisible to the naked eye as the wavelengths occur in the range of the electromagnetic spectrum which is longer than that which the eye can detect.

There are multiple situations in which infrared thermography can be useful in historic buildings. The information it provides can help improve understanding of a problem, as well as determine the performance characteristics of a building and assess its structural and environmental integrity.

The key to interpreting thermal images is based on the assignment of the 'iron scale', associating zones of higher thermal emission with lighter colours and zones of lower thermal emission with progressively darker colours. Under thermal transient conditions, the thermal image highlights the structure underneath the plaster, which responds differently to heating depending on the different thermal emissivity of the materials: for example, in a ceiling, the concrete areas (beams and joists) are clearly defined in their contours, which are darker than the areas occupied by the brick blocks.

The test was carried out from around 10 a.m. on 11 February 2021 under natural thermal transient conditions with the aim of non-destructively detecting the presence of moisture and/or seepage. A total of 98 thermographic surveys were carried out, distributed inside and outside the church. The thermographic investigations are carried out with a Flir thermal imaging camera, model T420bx. Some images taken

are presented below to understand the main issues that the construction under analysis suffers from.

The Figure 1-36 was taken in the intrados of a vault. From it is possible to notice that there is fracture of considerable size in the middle part, and so many little fractures around.


Figure 1-36.

Another representation of the intrados of a vault is given by the Figure 1-37. From this image is possible to notice the moisture infiltration which is represented with a darker colour in next to the rib.

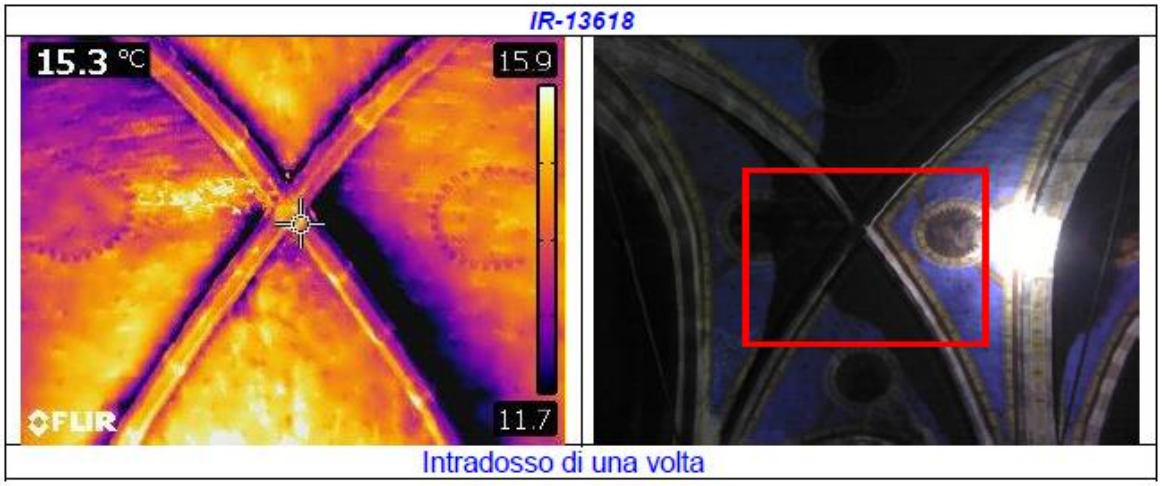


Figure 1-37.

A crack in correspondence with a stained-glass window in the presbyterium is represented by the Figure 1-38.

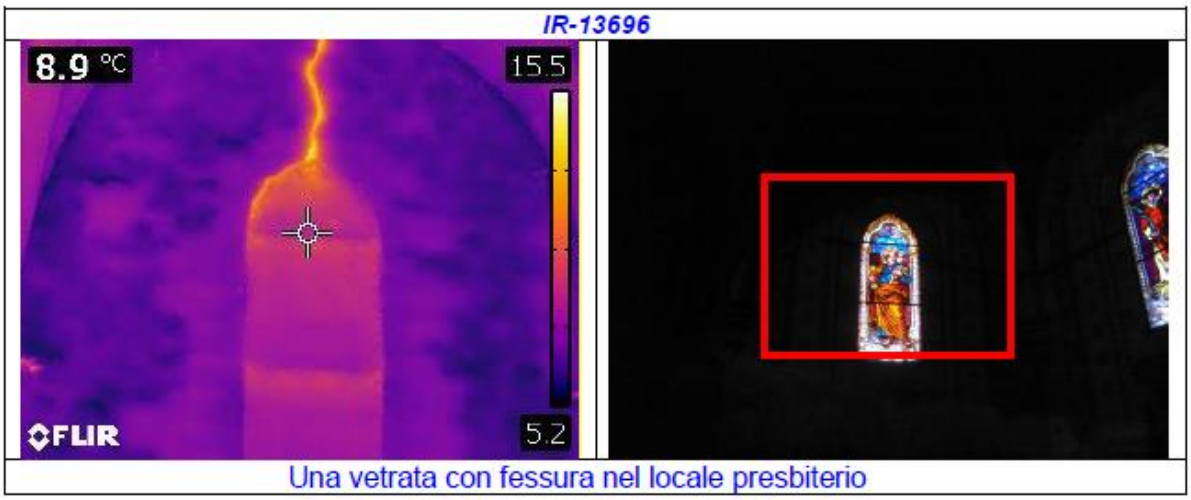


Figure 1-38.

The Figure 1-39 represents the external face with buffered opening, from the image is possible to understand the presence of a crack in the middle part of the wall.

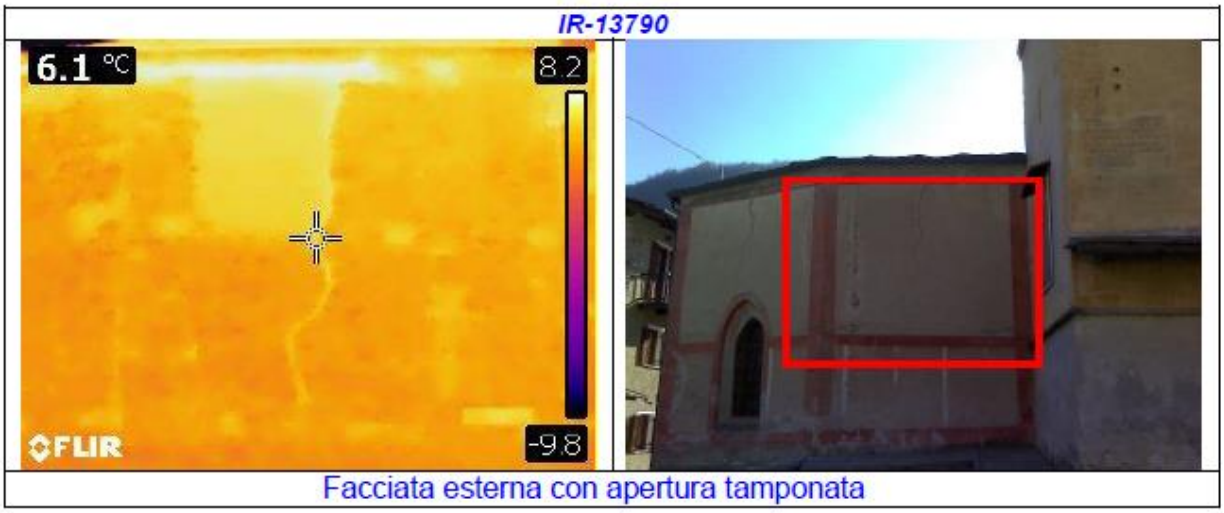


Figure 1-39.

With all the above tests it is thus possible to have a deeper knowledge of the materials that constitute the church, in the same way the geometry of the church can be confirmed. Although the tests carried out on the construction give an idea of the materials used in the construction and, more importantly, their mechanical characteristics, it is not possible to fully trust in them.

The tests that have been carried out do not a complete stratigraphy of the walls that are being analysed, and consequently it is not possible to know what there is beyond the first superficial centimetres that have been removed, leaving a big question mark.

Among all the tests available on the market, the one that, due to its characteristics, would have been the most suitable to solve this problem is the endoscopy test. It consists of observing natural or artificial cavities (specially created with core drills or drills) with special instruments. This test on masonry allows knowledge of the stratigraphy, type, morphology, and state of preservation of the materials passed through. It can also be carried out on load bearing and load-bearing structures of flat floors.

# 2

# Seismic safety assessment

This chapter can be divided into two processes. The first process undertaken was the determination of the mechanical characteristics of the materials comprising the construction. The second process is related to a seismic safety assessment, which involves evaluating the integrity and safety of the structure in relation to potential seismic risks.

## 2.1 Knowledge levels and confidence factors

Once the construction has been identified, in relation to the in-depth geometric survey and the material-constructive, mechanical and on the ground and foundations, the designer assumes a confidence factor FC, between 1 and 1.35, which makes it possible to graduate the reliability of the structural analysis model and the evaluation of the of seismic safety.

There are several models that apply different confidence factors to assessing seismic safety, they can be grouped as follows.

- Models that consider the deformability and strength of materials and structural elements.

- Models that consider the limit equilibrium of the different elements of the construction, thinking of the masonry material as rigid and non-tensile resistant (creation of a kinematics of rigid blocks, through the introduction of appropriate disconnections).

In the first case, the confidence factor is applied to the properties of the materials, reducing both elastic modulus and strengths. The starting values of the mechanical properties to which the confidence factor will be defined in the usual ranges of construction practice of the time, based on the findings of the material survey and construction details. In the second case, i.e. rigid body models, where the resistance of the material is ignored, the confidence factor is applied directly to the structure's capacity, i.e. by reducing the acceleration. [1]

As previously mentioned in the chapter 1.5 the Italian Technical Standard for Construction (NTC 2018) defines different kind of tests that can be performed in an existing building, these tests are differentiated by levels which range from very weak to very strong in terms of the information obtained. In relation with these tests, the Italian code, in the paragraph C8.5.4 defines the knowledge levels and their confidence factors as follows:

- LC1: is considered achieved when, as a minimum, the historical-critical analysis commensurate with the level considered, the complete geometric survey and limited investigations of construction details, limited tests on the mechanical properties of materials have been carried out, the corresponding confidence factor is **FC=1.35.**

- LC2: is understood to be achieved when, as a minimum, the historical-critical analysis commensurate with the level considered, the complete geometric survey and extensive investigations of construction details, extensive tests on the mechanical properties of materials have been carried out, the corresponding confidence factor is **FC=1.2.**
- LC3: is understood to have been achieved when the historical-critical analysis commensurate with the level considered has been carried out, the geometric survey, complete and accurate in every part, and exhaustive investigations of construction details, exhaustive tests on the mechanical characteristics of materials, the corresponding confidence factor is **FC=1.** [12]

In line with the above- mentioned regulations, and evaluating the surveys carried out and the information available, it is possible to establish that the level of knowledge of the structure under examination is LC2, which corresponds to a confidence factor of 1.2.

On the other hand, in the chapter 4 of the "Guidelines for evaluation and reduction of seismic risk of cultural heritage" the route to be followed to identify the construction to be able to then go in the process of dine a level of knowledge and a confidence factor. The path indicated in the guidelines can be divided into the following activities:

- Identifying the building, is the first phase of knowledge and consists of assessing the relationship of the building with the surrounding urban context, the presence of elements of where to carry out possible reinforcement works and identify possible areas of sacrifice where to carry out destructive investigations.

- Complete geometric survey of the building, identifying the plano-altimetrical characteristics of all the masonry elements and assessing the cracks, trying to identify the causes and possible evolutions by classifying the lesions from a geometric point of view (extension and amplitude) as well as kinematically (detachment rotation, sliding, displacement out of plane).

- Identifying the path of construction of the artefact and the modifications undergone over time, paying particular attention to the successive construction of the various portions of the building to identify possible areas of discontinuity in the material.

- Identify the constituent elements of the resistant organism paying particular attention to construction techniques, construction details and connections between the elements.

- Identifying materials by assessing both the level of degradation and mechanical properties from a visual survey to the use of both destructive tests (such as example the use of the double flat jack to determine the modulus of elasticity modulus and compressive strength) and non-destructive (sonic and ultrasonic).

- Knowledge of the subsoil and foundation structures, with reference to variations over time and related instabilities using available documentation combined with possible non-destructive testing.

A very similar value could be obtained using the Figure 2-1, that is a table given by the “Guide lines for evaluation and reduction of seismic risk of cultural heritage”, it is possible to determine the confidence factor by defining several partial confidence factors, on the basis of the numerical coefficients given in the aforementioned table, the values of which are associated with the survey categories and the level of depth reached in them:

$$F_C = 1 + \sum_{k=1}^{4} F_{Ck} \qquad (1)$$

Tabella 4.1
Definizione dei livelli di approfondimento delle indagini sui diversi aspetti della conoscenza e relativi fattori parziali di confidenza.

| Rilievo geometrico | Rilievo materico e dei dettagli costruttivi | Proprietà meccaniche dei materiali | Terreno e fondazioni |
|---|---|---|---|
| rilievo geometrico completo<br>$F_{C1} = 0.05$ | limitato rilievo materico e degli elementi costruttivi<br>$F_{C2} = 0.12$ | parametri meccanici desunti da dati già disponibili<br>$F_{C3} = 0.12$ | limitate indagini sul terreno e le fondazioni, in assenza di dati geologici e disponibilità d'informazioni sulle fondazioni<br>$F_{C4} = 0.06$ |
| rilievo geometrico completo, con restituzione grafica dei quadri fessurativi e deformativi<br>$F_{C1} = 0$ | esteso rilievo materico e degli elementi costruttivi<br>$F_{C2} = 0.06$ | limitate indagini sui parametri meccanici dei materiali<br>$F_{C3} = 0.06$ | disponibilità di dati geologici e sulle strutture fondazionali; limitate indagini sul terreno e le fondazioni<br>$F_{C4} = 0.03$ |
| | esaustivo rilievo materico e degli elementi costruttivi<br>$F_{C2} = 0$ | estese indagini sui parametri meccanici dei materiali<br>$F_{C3} = 0$ | estese o esaustive indagini sul terreno e le fondazioni<br>$F_{C4} = 0$ |

Figure 2-1. Partial confidence factor. Table 4.1 of "Guidelines for evaluation and reduction of seismic risk of cultural heritage", paragraph 4.2.

Based on the data collected, the following partial coefficients were chosen:

$$F_{C_1} = 0$$

$$F_{C_2} = 0.12$$

$$F_{C_3} = 0.06$$

$$F_{C_4} = 0.03$$

Obtaining as a result,

$$F_C = 1 + 0 + 0.12 + 0.06 + 0.03$$

$$F_C = 1.21$$

The value obtained is higher than the one established by the level of confidence LC2.

## 2.2 Mechanical characterisation of the masonry

In correspondence with the paragraph C8.5.4.1 of NTC 2018, when the level of knowledge is LC2, the values of the mechanical parameters to be used are defined as follows: for the resistance and the elastic modulus the mean values given by the Figure 1-35 must be used.

Then by averaging these values it is possible to obtain the mechanical parameters of interest for the masonry material. Where, f is related to the average compressive strength, $\tau_0$ is the average shear strength in the absence of normal stresses, fv0 is the average shear strength in the absence of normal stresses, E is the mean value of the normal modulus of elasticity, G is the mean value of the tangential modulus of elasticity and w is the mean specific gravity. These parameters will be implemented in the finite element model of the church that will be developed in a next chapter.

| | Knowledge level (LC) | Reliability factor (FC) | Mechanical parameters | | | | | |
|---|---|---|---|---|---|---|---|---|
| POINT | | | f (N/mm2) | tau0 (N/mm2) | fv0 | E | G | w |
| M1 | LC2 | 1.2 | 1.50 | 0.03 | - | 870.00 | 290.00 | 19.00 |
| M2 | | | 1.50 | 0.03 | - | 870.00 | 290.00 | 19.00 |
| M3 | | | 1.50 | 0.03 | - | 870.00 | 290.00 | 19.00 |
| M4 | | | 1.50 | 0.03 | - | 870.00 | 290.00 | 19.00 |
| M5 | | | 3.45 | 0.09 | 0.20 | 1500.00 | 500.00 | 18.00 |
| M6 | | | 3.45 | 0.09 | 0.20 | 1500.00 | 500.00 | 18.00 |
| M7 | | | 1.50 | 0.03 | - | 870.00 | 290.00 | 19.00 |
| M8 | | | 1.50 | 0.03 | - | 870.00 | 290.00 | 19.00 |

Table 2-1. Final mechanical parameters of the masonry under examination.

## 2.3 The seismic behavior of historical masonry buildings

Masonry churches represent a not insignificant portion of the Italian building fabric and are those that potentially, in occasion of seismic events, can cause a high number of victims. Therefore, due to their high seismic vulnerability, they contribute significantly increase the national seismic risk. [13]

The historic masonry structures constitute an extremely diverse and complex set for types and construction techniques, for which the analysis of their structural behaviour and the evaluation of their safety are conditioned by considerable uncertainties in the definition of the mechanical properties of the materials and the conditions of

constraint between the elements. As far as the masonry is the result of a combination of materials, its characteristics are variable. For instance the constituent material of the elements could be stone, brick, unfired earth, etc. and used in a mixed manner, the size and shape of the elements is also variable, the assembly technique could be performed in different ways (dry or with mortar joints), the texture of the materials is variable and the arrangement of the elements.

The historic masonry constructions were not designed according to the principles of mechanics of materials and structures, but rather based on intuition and observation, observing rigid bodies in equilibrium, and experimenting with how they behaved. The guidelines identify mainly elements for assessing the safety of a building:

- Confirm that a construction agrees with the rules of art.
- "History's 'testing", to which the existence of the building itself provides testimony. Such a test, however, is often insufficient regarding seismic risk prevention, since a construction (even an ancient one) may not yet have been hit by a violent earthquake, the one that is assumed by the standards to assess safety about the ultimate limit state.
- The seismic activity present in the area where the construction is located, since in high seismic hazard areas retrofitting works were introduced in anticipation of the earthquake. On the other hand, in areas where the seismic hazard is low, these works are introduced once the damage is already present.

Based on the description of the structure and its seismic behaviour, different analysis methods can be used for existing masonry buildings. It is essential for the structural capacity and seismic safety of cultural heritage buildings to be evaluated with an appropriate analysis method. The following can be mentioned in particular:

- Linear static analysis
- Modal dynamic analysis
- Non-linear static analysis
- Non-linear dynamic analysis

## 2.4 Assessment of building safety

To assess the safety of the structure, the guidelines define 3 different levels to be analysed.

-LV1: qualitative analysis and evaluation with simplified mechanical models. It is possible to evaluate seismic safety using simplified methods capable of estimating the ground acceleration corresponding to reaching an **ultimate limit state.** Nevertheless, this acceleration value, compared to a site's characteristic peak acceleration, can only be used to determine intervention priorities using a seismic safety index (IS). The seismic safety index **IS** defined as follows:

$$I_s = \frac{a_{SLU}}{\gamma_I S a_g} \tag{2}$$

Where from the equation (1) the following coefficients can be explained:

$a_{SLU}$ is the ground acceleration leading to the ultimate limit state.

$S$ is the factor that considers the stratigraphic profile of the foundation subsoil and any morphologic effects.

$\gamma_I$ is a coefficient of significance.

$a_g$ is the site reference acceleration.

Seismic safety index values greater than 1 indicate that the building is suitable to withstand the seismic action expected in the area. On the contrary, if the seismic safety index is less than one, the safety of the building is less than desirable, consistent with the requirements for suitable constructions.

-LV2: Assessment of individual macro-elements (local collapse mechanisms). Restoration work on individual parts of the building is subject to this level of assessment, also in this case is possible to use local models related to specific parts of the building called macro-elements. These macro-elements can be defined as “parts of the church with architecturally identifiable features (façade, apse, truncated arch) with significantly different seismic responses to the rest of the building”. In general, the most effective and easy tool for such an assessment is kinematic analysis, which can be linear or non-linear. There is a risk that the results that are obtained may be overly cautious if the various construction details that determine the actual behaviour of the structure are not considered: chains, anchoring between orthogonal

masonry, masonry texture, etc. Therefore, for each macro-element analysed, the comparison of the ultimate limit state accelerations before and after the intervention on the construction allows a judgement to be made on the degree of improvement obtained.

-LV3: Overall assessment of the seismic response of the building. In this level of assessment, the seismic safety of the building is considered as a whole, that is, the ground acceleration at the ultimate limit state of the building, or individually significant parts of that building (macro-elements). This level should be adopted whenever interventions are designed that alter the established functioning of the building and, in any case, when the renovation is intended for a building of a strategic nature, since knowing the safety of such structures is of great social importance.

Before going on with the analysis, it is of vital importance to define the limit states to which a structure may be subjected. A limit state in structural engineering is defined as a condition, which if exceeded, the structure under analysis does not satisfy the requirements under which it was designed. It is possible to distinguish between ultimate limit states and exercise limit states.

The SLU (Ultimate Limit States) could be defined as extreme values of load-bearing capacity or structural failures that may endanger lives. This state is motivated by the desire to safeguard the building and the safety of the occupants when earthquakes occur rarely and strongly. According to the Italian code for seismic actions the ultimate limit states are subdivided into:

- Life-sustaining limit state (SLV): because of the earthquake, non-structural and plant engineering components of the building rupture and collapse, and structural components suffer significant damage with a significant loss of stiffness in relation to horizontal movements.
- Collapse Prevention Limit State (SLC): due to the earthquake, the non-structural and plant engineering components of the building collapsed and suffered severe damage, while the structural components were severely damaged. There is still a margin of safety against collapse for vertical actions and a small margin of safety against collapse against horizontal actions.

While the exercise limit states, are states beyond which the operational requirements can no longer be met. These limit states are aimed at limiting damage from less

intense but more frequent earthquakes. There are two kinds of damage or deformation caused by exceeding an operating limit state: the first scenario is reversible and will cease as soon as the cause that caused the overshoot is removed. A second scenario occurs when unacceptable permanent damage or deformation arises that cannot be fixed by eradicating their cause. With respect to seismic actions (dynamic SLE), the limit states are subdivided into:

- Serviceability Limit State (SLO): following the earthquake, the building (including structural elements, non-structural elements, etc.) must not suffer significant damage and interruption of use.
- Damage limit state (SLD): following the earthquake, the building (including structural elements, non-structural elements, relevant equipment, etc.) suffers damage such that it does not put users at risk and does not significantly compromise the capacity for resistance and rigidity against vertical and horizontal actions, remaining immediately usable even if part of the equipment is interrupted. [12]

## 2.5 Simplified model for estimating ground acceleration corresponding to limit states (LV1)

For most churches, the assumption of unitary and overall behaviour is hardly useful. Consequently, due to the considerable typological and constructional diversity of churches, a simplified mechanical model based on a limited number of parameters should not be used for evaluating seismic safety. An alternative for assessing LV1 is to make use of the parameters of the damage and vulnerability. The maximum ground acceleration corresponding to the different limit states can be related to a numerical indicator, the vulnerability index $i_V$, obtained through an appropriate combination of scores assigned to the different elements of vulnerability and earthquake protection.

### 2.5.1 Seismic safety levels

A reference level of seismic safety must be established, distinguished by the characteristics and use of the buildings, as well as the more or less serious consequences of their damage. For that objective some parameters will be defined:

- $V_N$ : Nominal life, it is defined as the number of years in which the structure, provided it is subject to the necessary maintenance, is expected to maintain specific performance levels or for which seismic improvements are planned, if required. The minimum values of VN to be adopted for the different types of construction are given in Table 2-2. Culture assets should have a long nominal life to ensure their preservation over time, even in the face of seismic activities with high return periods. In the case of the church under investigation the nominal life that will be assumed is equal to 50 years.
- $C_U$ : usage class. In terms of the consequences of an operational interruption or collapse, according to the normative, constructions can be categorized into use classes as follows:

Class I: Buildings with only occasional presence of people, agricultural buildings.

**Class II: Buildings whose use involves normal crowding, with no environmentally hazardous contents and no essential public and social essentials.**

Class III: Buildings whose use involves significant crowding. Industries with environmentally hazardous activities.

Class IV: strategic building and very frequent use and/or with significant crowding.

Each use class corresponds to a use coefficient, which can be extracted from the Table 2-3.

Focusing attention on the case study, the church can be considered to fall into use class II, because of the use to which it is devoted and because of the presence of a normal crowd during its use period. For that reason, the coefficient $C_U$ is equal to 1.

**Tab. 2.4.II** – *Valori del coefficiente d'uso* $C_U$

| CLASSE D'USO | I | II | III | IV |
|---|---|---|---|---|
| COEFFICIENTE $C_U$ | 0,7 | 1,0 | 1,5 | 2,0 |

Table 2-3 - Tabl2.4.II "Valori del coefficiente d'uso CU" extracted from "Normative tecniche per

A reference period is used to calculate the seismic action acting on the building, this reference period is obtained by multiplying the nominal life by the use coefficient. In this way, once both coefficients have been determined, it is possible to determine the reference period, as indicated by the following formula.

$$V_R = V_N \, \mathrm{C_u} \tag{3}$$

The Table 2-4 gives an overview of the parameters of interest.

| | Unit | Value |
|---|---|---|
| Nominal Life | Years | 50 |
| usage class | | III |
| Use coefficient | | 1.5 |
| Life of reference | Years | 75 |

Table 2-4. Parameters of the construction.

In relation to the reference period $V_R$ and the considered limit state, to which a probability of exceeding $P_{VR}$ in the reference period is assigned, a reference period of the considered seismic action can be evaluated $T_R$. A return period can be defined as the *"time span or number of years that, on average, it is believed to be equaled or exceeded, i.e., the frequency with which an event occurs".* [14]

The following formula can be used to calculate the return period:

$$T_R = -\frac{V_R}{\ln\left(1 - P_{V_R}\right)} = \frac{V_N \, \mathrm{C_u}}{\ln\left(1 - P_{V_R}\right)} \tag{4}$$

The $P_{V_R}$ exceedance probability is a function of the limit state and is defined through Table 3.1.I of NTC18 (Ministerial Decree of 17 January 2018).

| Stati Limite | | $P_{V_R}$: Probabilità di superamento nel periodo di riferimento $V_R$ |
|---|---|---|
| Stati limite di esercizio | SLO | 81% |
| | SLD | 63% |
| Stati limite ultimi | SLV | 10% |
| | SLC | 5% |

Table 2-5. Probability of exceeding $P_{V_R}$ as a function of the limit state considered. Table 3.1.I from NTC18.

Then, based on the limit states of interest, as a function of the probability of exceedance, the periods of return can be determined by applying equation 3. This was carried out and is reported in the table Table 2-6.

| Limit state | $P_{VR}$ [%] | $T_R$[years] |
|---|---|---|
| SLD | 63 | 50 |
| SLV | 10 | 475 |

Table 2-6. Exceedance probabilities and reference periods for the limit states considered.

### 2.5.2 Subsoil category and topographical conditions

As determined in chapter 1.5, the terrain class is C, while the topographic category is T2. Based on the table 3.2.III of NTC18 (Ministerial Decree of 17 January 2018), this type of terrain presents slopes with medium inclination greater than 15 degrees.

| Categoria | Caratteristiche della superficie topografica |
|---|---|
| T1 | Superficie pianeggiante, pendii e rilievi isolati con inclinazione media $i \leq 15°$ |
| T2 | Pendii con inclinazione media $i > 15°$ |
| T3 | Rilievi con larghezza in cresta molto minore che alla base e inclinazione media $15° \leq i \leq 30°$ |
| T4 | Rilievi con larghezza in cresta molto minore che alla base e inclinazione media $i > 30°$ |

Table 2-7. Topographical categories. Table 3.2.III from NTC18

### 2.5.3 Elastic spectrum in accelerations for the Damage limit state (SLD) and Life-sustaining limit state (SLV)

To assess seismic action, sub-soil and topographical characteristics are considered. With the help of the excel spreadsheet provided by the superior council of public works, it is possible to obtain the following parameters:

- The maximum horizontal acceleration at the site $a_g$.
- The amplification factor of the spectrum under horizontal acceleration $F_0$.
- The period of the constant velocity section in the horizontal acceleration spectrum $T^*$.

| | SLD | SLV |
|---|---|---|
| $T_R$ | 50 years | 475 years |
| $a_g$ | 0.055 g | 0.136 g |
| $F_0$ | 2.425 | 2.481 |
| $T_c^*$ | 0.227 s | 0.273 s |

Table 2-8. Frassino's seismic parameters for different limit states.

Then, the S coefficient considers topographical conditions and terrain type. It is calculated as:

$$S = S_S\, S_T \tag{5}$$

Where:

$S_S$ is the stratigraphic coefficient and it is calculated using the formulas proposed in the NTC18 standards (Ministerial Decree of 17 January 2018).

| Categoria sottosuolo | $S_S$ | $C_C$ |
|---|---|---|
| A | 1,00 | 1,00 |
| B | $1,00 \le 1,40 - 0,40 \cdot F_o \cdot \frac{a_g}{g} \le 1,20$ | $1,10 \cdot (T_C^*)^{-0,20}$ |
| C | $1,00 \le 1,70 - 0,60 \cdot F_o \cdot \frac{a_g}{g} \le 1,50$ | $1,05 \cdot (T_C^*)^{-0,33}$ |
| D | $0,90 \le 2,40 - 1,50 \cdot F_o \cdot \frac{a_g}{g} \le 1,80$ | $1,25 \cdot (T_C^*)^{-0,50}$ |
| E | $1,00 \le 2,00 - 1,10 \cdot F_o \cdot \frac{a_g}{g} \le 1,60$ | $1,15 \cdot (T_C^*)^{-0,40}$ |

Table 2-9. Table 3.2.IV from NTC18.

In contrast, the parameter relating to topographical conditions ST is taken from Table 3.2.V. of the regulations (Ministerial Decree of 17 January 2018).

| Categoria topografica | Ubicazione dell'opera o dell'intervento | $S_T$ |
|---|---|---|
| T1 | - | 1,0 |
| T2 | In corrispondenza della sommità del pendio | 1,2 |
| T3 | In corrispondenza della cresta di un rilievo con pendenza media minore o uguale a 30° | 1,2 |
| T4 | In corrispondenza della cresta di un rilievo con pendenza media maggiore di 30° | 1,4 |

Table 2-10. Table. 3.2.V from NTC18. · Maximum values of topographic amplification coefficient ST.

| | SLD | SLV |
|---|---|---|
| Terrain class | C | |
| Topographic category | T2 | |
| $S_S$ | 1.5 | 1.5 |
| $S_T$ | 1.2 | 1.2 |
| $S$ | 1.8 | 1.8 |
| $a_g$ | 0.055 g | 0.136 g |
| $a_g S$ | 0.099 | 0.245 |

2-11. Summary of seismic parameters for different limit states.

### 2.5.4 Vulnerability index

The methodology considers 28 damage mechanisms associated with the different macro-elements that may exist in a church. With reference to the vulnerability assessment, it is necessary to detect those typological and construction details that play a fundamental role in the seismic response of the building. Indicators of vulnerability and anti-seismic protection are considered.

According to statistics, the seismic behaviour of the entire building is represented by a vulnerability index that ranges from 0 to 1, based on a weighted average of the different parts:

$$i_V = \frac{1}{6}\frac{\sum_{k=1}^{28}\rho_K\,(\boldsymbol{v_{ki}} - \boldsymbol{v_{kp}})}{\sum_{k=1}^{28}\rho_K} + \frac{1}{2} \tag{6}$$

From the above formula, the behaviour of the entire building depends on the weight given to each damage mechanism that may be triggered by the earthquake. Where for the k.th mechanism $v_{ki}$ and $v_{kp}$ are derived from research of the vulnerability indicators and the earthquake-proof structures. Table 2-12 provides a vulnerability score assessment for each damage mechanism. While the coefficient $\rho_K$ is the weight attributed to the mechanism, it adopts a value of 0 for the mechanisms that could not have been activated in the church, due to the absence of the macro-element, while it is between 0.5 and 1 in the other cases.

| Numero degli indicatori di vulnerabilità o dei presidi antisismici | Giudizio dell'efficacia | $v_k$ |
|---|---|---|
| almeno 1 | 3 | 3 |
| almeno 2 | 2 | |
| 1 | 2 | 2 |
| almeno 2 | 1 | |
| 1 | 1 | 1 |
| nessuno | 0 | 0 |

Table 2-12- Table 5.1 of the "Linee guida per la valutazione e riduzione del rischio sismico del patrimonio culturale"

In summary, the procedure to be followed is to rate each feature of the seismic structures and vulnerability indicators identified in the guideline from 1 to 3 for each mechanism analysed.

As a first step, the mechanisms that can occur in the church must be identified, according to the type of structure and macro-elements present. The mechanisms defined by the regulation are the following:

- **Overturning of the façade**. It is characterized by the detachment of the façade from the walls or visible detachment out of lead. (1)
- **Mechanisms at the top of the façade**. This mechanism consists in the tipping of the gable, with horizontal or V-shaped lesion, masonry disintegration or kerb sliding and rotation of trusses. (2)
- **Mechanisms in the plane of the façade**. Inclined injuries (shear), vertical or curved injuries (rotation), other cracks or displacements. (3)
- **Narthex:** Injuries in arches or in entablature due to rotation of columns - Detachment from the façade – Hammering. (4)
- **Transverse response of the hall**. Injuries in the arches (with possible continuation in the vault), rotations of side walls, shear injuries in vaults, out-of-lead and crushing in columns. (5)

- **Shear mechanisms in the side walls (longitudinal response)**. This mechanism is composed of inclined injuries (single or crossed), injuries in correspondence with the discontinuities in masonry. (6)
- **Longitudinal response of the colonnade**. Cross-sectional arches or lintels that experience crushing and/or shear injuries, pillar bases that sustain crushing and/or shear injuries. (7)
- **Central nave vaults**. Disconnections between the vaults and the arches in the central hall. (8)
- **Lateral nave vaults**. Disconnections or injuries to vaults or arches. (9)
- **Overturning the walls of transept ends**. Detachment of the front wall from the side walls · Overturning or disintegration of the tympanum at the top. (10)
- **Shear mechanisms in the transept walls**. Inclined injuries (single or crossed) · Injuries through discontinuities. (11)
- **Transept vaults.** Injuries in vaults or disconnections from arches and side walls. (12)
- **Triumphal arches**. Injuries in the arch, crushing or horizontal injuries at the base of the piers. (13)
- **Dome - drum/timber.** Injuries in the dome (arch) with possible continuation in the drum. (15)
- **Overturning of the apse**. Vertical or arcuate lesions in apse walls · Vertical lesions in polygonal apses · U-shaped lesion in semicircular apses. (16)
- **Shear mechanisms in the presbytery or apse**. Inclined injuries (single or crossed) · Injuries at of wall discontinuities. (17)
- **Presbytery or apse vaults**. Injuries in the vaults or disconnections from the arches or side walls. (18)

- **Roofing elements: hall**. Injuries near the heads of the wooden beams, sliding of the beams - Disconnections between kerb and masonry - Significant movements of the roof covering. (19)
- **Mechanisms in roof elements – transept**. Injuries close to the heads of the wooden beams, sliding of the beams - Disconnections between the kerb and masonry - Significant movements of the roof covering. (20)
- **Roofing elements: apse**. Injuries close to the heads of the wooden beams, sliding of the beams - Disconnections between the kerb and masonry - Significant movements of the roof covering (21).
- **Overturning of the chapels.** Detachment of the front wall from the side walls. (22)
- **Shear mechanisms in chapel walls.** Inclined injuries (single or crossed) - Injuries at of wall discontinuities. (23)
- **Vaults of the chapels.** Lesions in the vaults or disconnections from the side walls. (24)
- **Interactions in the vicinity of irregularities plano-altimetrical irregularities.** Movement at construction discontinuities - Injuries in masonry by hammering. (25)
- **Projections (sail, spires, pinnacles, statues)**. Evidence of permanent rotation or sliding – Injuries. (26)
- **Bell tower**. Injuries near the detachment from the body of the church - Shear or sliding - Vertical or curved injuries (ejection of one or more corners). (27)
- **Bell cell**. Injuries in the arches - Rotations or sliding of the piers. (28)

The following figures, Figure 2-2, Figure 2-3 and Figure 2-4 extracted from the "Guidelines for evaluation and reduction of seismic risk of cultural heritage" give a more exhaustive understanding of the above-mentioned mechanisms.

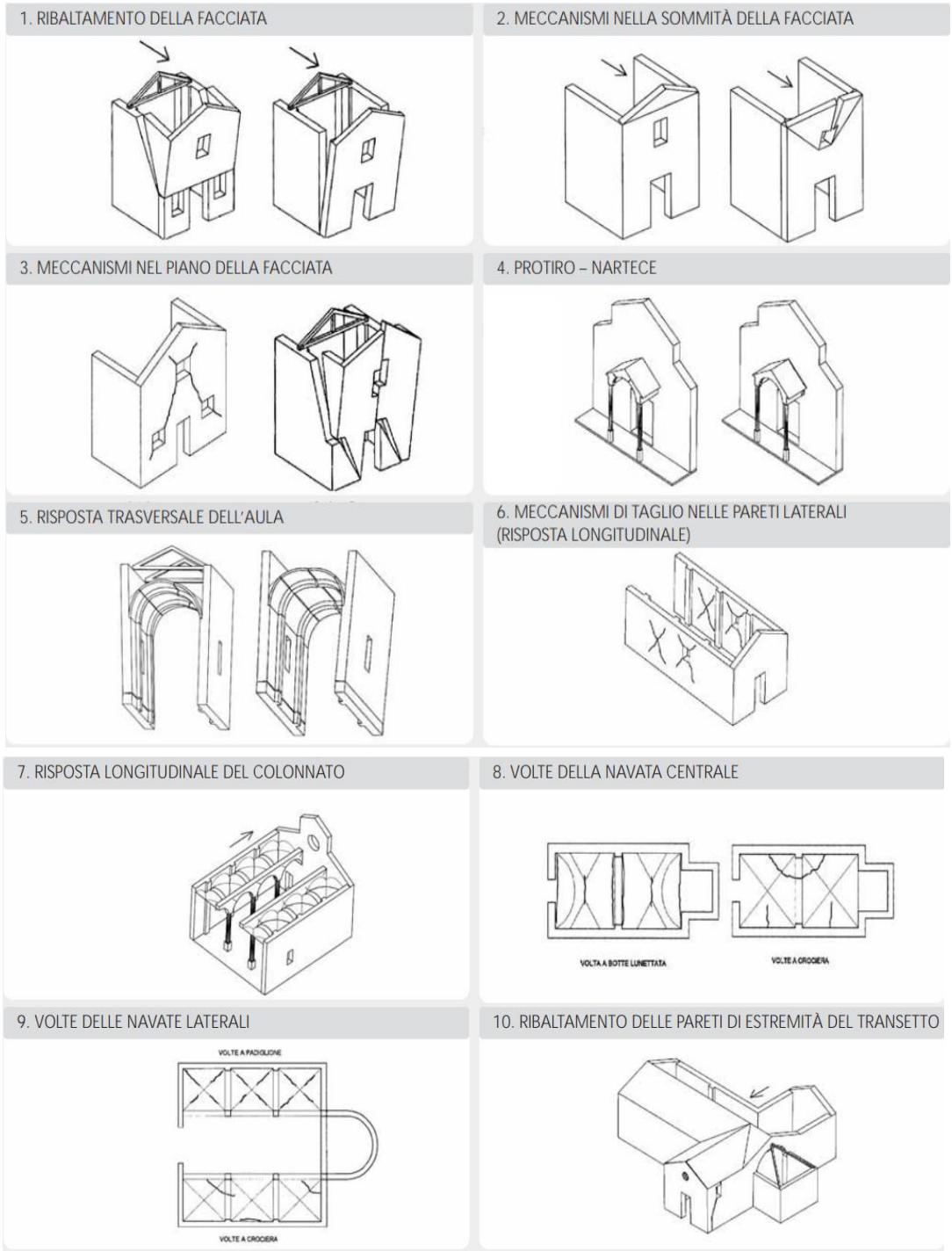


Figure 2-2. Collapse mechanisms extracted from the Annex C of the "Guidelines for evaluation and reduction of seismic risk of cultural heritage".

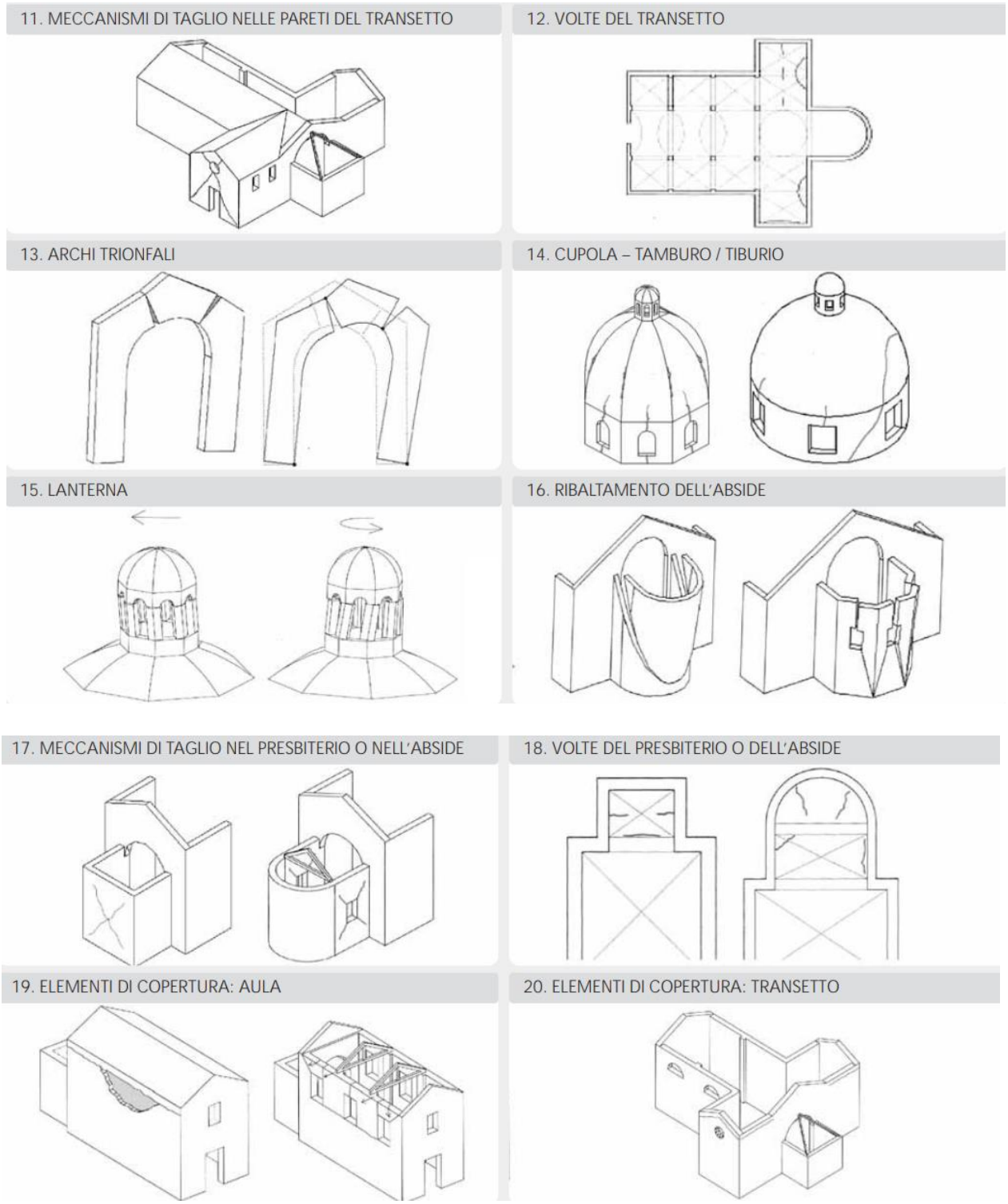


Figure 2-3. Collapse mechanisms extracted from the Annex C of the "Guidelines for evaluation and reduction of seismic risk of cultural heritage".

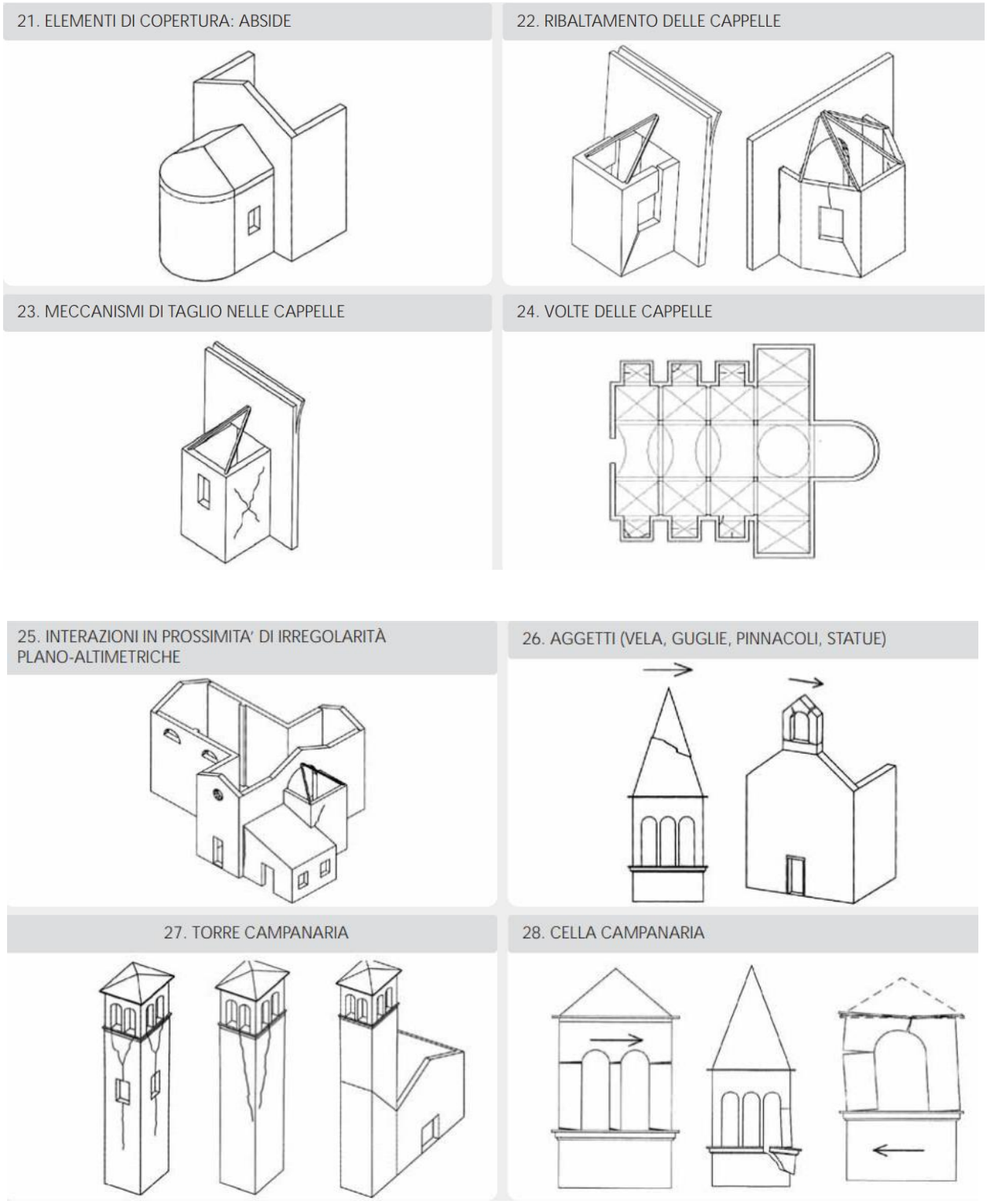


Figure 2-4. Collapse mechanisms extracted from the Annex C of the "Guidelines for evaluation and reduction of seismic risk of cultural heritage".

Of the 28 possible damage mechanisms defined by the "Guidelines for evaluation and reduction of seismic risk of cultural heritage" [1], only the following are likely to occur in the church under study:

- **Overturning of the façade**. (1)
- **Mechanisms at the top of the façade**. (2)
- **Mechanisms in the plane of the façade**. (3)
- **Transverse response of the hall**. (5)
- **Shear mechanisms in the side walls (longitudinal response)**. (6)
- **Longitudinal response of the colonnade**. (7)
- **Central nave vaults**. (8)
- **Lateral nave vaults**. (9)
- **Overturning of the apse**. (16)
- **Shear mechanisms in the presbytery or apse**. (17)
- **Presbytery or apse vaults**. (18)
- **Roofing elements: hall**. (19)
- **Roofing elements: apse**. (21)
- **Interactions in the vicinity of irregularities plano-altimetrical irregularities.** (25)
- **Projections (sail, spires, pinnacles, statues)**. (26)
- **Bell tower**. (27)
- **Bell cell**. (28)

Then, for the 17 possible collapse mechanisms in the church, the values to be attributed to the anti-seismic restraints and vulnerability indicators must be chosen. It is necessary to assign a score from 1 to 3 for every detected control indicator or vulnerability indicator.

By analyzing Table 2-12 , it is possible to determine the values of **vki** and **vkp** to use in the Equation 1 for vulnerability index calculation.

| **Overturning of the façade ( 1)** | $\rho_k = 1$ |
|---|---|
| **Earthquake-proofing** | Efficiency |
| Presence of longitudinal chains. | 0 |
| Presence of effective contrasting elements (buttresses, leaning bodies, other buildings). | 1 |
| Good quality interlocking between the façade and the walls of the nave. | 0 |
| **Vulnerability indicators** | Severity |
| Presence of pushing elements (roof struts, vaults, arches). | 3 |
| Presence of large openings in the side walls near the cantonal. | 0 |

| **Mechanisms at the top of the façade ( 2 )** | $\rho_k = 1$ |
|---|---|
| **Earthquake-proofing** | Efficiency |
| Presence of point connections with roof elements | 0 |
| Presence of roof bracing | 0 |
| Presence of lightweight kerbs (reticulated metal, reinforced masonry, other). | 0 |
| **Vulnerability indicators** | Severity |
| Presence of large openings | 1 |
| The presence of a sail top of great size and weight. | 3 |
| Rigid kerbs, reinforced concrete ridge beam, heavy reinforced concrete roofing. | 0 |

| **Mechanisms in the plane of the façade ( 3 )** | $\rho_k = 1$ |
|---|---|
| **Earthquake-proofing** | Efficiency |
| Presence of a chain in the counter facade | 3 |
| Lateral contrast provided by adjoining bodies, in other words church embedded in aggregate. | 1 |
| **Vulnerability indicators** | Severity |
| Presence of large or numerous openings (even if plugged) | 2 |
| High slenderness (height/width ratio) | 0 |

| **Transverse response of the hall ( 5 )** | $\rho_k = 1$ |
|---|---|
| **Earthquake-proofing** | Efficiency |
| Presence of external pilasters or buttresses. | 0 |
| Presence of adjacent outbuildings. | 2 |
| Presence of transverse chain. | 3 |
| **Vulnerability indicators** | Severity |
| Presence of walls with high slenderness. | 0 |
| The presence of vaults and arches. | 3 |

| **Shear mechanisms in the side walls (longitudinal response) ( 6 )** | $\rho_k = 1$ |
|---|---|
| **Earthquake-proofing** | Efficiency |
| Uniform masonry (one construction phase) and good quality. | 1 |
| Presence of good lintels in openings. | 0 |
| Presence of lightweight kerbs (reticulated metal, reinforced masonry, other). | 0 |
| **Vulnerability indicators** | Severity |
| Presence of large openings or large areas with masonry of limited thickness. | 0 |
| Very rigid reinforced concrete kerbs, heavy reinforced concrete roofing. | 0 |

| **Longitudinal response of the colonnade. ( 7 )** | $\rho_k = 1$ |
|---|---|
| **Earthquake-proofing** | Efficiency |
| Presence of longitudinal chains | 0 |
| Presence of buttresses in the façade | 0 |
| **Vulnerability indicators** | Severity |
| The presence of heavy vaults in the nave. | 3 |
| Heavy concrete roofing, reinforced caps of significant thickness in the vaults. | 0 |

| **Central nave vaults. ( 8 )** | $\rho_k = 1$ |
|---|---|
| **Earthquake-proofing** | Efficiency |
| Presence of chains in effective position. | 2 |
| Presenza di rinfianchi o frenelli. | 0 |
| **Vulnerability indicators** | Severity |
| Presence of concentrated loads transmitted by the roof | 3 |
| Sheet vaults, especially on large spans. | 0 |
| Presence of fanlights or interruptions and irregularities in the profile of the vaults. | 3 |

| **Lateral nave vaults. ( 9 )** | $\rho_k = 1$ |
|---|---|
| **Earthquake-proofing** | Efficiency |
| Presence of chains in effective position. | 2 |
| Presenza di rinfianchi o frenelli. | 0 |
| **Vulnerability indicators** | Severity |
| Presence of concentrated loads transmitted by the roof | 3 |
| Sheet vaults, especially on large spans. | 0 |
| Presence of fanlights or interruptions and irregularities in the profile of the vaults. | 3 |

| **Overturning of the apse. ( 16 )** | $\boldsymbol{\rho_k = 0.5}$ |
|---|---|
| **Earthquake-proofing** | Efficiency |
| Presence of hoops (semi-circular and polygonal) or chains (rectangular). | 0 |
| Presence of effective counteracting elements (buttresses, leaning bodies). | 0 |
| The presence of braced, non-pushing roofing. | 0 |
| **Vulnerability indicators** | Severity |
| Presence of severe weakening due to the presence of openings (even plugged) in the walls. | 1 |
| Presence of pushing vaults. | 3 |
| Rigid kerbs, heavy roofing, reinforced concrete struts. | 0 |

| **Shear mechanisms in the presbytery or apse. ( 17 )** | $\boldsymbol{\rho_k = 0.5}$ |
|---|---|
| **Earthquake-proofing** | Efficiency |
| Uniform masonry (one construction phase) and good quality. | 1 |
| Presence of good lintels in openings. | 0 |
| Presence of lightweight kerbs (reticulated metal, reinforced masonry, other). | 0 |
| **Vulnerability indicators** | Severity |
| Presence of large openings or large areas with masonry of limited thickness. | 0 |
| Very rigid reinforced concrete kerbs, heavy reinforced concrete roofing. | 0 |

| **Presbytery or apse vaults. ( 18 )** | $\boldsymbol{\rho_k = 0.5}$ |
|---|---|
| **Earthquake-proofing** | Efficiency |
| Presence of chains in effective position. | 2 |
| Presenza di rinfianchi o frenelli. | 0 |
| **Vulnerability indicators** | Severity |
| Presence of concentrated loads transmitted by the roof. | 3 |
| Sheet vaults, especially on large spans. | 0 |
| Presence of fanlights or interruptions and irregularities in the profile of the vaults. | 2 |

| **Roofing elements: hall. ( 19 )** | $\boldsymbol{\rho_k = 0.5}$ |
|---|---|
| **Earthquake-proofing** | Efficiency |
| Presenza di cordoli leggeri (metallici reticolari, muratura armata, altro) | 0 |
| Presence of beam connections to masonry. | 0 |
| The presence of good connections between the roof frame elements roof. | 0 |
| **Vulnerability indicators** | Severity |
| Presence of statically pushing roofing. | 3 |
| Presence of rigid kerbs, heavy covering. | 0 |
| **Roofing elements: apse. ( 21 )** | $\boldsymbol{\rho_k = 0.5}$ |
| **Earthquake-proofing** | Efficiency |
| Presenza di cordoli leggeri (metallici reticolari, muratura armata, altro) | 0 |
| Presence of beam connections to masonry. | 0 |
| The presence of good connections between the roof frame elements roof. | 0 |
| **Vulnerability indicators** | Severity |
| Presence of statically pushing roofing. | 3 |

| | |
|---|---|
| Presence of rigid kerbs, heavy covering. | 0 |

| **Interactions in the vicinity of irregularities plano-altimetrical irregularities ( 25 )** | $\rho_k = 1$ |
|---|---|
| **Earthquake-proofing** | Efficiency |
| Presence of an adequate connection between masonry of different phases different phases. | 0 |
| Presence of connecting chains. | 0 |
| **Vulnerability indicators** | Severity |
| Presence of a high stiffness difference between the two bodies. | 3 |
| Possibility of concentrated actions transmitted by the connection. | 0 |

| **Projections (sail, spires, pinnacles, statues). ( 26 )** | $\rho_k = 0.5$ |
|---|---|
| **Earthquake-proofing** | Efficiency |
| Presence of masonry connection pins or retaining elements. | 0 |
| Elements of limited importance and size. | 1 |
| Monolithic masonry (with square ashlars or otherwise of good quality). | 0 |
| **Vulnerability indicators** | Severity |
| Elements of high slenderness. | 1 |
| Supporting the underlying masonry in falsework | 0 |
| Asymmetrical position in relation to the underlying element (especially if the overhang has considerable mass). | 0 |

| **Bell tower. ( 27 )** | $\boldsymbol{\rho_k = 1}$ |
|---|---|
| **Earthquake-proofing** | Efficiency |
| Uniform masonry (one construction phase) and good quality. | 1 |
| Presence of chains at different orders. | 0 |
| The presence of adequate distance from church walls (if adjacent). | 0 |
| The presence good connection with church walls (if incorporated). | 0 |
| **Vulnerability indicators** | Severity |
| Presence of significant openings on several levels. | 0 |
| Asymmetrical constraint on masonry at base (incorporated tower). | 2 |
| Irregular ground support of the tower (presence of arches on some sides, cantilevered walls). | 0 |

| **Bell cell. ( 28 )** | $\boldsymbol{\rho_k = 1}$ |
|---|---|
| **Earthquake-proofing** | Efficiency |
| The presence of squat piers and/or arches of reduced span. | 0 |
| Presence of chains or rims. | 0 |
| **Vulnerability indicators** | Severity |
| Presence of heavy cover or other significant masses. | 2 |
| Presence of pushing cover. | 0 |

Once each mechanism has been analyzed, the results obtained can be summarized in the Table 2-13. Whereas already mentioned above, $v_{ki}$ is related with the vulnerability indicators and $v_{kp}$ is related with the earthquake proofing that the structure has. Furthermore, from the Table 2-13. it can be noted that the mechanisms that tend to increase vulnerability, i.e. those that cause the index to increase are: Central nave vaults ( 8 ), Lateral nave vaults ( 9 ) and Overturning of the apse ( 16 ).

| Mechanism(k-th) | $\rho_K$ | $\sum v_{ki}$ | $\sum v_{kp}$ | $\Delta v$ |
|---|---|---|---|---|
| 1 | 1 | 3 | 2 | 1 |
| 2 | 1 | 4 | 0 | 4 |
| 3 | 1 | 2 | 4 | -2 |
| 5 | 1 | 3 | 5 | -2 |
| 6 | 1 | 0 | 1 | -1 |
| 7 | 1 | 3 | 0 | 3 |
| 8 | 1 | 6 | 2 | 4 |
| 9 | 1 | 6 | 2 | 4 |
| 16 | 0.5 | 4 | 0 | 4 |
| 17 | 0.5 | 0 | 1 | -1 |
| 18 | 0.5 | 5 | 2 | 3 |
| 19 | 0.5 | 3 | 0 | 3 |
| 21 | 0.5 | 3 | 0 | 3 |
| 25 | 1 | 3 | 0 | 3 |
| 26 | 0.5 | 1 | 1 | 0 |
| 27 | 1 | 2 | 1 | 1 |
| 28 | 1 | 2 | 0 | 2 |

Table 2-13. Summary of the various mechanisms with their respective vulnerability index and proofing index.

Applying the Equation 6, the vulnerability index obtained is equal to **0.774.** Once calculated the vulnerability index the "Guidelines for evaluation and reduction of seismic risk of cultural heritage", also provides the equations to be used for the calculation of ground acceleration for the different limit states. These equations are:

$$a_{SLD}S = 0.025 \times 1.8^{2.75-3.44\, i_v} \tag{7}$$

$$a_{SLV}S = 0.025 \times 1.8^{5.1-3.44\, i_v} \tag{8}$$

By replacing in the equations 6 and 7 with the value of the vulnerability index obtained, the accelerations obtained as results are:

$$a_{SLD}S = 0.0263\, g$$

$$a_{SLV}S = 0.1048\, g$$

The return periods corresponding to the limit states considered (SLD and SLV) can be obtained by interpolating between the known values for the predefined return periods. The regulation gives the following formula.

$$T_{SLV} = T_{R1} \times 10^{\log\left(\frac{T_{R2}}{T_{R1}}\right)\log\left(\frac{a_{SLV}S}{FCa_1S_1}\right)\log\left(\frac{a_2S_2}{a_1S_1}\right)} \quad (9)$$

Where:

- TR1 and TR2 are the return periods for which the seismic hazard is provided, within which TSLV is included.
- $a_1S_1$ and $a_2S_2$ are the corresponding values of the peak acceleration on rigid ground and the coefficient considering the subsoil category and the topographical conditions.
- FC is the confidence factor, defined according to the level of in-depth knowledge.

Table 2-14 summarizes the parameters to be used in the formula 8, and at the end the return periods are obtained.

| | |
|---|---|
| $T_{R1}$ | 50 |
| $T_{R2}$ | 475 |
| $a_{SLD}S$ | 0.02633 |
| $a_{SLV}S$ | 0.10479 |
| FC | 1.2 |
| $a_1S_1$ | 0.099 |
| $a_2S_2$ | 0.245 |
| $T_{SLV}$ | 452 |
| $T_{SLD}$ | 28 |

Table 2-14. Calculation of return periods corresponding to the attainment of limit states SLV and SLD.

Given all these quantities, it is now possible to calculate the seismic safety index IS through the following formulations:

$$I_{S,SLV} = \frac{T_{SLV}}{T_{R,SLV}} = \frac{452\ \text{years}}{475} = 0.953 \tag{10}$$

$$I_{S,SLD} = \frac{T_{SLD}}{T_{R,SLD}} = \frac{28\ \text{years}}{50\ \text{years}} = 0.560 \tag{11}$$

In conclusion, after having analyzed the results of the indexes, it can be said that both are lower than 1, it means that in presence of an earthquake the structural components will suffer significant damage with a huge loss of stiffness in relation to horizontal movements, that it is the case of the life sustaining limit state. While in the case of the Damage limit state (SLD), the building will suffer damage such that it does not put users at risk and does not significantly compromise the capacity for resistance and rigidity against vertical and horizontal actions, remaining immediately usable even if part of the equipment is interrupted.

# 3

# Models of the church

This chapter aims to develop the various models that will be carried out of the church, starting with the geometric model and then with the numerical model.

The concept of geometric modelling refers to the set of methods used to define the shape and other characteristics of objects. On the other hand, the numerical model is related with the Finite Element Method, that is a numerical method used to perform a finite element analysis (FEA) of any given physical phenomenon of a structure in order to determine how it will behave in the future or how it actually behaves. As an approximation method, FEM is one that subdivides a complex space or domain into a number of small, countable, and finite number of pieces (hence the name finite elements) whose behavior can be described by a relatively simple equation that fits the space or domain. [2]

## 3.1 Geometrical Models

From the information gathered and received from different sources, it was possible to construct two geometrical models of the structure.

The first geometrical model, was performed using the software AutoCAD. An AutoCAD program is a computer-aided design (CAD) program that is used for the creation of both 2-D and 3-D designs and drafting. It was one of the first CAD programs to be developed and marketed by a company called Autodesk Inc. , also it was one of the first CAD programs designed to run on personal computers. [15]

As a first point of departure, the plans already obtained were used to draw the middle line of each wall, trying to uniform the thicknesses, which will be of vital importance later on in the numerical model. With a pink dashed line, the middle line of the walls is identified in the Figure 3-1. Then, on the basis of the sections obtained from old plans, from photographic dot plotting and from other sources, it was possible to determine the height of the walls that make up the church, the bell tower, and the inclination of the roofs. This geometry was captured in a 3D model, from which axonometric views were obtained and are shown in the Figure 3-2 and Figure 3-3.

It is important to mention that this model is made up exclusively of lines, which interconnected with each other form a geometry, but these lines do not contain relevant information of the structure, it is only a geometric representation.

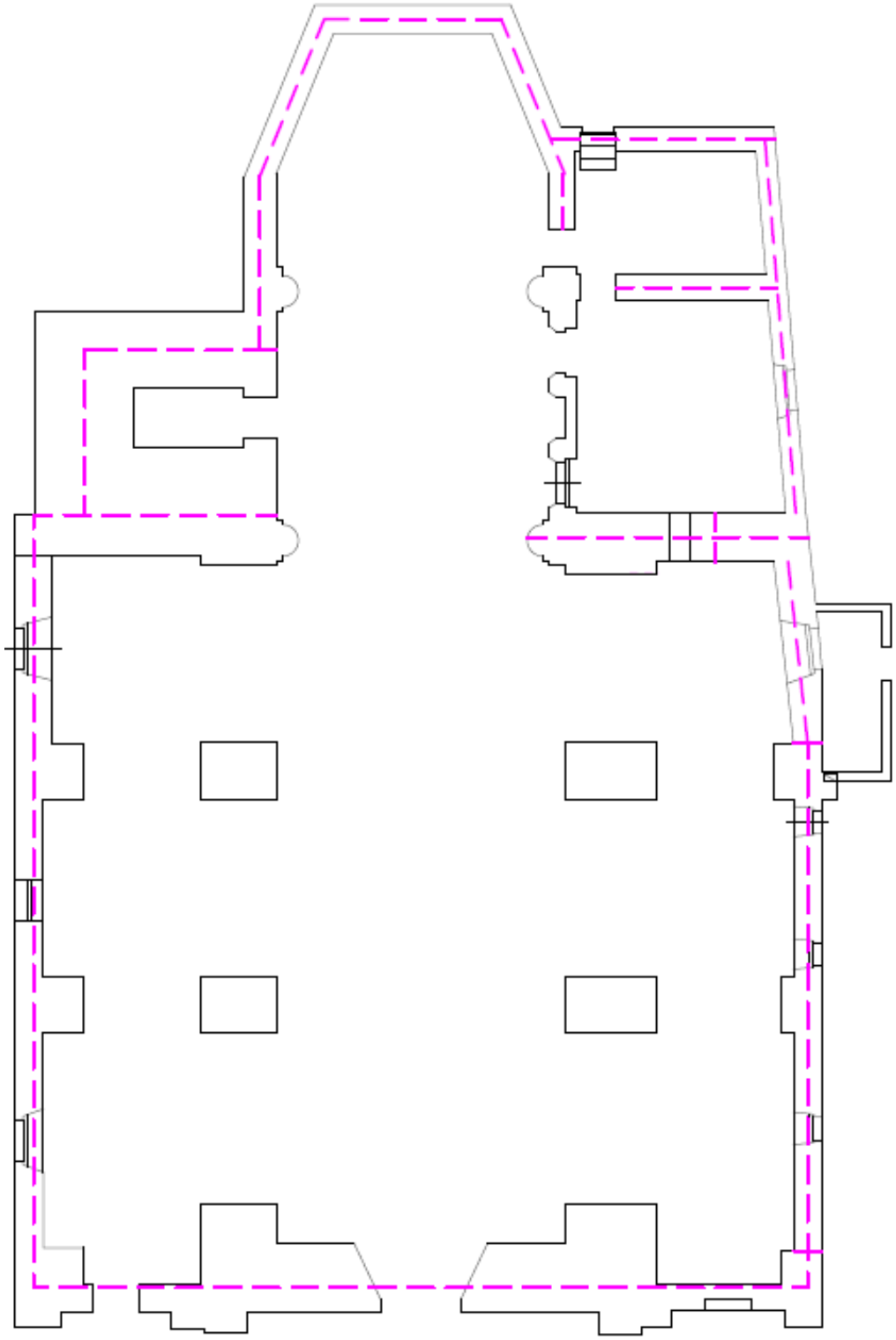

Figure 3-1. Structural plan with midline identification.

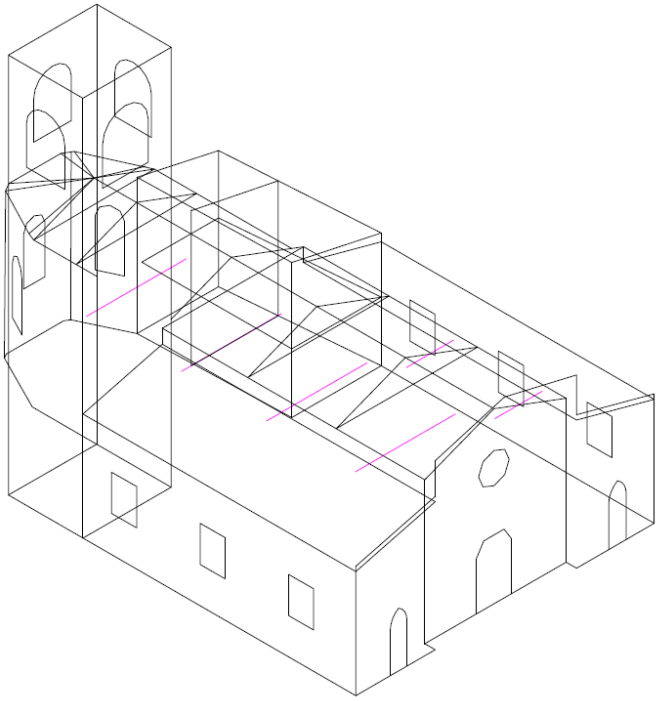

Figure 3-2. Axonometric view N°1.

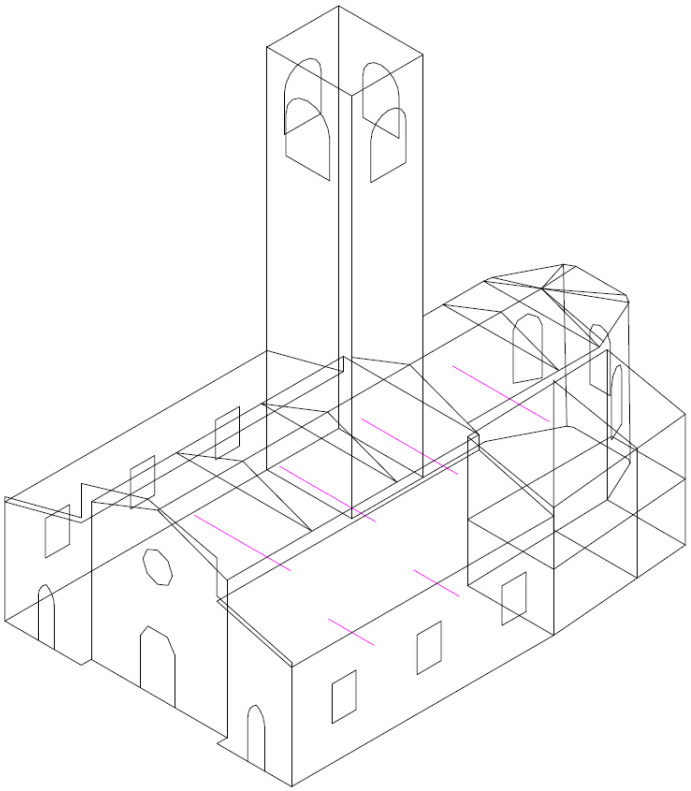

Figure 3-3. Axonometric view N°2.

## 3.2 Finite element method

The first step in thinking about the finite element model was to build a geometrical model that would then allow the application of this calculation methodology. FEA NX software was used for this purpose. Based on the finite element solution methodology, FEA NX has been developed for the simulation of advanced nonlinear and detailed analysis for civil and structural engineering applications based on advanced nonlinear analysis. The software has state-of-the-art modelling tools and, thanks to its compatibility with other formats, very advanced modelling levels can be achieved in a short time. The powerful meshing and solver allow the finite element model that best represents the previously created solid geometry to be accurately represented and solved.

The use of this program was mainly aimed at the creation of the complex geometries of the structure, especially the vaults. The initial step within the software was to import the geometric model previously made by Autocad. The interoperability between the two programs is medium level, since the information is not lost, i.e., the import is complete, but there are problems in the sense that DXF files created on AutoCAD do not have tolerance that can determine the connectivity between endpoints. Although edges may seem connected to the naked eye, they maybe intersected or not connected after import, for this reason was necessary to check the edges of the AutoCAD DXF file before importing.

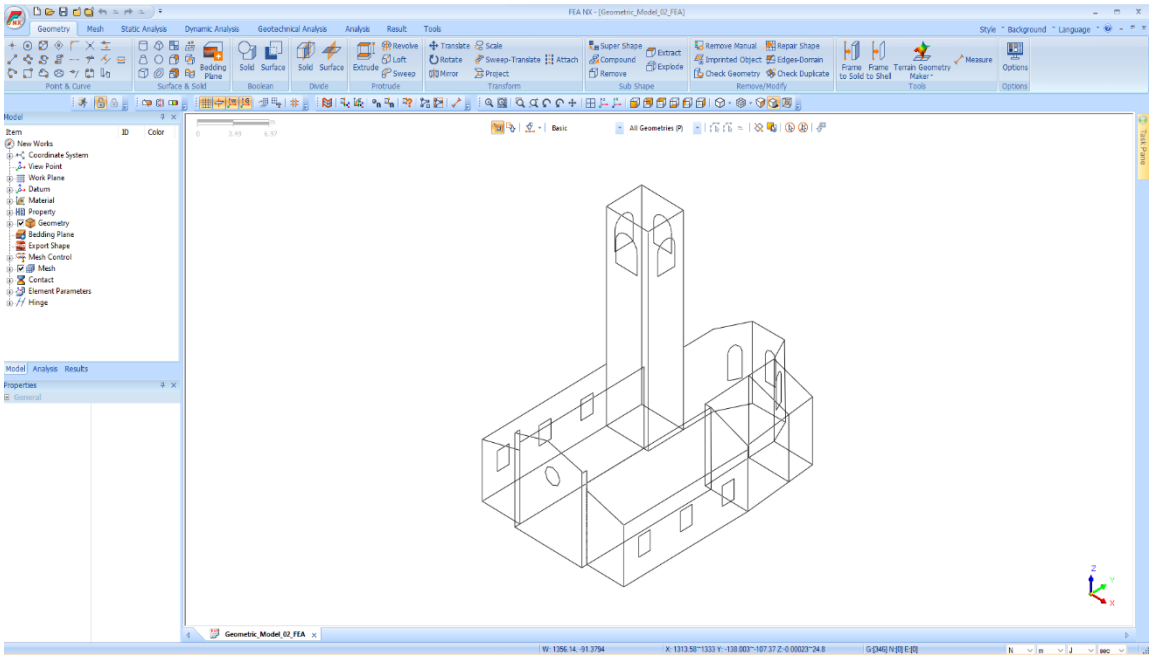

Figure 3-4. Autocad 3D model imported into FEA NX.

For the reasons listed above, it was not convenient to work on the 3D model generated in AutoCAD. Therefore, what was done was to import the structural plan with midline identification, the geometry was mapped out using the tools of the software itself, taking the measurements provided by the 3D model as a reference.

The next step was the creation of the walls, starting with the perimeter walls and then the inner walls. These were created with the command “Make Face” (Geometry → Surface & Solid → Make Face), have been realized two-dimensional plane surfaces by selecting the contour lines within which the created the surface considering that there are no restrictions on the number of lines selected. In some cases, the problem was related to the fact that the lines did not intersect each other and in many cases, it was necessary to recreate these lines with the command “Line” (Geometry → Point & Curve → Line). The tolerance value, which serves to verify that the lines belong to the same plane, has been 0.0001 m.

At the same time, the presence of the openings was considered in the creation of the walls, simply outlining the parts to be made into a forum. The result obtained is represented by the Figure 3-5.

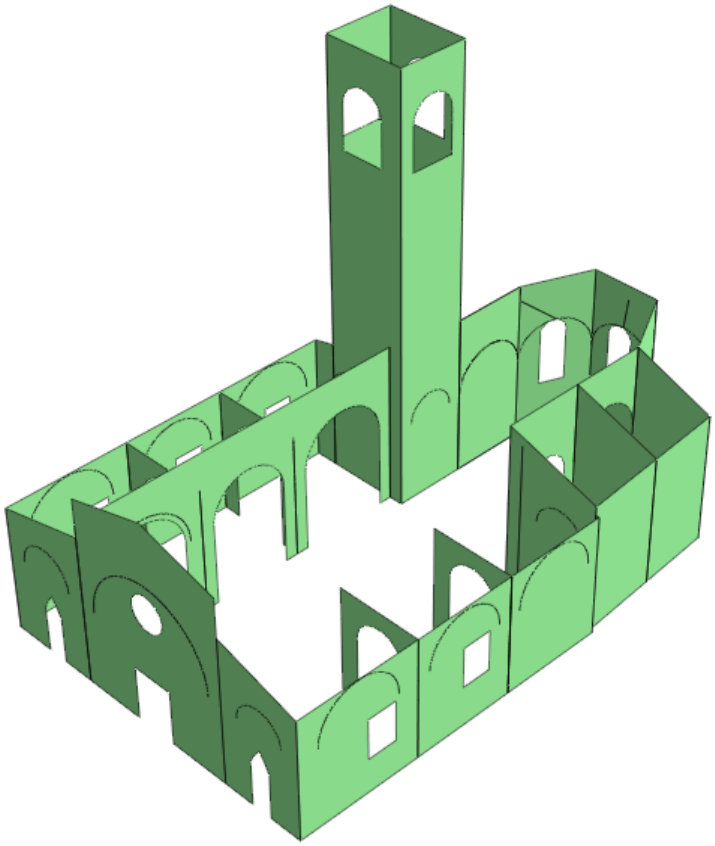

Figure 3-5 · Geometrical model of the walls.

After defining the perimeter and interior walls, the next step was the design of the vaults, starting with the vaults of the lateral aisle. As was mentioned in the previous paragraphs, the type of vaults present in the construction are cross vaults, that in the Italian language is *"volta a crociera"*. This type of structure is created by the intersection of two equal and orthogonal barrel vaults, at the intrados of which are two curved corners running from one corner to the opposite corner. In order to design the geometry, the dimensions in plan were taken, considering the columns and the walls that separate one nave from the other as support points for the vaults, then the arches were designed. The reasoning followed in order to realize the geometry can be seen in the Figure 3-6.

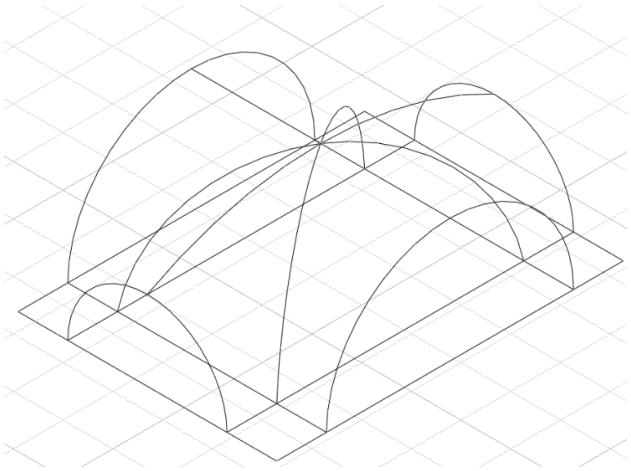

Figure 3-6. Dimensions and arches of a lateral nave cross vault.

Once geometry was created, the next step was to create the surfaces, the creation was possible to define thanks to the intersection of the arcs with the lines that defined a surface. Each vault was generated by 8 surfaces, that all intersect at the upper point. The command used was the same as for the walls “Make Face”. Then, in order to obtain a coherent mesh, it was necessary to join these different surfaces in order to create a single surface. This was done with the command “Boolean Surface”, where the command sew was selected.

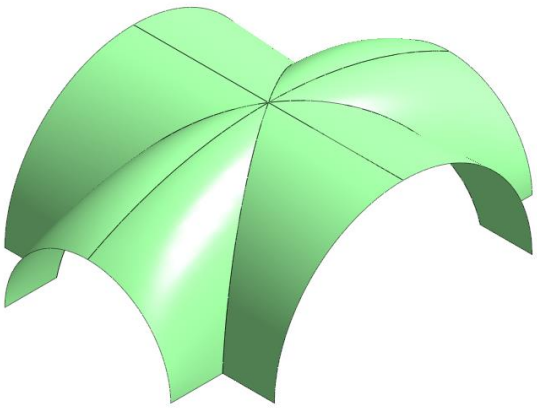

Figure 3-7. Geometrical model of the cross vaults on the lateral aisles.

The vaults of the central aisle were created following the same procedure, because of the fact that they are also considered to be cross vaults.

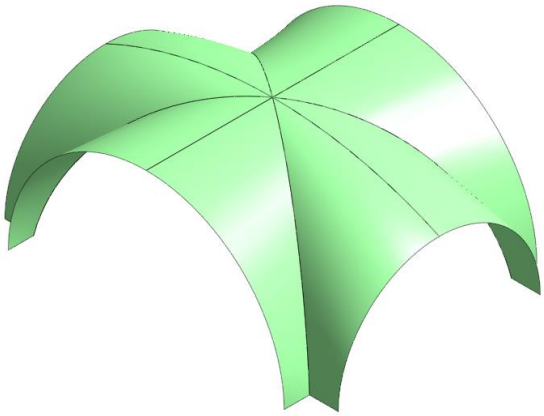

Figure 3-8. Geometrical model of the cross vaults on the central aisles.

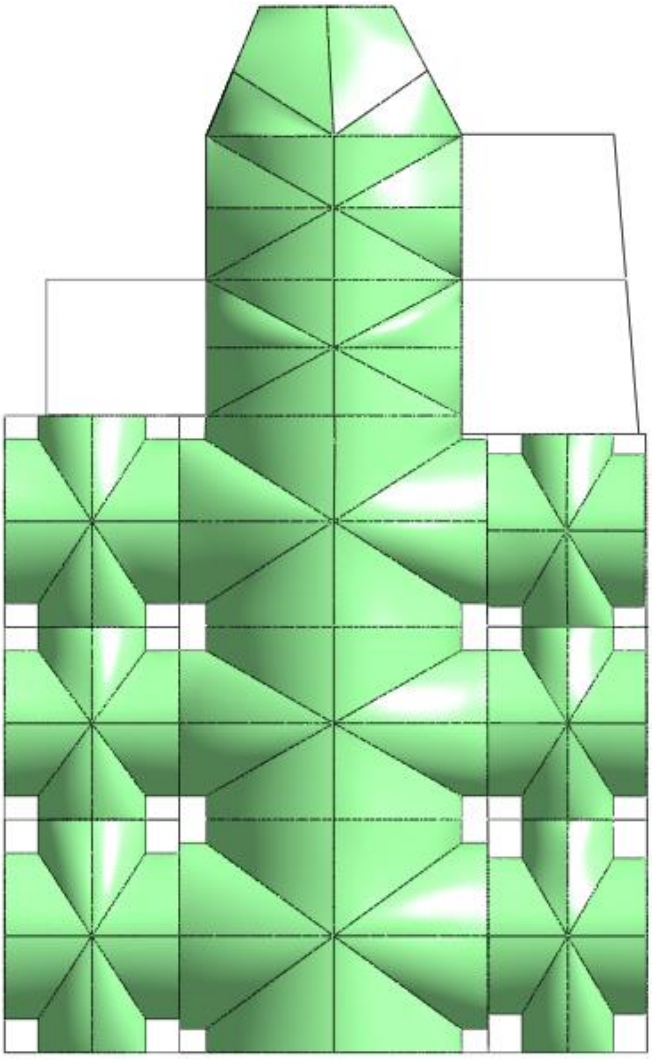

Figure 3-9. Plan view of the model after the addition of the vaults.

Then, after having made the vaults, the model obtained is represented by the Figure 3-10.

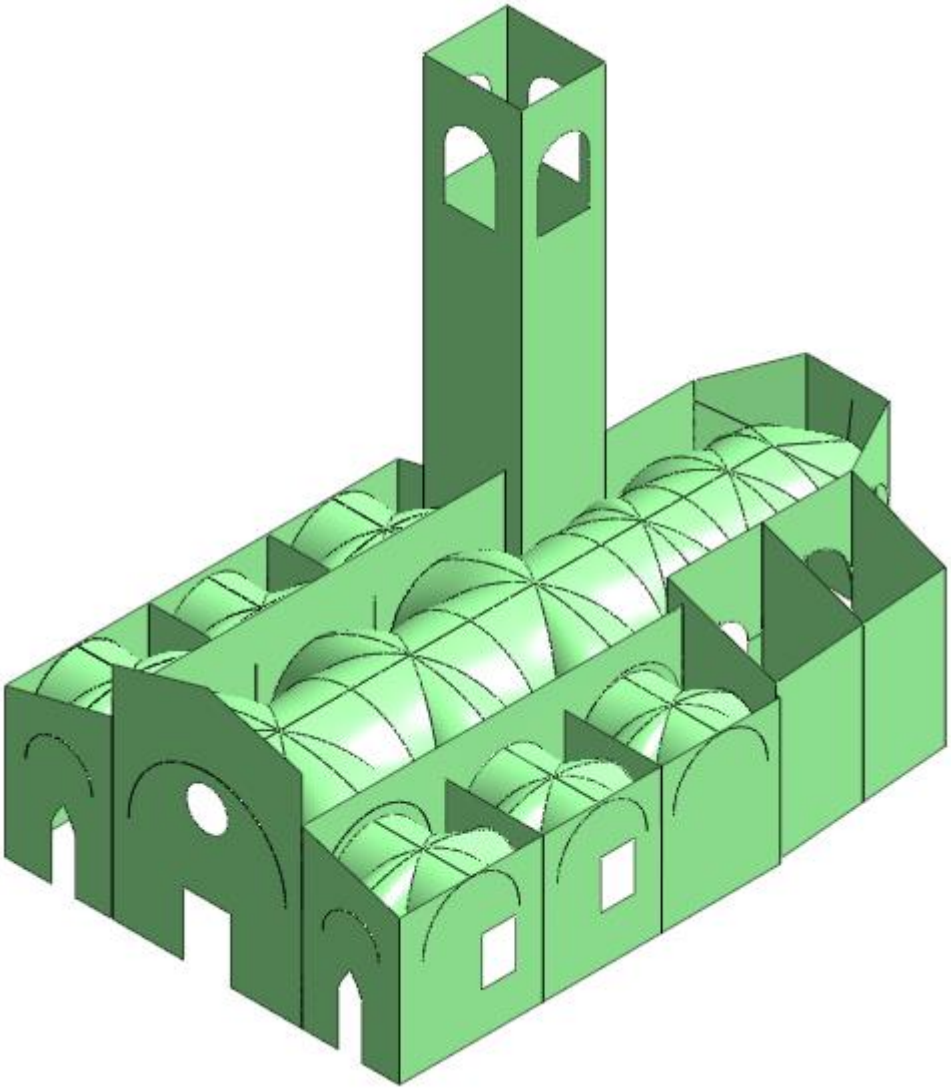

Figure 3-10. Complete model of the church.

As it is possible to observe in the geometric model made and presented in the previous figures, all the elements present in the figure are two-dimensional elements, this implies that one of the sizes that make up these elements is much smaller with respect to the others, and in all cases this dimension is the thickness. It is known that two-dimensional elements can present three different types of behavior.

The first behavior is known as “Slab Behavior” in which each node of the element has two degrees of freedom, i.e., two translations in the plane of the element. It is used to represent plane stress states and the stressful actions lie in the plane of the element. It is an element with membrane rigidity and transmits only stresses in its plane.

The second is the “Plate Behavior” where each node of this element has three degrees of freedom, one translation orthogonal to the mean plane of the element and two rotations about the two axes belonging to the plane of the element. It is an element with flexural rigidity and transmits shear and bending stresses. The stress actions are orthogonal to the plane of the element.

The “Shell Behavior”, which is used for the modelling of elements such as walls, foundation slabs, footings, is characterized by the superposition of two plate and slab behavior mentioned before. It is an element with both flexural and membranous stiffness and can be used to reproduce the generic behavior of a plane structural element. Due to the above, the type of behavior adopted in the modelling of the structural elements, walls, and vaults, is shell behavior.

Once the structural characteristics of the elements under analysis are understood, the second phase of the modelling is carried out.

The second phase is the definition of the mesh, the representation of the essential elements for getting accurate results from an FEA model. In Finite Element Method, is necessary the creation of a mesh which splits the domain into a discrete number of elements for which the solution can be calculated. The data is then interpolated across the whole domain. To accurately discretize stress gradients, the mesh's elements must consider a variety of factors. Since the designs are better sampled across the physical domains, the solution is typically more accurate the smaller the mesh size. The trade-off is that longer solve times result from larger simulations as accuracy increases.

Before starting to define the mesh, it was necessary to define the material of which each element is composed and its thickness. As far as the material is concerned, its properties were inserted according to the material properties obtained in the chapter 1.5.

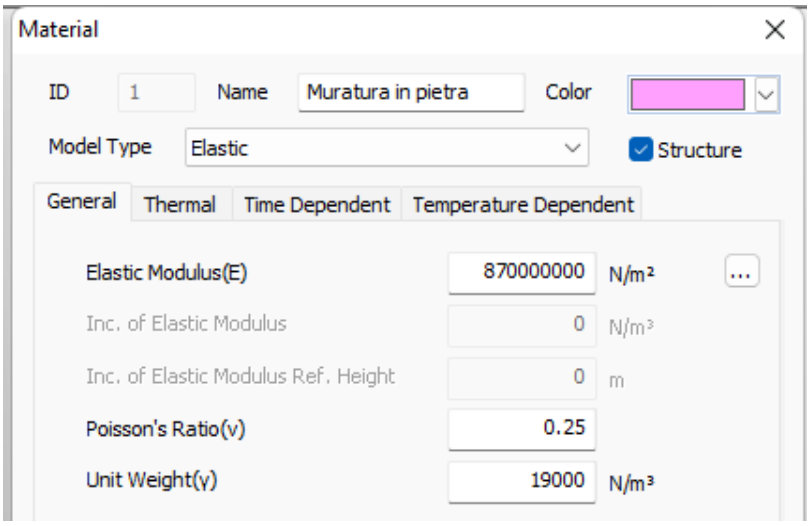


Figure 3-11. Mechanical properties assigned to "messy stone masonry".

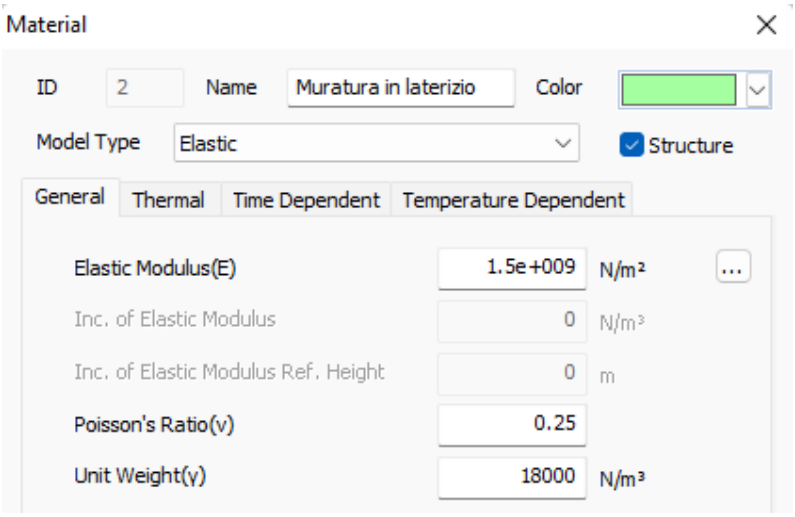


Figure 3-12. Mechanical properties assigned to “solid brick and cement mortar masonry”.

Considering the plan of the midline of the various walls, the different wall thicknesses were determined. The Figure 3-13 shows a dimensioned plan which allows the different thicknesses to be visualized.

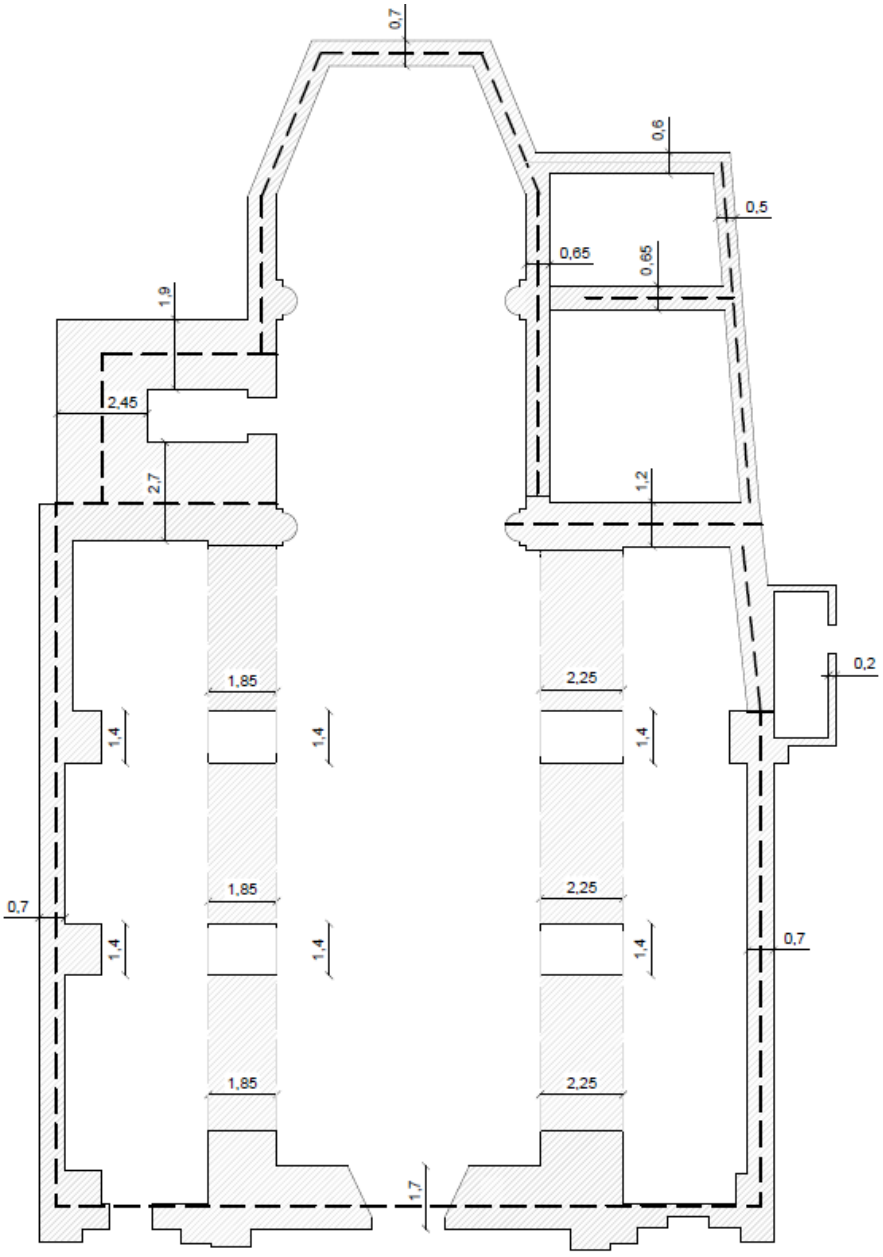


Figure 3-13. Thickness of the walls.

The process of meshing the structure was carried out after determining the thicknesses, materials, and geometry to be used, allowing for a seamless transition in the process. The software's powerful mesh generation capabilities made the process easier by automatically generating the desired mesh sizes. The selected meshing method was based on size, for the vaults  the mesh size chosen was 30 cm, while for

the walls, the mesh size was between 50 - 70 cm., this choice is justified by the fact of providing an aspect ratio" closest to 1.0. Therefore, great attention was given to the congruency of the mesh to ensure accurate analysis. Overall, the use of size-based meshing method with a set size of 30 cm and 50-70 cm allowed for an efficient and uniform meshing process to be carried out, providing a foundation for reliable structural analysis. The shows the final arrangement of the meshes in the structure.

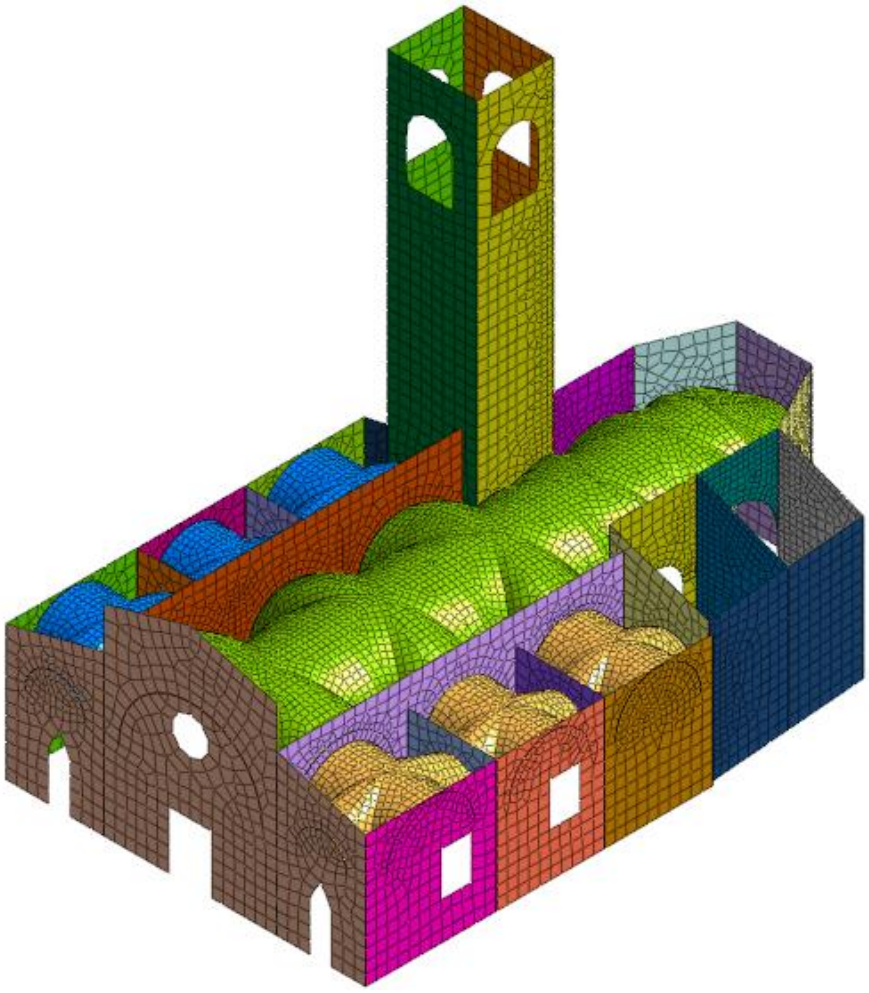

Figure 3-14. Structure's mesh.

Even though the software is very efficient when it is used to make the meshes, in some cases it was necessary to "fixed the mesh" to guarantee the congruence between the different parts of the structure. This operation was carried out in different ways, the main one was by printing the curve that defined each surface on the adjacent one, it was performed with the "Imprint" command, then using the tool "Size control", the imprinted edged was selected and divided in an interval length. In this way, when the meshing was done, the software automatically recognised that the mesh had to be resharpened in that area. Another method used was the "merge nodes" method, where

each mesh was checked in detail and in cases where adjacent nodes did not match, they were manually joined together. The most critical areas were the junctions between vaults and walls, where an inconsistent and unfair meshing could have led to incorrect results. Because of this, special attention was devoted to these cases.

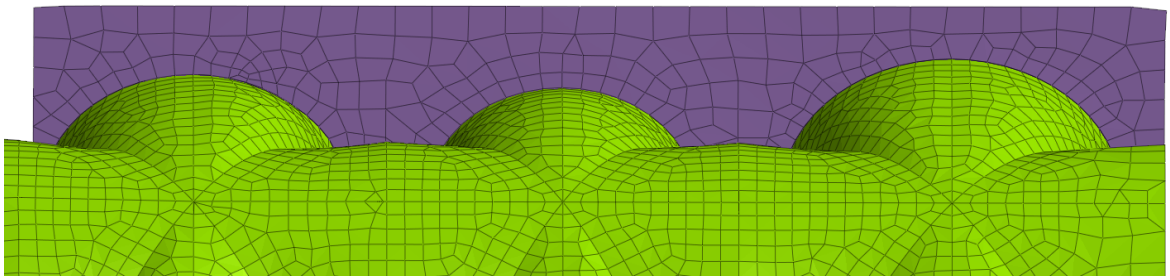

Figure 3-15. Joint detail between vaults and the central wall.

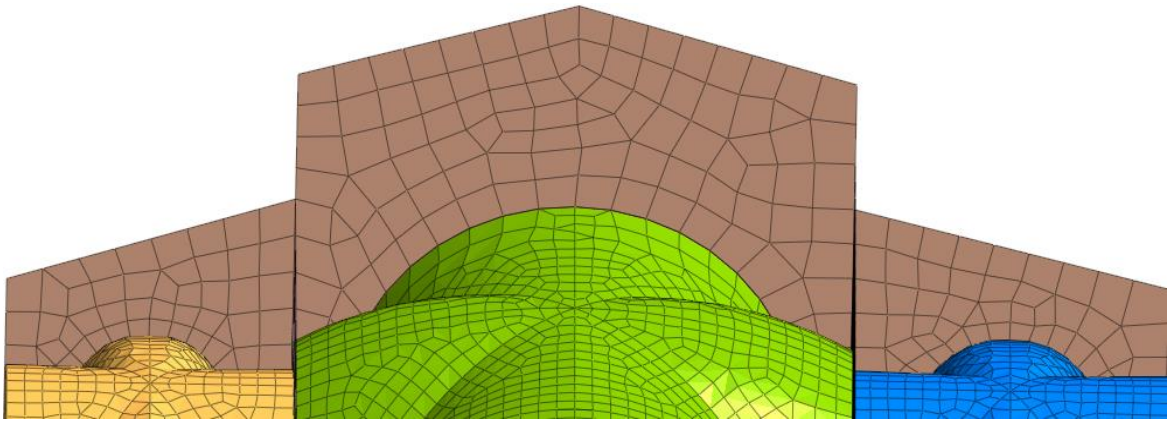

Figure 3-16. Detail of the junction between vaults and the façade wall.

After defining the mesh, the subsequent step was to export the generated FEA NX model to Midas Gen using an *.mgt file. Initially, the Midas software could not recognize this model due to poorly defined mesh elements with overlapping. These errors were quickly identified in the 'Analysis message window' of Midas Gen. Then, the errors were resolved, resulting in the final model being successfully imported into the software.

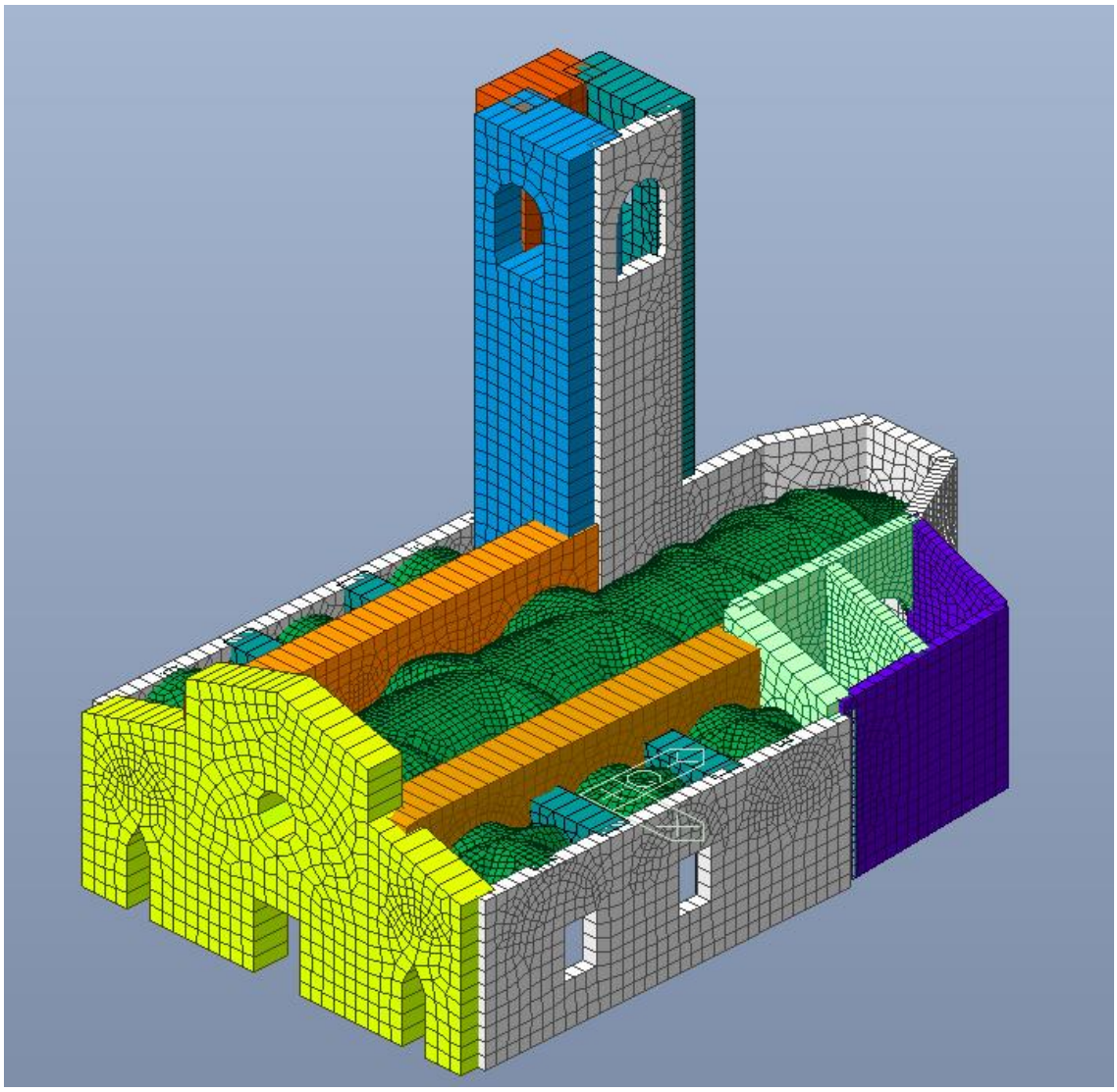

Figure 3-17. Result of the imported model in Midas Gen.

The first step within the software was the definition of the boundary conditions, these are characterized by not allowing the displacements at the base, it means that the displacements in x,y and z direction are restricted at the base of the structure. In the case of rotations, these were not restricted, as the walls can be overturned due to horizontal loads.

As specified in previous chapters, the various investigations that were carried out in the church reveal that the building has chains that fit between the walls of the side and central corridors, these chains are recognize as a structural intervention in order to give strength to the vaults. For the aforementioned reason, it was important to consider the presence of these elements in the FEM model. The chains were introduced in the Midas

model as “Tension Only” elements and its cross section is of 50 mm x 20 mm (rectangular section).

The roof of the structure was not considered in the modelling, as can be seen in the images. The choice to build the roof structure in a different model is justified by the fact that the roof does not have a bracing structure, because of this there was a possibility that when the seismic force was inserted into the model, parasitic modes of vibration with a very low excitation mass could occur.

For this reason, the roof was modelled separately, taking as a reference the existing documentation and drawings. Regarding the calculation, all loads relevant to the roof were assigned to this model, where the reactions were then determined and applied as point loads to the walls supporting the ceiling.

The figure Figure 3-18 shows the configuration in section of the roof, where it is possible to observe the different parts that compose it with their corresponding dimensions. Once the sections of these elements were recognized, the next step was to investigate the type of wood it was made of. Since the type of material was not known for certain, a type GL20h was adopted for the purposes of the calculation, which has the most severe resistance characteristics, thus being in safety's favor.

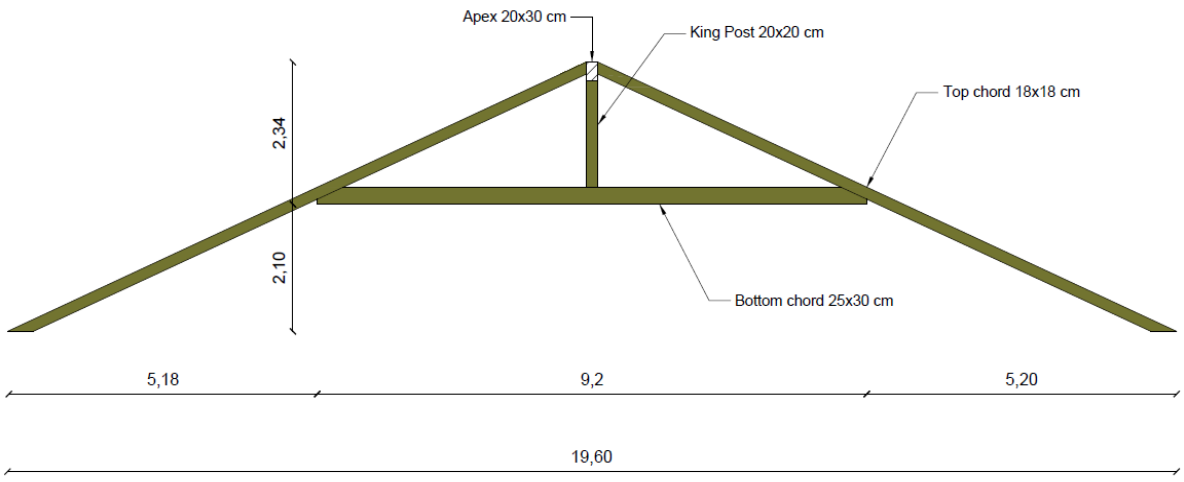


Figure 3-18. Configuration of the wood roof.

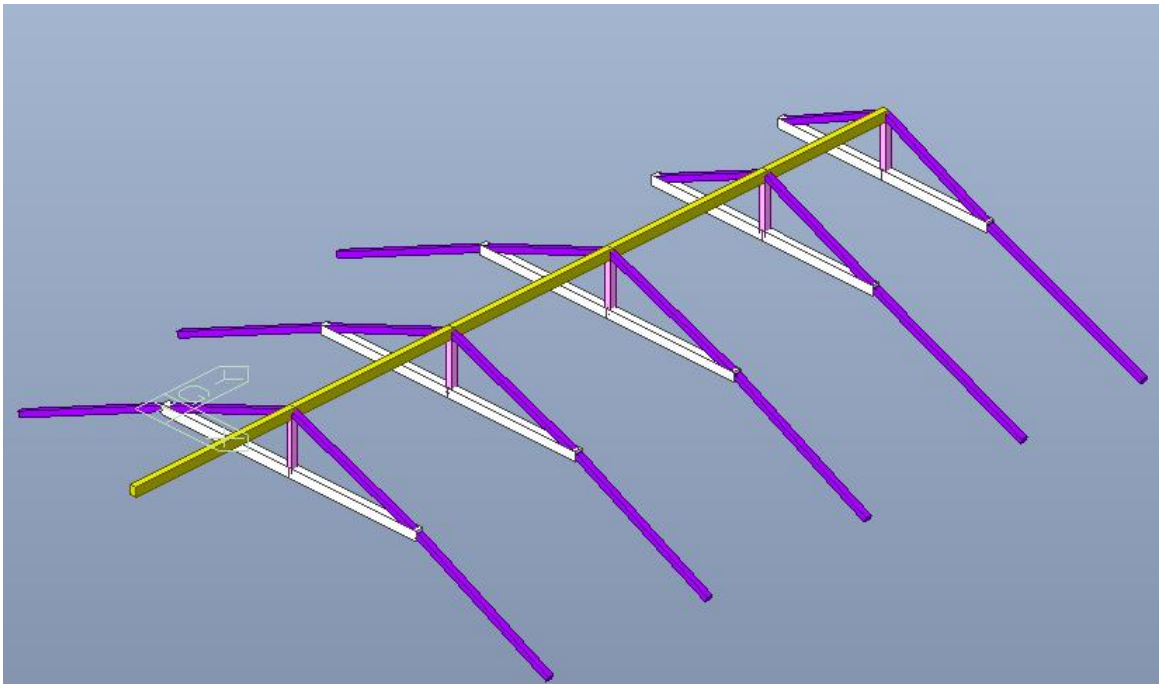

Figure 3-19. Calculation model of the roof -Midas gen.

The calculation model for the wooden roof of the church is shown in the Figure 3-19. As can be seen, the roof is not completely symmetrical, as it extends to the end in the right aisle, while in the left aisle it stops when it ends (intersection with the bell tower).

Existing buildings made of load- bearing masonry very often have roofs of the push-on type, this means that when it is subjected only to vertical loads, it generates a horizontal thrust on the perimeter walls on which it unloads. In this configuration, the horizontal thrust on the supporting perimeter walls increases as the weight of the roof increases and as its deformability increases. This means that a horizontal component due to roof thrust was considered in the analysis and for this reason, the roof boundary condition is one that allows for horizontal movements in one direction.

## 3.3 Analysis of the loads to be applied on the model.

The concept of load can be defined as the forces that cause stress, deformation, or accelerations. A structure or its components suffer stress or displacement as a result of these loads. When designing a structure or verifying the state of an existing building , various structural loads must be considered, such as dead loads, live loads, etc.

In the case of the building under analysis, the loads to be considered have been considered following the Eurocode 1: actions on structures, and also taking as reference the Italian regulation, “Norme techniche per le costruzioni” (NTC2018), which was of vital importance for the use of specific coefficients that depend on each country.

### 3.3.1 Permanent structural load.

The permanent structural loads depend on the self-weight of the materials and the geometric dimensions of the structural parts that make up the building. Since the correct characteristics were assigned to the materials during the modelling phase, Midas GEN was able to automatically assign the self-weight of the masonry elements.

As mentioned in previous chapters, in the cathedral two types of masonry can be identified, which have the weights indicated in the Table 2-1. In addition to the masonry material, the own wight of the wood roof must also be considered. To establish its density the table 3.1.I from the “NTC 2018” was used, obtaining a value of 6kN/m$^3$.

Lastly, another permanent structural load to be considered is the vault filling, for this a concrete thickness equal to 5 cm placed on top of the vaults was contemplated. It is a concrete of very low quality with a considerable level of deterioration, for this reason the density assumed was 18kN/m$^3$.

The summarizes the specific weight values adopted for each material.

| Material | Density (kN/m3) |
|---|---|
| Stone masonry | 19 |
| Brickwork | 18 |
| Wood | 8 |
| Concrete | 18 |

Table 3-1. Weights per unit volume automatically assigned by Midas GEN.

In the case of the materials themselves and their dimensions, the software automatically considers the weight of each structural element.

On the other hand, in the case of the wooden roof, in order to consider the action of its own weight on the structure, it was necessary to perform a weight distribution, which means to have taken from the simplified model of the roof the reactions that were produced due to the own weight of this structure and to place them as point loads on the walls that support the roof structure.

It is important to mention that not all the structural elements that make up the roof were modelled, for instance the roof batten (that in Italian means “terzere”) and the purlins (“correnti” in Italian) were not inserted in the model. In order to consider, the action of the elements, the following procedure was carried out: firstly, the volume of each of the elements was taken, considering the dimensions and quantity present, this information was obtained from the different plans of the church. Then, this volume was multiplied by the specific weight of the wood considered, thus obtaining a point load, then this load was divided by the total area of the roof, thus obtaining a surface load. But in the calculation model it was necessary to insert the linear load that would be supported by each of the elements that make up the roof (beams), for this reason it was worked with influence thicknesses, i.e., how much roof load would reach each beam. Because of this, the beams on the sides will have a greater thickness of influence, and as a consequence a greater amount of load will be applied to them.

The aforementioned approach has been applied for the roof of the central nave and also for roof of the right and left lateral aisles.

Finally, in the case of the vaults the weight of the fill above them was applied as a pressure load. In other words, the density of the concrete was multiplied by the thickness of the layer that covers them, thus obtaining a load of 0.9 $kN/m^2$.

### 3.3.2 Permanent non-structural load.

The Italian standard defines this type of load as “the loads present on the construction during its normal operation, such as those related to external infills, internal partitions, screeds, insulation, floors and walls”. Also in this case, the actions

are derived from the geometric dimensions and weights per unit of volume of the materials from which the non-structural parts of the construction are made.

In the case of the construction under examination, the non-structural loads are given by the action of the roof in stone for the central nave and for the lateral aisles. The weight per unit area considered for this roof was 1.5 kN/m2, which includes the weight of the planking, laths, and the stone slab. In this case, the same reasoning as for the structural load was applied, taking the weight per unit of roof surface, multiplied by a thickness of influence, thus obtaining a load per unit length, which would then be applied to the beams that make up the structural model.

The tables below summarize the above for the weight of the structural elements of the roof (referred to as G1) as well as for the non-structural elements of the roof (G2).[12]

| Central aisle roof configuration (G1) | | | | | |
|---|---|---|---|---|---|
| Truss elements | b | h | l | n° | Volume |
| | [m] | [m] | [m] | | [m3] |
| Roof batten (Terzere ) | 0.10 | 0.10 | 5.75 | 20.00 | 1.15 |
| Purlins (Correnti) | 0.10 | 0.05 | 5.00 | 10.00 | 0.25 |
| | | | | Total | 1.40 |

| G2 | Weight |
|---|---|
| | [kN/m2] |
| Roof (tavolato + listelli + losa pietra) | 1.5 |

| Central aisle roof loads (G1 and G2) | | | | | |
|---|---|---|---|---|---|
| | Volume | Unitary weight | Area | Load | |
| | [m3] | [kN/m3] | [m2] | kN/m2 | |
| Truss elements | 1.40 | 8.00 | 247.20 | 0.05 | G1 |
| Roof | | | | 1.50 | G2 |

| G1 | | | |
|---|---|---|---|
| N° | Width | Width of influence | Lineal Load |
| | [m] | [m] | kN/m |
| 1 | 5.75 | 8.63 | 0.39 |
| 2 | 5.75 | 5.75 | 0.26 |
| 3 | 5.75 | 5.75 | 0.26 |
| 4 | 5.75 | 5.05 | 0.23 |
| 5 | 4.35 | 4.35 | 0.20 |

| G2 | | | |
|---|---|---|---|
| N° | Width | Width of influence | Lineal Load |
| | [m] | [m] | kN/m |
| 1 | 5.75 | 8.63 | 12.94 |
| 2 | 5.75 | 5.75 | 8.63 |
| 3 | 5.75 | 5.75 | 8.63 |
| 4 | 5.75 | 5.05 | 7.58 |
| 5 | 4.35 | 4.35 | 6.53 |

Figure 3-20. Determination of the permanent structural and non-structural loads to be applied to the central nave.

| Lateral right aisle roof configuration | | | | | |
|---|---|---|---|---|---|
| Truss elements | b | h | l | n° | Volume |
| | [m] | [m] | [m] | | [m3] |
| Roof batten (Terzere ) | 0.10 | 0.10 | 5.75 | 10.00 | 0.575 |
| Correnti | 0.10 | 0.05 | 5.75 | 5.00 | 0.14 |
| | | | | **Total** | **0.72** |

| G2 | Weight |
|---|---|
| | [kN/m2] |
| Roof (tavolato + listelli + losa pietra) | 1.5 |

| Lateral right aisle roof configuration load | | | | | |
|---|---|---|---|---|---|
| | Volume | Unitary weight | Area | Load | |
| | [m3] | [kN/m3] | [m2] | kN/m2 | |
| Truss elements | 0.72 | 8.00 | 130.64 | 0.04 | G1 |
| Roof | | | | 1.50 | G2 |

| G1 | | | |
|---|---|---|---|
| N° | Width | Width of influence | Lineal Load |
| | [m] | [m] | kN/m |
| 1 | 5.75 | 8.63 | 0.38 |
| 2 | 5.75 | 5.75 | 0.25 |
| 3 | 5.75 | 5.75 | 0.25 |
| 4 | 5.75 | 5.05 | 0.22 |
| 5 | 4.35 | 4.35 | 0.19 |

| G2 | | | |
|---|---|---|---|
| N° | Width | Width of influence | Lineal Load |
| | [m] | [m] | kN/m |
| 1 | 5.75 | 8.63 | 12.94 |
| 2 | 5.75 | 5.75 | 8.63 |
| 3 | 5.75 | 5.75 | 8.63 |
| 4 | 5.75 | 5.05 | 7.58 |
| 5 | 4.35 | 4.35 | 6.53 |

Figure 3-21. Determination of the permanent structural and non-structural loads to be applied to the lateral right aisle.

| Lateral left aisle configuration | | | | | |
|---|---|---|---|---|---|
| Truss elements | b | h | l | n° | Volume |
| | [m] | [m] | [m] | | [m3] |
| Roof batten (Terzere ) | 0.10 | 0.10 | 5.75 | 3.00 | 0.173 |
| Correnti | 0.10 | 0.05 | 5.75 | 5.00 | 0.14 |
| | | | | **Total** | **0.32** |

| | Weight |
|---|---|
| | [kN/m2] |
| Roof (tavolato + listelli + losa pietra) | 1.5 |

| Lateral left aisle configuration load | | | | | |
|---|---|---|---|---|---|
| | Volume | Unitary weight | Area | Load | |
| | [m3] | [kN/m3] | [m2] | kN/m2 | |
| Truss elements | 0.32 | 8.00 | 190.03 | 0.01 | G1 |
| Roof | | | | 1.50 | G2 |

| G1 | | | |
|---|---|---|---|
| N° | Width | Width of influence | Lineal Load |
| | [m] | [m] | kN/m |
| 1 | 5.75 | 8.63 | 0.11 |
| 2 | 5.75 | 5.75 | 0.08 |
| 3 | 5.75 | 2.88 | 0.04 |

| G2 | | | |
|---|---|---|---|
| N° | Width | Width of influence | Lineal Load |
| | [m] | [m] | kN/m |
| 1 | 5.75 | 8.63 | 12.94 |
| 2 | 5.75 | 5.75 | 8.63 |
| 3 | 5.75 | 2.88 | 4.31 |

Figure 3-22. Determination of the permanent structural and non-structural loads to be applied to the lateral left aisle.

### 3.3.3 Wind action.

Wind pressures change over time and exert direct pressure on enclosed structures' exterior surfaces. However, because the external surface is porous, wind pressures also indirectly affect the internal surfaces. [16]

A condensed set of pressures or forces that have effects comparable to the extreme ones of a turbulent wind are used to illustrate the wind action.

For the calculation of these pressure forces, the Eurocode, chapter 1.4, and the Italian standard were used as a reference. In order to obtain the value of the acting wind pressure, a certain number of values have to be determined first, beginning with the fundamental value of the wind velocity.

The fundamental value of the basic wind velocity, $v_{b,0}$, is the characteristic 10 minutes mean wind velocity at 10m above ground level in open country terrain with low vegetation such as grass and isolated obstacles separated by at least 20 obstacle heights, regardless of wind direction or time of year. The Eurocode prescribes the equation 4.1 for the calculation of this value.

$$\mathbf{v_b} = \boldsymbol{C_{dir}}\, \boldsymbol{C_{season}} \boldsymbol{V_{b,0}} \tag{12}$$

Where:

$\mathbf{v_b}$ is the basic wind velocity, defined as a function of wind direction and time of year at 10 m above gorund of terrain category II.

$\boldsymbol{V_{b,0}}$ is the fundamental value of the basic wind velocity.

$\mathbf{C_{dir}}$ is the directional factor.

$\boldsymbol{C_{season}}$ is the season factor.

For the determination of these parameters the National Annex was used, using the Italian regulation as a reference, the season factor was assumed equal to 1. And the equation 12 is transformed in:

$$\mathbf{v_b} = \boldsymbol{C_a V_{b,0}} \tag{13}$$

Where:

$\boldsymbol{C_a}$ is an altitude coefficient.

For the value of the basic wind velocity, the Italian regulation provides a table in which, depending on the region in which the building is located, a series of parameters, among which is the base reference speed.

Tab. 3.3.I -*Valori dei parametri* $v_{b,0}$, $a_0$, $k_s$

| Zona | Descrizione | $v_{b,0}$ [m/s] | $a_0$ [m] | $k_s$ |
|---|---|---|---|---|
| 1 | Valle d'Aosta, Piemonte, Lombardia, Trentino Alto Adige, Veneto, Friuli Venezia Giulia (con l'eccezione della provincia di Trieste) | 25 | 1000 | 0,40 |
| 2 | Emilia Romagna | 25 | 750 | 0,45 |
| 3 | Toscana, Marche, Umbria, Lazio, Abruzzo, Molise, Puglia, Campania, Basilicata, Calabria (esclusa la provincia di Reggio Calabria) | 27 | 500 | 0,37 |
| 4 | Sicilia e provincia di Reggio Calabria | 28 | 500 | 0,36 |
| 5 | Sardegna (zona a oriente della retta congiungente Capo Teulada con l'Isola di Maddalena) | 28 | 750 | 0,40 |
| 6 | Sardegna (zona a occidente della retta congiungente Capo Teulada con l'Isola di Maddalena) | 28 | 500 | 0,36 |
| 7 | Liguria | 28 | 1000 | 0,54 |
| 8 | Provincia di Trieste | 30 | 1500 | 0,50 |
| 9 | Isole (con l'eccezione di Sicilia e Sardegna) e mare aperto | 31 | 500 | 0,32 |

Figure 3·23 .Table 3.3.I from the NTC 2018.

The building under analysis is located in Frassino, province of Cuneo, it is part of the Piedmont region, for this reason the zone to be considered is 1. Then, for the determination of the Ca coefficient, the regulations give us two formulas to use, for which the election of one or the other depends on the height above sea level at which the site is situated. According to the table and the zone mentioned above, the maximum height above sea level is 1000m. Analyzing the site where the building is located, it is 750 m above sea level, for this reason the formula to be used is the first one that prescribes that the coefficient Ca is equal to 1.

$$C_a = 1 \text{ for } a_S \leq a_0 \tag{14}$$

$$C_a = 1 + k_s\left(\frac{\mathrm{a_s}}{\mathrm{a_0}} - 1\right) \text{ for } \mathrm{a_0} \le \mathrm{a_s} \le 1500\mathrm{m} \tag{15}$$

So, at the end it is possible to obtain:

$$\mathbf{v_b} = 1 \times 25\frac{m}{s} = \mathbf{25}\frac{\boldsymbol{m}}{\boldsymbol{s}} \tag{16}$$

Then, the reference velocity is defined as the average value over 10 minutes, at a height of 10 m above ground level on a flat and homogeneous terrain of exposure category II, referring to the design return period TR.

$$\mathrm{v_r} = \mathrm{v_b c_r} \tag{17}$$

The regulations allow us to assume for a return period equal to 50 years a value of the return coefficient equal to 1.

Obtaining as a result,

$$\mathrm{v_r} = 25\frac{m}{s} \times 1 = 25\frac{m}{s} \tag{18}$$

After obtaining the reference velocity, the wind pressure is calculated. It is given by the following equation:

$$\mathrm{p} = \mathrm{q_r}\,\mathrm{C_e}\,C_p\,C_d \tag{19}$$

Where:

$\mathrm{q_r}$ is the reference kinetic pressure.

$\mathrm{C_e}$ is the exposure coefficient.

$\mathrm{C_p}$ is the pressure coefficient.

$\mathrm{C_d}$is the dynamic coefficient.

In order to obtain the value of the wind pressure, the first step was the determination of the kinetic pressure. The Italian regulation defines the formula to determine it as follows:

$$q_r = \frac{1}{2}\, p\, v_r^2 \tag{20}$$

Where:

$v_r$ is the reference velocity that was already obtained.

p is the air density assume as $1{,}25\,\frac{kg}{m^3}$.

$$q_r = \frac{1}{2} \times 1{,}25 \times \frac{kg}{m^3} \times 25\,\frac{m}{s} \tag{21}$$

$$\mathbf{q_r = 390.625\,\frac{N}{m^2}} \tag{22}$$

The second step was to define the exposure coefficient, it depends on the height z above ground of the location in consideration, the topography of the terrain and the exposure category of the site where the building stands.

The definition of the terrain roughness class started with the Table. 3.3.III given by the Italian regulation. Since the town of Frassino is a town with a small number of buildings, which do not exceed 15 m in height, the standard prescribes in this case that the roughness class of the terrain is B.

**Tab. 3.3.III** - *Classi di rugosità del terreno*

| Classe di rugosità del terreno | Descrizione |
|---|---|
| A | Aree urbane in cui almeno il 15% della superficie sia coperto da edifici la cui altezza media superi i 15 m |
| B | Aree urbane (non di classe A), suburbane, industriali e boschive |
| C | Aree con ostacoli diffusi (alberi, case, muri, recinzioni,....); aree con rugosità non riconducibile alle classi A, B, D |
| D | a) Mare e relativa fascia costiera (entro 2 km dalla costa);<br>b) Lago (con larghezza massima pari ad almeno 1 km) e relativa fascia costiera (entro 1 km dalla costa)<br>c) Aree prive di ostacoli o con al più rari ostacoli isolati (aperta campagna, aeroporti, aree agricole, pascoli, zone paludose o sabbiose, superfici innevate o ghiacciate, ....) |

L'assegnazione della classe di rugosità non dipende dalla conformazione orografica e topografica del terreno. Si può assumere che il sito appartenga alla Classe A o B, purché la costruzione si trovi nell'area relativa per non meno di 1 km e comunque per non meno di 20 volte l'altezza della costruzione, per tutti i settori di provenienza del vento ampi almeno 30°. Si deve assumere che il sito appartenga alla Classe D, qualora la costruzione sorga nelle aree indicate con le lettere a) o b), oppure entro un raggio di 1 km da essa vi sia un settore ampio 30°, dove il 90% del terreno sia del tipo indicato con la lettera c). Laddove sussistano dubbi sulla scelta della classe di rugosità, si deve assegnare la classe più sfavorevole (l'azione del vento è in genere minima in Classe A e massima in Classe D).

Figure 3-24.Terrain's roughness class.

Once the roughness has been obtained and depending on the zone where the building is located, it is possible to determine the exposure class of the site. It was done using the tables 3.3.2 from the Italian regulation, the table used was chosen in function of the zone where the building is located, as said before the zone is 1, then entering with the roughness of the terrain and with the altitude, it is possible to determine the exposure category, in this case was class 4.

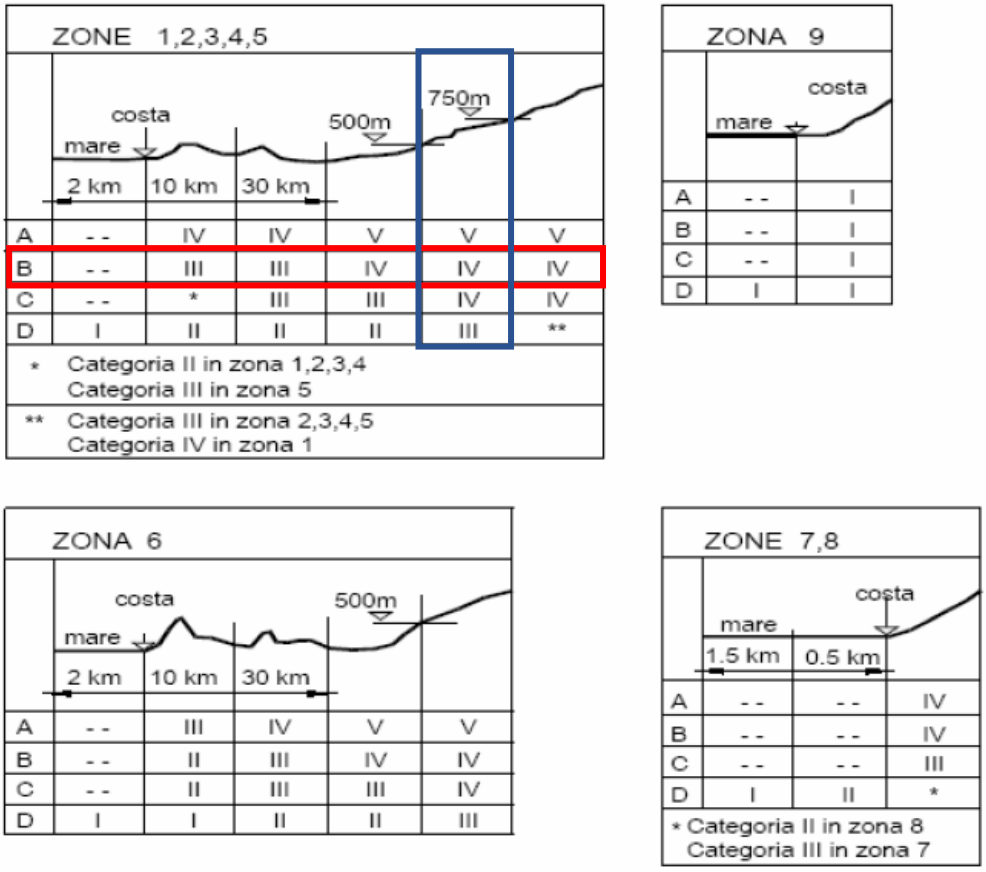


Figure 3-25. Definition of exposure categories. Table 3.3.2 from the NTC2018.

Once the exposure category has been determined, it is possible to obtain the parameters necessary for the definition of the exposure coefficient, these parameters are provided by Table 3.3.II of the Italian standards.

**Tab. 3.3.II** - *Parametri per la definizione del coefficiente di esposizione*

| Categoria di esposizione del sito | $K_r$ | $z_0$ [m] | $z_{min}$ [m] |
|---|---|---|---|
| I | 0,17 | 0,01 | 2 |
| II | 0,19 | 0,05 | 4 |
| III | 0,20 | 0,10 | 5 |
| IV | 0,22 | 0,30 | 8 |
| V | 0,23 | 0,70 | 12 |

Figure 3-26. Table 3.3.II Parameters for defining the exposure coefficient.

Once these parameters have been obtained, it is possible to determine the exposure coefficient. As it is possible to observe, the Italian regulations provide two formulas to be implemented to determine this coefficient, and this is a function of the height at

which the wind pressure is determined. When the height is less than the minimum height given as a parameter, this coefficient adopts a value equal to one, whereas when a greater height is analyzed, it is necessary to apply a formula in which the height ratio, and the topographical coefficient are considered.

Since no topographical coefficient was specified, the regulations allow us to assume a value equal to 1, $C_t = 1$.

$$C_e\,(z) = C_e\,(z_{\min}) \text{ when } \mathrm{z} < \mathrm{zmin} \tag{23}$$

$$C_e = k_r^2 c_t \ln\left(\frac{z}{z_0}\right)\left[7 + c_t \ln\left(\frac{z}{z_0}\right)\right] \quad \mathrm{z} \geq \mathrm{zmin} \tag{24}$$

As mentioned above, the exposure coefficient depends on the height at which the wind pressure is being calculated, therefore, as the wind is not represented by a linear function, what has been decided to do is to divide the walls on which the wind impacts into several pieces. In this way the variation of the wind function at different levels was considered. The Figure 3-27 and Figure 3-28 represents the division made for each wall.

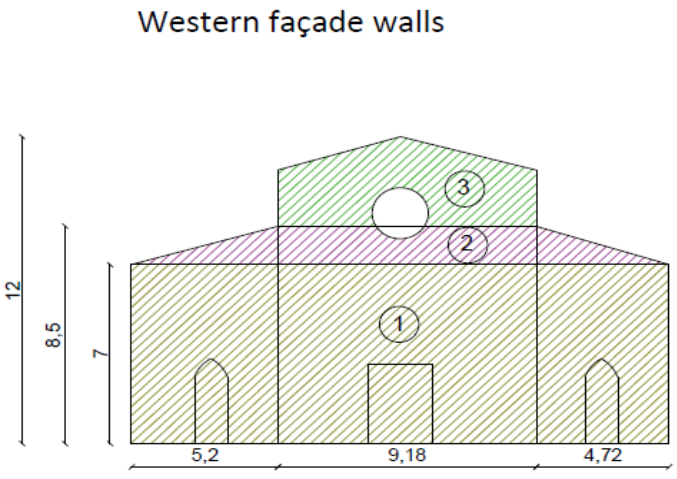


Figure 3-27 – Division of the western façade walls.

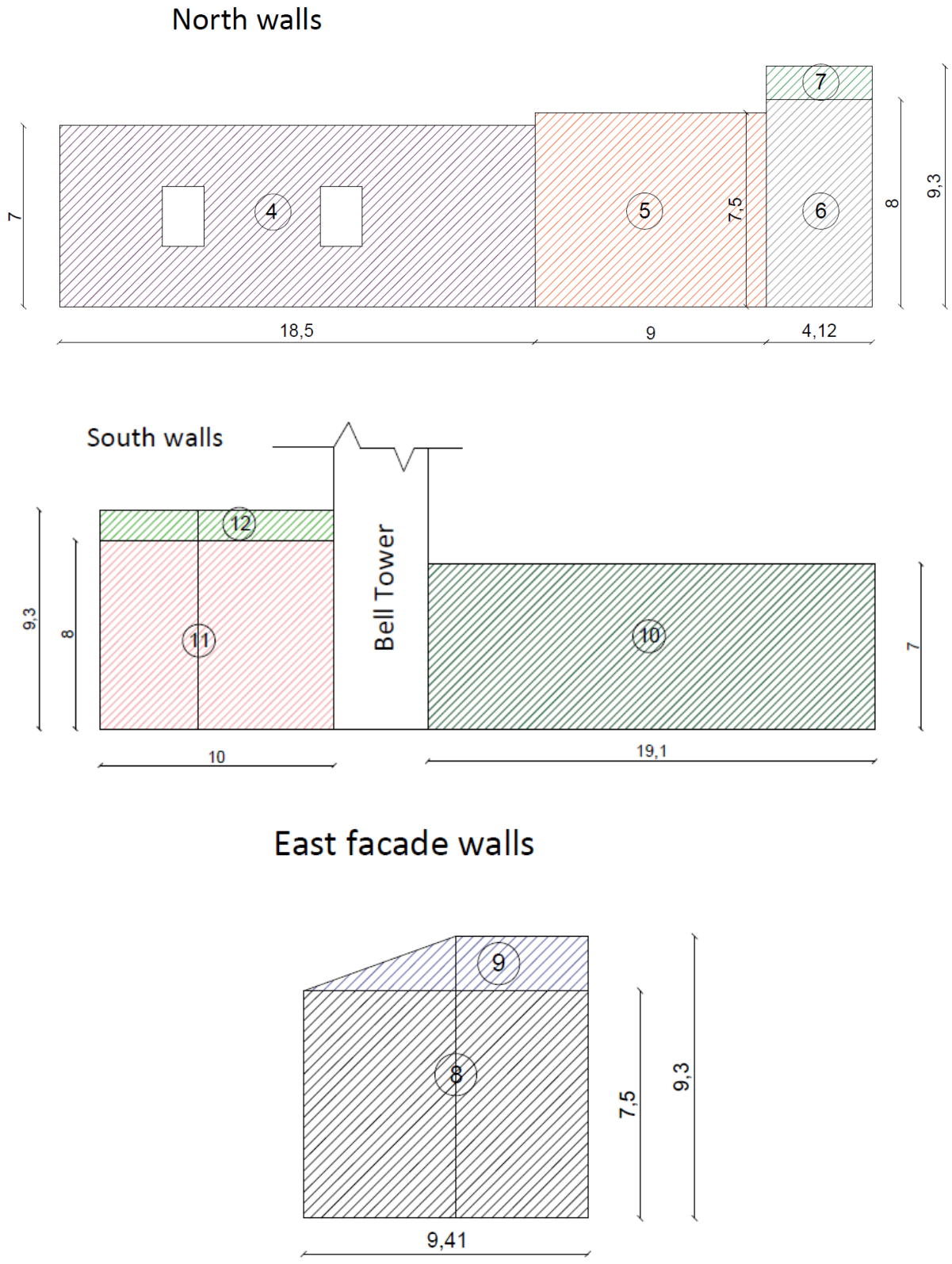


Figure 3-28 – Division of the north, south and east façade walls.

The Table 3-2 shows the walls that were considered, with their corresponding division into levels and as a result the exposure coefficient used to then calculate the acting pressure.

| Exposure coefficient Ce | | | | | | | |
|---|---|---|---|---|---|---|---|
| **Description** | **Subdivision** | **z** | **z0** | **zmin** | **kr** | **ct** | **ce** |
| | | **[m]** | **[m]** | **[m]** | | | |
| Western façade walls | 1 | 7.00 | 0.30 | 8.00 | 0.22 | 1.00 | 1.00 |
| | 2 | 8.50 | 0.30 | 8.00 | 0.22 | 1.00 | 1.67 |
| | 3 | 12.00 | 0.30 | 8.00 | 0.22 | 1.00 | 1.91 |
| North façade walls | 4 | 7.00 | 0.30 | 8.00 | 0.22 | 1.00 | 1.00 |
| | 5 | 7.50 | 0.30 | 8.00 | 0.22 | 1.00 | 1.00 |
| | 6 | 8.00 | 0.30 | 8.00 | 0.22 | 1.00 | 1.00 |
| | 7 | 10.30 | 0.30 | 8.00 | 0.22 | 1.00 | 1.80 |
| East façade walls | 8 | 7.50 | 0.30 | 8.00 | 0.22 | 1.00 | 1.00 |
| | 9 | 9.30 | 0.30 | 8.00 | 0.22 | 1.00 | 1.73 |
| South walls | 10 | 7.00 | 0.30 | 8.00 | 0.22 | 1.00 | 1.00 |
| | 11 | 8.00 | 0.30 | 8.00 | 0.22 | 1.00 | 1.00 |
| | 12 | 9.30 | 0.30 | 8.00 | 0.22 | 1.00 | 1.73 |
| Bell Tower | 13 | 8.00 | 0.30 | 8.00 | 0.22 | 1.00 | 1.00 |
| | 14 | 16.00 | 0.30 | 8.00 | 0.22 | 1.00 | 2.11 |
| | 15 | 26.60 | 0.30 | 8.00 | 0.22 | 1.00 | 2.49 |

Table 3-2. Exposure coefficient Ce.

As it is possible to observe from the table, the exposure coefficient increases with height, in very tall structures, such as in the bell tower, the wind pressure at the top will have a greater influence. In the case of the dynamic coefficient this was assumed to be equal to 1, $C_d = 1$.

Before proceeding to the determination of the pressure coefficient, it is necessary to specify that the action of the wind must be considered in both directions , that is to say that the same surface can be subjected to upwind or downwind. The Figure 3-29 depicts the aforementioned.

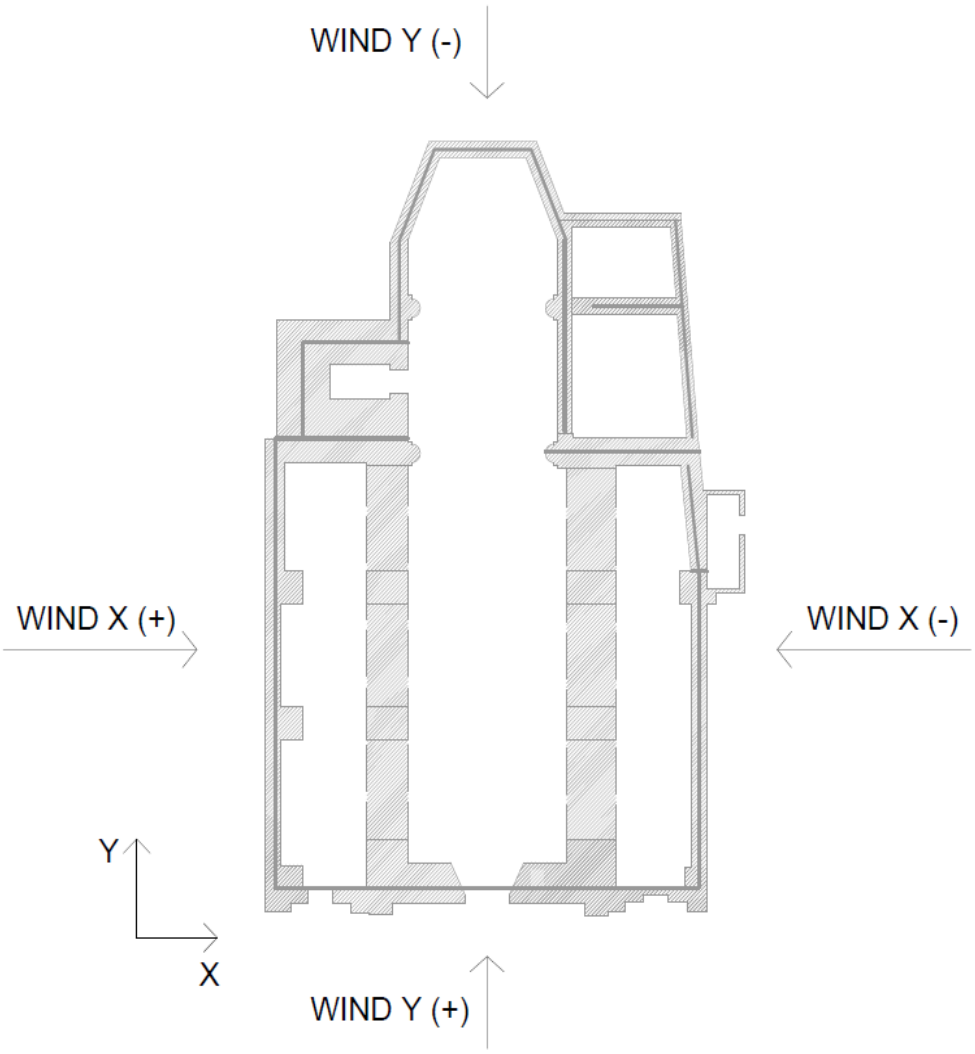


Figure 3-29. Wind scheme.

For determining the pressure coefficient $C_p$, several factors must be considered. First and foremost, it must be recognized that surfaces can be affected directly or indirectly by wind, resulting in pressure or depression.

As a result, two types of surfaces are defined, upwind surfaces are those that are directly impacted by the wind and are susceptible to pressure while downwind surfaces are those that are not directly affected by the wind and are subject to depression.

For the calculation of the pressure coefficient, reference was made to "Circolare 617/2009". The pressure coefficient is given by the sum of the internal pressure coefficient and the external pressure coefficient. First of all, the external pressure coefficient depends on whether the surface is subjected to under or over pressure, and on the ratio between the height and the length of the wall orthogonal to the wall under analysis.

**Tabella G.I** – Edifici a pianta rettangolare: $c_{pe}$ per facce sopravento, sottovento e laterali.

| Faccia sopravento | Facce laterali | Faccia sottovento |
|---|---|---|
| $h/d \leq 1$: $c_{pe} = 0,7 + 0,1 \cdot h/d$<br>$h/d > 1$: $c_{pe} = 0,8$ | $h/d \leq 0,5$: $c_{pe} = -0,5 - 0,8 \cdot h/d$<br>$h/d > 0,5$: $c_{pe} = -0,9$ | $h/d \leq 1$: $c_{pe} = -0,3 - 0,2 \cdot h/d$<br>$1 < h/d \leq 5$: $c_{pe} = -0,5 - 0,05 \cdot (h/d - 1)$ |

Figure 3-30. Table G.I from the "Circolare 617/2009".

On the other hand, in the case of the internal pressure coefficient, as the number of openings in the structure is less than 1/3 of the total surface area, the internal pressure coefficient adopted is equal to **0.2**. The most severe combination must be considered when determining the final pressure coefficient.

The Table 3-3 presents the values obtained for the pressure coefficients in the various walls and in turn in the various divisions adopted.

| Pressure coefficient Cp | | | | | | | | | |
|---|---|---|---|---|---|---|---|---|---|
| Position | Description | Subdivision | h [m] | d [m] | h/d | Equation | Cpe | Cpi | Cp |
| Upwind | Western façade walls | 1 | 7.00 | 27.50 | 0.25 | Calculate | 0.73 | 0.20 | 0.93 |
| | | 2 | 8.50 | 27.50 | 0.31 | Calculate | 0.73 | 0.20 | 0.93 |
| | | 3 | 12.00 | 27.50 | 0.44 | Calculate | 0.74 | 0.20 | 0.94 |
| | North façade walls | 4 | 7.00 | 20.00 | 0.35 | Calculate | 0.74 | 0.20 | 0.94 |
| | | 5 | 7.50 | 20.00 | 0.38 | Calculate | 0.74 | 0.20 | 0.94 |
| | | 6 | 8.00 | 20.00 | 0.40 | Calculate | 0.74 | 0.20 | 0.94 |
| | | 7 | 10.30 | 20.00 | 0.52 | Calculate | 0.75 | 0.20 | 0.95 |
| | East façade walls | 8 | 7.50 | 27.50 | 0.27 | Calculate | 0.73 | 0.20 | 0.93 |
| | | 9 | 9.30 | 27.50 | 0.34 | Calculate | 0.73 | 0.20 | 0.93 |
| | South walls | 10 | 7.00 | 20.00 | 0.35 | Calculate | 0.74 | 0.20 | 0.94 |
| | | 11 | 8.00 | 20.00 | 0.40 | Calculate | 0.74 | 0.20 | 0.94 |
| | | 12 | 9.30 | 20.00 | 0.47 | Calculate | 0.75 | 0.20 | 0.95 |
| | Bell Tower | 13 | 8 | 19.00 | 0.42 | Calculate | 0.74 | 0.20 | 0.94 |
| | | 14 | 16 | 19.00 | 0.84 | Calculate | 0.78 | 0.20 | 0.98 |
| | | 15 | 26.6 | 19.00 | 1.40 | 0.8 | 0.80 | 0.20 | 1.00 |
| | | | | | | | | | |
| Downwind | Western façade walls | 1 | 7.00 | 27.50 | 0.25 | 1 | -0.35 | 0.20 | -0.55 |
| | | 2 | 8.50 | 27.50 | 0.31 | 1 | -0.36 | 0.20 | -0.56 |
| | | 3 | 12.00 | 27.50 | 0.44 | 1 | -0.39 | 0.20 | -0.59 |
| | North façade walls | 4 | 7.00 | 20.00 | 0.35 | 1 | -0.37 | 0.20 | -0.57 |
| | | 5 | 7.50 | 20.00 | 0.38 | 1 | -0.38 | 0.20 | -0.58 |
| | | 6 | 8.00 | 20.00 | 0.40 | 1 | -0.38 | 0.20 | -0.58 |
| | | 7 | 10.30 | 20.00 | 0.52 | 1 | -0.40 | 0.20 | -0.60 |
| | East façade walls | 8 | 7.50 | 27.50 | 0.27 | 1 | -0.35 | 0.20 | -0.55 |
| | | 9 | 9.30 | 27.50 | 0.34 | 1 | -0.37 | 0.20 | -0.57 |
| | South walls | 10 | 7.00 | 20.00 | 0.35 | 1 | -0.37 | 0.20 | -0.57 |
| | | 11 | 8.00 | 20.00 | 0.40 | 1 | -0.38 | 0.20 | -0.58 |
| | | 12 | 9.30 | 20.00 | 0.47 | 1 | -0.39 | 0.20 | -0.59 |
| | Bell Tower | 13 | 8.00 | 19.00 | 0.42 | 1 | -0.38 | 0.20 | -0.58 |
| | | 14 | 16.00 | 19.00 | 0.84 | 1 | -0.47 | 0.20 | -0.67 |
| | | 15 | 26.60 | 19.00 | 1.40 | 2 | -0.58 | 0.20 | -0.78 |
| | | | | | | | | | |

Table 3-3. Determination of the pressure coefficient.

After the pressure coefficients were determined for each of the walls and their divisions, the next step was to determine the pressure value to be applied by using the formula 19. The results obtained are shown in the table, as can be seen in the table, as it is possible to see there was a distinction made in the determination of the pressure for the surfaces that are located at upwind or downwind as a consequence of the direction of the wind. This means for example if the wind is considered to act in positive x-direction, the walls located on the north façade will be in an upwind condition while those located on the south façade will be in a downwind condition, as a consequence the pressure values to be used will be different.

| Position | Description | Subdivision | z | $q_r$ | $C_e$ | $C_d$ | $C_p$ | p | p |
|---|---|---|---|---|---|---|---|---|---|
| | | | [m] | [N/m2] | | | | [N/m2] | [kN/m2] |
| Upwind | Western façade walls | 1 | 7.00 | 390.63 | 1.00 | 1.00 | 0.93 | 361.51 | 0.36 |
| | | 2 | 8.50 | 390.63 | 1.67 | 1.00 | 0.93 | 608.80 | 0.61 |
| | | 3 | 12.00 | 390.63 | 1.91 | 1.00 | 0.94 | 703.46 | 0.70 |
| | North façade walls | 4 | 7.00 | 390.63 | 1.00 | 1.00 | 0.94 | 365.23 | 0.37 |
| | | 5 | 7.50 | 390.63 | 1.00 | 1.00 | 0.94 | 366.21 | 0.37 |
| | | 6 | 8.00 | 390.63 | 1.00 | 1.00 | 0.94 | 367.19 | 0.37 |
| | | 7 | 10.30 | 390.63 | 1.80 | 1.00 | 0.95 | 670.23 | 0.67 |
| | East façade walls | 8 | 7.50 | 390.63 | 1.00 | 1.00 | 0.93 | 362.22 | 0.36 |
| | | 9 | 9.30 | 390.63 | 1.73 | 1.00 | 0.93 | 632.58 | 0.63 |
| | South walls | 10 | 7.00 | 390.63 | 1.00 | 1.00 | 0.94 | 365.23 | 0.37 |
| | | 11 | 8.00 | 390.63 | 1.00 | 1.00 | 0.94 | 367.19 | 0.37 |
| | | 12 | 9.30 | 390.63 | 1.73 | 1.00 | 0.95 | 641.17 | 0.64 |
| | Bell Tower | 13 | 8.00 | 390.63 | 1.00 | 1.00 | 0.94 | 368.01 | 0.37 |
| | | 14 | 16.00 | 390.63 | 2.11 | 1.00 | 0.98 | 812.21 | 0.81 |
| | | 15 | 26.60 | 390.63 | 2.49 | 1.00 | 1.00 | 973.83 | 0.97 |
| | | | | | | | | | |
| Downwind | Western façade walls | 1 | 7.00 | 390.63 | 1.00 | 1.00 | -0.55 | -215.20 | -0.22 |
| | | 2 | 8.50 | 390.63 | 1.67 | 1.00 | -0.56 | -367.42 | -0.37 |
| | | 3 | 12.00 | 390.63 | 1.91 | 1.00 | -0.59 | -437.80 | -0.44 |
| | North façade walls | 4 | 7.00 | 390.63 | 1.00 | 1.00 | -0.57 | -222.66 | -0.22 |
| | | 5 | 7.50 | 390.63 | 1.00 | 1.00 | -0.58 | -224.61 | -0.22 |
| | | 6 | 8.00 | 390.63 | 1.00 | 1.00 | -0.58 | -226.56 | -0.23 |
| | | 7 | 10.30 | 390.63 | 1.80 | 1.00 | -0.60 | -424.75 | -0.42 |
| | East façade walls | 8 | 7.50 | 390.63 | 1.00 | 1.00 | -0.55 | -216.62 | -0.22 |
| | | 9 | 9.30 | 390.63 | 1.73 | 1.00 | -0.57 | -384.52 | -0.38 |
| | South walls | 10 | 7.00 | 390.63 | 1.00 | 1.00 | -0.57 | -222.66 | -0.22 |
| | | 11 | 8.00 | 390.63 | 1.00 | 1.00 | -0.58 | -226.56 | -0.23 |
| | | 12 | 9.30 | 390.63 | 1.73 | 1.00 | -0.59 | -401.71 | -0.40 |
| | Bell Tower | 13 | 8.00 | 390.63 | 1.00 | 1.00 | -0.58 | -228.21 | -0.23 |
| | | 14 | 16.00 | 390.63 | 2.11 | 1.00 | -0.67 | -551.61 | -0.55 |
| | | 15 | 26.60 | 390.63 | 2.49 | 1.00 | -0.78 | -759.59 | -0.76 |
| | | | | | | | | | |

Figure 3-31. Pressure of the wind in each wall.

In the Midas gen software, the wind pressure was inserted as "pressure loads" on each of the walls under analysis, defining the wind load as a live load. In this type of load definition, it can be decided whether the pressure will be on local or global axes, always the global axes of the project were chosen as reference and in the case of the wind direction the Y or X axes, depending on the case.

### 3.3.4 Snow load.

The weight of accumulated snow and ice on a building's roof causes a downward pressure on the roof. The load caused by snow on roofs will be evaluated using the following expression, which is provided by the Italian regulation.

$$q_s = q_{sk}\,\mu_i\,C_E\,C_t \tag{25}$$

Where:

$q_{sk}$: is the reference value of the snow load on the ground.

$\mu_i$: is the shape coefficient of the roof.

$C_E$: is the exposure coefficient.

$C_t$: is the thermal coefficient.

The first step in determining the snow load is to determine the reference value. For this purpose, paragraph 3.4.2 of the Italian regulation was used, where it is stated that *"given the differing amounts of snowfall from location to region, the snow load on the ground is determined by the local climate and exposure conditions".*

In turn, as for the wind load, the regulation divides the country into different zones, where the expression to determine this reference value differs from region to region. In the case of the construction under study, it is located in zone 1, defined as alpine.

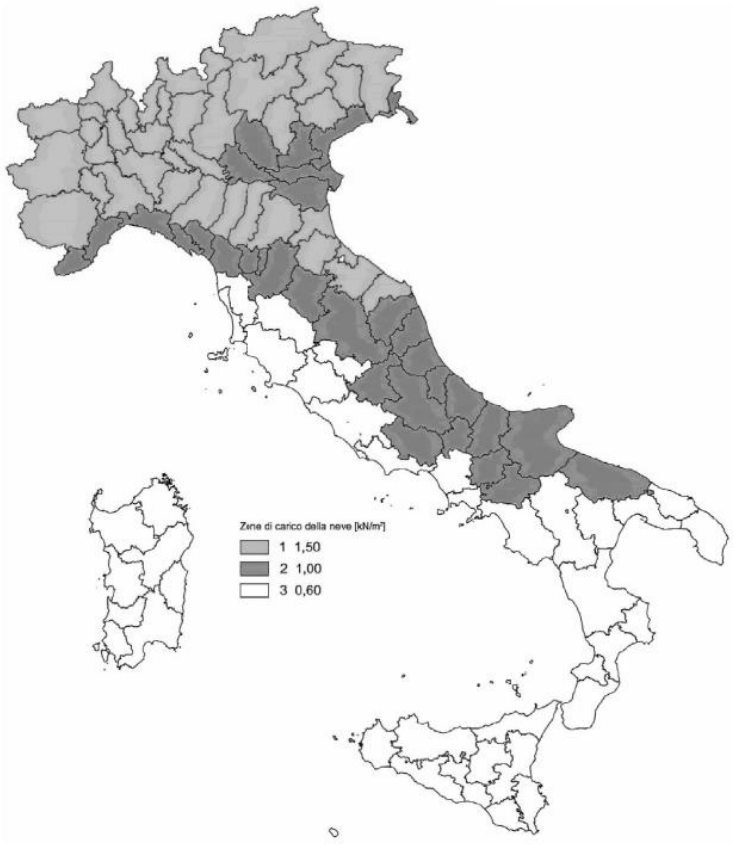


Figure 3-32. Figure 3.4.1 from the NTC2018 - Snow load zones.

As previously stated, the reference value also depends on the altitude, therefore there are two different formulas to be used depending on the altitude of the area under analysis. The formulas given by the regulations are the following.

$$q_{sk} = 1{,}50 \frac{kN}{m^2} \qquad \text{for } a_s \leq 200 \text{ m} \tag{26}$$

$$q_{sk} = 1{,}39 \left[1 + \left(\frac{a_s}{728}\right)^2\right] \frac{kN}{m^2} \qquad \text{for } a_s > 200 \text{ m} \tag{27}$$

In the case of the building under analysis, the altitude at which it is located is 750 m above sea level, for this reason the formula to be used is 27.

$$q_{sk} = 1{,}39 \left[1 + \left(\frac{750}{728}\right)^2\right] \frac{kN}{m^2} = 2{,}87 \frac{kN}{m^2} \quad (28)$$

Once the reference value was obtained, the next step was to determine the shape coefficient of the roof. The shape coefficients of roofs depend on the shape of the roof itself and the inclination on the horizontal of its component parts and the local climatic conditions of the site where the building stands.

The regulations make a distinction between single-pitch and double-pitch roofing, in the case of the roof in question, it is a double pitch roof, with an equal inclination of both part that compose the roof lower than 30°.

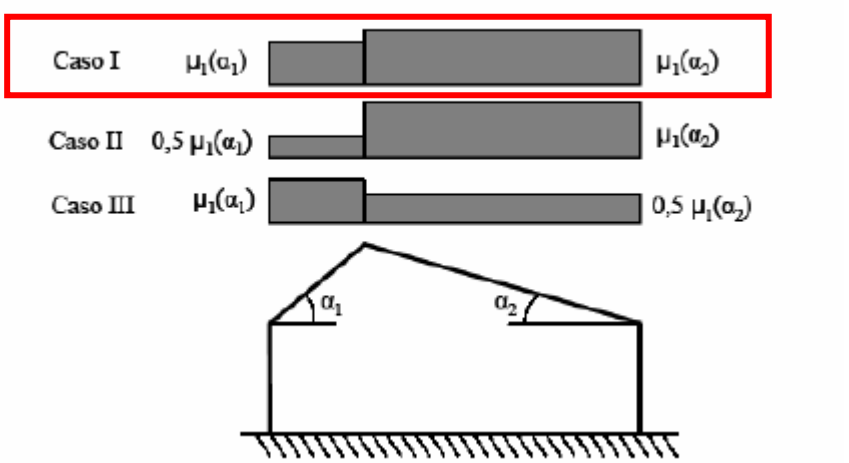


Figure 3-33. Figure 3.4.3 from the NTC2018 - Load conditions for two-pitch roofs.

In this way, using the table 3.4.II given by the Italian regulation, it is possible to obtain the shape coefficient, that in this case is equal to $\mu_1 = 0{,}8$.

**Tab. 3.4.II** – *Valori del coefficiente di forma*

| Coefficiente di forma | $0° \leq \alpha \leq 30°$ | $30° < \alpha < 60°$ | $\alpha \geq 60°$ |
|---|---|---|---|
| μ1 | 0,8 | $0{,}8 \cdot \frac{(60-\alpha)}{30}$ | 0,0 |

Figure 3-34. Table 3.4.II from the NTC2018 - shape coefficient values.

The third step was the determination of the exposure coefficient, which considers the specific characteristics of the area where the structure is located. The table 3.4.1 of the Italian standard, which reflects the topography of the site, was used for its determination. In the case of the topography of the area we are analyzing, it can be considered as "normal", which is defined as *"areas where there is no significant snow removal on the wind-generated construction, due to the ground, other constructions or trees"*. Thus, an exposure coefficient is obtained equal to $C_E = 1$.

**Tab. 3.4.I** – *Valori di $C_E$ per diverse classi di esposizione*

| Topografia | Descrizione | $C_E$ |
|---|---|---|
| Battuta dai venti | Aree pianeggianti non ostruite esposte su tutti i lati, senza costruzioni o alberi più alti | 0,9 |
| Normale | Aree in cui non è presente una significativa rimozione di neve sulla costruzione prodotta dal vento, a causa del terreno, altre costruzioni o alberi | 1,0 |
| Riparata | Aree in cui la costruzione considerata è sensibilmente più bassa del circostante terreno o circondata da costruzioni o alberi più alti | 1,1 |

Figure 3-35. Table 3.4.1 from the NTC2018 - Values of the exposure coefficient for different exposure classes.

The last coefficient to be determined is the thermal coefficient which contemplates the reduction in snow load, due to melting, caused by the loss of heat from the construction. The coefficient depends on the thermal insulation properties of the material used in the roof. The building under study is antique, and at that time thermal insulation was not discussed, and also because thermal insulation was not included in the interventions that were carried out on the building. For all the above considerations and in order to be in favor of safety, the value of the thermal coefficient adopted is equal to $C_t = 1$.

Finally, once all the coefficients necessary for the calculation of the snow load were obtained, the equation 24 was applied to obtain the value of the snow load. The summarizes the value of the coefficients obtained and the snow load value obtained.

| | | |
|---|---|---|
| as | 750.00 | [m] |
| qsk | 2.87 | [kN/m2] |
| u1 | 0.80 | - |
| u2 | 0.80 | - |
| Ce | 1.00 | - |
| Ct | 1.00 | - |
| qs | 2.29 | [kN/m2] |

Table 3-4. Calculation of the snow load.

As previously mentioned, the snow load is a value that influences the roof of the building. For this reason, what was done, as in the case of structural and non-structural permanent weight, was to determine the amount of load per linear meter that would be carried by the roof beams. It was carried out by means of multiplying the load per unit area determined by the influence thickness of each beam. This was done both for the roof of the central nave and for the roof of the side aisles. The table which follows summarizes the previously mentioned, where it is possible to read the value of the load applied to each beam.

| Central Nave | | | |
|---|---|---|---|
| N° | Width | Width of influence | Load |
| | [m] | [m] | [kN/m] |
| 1 | 5.75 | 8.63 | 19.77 |
| 2 | 5.75 | 5.75 | 13.18 |
| 3 | 5.75 | 5.75 | 13.18 |
| 4 | 5.75 | 5.05 | 11.58 |
| 5 | 4.35 | 4.35 | 9.97 |

| Right lateral nave | | | |
|---|---|---|---|
| N° | Width | Width of influence | Load |
| | [m] | [m] | [kN/m] |
| 1 | 5.75 | 8.63 | 19.77 |
| 2 | 5.75 | 5.75 | 13.18 |
| 3 | 5.75 | 5.75 | 13.18 |
| 4 | 5.75 | 5.05 | 11.58 |
| 5 | 4.35 | 4.35 | 9.97 |

| Leftt lateral nave | | | |
|---|---|---|---|
| N° | Width | Width of influence | Load |
| | [m] | [m] | [kN/m] |
| 1 | 5.75 | 8.63 | 19.77 |
| 2 | 5.75 | 5.75 | 13.18 |
| 3 | 5.75 | 2.88 | 6.59 |

Table 3-5. Value of the lineal load due to snow to applied to each beam.

As mentioned in other load cases, the reactions produced by the snow load were read from the roof model and then applied as wall actions in the global model.

The snow load, besides influencing the roofs of the central and side aisles, also affects the roof of the bell tower, which is the reason for applying this load to this area as well. In the Midas gen software this load was applied as "Floor load". This command is characterized by the conversion of pressure loads into effective loads acting on beams or walls.[17]

### 3.3.5 Overload.

The overloads, or imposed loads, include the loads related to the destination of use of the structure, it is important to consider that these are live loads. Italian norms in the paragraph 3.1.4, depending on the category of use of the buildings, provide an overload value to be used.

In the case of the building in question, it falls into category H, where it refers to roofs accessible only for maintenance and repair work, this is because the second level of the building, i.e., the gap between the vaults and the wood roof it does not have use for anything other than maintenance. Also, another area where the presence of this live load was considered is the upper part of the bell tower roof since the top of the tower has to be accessed for maintenance work on the roof as well as on the bell.

The Figure 3-36 represents the table 3.1.II of the Italian standards, where for each category the value of the uniformly distributed vertical load to be applied on the roof of the building under analysis is given. In the case of the church, the value to be applied on the vaults and on the top roof of the bell tower is **0.5 kN/m$^2$.**

| Cat. | Ambienti | $q_k$ [kN/m²] | $Q_k$ [kN] | $H_k$ [kN/m] |
|---|---|---|---|---|
| A | **Ambienti ad uso residenziale** | | | |
| | Aree per attività domestiche e residenziali; sono compresi in questa categoria i locali di abitazione e relativi servizi, gli alberghi (ad esclusione delle aree soggette ad affollamento), camere di degenza di ospedali | 2,00 | 2,00 | 1,00 |
| | Scale comuni, balconi, ballatoi | 4,00 | 4,00 | 2,00 |
| B | **Uffici** | | | |
| | Cat. B1 Uffici non aperti al pubblico | 2,00 | 2,00 | 1,00 |
| | Cat. B2 Uffici aperti al pubblico | 3,00 | 2,00 | 1,00 |
| | Scale comuni, balconi e ballatoi | 4,00 | 4,00 | 2,00 |
| C | **Ambienti suscettibili di affollamento** | | | |
| | Cat. C1 Aree con tavoli, quali scuole, caffè, ristoranti, sale per banchetti, lettura e ricevimento | 3,00 | 3,00 | 1,00 |
| | Cat. C2 Aree con posti a sedere fissi, quali chiese, teatri, cinema, sale per conferenze e attesa, aule universitarie e aule magne | 4,00 | 4,00 | 2,00 |
| | Cat. C3 Ambienti privi di ostacoli al movimento delle persone, quali musei, sale per esposizioni, aree d'accesso a uffici, ad alberghi e ospedali, ad atri di stazioni ferroviarie | 5,00 | 5,00 | 3,00 |
| | Cat. C4. Aree con possibile svolgimento di attività fisiche, quali sale da ballo, palestre, palcoscenici. | 5,00 | 5,00 | 3,00 |
| | Cat. C5. Aree suscettibili di grandi affollamenti, quali edifici per eventi pubblici, sale da concerto, palazzetti per lo sport e relative tribune, gradinate e piattaforme ferroviarie. | 5,00 | 5,00 | 3,00 |
| | Scale comuni, balconi e ballatoi | Secondo categoria d'uso servita, con le seguenti limitazioni | | |
| | | ≥ 4,00 | ≥ 4,00 | ≥ 2,00 |
| D | **Ambienti ad uso commerciale** | | | |
| | Cat. D1 Negozi | 4,00 | 4,00 | 2,00 |
| | Cat. D2 Centri commerciali, mercati, grandi magazzini | 5,00 | 5,00 | 2,00 |
| | Scale comuni, balconi e ballatoi | Secondo categoria d'uso servita | | |
| E | **Aree per immagazzinamento e uso commerciale ed uso industriale** | | | |
| | Cat. E1 Aree per accumulo di merci e relative aree d'accesso, quali biblioteche, archivi, magazzini, depositi, laboratori manifatturieri | ≥ 6,00 | 7,00 | 1,00* |
| | Cat. E2 Ambienti ad uso industriale | da valutarsi caso per caso | | |
| F-G | **Rimesse e aree per traffico di veicoli (esclusi i ponti)** | | | |
| | Cat. F Rimesse, aree per traffico, parcheggio e sosta di veicoli leggeri (peso a pieno carico fino a 30 kN) | 2,50 | 2 x 10,00 | 1,00** |
| | Cat. G Aree per traffico e parcheggio di veicoli medi (peso a pieno carico compreso fra 30 kN e 160 kN), quali rampe d'accesso, zone di carico e scarico merci. | da valutarsi caso per caso e comunque non minori di | | |
| | | 5,00 | 2 x 50,00 | 1,00** |
| H-I-K | **Coperture** | | | |
| | Cat. H Coperture accessibili per sola manutenzione e riparazione | 0,50 | 1,20 | 1,00 |
| | Cat. I Coperture praticabili di ambienti di categoria d'uso compresa fra A e D | secondo categorie di appartenenza | | |
| | Cat. K Coperture per usi speciali, quali impianti, eliporti. | da valutarsi caso per caso | | |

* non comprende le azioni orizzontali eventualmente esercitate dai materiali immagazzinati.
** per i soli parapetti o partizioni nelle zone pedonali. Le azioni sulle barriere esercitate dagli automezzi dovranno essere valutate caso per caso.

Figure 3-36. Table. 3.1.II from the NTC2018 - Overload values for the different categories of building use.

This load in the Midas gen software was applied as "pressure load", adopting the global Z-direction as the load direction in the case of the central and lateral nave. On the other hand, in order to represent the effect of this load in the bell tower structure it was inserted as a “Floor Load”. In turn, the load case corresponds to a live load type.

### 3.3.6 Seismic action.

Seismic activity is characterized by the kinds, frequency, and size of earthquakes that occur throughout time in a specific region.

For the determination of the seismic action, reference is made to paragraph 3.2 of the Italian regulations (NTC 2018). It states that the design seismic actions, on the basis of which compliance with the various limit states considered is to be assessed, are defined from the 'basic seismic hazard' of the construction site and are a function of the morphological and stratigraphic characteristics that determine the local seismic response.

For the purposes of these regulations, spectral shapes are defined for each of the $P_{V_R}$ exceedance probabilities during the reference period VR, from the values of the following parameters on a rigid horizontal reference site:

- $a_g$ is the maximum horizontal acceleration at the site.
- $F_0$ is the maximum value of the spectrum amplification factor in acceleration horizontal.
- $T_C^*$ reference value for determining the start period of the constant-velocity section of the horizontal acceleration spectrum.

It is important to note that in the case of the building under analysis, referring to paragraph 7.2.2 of the NTC 2018, the vertical component of the seismic event must be considered since it prescribes the consideration of the vertical component when thrust structures are present within the building, in this case the roof. As stated above, the vertical component of the seismic event must be taken into consideration.

The response spectrum is a graph which, as a function of the oscillation period known as T, gives the maximum response in terms of velocity, acceleration, and displacement of an SDOF (single degree of freedom) or damped simple oscillator. The correlation between systems of one degree of freedom and the complex structures being analysed is that the latter can be decomposed into systems of N degrees of freedom, and this is what is done in modal analysis. For this reason, response spectrums are of such importance.

For the determination of the response spectrum (in the vertical and horizontal directions) to be inserted in Midas GEN, the spreadsheet downloadable from the website of the "Superior Council of Public Works" was used.

This spreadsheet is divided into 3 phases. The first one is related to the determination of the seismic hazard of the site, where the location of the building site must be inserted, as it is calculated as a function of geographical coordinates (longitude and latitude).

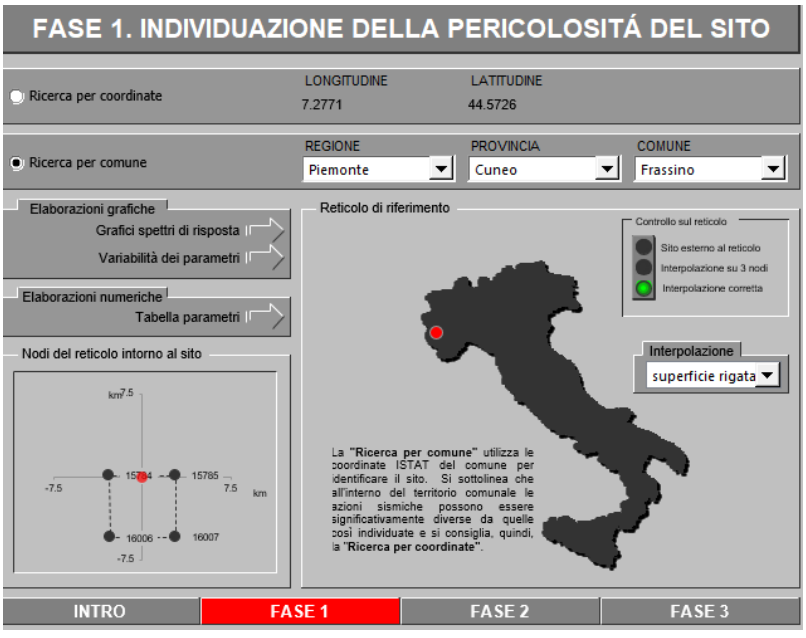


Figure 3-37. Identification of the seismic hazard of the site (Response Spectra Calculation Sheet - Step 1).

In the second step, which is related to the selection of the projection strategy, it was necessary to enter the nominal life of the construction $V_N$ and the usage coefficient $C_u$, these parameters have already been calculated earlier, in chapter 2.5.1.

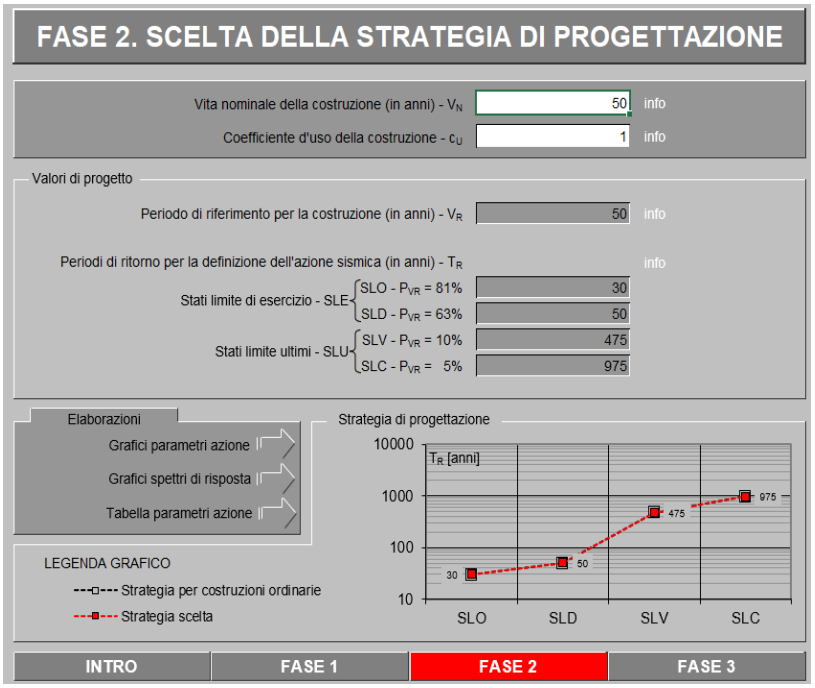


Figure 3-38. Choice of design strategy (Response Spectra Spreadsheet - Step 2).

The third and last phase corresponds to the determination of the design of the action. For which it is necessary to define certain parameters, the first of which is related to the limit state under consideration, both the Limit State of Life and the Limit State of Damage are examined, the former is used to carry out the verification of sections, the latter to analyze displacements.

Then, the subsoil category ( C ) and the topographical category (T2) are inserted. It is essential to point out a final factor that needs to be introduced in this last step, which is the behavior factor. The behavior factor is a pure number indicated in the Standard by the letter q. This factor has the function of scaling the ordinates of the elastic response spectrum by reducing them, thus giving rise to the design spectrum for verification at the Ultimate Limit States in seismic combination. Applying the behavior factor to the ordinates of the Elastic Response Spectrum causes the structure

under analysis to experience lower seismic accelerations than it would if its behavior were indefinitely elastic.

Due to the fact that masonry is considered a material with a low ductility, added to the fact that the constituent material is also of a very low quality, and also the malt, in order to be in favor of safety it was decided to take a value of behavior factor equal to 1.5, in this way the seismic that was considered to reach the structure is not reduced in a considerable way.

When considering seismic action, two different states were considered: the ultimate limit state and the life-sustaining limit state. In both cases, the value of the seismic acceleration varies.

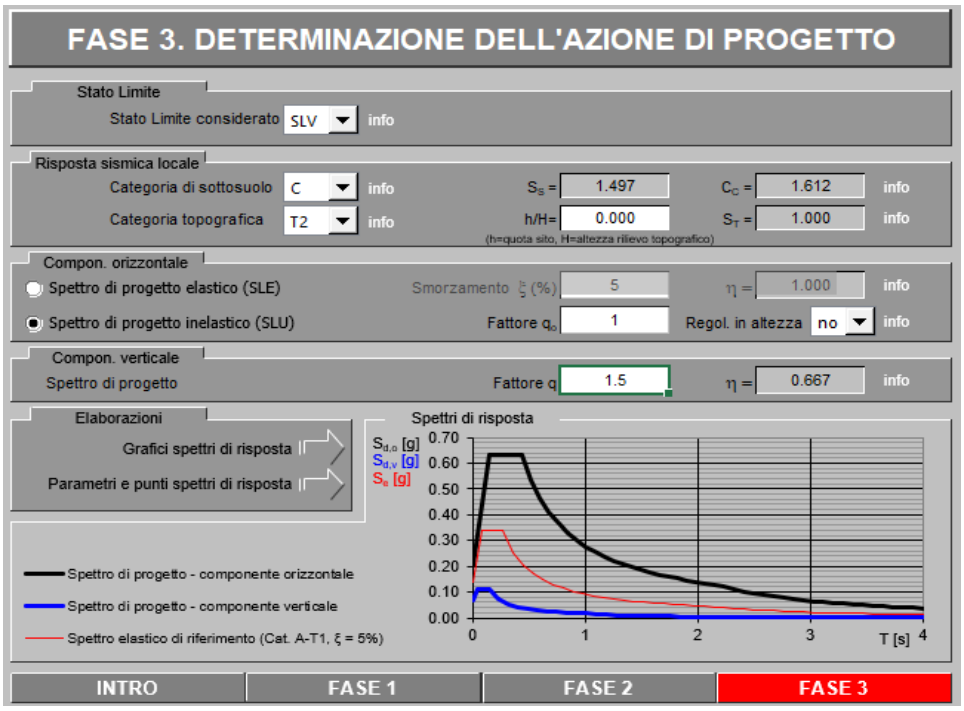


Figure 3-39. Determination of the design action for the Life Sustaining Limit State (Response Spectra Calculation Sheet - Step 3).

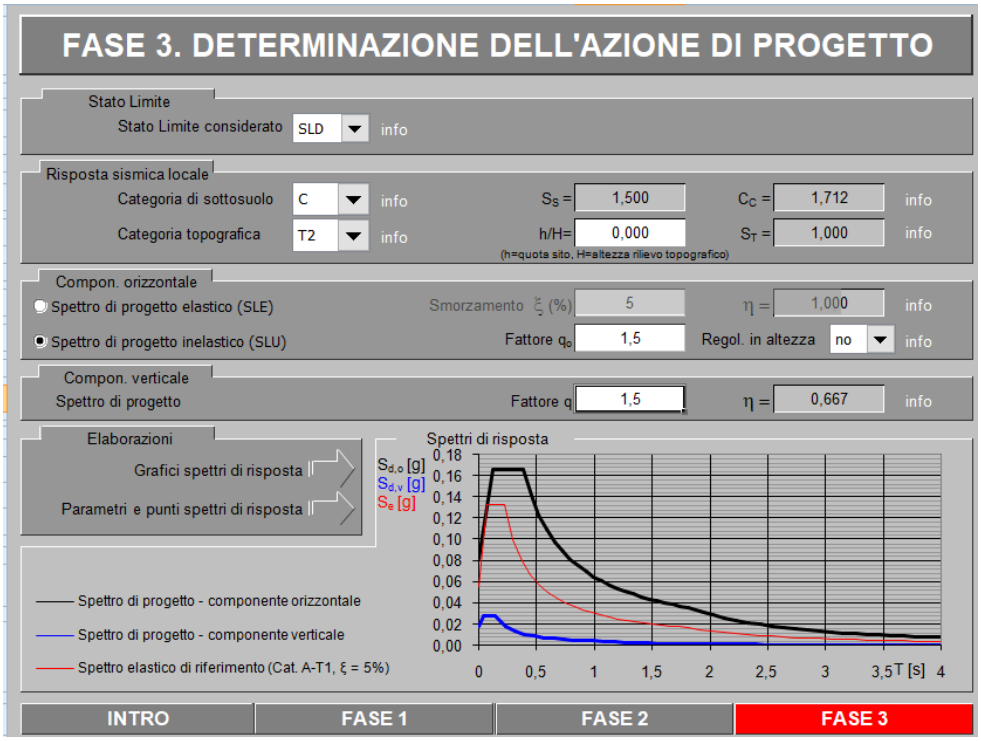


Figure 3-40. Determination of the design action for the Ultimate Limit State (Response Spectra Calculation Sheet - Step 3).

The spreadsheet, after entering all the required parameters, is able to provide the response spectra, the points of which will be imported into Midas GEN.

In particular, response spectra were obtained for the Limit state for safeguarding life (SLV) and the Ultimate limit state SLD) for both the horizontal and vertical components, both from a graphical point of view and in table form.

The most important parameters that will later be used to design the spectrum in Midas GEN, can be summarized in the Table 3-6 and in the Table 3-7.

| Spectrum parameters Life Sustaining Limit State (SLV) | | | |
|---|---|---|---|
| Horizontal Design Spectrum | Soil Factor (S) | 1.8 | |
| | Tb | 0.15 | |
| | Tc | 0.44 | |
| | Td | 2.14 | |
| | ag | 0.136 | g |
| | F0 | 2.481 | |
| | Tc* | 0.273 | |
| | q | 1.5 | |
| | Max period | 4 | sec |
| Vertical design spectrum | Soil Factor (S) | 1 | |
| | Tb | 0.05 | |
| | Tc | 0.15 | |
| | Td | 1 | |
| | ag | 0.068 | g |
| | F0 | 3.511 | |
| | Tc* | 0.15 | |
| | q | 1 | |
| | Max period | 4 | sec |

Table 3-6- Spectrum parameters of the Life Sustaining Limit State (SLV) to be used in Midas GEN.

| Spectrum parameters Ultimate Limit State (SLD) | | | |
|---|---|---|---|
| Horizontal Design Spectrum | Soil Factor (S) | 1.5 | |
| | Tb | 0.13 | |
| | Tc | 0.389 | |
| | Td | 1.819 | |
| | ag | 0.055 | g |
| | F0 | 2.425 | |
| | Tc* | 0.277 | |
| | q | 1.5 | |
| | Max period | 4 | sec |
| Vertical design spectrum | Soil Factor (S) | 1 | |
| | Tb | 0.05 | |
| | Tc | 0.15 | |
| | Td | 1 | |
| | ag | 0.017 | g |
| | F0 | 0.767 | |
| | Tc* | 0.15 | |
| | q | 1 | |
| | Max period | 4 | sec |

Table 3-7. Spectrum parameters of the Ultimate Limit State (SLU) to be used in Midas GEN.

The insertion of the seismic action within the models follows a somewhat different procedure from that followed for the assignment of other loads. In this case, the

software is loaded with the points of the horizontal and vertical response spectra, separately, which were previously calculated using the RS Functions (Response Spectrum Functions) command. The horizontal and vertical response spectra were reconstructed with the parameters given above.

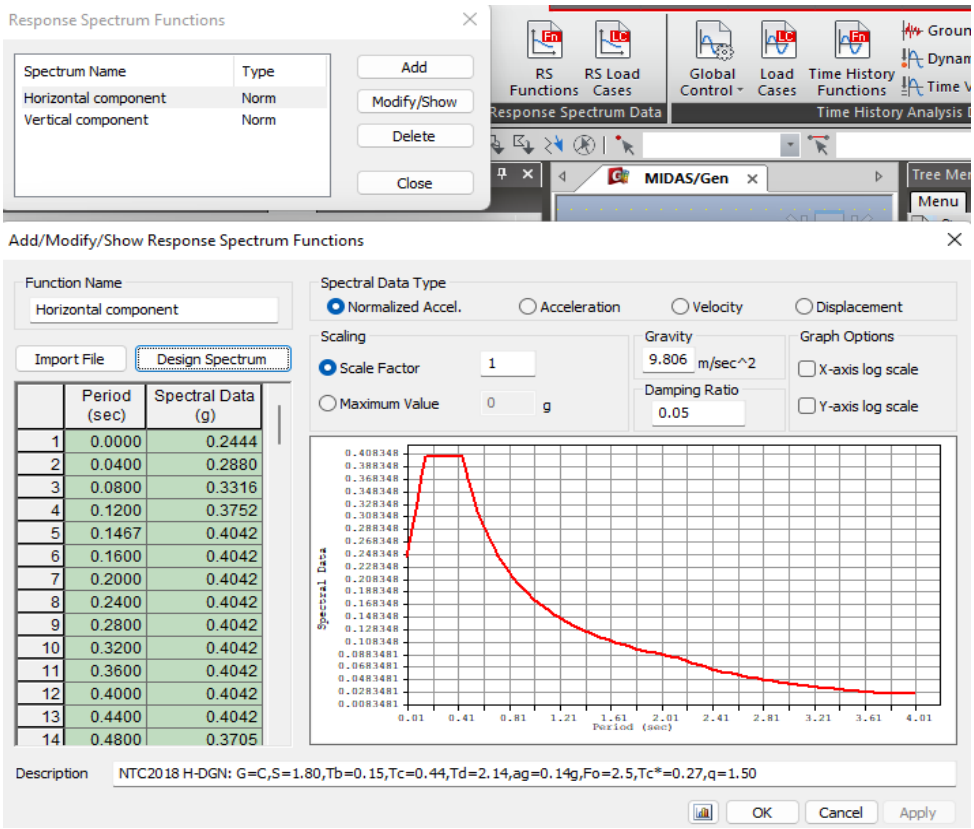


Figure 3-41. RS Functions command for horizontal spectrum at SLV.

Once the response spectra have been loaded, load cases are created using the command RS Load Cases (Response Spectrum Load Cases). For each model, there are three load cases one in the X direction (EX), one in the Y direction (EY) and one in the Z direction (EZ). The first is created from the horizontal response spectrum with an angle equal to zero, for the second the horizontal response spectrum is always used but with an angle of angle of ninety degrees, the third load case is based on the vertical response spectrum.

| LoadCase | Direction | Scale |
|---|---|---|
| EX | X-Y | 1 |
| EY | X-Y | 1 |
| EZ | Z | 1 |

Figure 3-42. Load cases for response spectra created on Midas GEN.

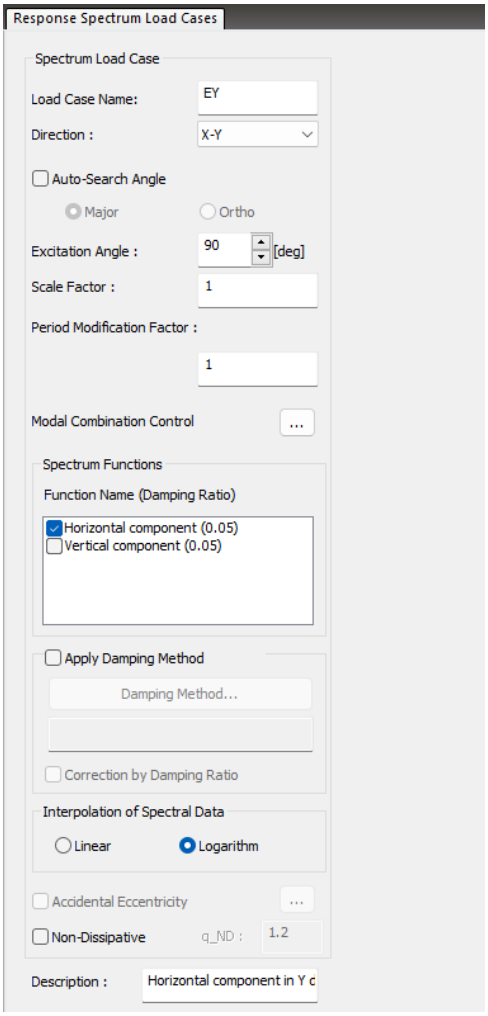


Figure 3-43. RS Load Cases command window of Midas GEN.

Using the Eigenvalues analysis control an analysis was set up according to the Lanczos method, the number of vibration modes chosen in order to have accurate results and acceptable resolution times is 60. Also, the amount of vibration modes

considered is also a function of the percentage of total mass they excite, as will be discussed later.

### 3.3.7 Combination of the actions.

For the combination of actions, reference was made to Chapter 2 of NTC18, which provides a semi-probabilistic limit state method for safety assessment based on the use of partial coefficients. For the purposes of limit state verifications, the Italian regulation defines different combinations of actions in paragraph 2.5.3 · Combination of actions. In the case of the church under study, there are three combinations of actions in the structure. The first one is called “fundamental combination” which is used for the ultimate limit state. The second combination is the seismic combination, which is used for the ultimate and operating limit states related to seismic action. The third combination considered is the characteristic combination, which is considered "rare" and is normally used for serviceability limit states. This last combination was mainly used when analyzing the displacements.

- Combinazione fondamentale, generalmente impiegata per gli stati limite ultimi (SLU):

$$\gamma_{G1} \cdot G_1 + \gamma_{G2} \cdot G_2 + \gamma_P \cdot P + \gamma_{Q1} \cdot Q_{k1} + \gamma_{Q2} \cdot \psi_{02} \cdot Q_{k2} + \gamma_{Q3} \cdot \psi_{03} \cdot Q_{k3} + \ldots \quad [2.5.1]$$

- Combinazione caratteristica, cosiddetta rara, generalmente impiegata per gli stati limite di esercizio (SLE) irreversibili:

$$G_1 + G_2 + P + Q_{k1} + \psi_{02} \cdot Q_{k2} + \psi_{03} \cdot Q_{k3} + \ldots \quad [2.5.2]$$

- Combinazione frequente, generalmente impiegata per gli stati limite di esercizio (SLE) reversibili:

$$G_1 + G_2 + P + \psi_{11} \cdot Q_{k1} + \psi_{22} \cdot Q_{k2} + \psi_{23} \cdot Q_{k3} + \ldots \quad [2.5.3]$$

- Combinazione quasi permanente (SLE), generalmente impiegata per gli effetti a lungo termine:

$$G_1 + G_2 + P + \psi_{21} \cdot Q_{k1} + \psi_{22} \cdot Q_{k2} + \psi_{23} \cdot Q_{k3} + \ldots \quad [2.5.4]$$

- Combinazione sismica, impiegata per gli stati limite ultimi e di esercizio connessi all’azione sismica E:

$$E + G_1 + G_2 + P + \psi_{21} \cdot Q_{k1} + \psi_{22} \cdot Q_{k2} + \ldots \quad [2.5.5]$$

- Combinazione eccezionale, impiegata per gli stati limite ultimi connessi alle azioni eccezionali A:

$$G_1 + G_2 + P + A_d + \psi_{21} \cdot Q_{k1} + \psi_{22} \cdot Q_{k2} + \ldots \quad [2.5.6]$$

Gli effetti dell'azione sismica saranno valutati tenendo conto delle masse associate ai seguenti carichi gravitazionali:

$$G_1 + G_2 + \sum_j \psi_{2j} Q_{kj} \,. \quad [2.5.7]$$

Figure 3-44. Action combinations NTC18, Section 2.5.3.

**Tab. 2.5.I** – *Valori dei coefficienti di combinazione*

| Categoria/Azione variabile | $\psi_{0j}$ | $\psi_{1j}$ | $\psi_{2j}$ |
|---|---|---|---|
| Categoria A - Ambienti ad uso residenziale | 0,7 | 0,5 | 0,3 |
| Categoria B - Uffici | 0,7 | 0,5 | 0,3 |
| Categoria C - Ambienti suscettibili di affollamento | 0,7 | 0,7 | 0,6 |
| Categoria D - Ambienti ad uso commerciale | 0,7 | 0,7 | 0,6 |
| Categoria E – Aree per immagazzinamento, uso commerciale e uso industriale Biblioteche, archivi, magazzini e ambienti ad uso industriale | 1,0 | 0,9 | 0,8 |
| Categoria F - Rimesse , parcheggi ed aree per il traffico di veicoli (per autoveicoli di peso ≤ 30 kN) | 0,7 | 0,7 | 0,6 |
| Categoria G – Rimesse, parcheggi ed aree per il traffico di veicoli (per autoveicoli di peso > 30 kN) | 0,7 | 0,5 | 0,3 |
| Categoria H - Coperture accessibili per sola manutenzione | 0,0 | 0,0 | 0,0 |
| Categoria I – Coperture praticabili | da valutarsi caso per caso | | |
| Categoria K – Coperture per usi speciali (impianti, eliporti, ...) | | | |
| Vento | 0,6 | 0,2 | 0,0 |
| Neve (a quota ≤ 1000 m s.l.m.) | 0,5 | 0,2 | 0,0 |
| Neve (a quota > 1000 m s.l.m.) | 0,7 | 0,5 | 0,2 |
| Variazioni termiche | 0,6 | 0,5 | 0,0 |

Figure 3-45. Values of combination coefficients - Table 2.5.1 from the NTC18.

The regulation specifies that the symbol "+" means combined with. As can be seen next to the load considered, depending on the type of combination, there are different coefficients. On the other hand, there are the combination coefficients $\psi_{oj}$ , $\psi_{1j}$ , $\psi_{2j}$ , which are given by table 2.5.1 (Figure 3-45) of the regulation. These coefficients depend on the category of use of the building and the type of action being considered.

In the case of the construction under examination, the coefficients used are those highlighted. As can be noted, in the case of roofs accessible only for maintenance, the values of these coefficients are zero in all cases.

On the other hand, in the combinations, the other coefficients that can be observed are the partial safety coefficients, which can be found in Table 2.6.1 of the Italian regulation. In order to determine them, it is first necessary to establish the type of approach. For the design of structural components that do not involve geotechnical actions the type of approach to adopt is A1.

**Tab. 2.6.I** – *Coefficienti parziali per le azioni o per l'effetto delle azioni nelle verifiche SLU*

| | | Coefficiente $\gamma_F$ | EQU | A1 | A2 |
|---|---|---|---|---|---|
| Carichi permanenti $G_1$ | Favorevoli | $\gamma_{G1}$ | 0,9 | 1,0 | 1,0 |
| | Sfavorevoli | | 1,1 | 1,3 | 1,0 |
| Carichi permanenti non strutturali $G_2$(1) | Favorevoli | $\gamma_{G2}$ | 0,8 | 0,8 | 0,8 |
| | Sfavorevoli | | 1,5 | 1,5 | 1,3 |
| Azioni variabili Q | Favorevoli | $\gamma_{Qi}$ | 0,0 | 0,0 | 0,0 |
| | Sfavorevoli | | 1,5 | 1,5 | 1,3 |

(1) Nel caso in cui l'intensità dei carichi permanenti non strutturali o di una parte di essi (ad es. carichi permanenti portati) sia ben definita in fase di progetto, per detti carichi o per la parte di essi nota si potranno adottare gli stessi coefficienti parziali validi per le azioni permanenti.

Figure 3-46. Table 2.6.I - Partial coefficients for actions- from NTC2018.

The coefficients for the combination of actions were entered by means of the command "Load Combination" in Midas GEN. For variable actions, all possible combinations were considered in order to capture the most severe combination.

Load Combination List

| | No | Name | Active | Type | Self Weight(ST) | Vault fill(ST) | Permanent structural load(ST) | Permanent non structural load(ST) | Overload(ST) | Snow(ST) | wind X+(ST) | wind X-(ST) | wind Y+(ST) | wind Y-(ST) | EX(RS) | EY(RS) | EZ(RS) |
|---|---|---|---|---|---|---|---|---|---|---|---|---|---|---|---|---|---|
| ▶ | 1 | SLU1_1 | Active | Add | 1.3000 | 1.3000 | 1.3000 | 1.3000 | 1.5000 | 0.7500 | 0.9000 | | | | | | |
| | 2 | SLU1_2 | Active | Add | 1.3000 | 1.3000 | 1.3000 | 1.3000 | 1.5000 | 0.7500 | | 0.9000 | | | | | |
| | 3 | SLU2_1 | Active | Add | 1.3000 | 1.3000 | 1.3000 | 1.3000 | 1.5000 | 0.7500 | | | 0.9000 | | | | |
| | 4 | SLU2_2 | Active | Add | 1.3000 | 1.3000 | 1.3000 | 1.3000 | 1.5000 | 0.7500 | | | | 0.9000 | | | |
| | 5 | SLU3_1 | Active | Add | 1.3000 | 1.3000 | 1.3000 | 1.3000 | 0.0000 | 1.5000 | 0.9000 | | | | | | |
| | 6 | SLU3_2 | Active | Add | 1.3000 | 1.3000 | 1.3000 | 1.3000 | 0.0000 | 1.5000 | | 0.9000 | | | | | |
| | 7 | SLU4_1 | Active | Add | 1.3000 | 1.3000 | 1.3000 | 1.3000 | 0.0000 | 1.5000 | | | 0.9000 | | | | |
| | 8 | SLU4_2 | Active | Add | 1.3000 | 1.3000 | 1.3000 | 1.3000 | 0.0000 | 1.5000 | | | | 0.9000 | | | |
| | 9 | SLU5_1 | Active | Add | 1.3000 | 1.3000 | 1.3000 | 1.3000 | 0.0000 | 0.7500 | 1.5000 | | | | | | |
| | 10 | SLU5_2 | Active | Add | 1.3000 | 1.3000 | 1.3000 | 1.3000 | 0.0000 | 0.7500 | | 1.5000 | | | | | |
| | 11 | SLU6_1 | Active | Add | 1.3000 | 1.3000 | 1.3000 | 1.3000 | 0.0000 | 0.7500 | | | 1.5000 | | | | |
| | 12 | SLU6_2 | Active | Add | 1.3000 | 1.3000 | 1.3000 | 1.3000 | 0.0000 | 0.7500 | | | | 1.5000 | | | |

Figure 3-47. Combination of the actions in Midas GEN.

As far as seismic action is concerned, the Italian regulation states that the response of the structure must be studied considering three different prevalent earthquake directions, along X, along Y and along Z. Seismic action along the prevailing direction of the earthquake is considered equal to 100%, while along the others equal to 30%. Furthermore, it is necessary to consider that seismic actions can have positive and negative signs. Ultimately, for the seismic actions the following 24 load combinations are obtained, applying the coefficients to the response spectra in the in the X, Y, Z directions equal to ±1 for the prevailing direction of the earthquake and ±0.30 for the orthogonal directions. The aforementioned is developed in the Table 3-8.

| Combination | Seismic direction | Ex | Ey | Ez |
|---|---|---|---|---|
| 1 | X | 1 | 0.3 | 0.3 |
| 2 | X | 1 | 0.3 | -0.3 |
| 3 | X | 1 | -0.3 | 0.3 |
| 4 | X | 1 | -0.3 | -0.3 |
| 5 | X | -1 | 0.3 | 0.3 |
| 6 | X | -1 | 0.3 | -0.3 |
| 7 | X | -1 | -0.3 | 0.3 |
| 8 | X | -1 | -0.3 | -0.3 |
| 9 | Y | 0.3 | 1 | 0.3 |
| 10 | Y | -0.3 | 1 | 0.3 |
| 11 | Y | 0.3 | 1 | -0.3 |
| 12 | Y | -0.3 | 1 | -0.3 |
| 13 | Y | -0.3 | -1 | 0.3 |
| 14 | Y | 0.3 | -1 | -0.3 |
| 15 | Y | 0.3 | -1 | 0.3 |
| 16 | Y | -0.3 | -1 | -0.3 |
| 17 | Z | 0.3 | 0.3 | 1 |
| 18 | Z | -0.3 | 0.3 | 1 |
| 19 | Z | 0.3 | -0.3 | 1 |
| 20 | Z | -0.3 | -0.3 | 1 |
| 21 | Z | -0.3 | 0.3 | -1 |
| 22 | Z | 0.3 | -0.3 | -1 |
| 23 | Z | 0.3 | 0.3 | -1 |
| 24 | Z | -0.3 | -0.3 | -1 |

Table 3-8. Combination of seismic actions.

Table 3-8 presents a total number of 24 seismic combinations considering that one direction prevails over the others, and moreover considering the different directions in which the seismic action can act. Further to these considerations, it is necessary to consider that seismic action is applied at the centre of gravity of the masses of each floor span. If the deck has a rectangular plan, the centre of gravity of the masses will coincide with the geometric centre of gravity.

To assume that the center of gravity of the masses coincides with the geometric center of gravity of the deck plan is the equivalent of saying that all the accidental loads are positioned so that the center of mass coincides with the geometric center of gravity of the deck. Such a situation is very unlikely to occur in reality. For this reason, “NTC2018” in paragraph 7.2.6 prescribes a measure to be taken to take account of randomness in the real position of the loads.

An incidental eccentricity with respect to its position as derived from the calculation shall be assigned to the centre of mass to consider the spatial variability of the seismic motion as well as any uncertainties. For buildings only and in the absence of more accurate determinations, the accidental eccentricity in each direction may not be less than 0.05 times the average building size measured perpendicular to the direction of

application of the seismic action. The effects of eccentricity were automatically calculated in the software.

With regard to actions other than earthquake, in the combination seismic, the permanent ones (both structural and non-structural) have coefficient 1, the actions variable actions of wind and snow in this case have a coefficient of 0 (zero).

What is important to mention is that in fact two global models were made, one considered as a "static" model and the other as a "dynamic" model. The second one is a copy of the first one with the addition of the seismic component. This was done for control purposes, since first an analysis was performed on the static model, and by checking the displacements it was understood whether the model was working correctly or not. At the beginning it was necessary to fix the lack of connection between mesh elements which gave displacements out of the acceptable ranges.

Once all these errors were fixed, the dynamic model was created. In which the modes of vibration were a fundamental element in understanding whether the connection between elements worked or not.

The two models will be of vital importance for the successive steps, in which the structural elements will be verified.

# 4

# Global analysis

Global mechanisms can be defined as those that involve the whole structure and engage the wall panels in their own plane. For the study of Frassino's church two analyses were conducted, from a static and dynamic point of view using Midas GEN. In which the deformation and stress states were evaluated.

In the case of the static study of the structure, the verification of the walls was carried out with the respective formulas prescribed by the Italian regulations, and the verification of the domes was carried out by applying a graphical method.

Finally, as far as the dynamic analysis is concerned, the vibration modes of the structure were analyzed, and the walls were verified using the corresponding standardized equations.

## 4.1 Static analysis

In carrying out the static analysis of the church, the fundamental combination is used, being the most severe combination of actions.

In the case of Midas Gen, it is possible to read the results in local coordinates, i.e., in the coordinates of each element, or in terms of the global axis of the structure. The first way presents the drawback that the elements are not always generated with the same order and with same orientation, which leads to different results between consecutive elements. For this reason, it was decided to work with the global axes of the structure, since, depending on the plane of interest, it is possible to impose the global axis.

In the assessment of the static model, the value of the displacements was of vital importance, as several mesh adjustments were made until the displacements were reasonable with the structure. For this reason, the self-weight load was of great assistance in evaluating the displacements to give an idea of whether the value of the displacements was reasonable or not.

Analyzing in the first instance, only the displacement that occurs in the z-direction due to the self-weight of the structure, from the Figure 4-1 can be seen that the most actively involved parties are the vaults and the bell tower.

Then, analyzing the fundamental combination, which turns out to be the most demanding. The results obtained were as shown in the figures Figure 4-1, Figure 4-2, Figure 4-3, Figure 4-4, Figure 4-5, Figure 4-6, Figure 4-7, Figure 4-8. The results presented are in unit of measurement centimeters (cm).

The resultant of the displacements is calculated with the following equation:

$$D_{xyz} = \sqrt{\mathrm{D}_{\mathrm{x}}^2 + \mathrm{D}_{\mathrm{y}}^2 + \mathrm{D}_{\mathrm{z}}^2} \tag{29}$$

From equation 28 it can be seen that the result obtained will always be positive, because the values are squared and then affected by a radical.

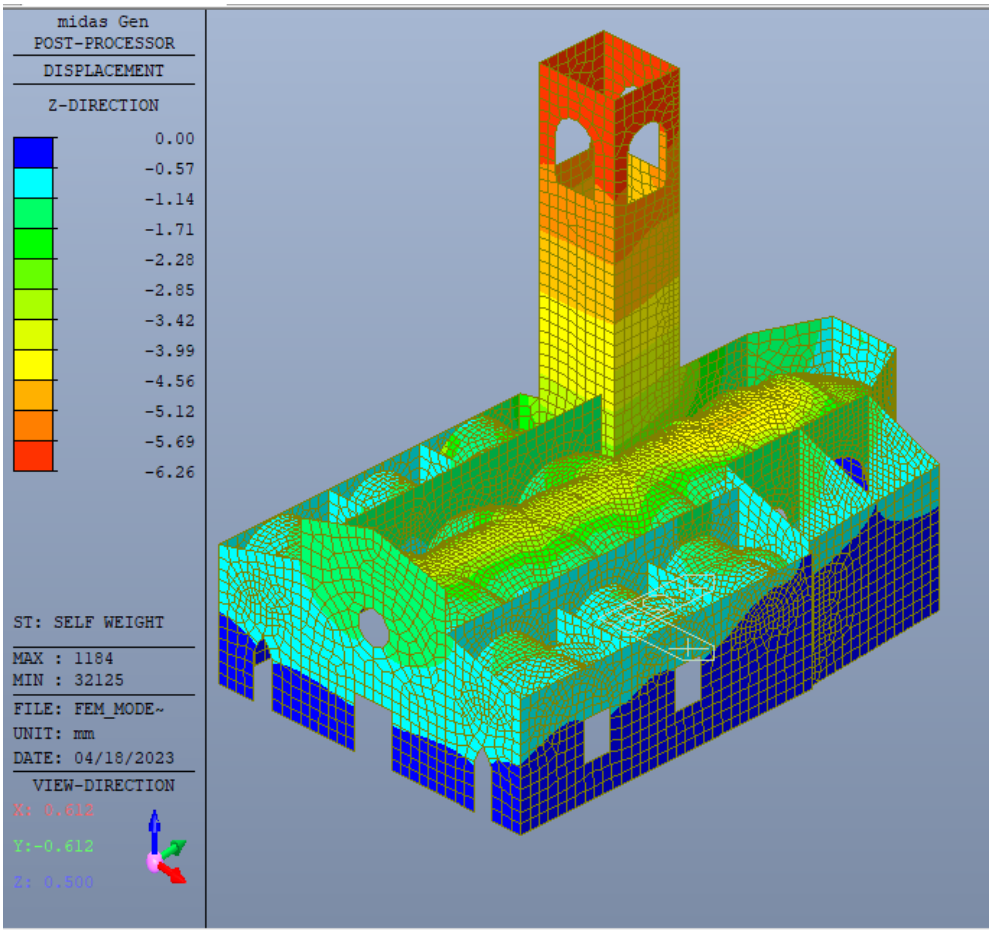


Figure 4-1. Displacement in the Z direction due to self-weight. Picture from Midas Gen.

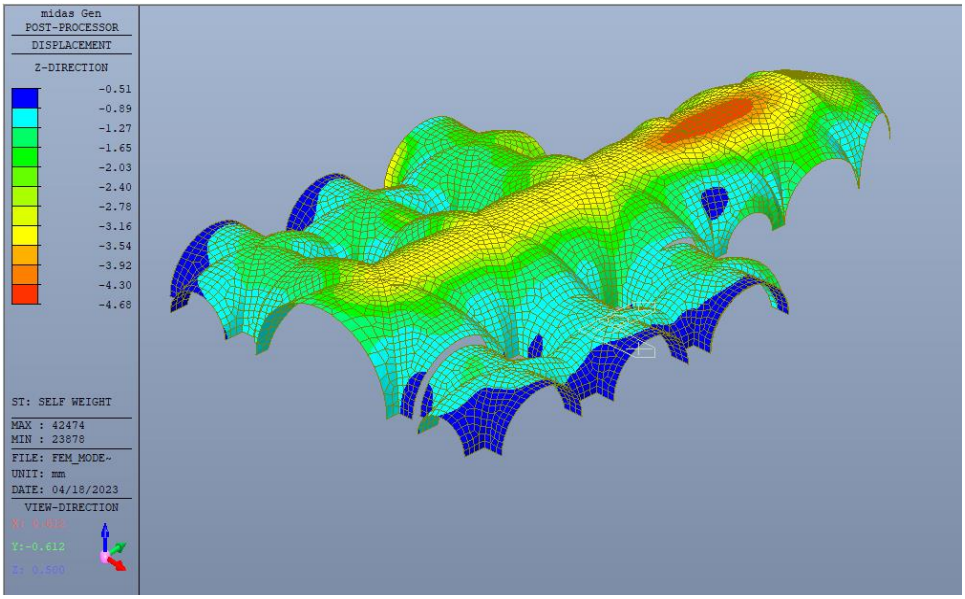


Figure 4-2. Displacements in Z direction in the vaults due to self-weight. Picture from Midas Gen.

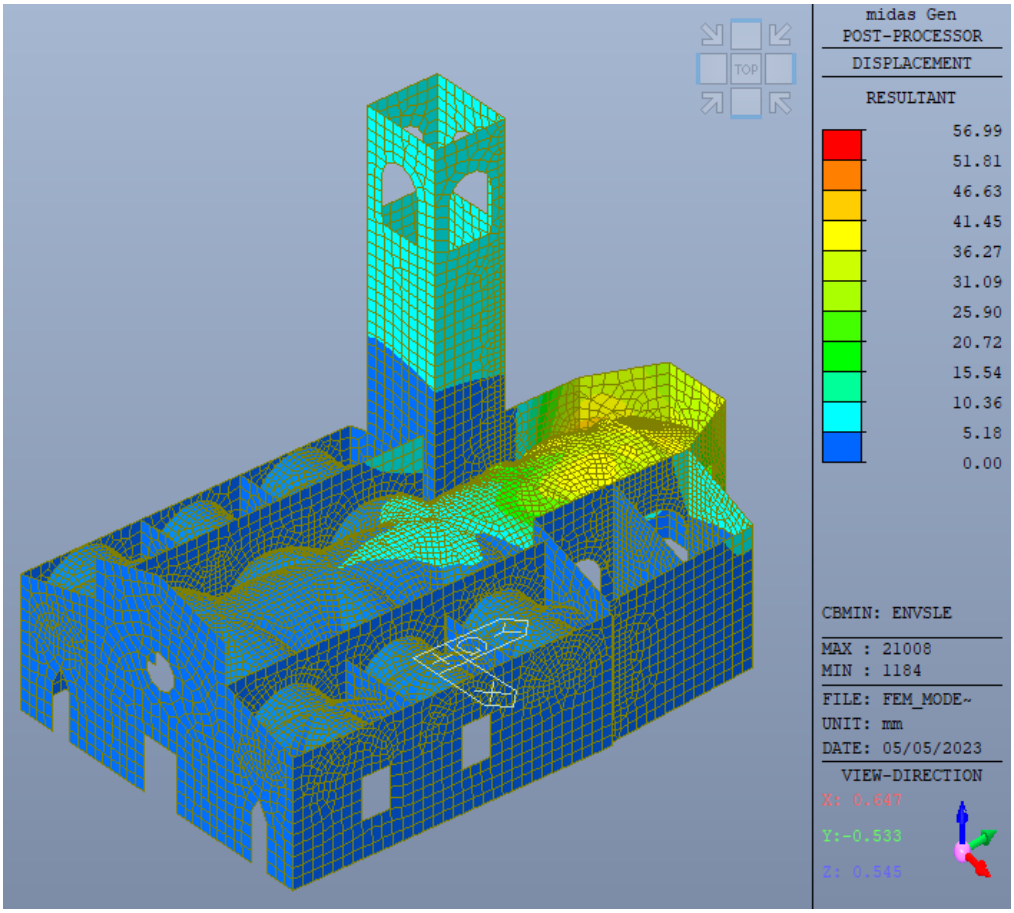


Figure 4-3. Resultant of the displacements – Serviceability Limit State (SLS) . Picture from Midas Gen.

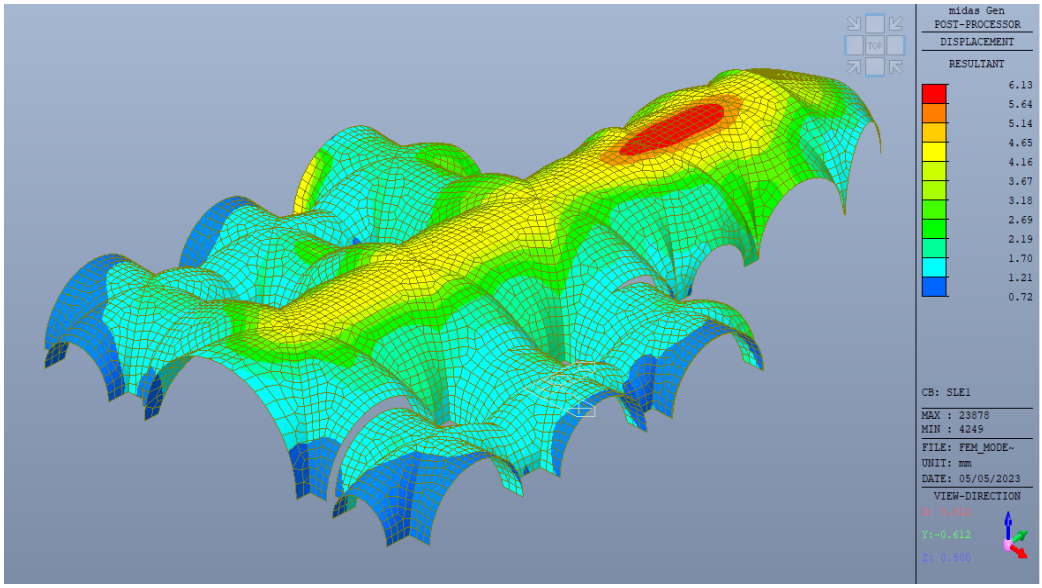


Figure 4-4. Resultant of the displacements – Serviceability Limit State (SLS) . Picture from Midas Gen.

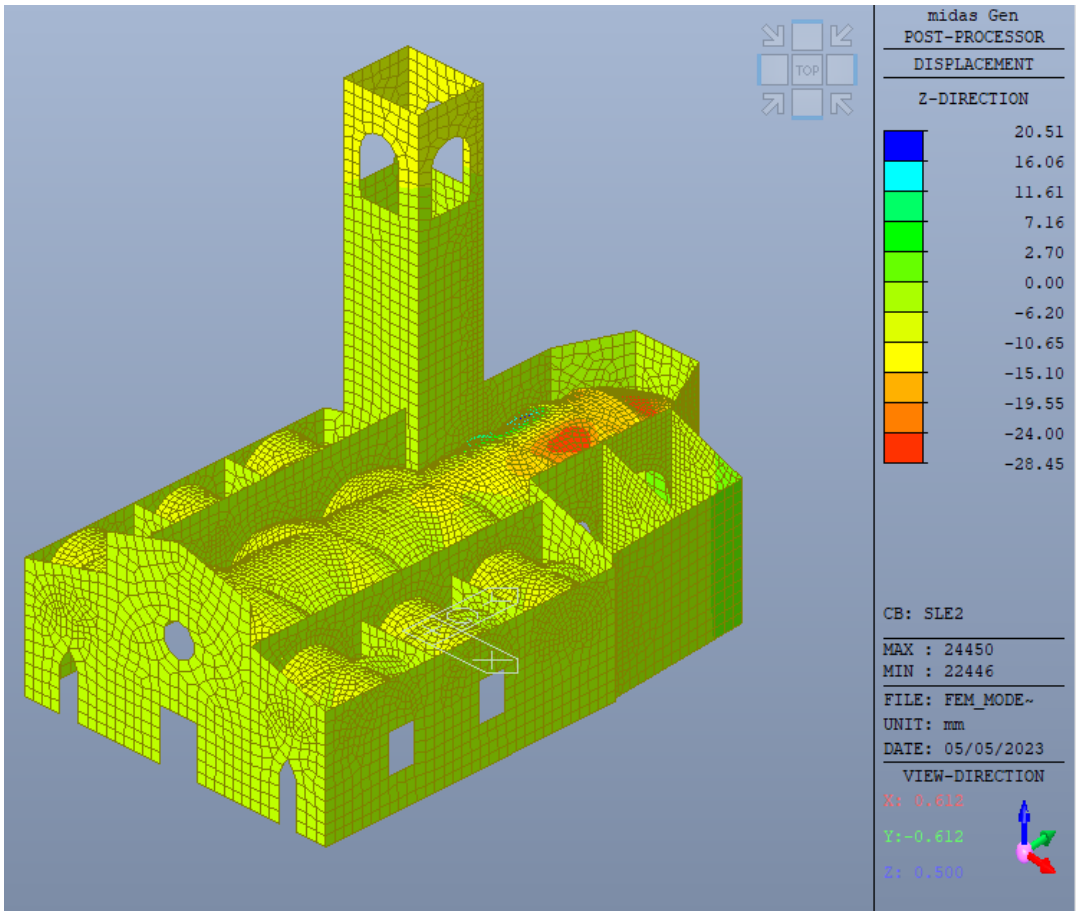


Figure 4-5. Displacements in the Z direction – Serviceability Limit State (SLS) . Picture from Midas Gen.

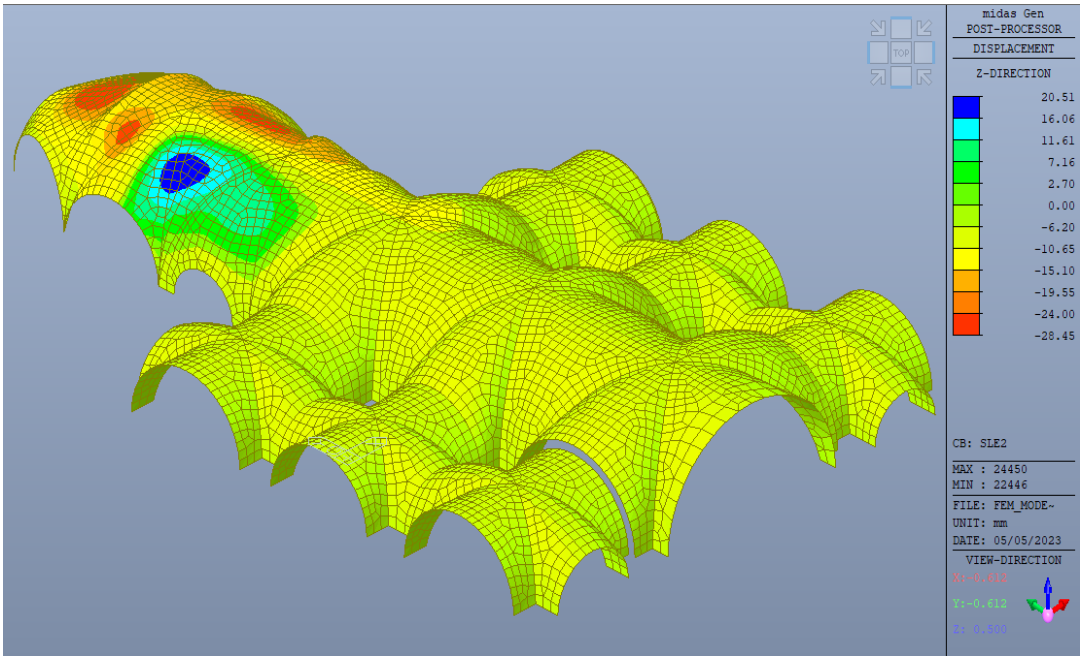


Figure 4-6. Displacements in the Z direction – Serviceability Limit State (SLS) . Picture from Midas Gen.

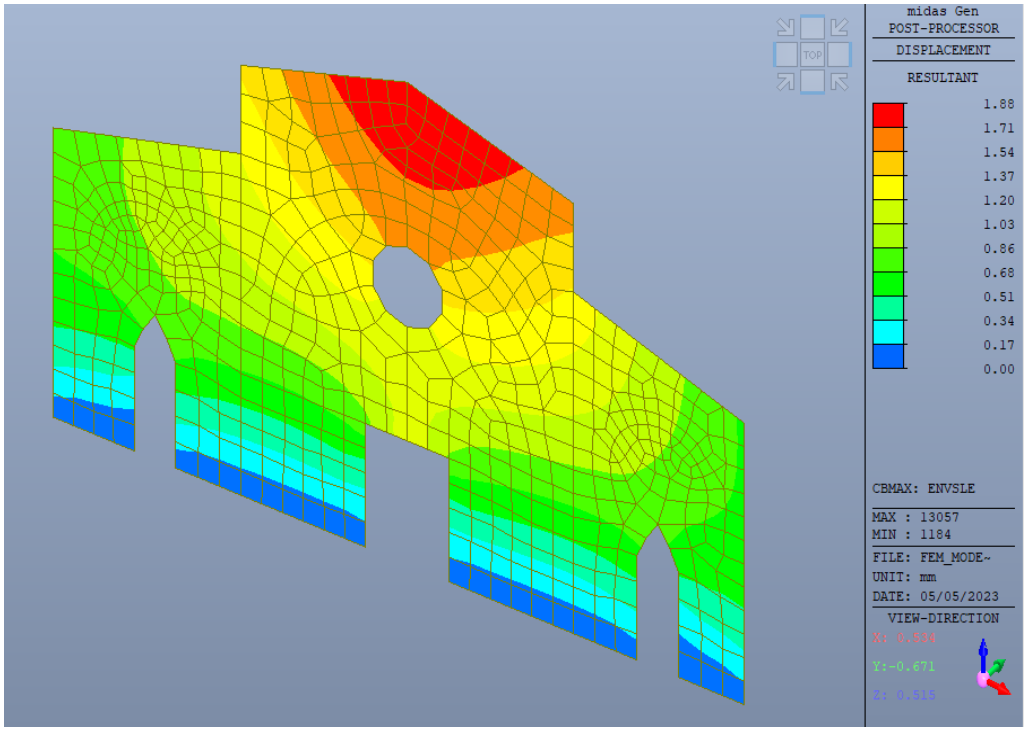


Figure 4-7. Resultant of the displacements – Serviceability Limit State (SLS) . Picture from Midas Gen.

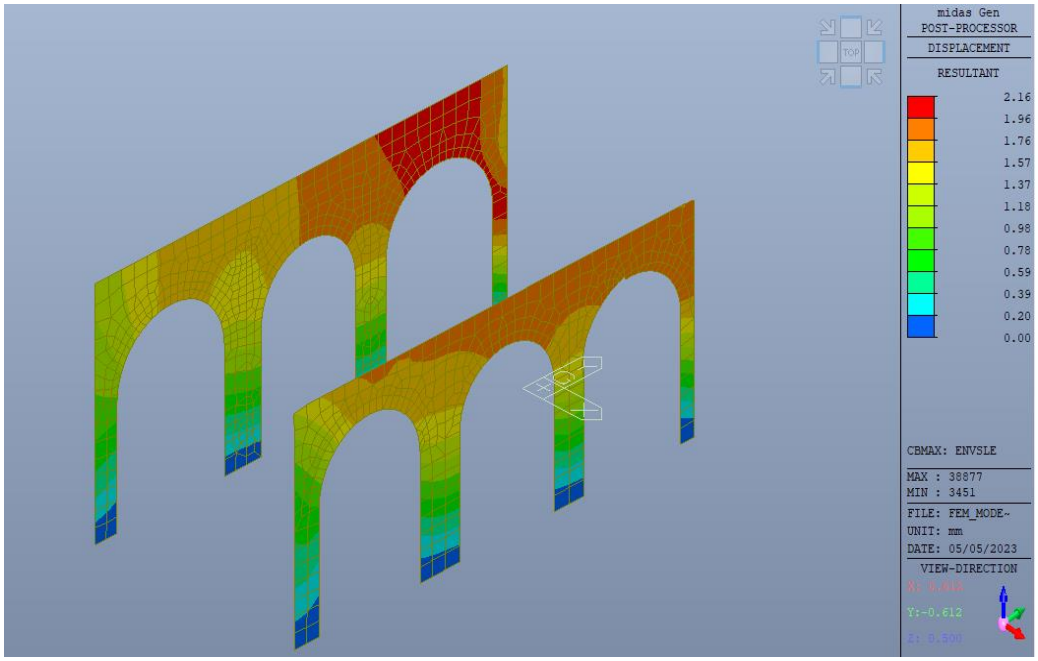


Figure 4-8. Resultant of the displacements – Serviceability Limit State (SLS) . Picture from Midas Gen.

As previously mentioned, the displacements were assessed in the serviceability limit state. Due to the load combination, the displacements are more significant.

From the Figure 4-3 it can be seen that the maximum displacement value, in terms of resultant, is at the top of the bell tower (20.72 mm). This structure is subjected to a considerable wind load, since, as specified above, this load increases with height. In addition, it must be considered that maintenance and snow load also fall directly on this part of the structure.

As far as the vaults are concerned, Figure 4-4 shows the resultant of the displacements, the maximum value is 6.13 mm. This value is found in the vicinity of the presbyterium vaults, in the middle. At the same time, it can be considered that due to the different geometry of the latter, the distribution of the forces and therefore of the displacement is not the same as that of the other vaults, which may be one of the main reasons why the displacement is higher than that of the others.

Analysing the Figure 4-7, where the displacements in the main façade can be observed, using the colour map as a guide, it can be noticed that the maximum values are given in the upper part, with a maximum value of 1.88 mm.

Figure 4-8 shows the walls of the central nave of the church, where it is possible to observe that the maximum displacement is at the top, with a value of 2.16 mm.

Regarding the evaluation of the stress state of the church, in the Midas Gen software it is possible to see the stresses acting on the various sections through the plate stresses command. At the same time the program allows us to view the stresses either at the top, at the bottom or on both sides. The choice of displaying the tensions was on both sides, where the top and bottom side stresses are shown at the same time while considering the thickness of the plate components. Also, linear interpolation is used to estimate the stresses through the thickness of the plate parts.

It is also important to understand in which direction to take the efforts, as the program allows us to work locally or globally. In the case under study, efforts were taken in the global components.

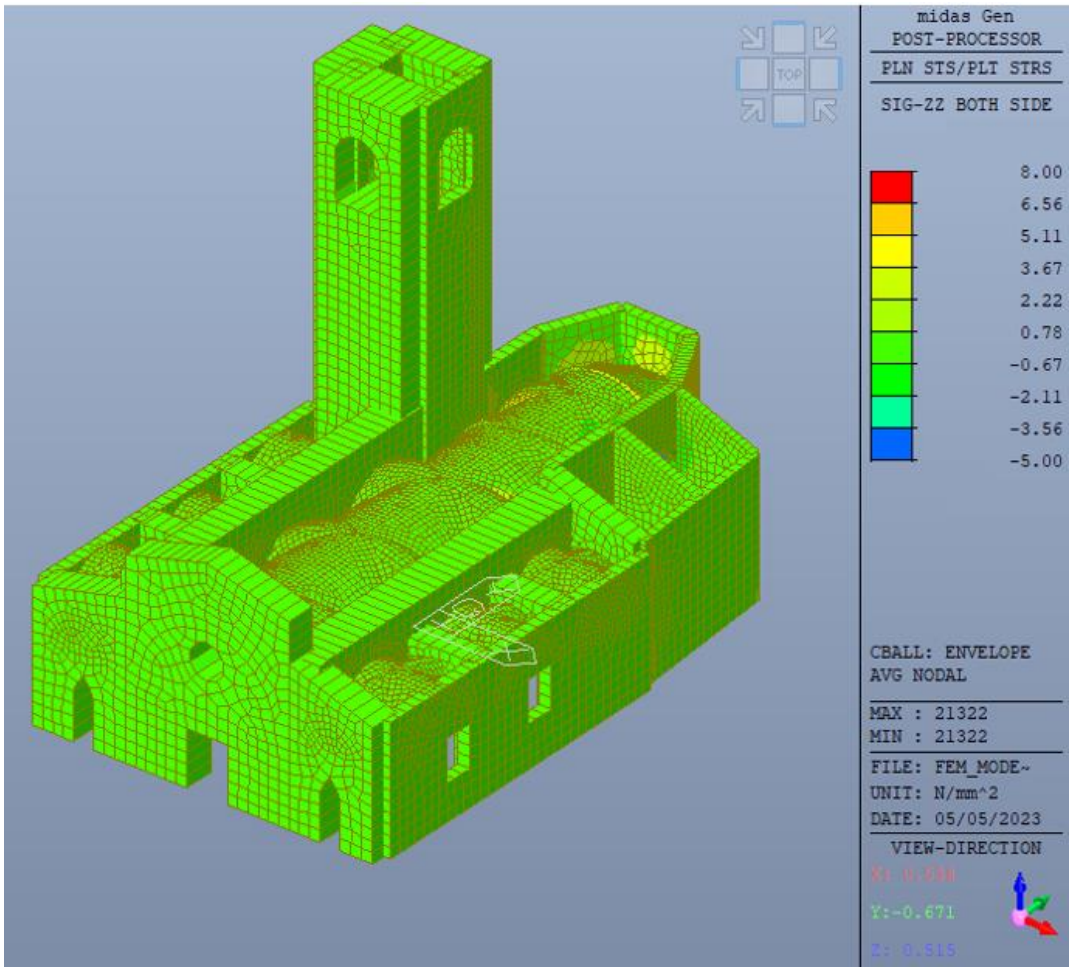


Figure 4-9. Stresses state of the Church $\sigma_{zz}$ component. Ultimate Limit State. Picture extracted from Midas Gen.

## 4.2 Dynamic analysis.

Dynamic analysis of structures is known to be divided into linear and non-linear analysis. In the case under study, a linear dynamic analysis, better known as modal analysis, was carried out.

The Italian standard, “Norme tecniche per le Costruzioni , in paragraph 7.3.3.1 defines what the linear dynamic analysis is. It states that this analysis consists of determining the modes of vibration of the construction by means of a modal analysis, and in determining the effects of seismic action, for each of the vibration modes identified.

In the case of a structure, vibrational modes are the shapes in which the structure will vibrate when it is excited. The vibrating modes of a structure are an intrinsic property, as they depend only on rigidity and mass. [18] The standard specifies that the vibration modes to be considered are those with a significant participating mass, i.e., greater than 5%. In turn, the total participating mass of the modes of vibration must be greater than 85%.

It is important to consider that during an earthquake, the maximum effects associated with one mode of vibration do not occur at the same time as the maximum effects associated with another mode of vibration. The standard specifies that these effects cannot be combined with each other by a simple sum, but a combination of the probabilistic type must be considered that considers this phase shift in time (between one mode and the other). This probabilistic combination of which the standard refers to is the “Complete Quadratic Combination”, known as CQC.

Through the Midas Gen software, it was possible to determine the vibrating modes of the structure, with the participating mass correlated to each mode. These are presented in the Table 4-1.

From the table mentioned previously, it is possible to observe that the first mode of vibration has a mass participating mainly in x, with a total of 19.781%, then mode 3 is the one in which more mass in the x-direction is mobilized. On the other hand, mode 4 is the one that moves mainly more mass in the y-direction. Finally, a significant quantity of mass mobilized in the z-direction starts to be found in mode 18, with a percentage equal to 35%.

| Mode No | Frequency | | Period | TRAN-X | | TRAN-Y | | TRAN-Z | |
|---|---|---|---|---|---|---|---|---|---|
| | (rad/sec) | (cycle/sec) | (sec) | MASS(%) | SUM(%) | MASS(%) | SUM(%) | MASS(%) | SUM(%) |
| 1 | 7.31 | 1.16 | 0.86 | 19.781 | 19.781 | 6.853 | 6.853 | 0.030 | 0.000 |
| 2 | 8.60 | 1.37 | 0.73 | 6.084 | 25.865 | 18.251 | 25.103 | 0.200 | 0.200 |
| 3 | 19.50 | 3.10 | 0.32 | 27.109 | 52.974 | 1.543 | 26.646 | 0.520 | 0.720 |
| 4 | 21.60 | 3.44 | 0.29 | 3.048 | 56.021 | 29.244 | 55.891 | 0.500 | 1.220 |
| 5 | 23.36 | 3.72 | 0.27 | 1.091 | 57.113 | 1.320 | 57.211 | 0.023 | 1.243 |
| 6 | 25.41 | 4.04 | 0.25 | 0.235 | 57.348 | 0.001 | 57.211 | 0.750 | 1.993 |
| 7 | 28.80 | 4.58 | 0.22 | 1.814 | 59.161 | 6.650 | 63.861 | 2.200 | 4.193 |
| 8 | 30.13 | 4.80 | 0.21 | 3.668 | 62.829 | 3.365 | 67.226 | 0.008 | 4.201 |
| 9 | 30.94 | 4.92 | 0.20 | 0.857 | 63.686 | 0.129 | 67.355 | 0.003 | 4.204 |
| 10 | 32.41 | 5.16 | 0.19 | 0.008 | 63.694 | 0.599 | 67.954 | 0.001 | 4.206 |
| 11 | 34.14 | 5.43 | 0.18 | 1.947 | 65.641 | 5.474 | 73.427 | 0.230 | 4.436 |
| 12 | 34.54 | 5.50 | 0.18 | 0.019 | 65.660 | 0.094 | 73.521 | 0.001 | 4.436 |
| 13 | 36.99 | 5.89 | 0.17 | 4.579 | 70.239 | 1.870 | 75.391 | 0.019 | 4.456 |
| 14 | 40.35 | 6.42 | 0.16 | 2.467 | 72.705 | 0.298 | 75.688 | 0.006 | 4.461 |
| 15 | 41.80 | 6.65 | 0.15 | 0.038 | 72.744 | 0.011 | 75.699 | 0.006 | 4.468 |
| 16 | 42.83 | 6.82 | 0.15 | 0.345 | 73.088 | 0.012 | 75.711 | 0.003 | 4.470 |
| 17 | 45.98 | 7.32 | 0.14 | 0.000 | 73.088 | 0.211 | 75.922 | 5.901 | 10.371 |
| 18 | 46.29 | 7.37 | 0.14 | 0.000 | 73.088 | 0.047 | 75.969 | 35.010 | 45.381 |
| 19 | 47.38 | 7.54 | 0.13 | 0.205 | 73.293 | 0.001 | 75.970 | 2.330 | 47.711 |
| 20 | 48.39 | 7.70 | 0.13 | 0.047 | 73.340 | 0.064 | 76.033 | 3.650 | 51.361 |
| 21 | 48.61 | 7.74 | 0.13 | 0.273 | 73.613 | 0.809 | 76.843 | 10.530 | 61.891 |
| 22 | 49.84 | 7.93 | 0.13 | 0.265 | 73.878 | 0.013 | 76.856 | 0.120 | 62.012 |
| 23 | 51.30 | 8.16 | 0.12 | 6.549 | 80.427 | 0.000 | 76.856 | 0.022 | 62.033 |
| 24 | 51.55 | 8.20 | 0.12 | 0.163 | 80.590 | 0.043 | 76.900 | 0.014 | 62.048 |
| 25 | 52.97 | 8.43 | 0.12 | 0.310 | 80.900 | 0.162 | 77.062 | 0.001 | 62.049 |
| 26 | 53.39 | 8.50 | 0.12 | 0.237 | 81.136 | 0.235 | 77.297 | 0.075 | 62.124 |
| 27 | 54.21 | 8.63 | 0.12 | 0.102 | 81.238 | 0.174 | 77.470 | 4.780 | 66.904 |
| 28 | 54.50 | 8.67 | 0.12 | 0.052 | 81.290 | 0.004 | 77.474 | 0.009 | 66.913 |
| 29 | 55.68 | 8.86 | 0.11 | 0.191 | 81.481 | 0.550 | 78.024 | 5.650 | 72.563 |
| 30 | 57.35 | 9.13 | 0.11 | 0.053 | 81.533 | 2.511 | 80.535 | 4.200 | 76.763 |
| 31 | 57.67 | 9.18 | 0.11 | 0.097 | 81.630 | 0.000 | 80.535 | 6.120 | 82.883 |
| 32 | 58.62 | 9.33 | 0.11 | 0.034 | 81.664 | 0.115 | 80.650 | 0.069 | 82.952 |
| 33 | 59.62 | 9.49 | 0.11 | 0.016 | 81.680 | 0.520 | 81.170 | 0.004 | 82.956 |
| 34 | 59.76 | 9.51 | 0.11 | 0.008 | 81.688 | 0.000 | 81.170 | 0.006 | 82.962 |
| 35 | 61.02 | 9.71 | 0.10 | 0.181 | 81.869 | 1.008 | 82.178 | 0.017 | 82.978 |
| 36 | 61.70 | 9.82 | 0.10 | 2.240 | 84.109 | 0.184 | 82.363 | 0.001 | 82.979 |
| 37 | 62.42 | 9.93 | 0.10 | 0.772 | 84.881 | 0.751 | 83.114 | 0.012 | 82.991 |
| 38 | 63.02 | 10.03 | 0.10 | 0.211 | 85.092 | 0.037 | 83.151 | 0.450 | 83.441 |
| 39 | 64.22 | 10.22 | 0.10 | 0.119 | 85.211 | 0.255 | 83.407 | 0.050 | 83.491 |
| 40 | 65.09 | 10.36 | 0.10 | 0.001 | 85.212 | 0.147 | 83.554 | 0.003 | 83.494 |
| 41 | 65.50 | 10.42 | 0.10 | 0.258 | 85.470 | 0.014 | 83.568 | 0.230 | 83.724 |
| 42 | 67.66 | 10.77 | 0.09 | 0.014 | 85.484 | 0.000 | 83.568 | 0.057 | 83.781 |
| 43 | 68.14 | 10.85 | 0.09 | 0.024 | 85.508 | 0.345 | 83.913 | 0.028 | 83.808 |
| 44 | 68.31 | 10.87 | 0.09 | 0.007 | 85.514 | 0.062 | 83.974 | 0.010 | 83.818 |
| 45 | 69.03 | 10.99 | 0.09 | 0.035 | 85.549 | 0.003 | 83.977 | 0.075 | 83.893 |
| 46 | 69.42 | 11.05 | 0.09 | 0.005 | 85.554 | 0.001 | 83.979 | 0.032 | 83.925 |
| 47 | 69.57 | 11.07 | 0.09 | 0.002 | 85.556 | 0.010 | 83.988 | 0.023 | 83.948 |
| 48 | 70.23 | 11.18 | 0.09 | 0.001 | 85.557 | 0.600 | 84.588 | 0.048 | 83.996 |
| 49 | 70.88 | 11.28 | 0.09 | 0.053 | 85.610 | 0.040 | 84.628 | 0.068 | 84.064 |
| 50 | 72.49 | 11.54 | 0.09 | 0.005 | 85.615 | 0.199 | 84.826 | 0.000 | 84.064 |
| 51 | 73.89 | 11.76 | 0.09 | 0.021 | 85.637 | 0.001 | 84.828 | 0.071 | 84.136 |
| 52 | 74.52 | 11.86 | 0.08 | 0.005 | 85.642 | 0.315 | 85.143 | 0.194 | 84.330 |
| 53 | 75.44 | 12.01 | 0.08 | 0.001 | 85.643 | 0.016 | 85.159 | 0.182 | 84.512 |
| 54 | 75.86 | 12.07 | 0.08 | 0.001 | 85.644 | 0.003 | 85.162 | 0.065 | 84.577 |
| 55 | 76.79 | 12.22 | 0.08 | 0.000 | 85.644 | 0.117 | 85.278 | 0.006 | 84.583 |
| 56 | 77.71 | 12.37 | 0.08 | 0.572 | 86.216 | 0.275 | 85.553 | 0.640 | 85.223 |
| 57 | 78.69 | 12.52 | 0.08 | 0.003 | 86.219 | 0.352 | 85.905 | 0.598 | 85.820 |
| 58 | 80.15 | 12.76 | 0.08 | 0.003 | 86.222 | 0.000 | 85.905 | 0.049 | 85.870 |
| 59 | 80.68 | 12.84 | 0.08 | 0.059 | 86.281 | 0.044 | 85.949 | 0.000 | 85.870 |
| 60 | 81.57 | 12.98 | 0.08 | 0.003 | 86.284 | 0.044 | 85.993 | 0.048 | 85.918 |

Table 4-1. Mode of vibration, frequency, period, percentage of participating mass and sum of the percentage of participating mass along X, Y and Z.

As it is known, each natural frequency has a corresponding mode, that is a shape that describes the deformation that the structure suffers. The first mode of vibration could be defined as the lowest frequency at which the deformation of the structure occurs. The Figure 4-10 represents the first mode of vibration of the building under analysis. It can be seen from the legend that is situated at the right part of the figure the percentage of mass mobilized in each direction, where the largest percentage is in the x direction.

Then, modes that mobilize a considerable amount of mass in various directions were considered. For this reason, in the figures Figure 4-11, Figure 4-12, Figure 4-13, Figure 4-14, Figure 4-15, Figure 4-16, Figure 4-17, Figure 4-18, the second, third, fourth, seventh, eighth, eleventh, thirteenth and eighteenth modes were considered.

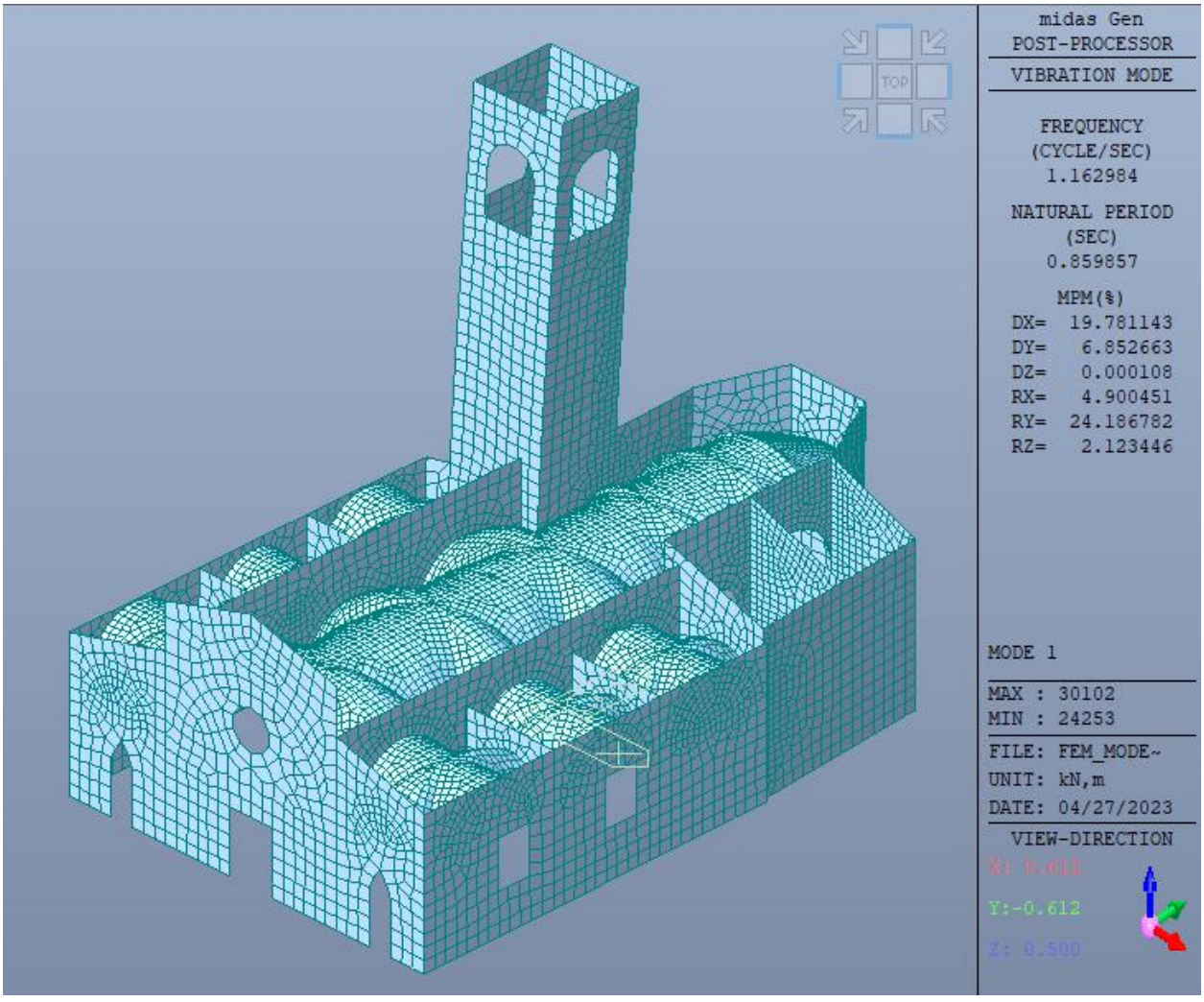


Figure 4-10. First mode of vibration. Extracted from Midas Gen.

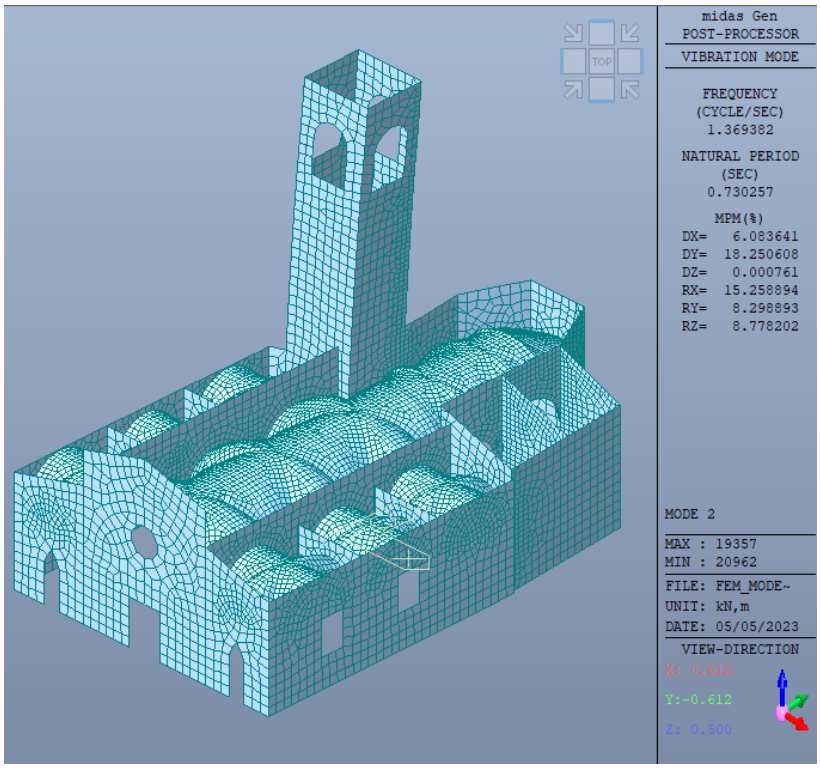


Figure 4-11. Second mode of vibration. Extracted from Midas Gen.

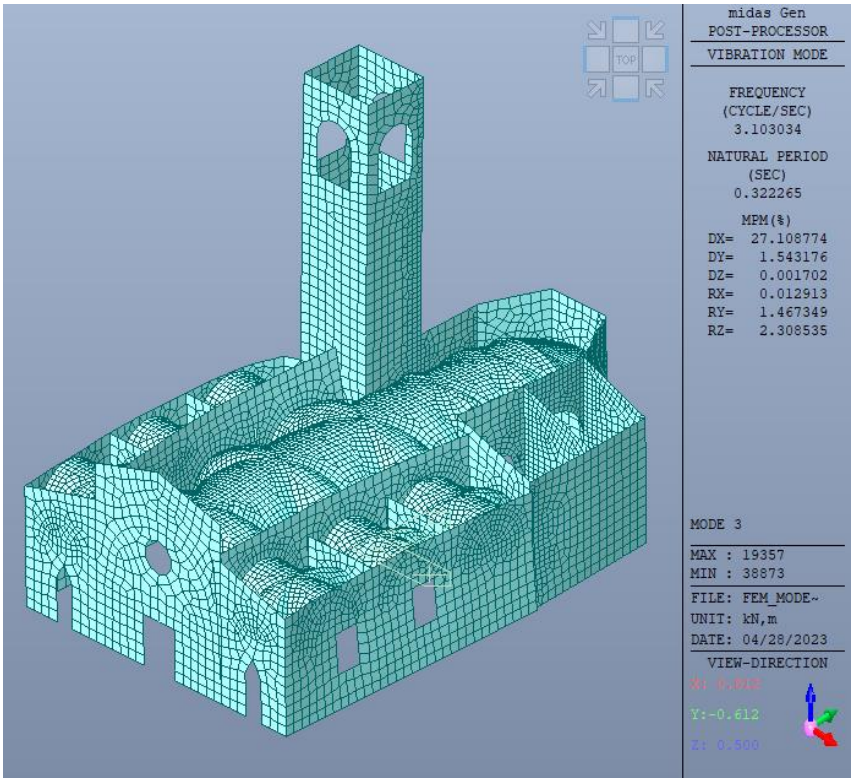


Figure 4-12. Third Mode of vibration. Extracted from Midas Gen.

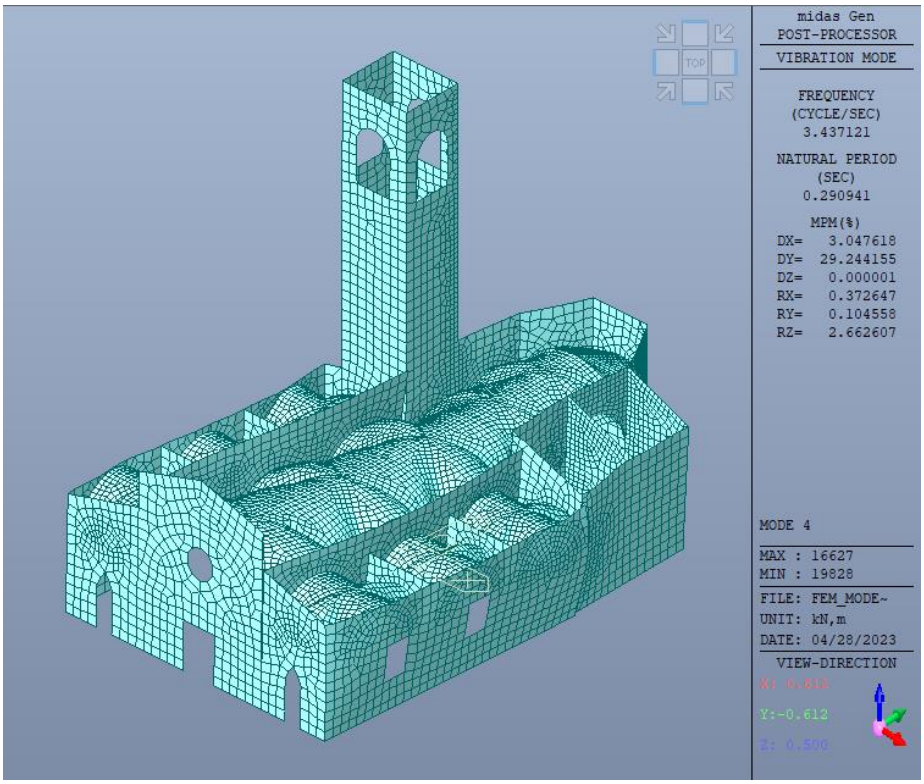


Figure 4-13. Fourth Mode of vibration. Extracted from Midas Gen.

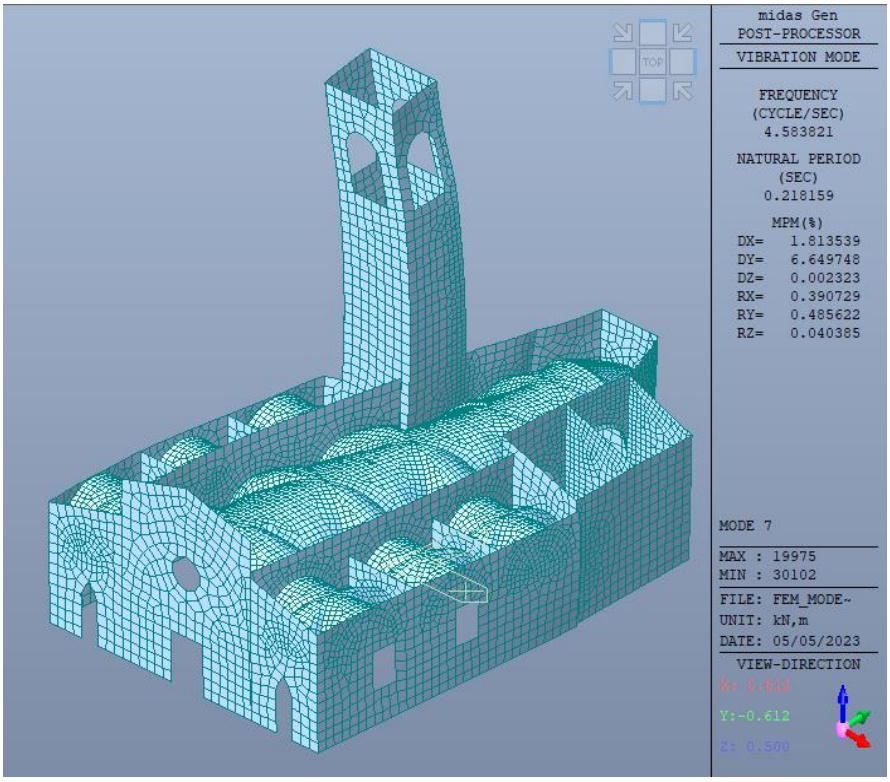


Figure 4-14. Seventh Mode of Vibration. Extracted from Midas Gen.

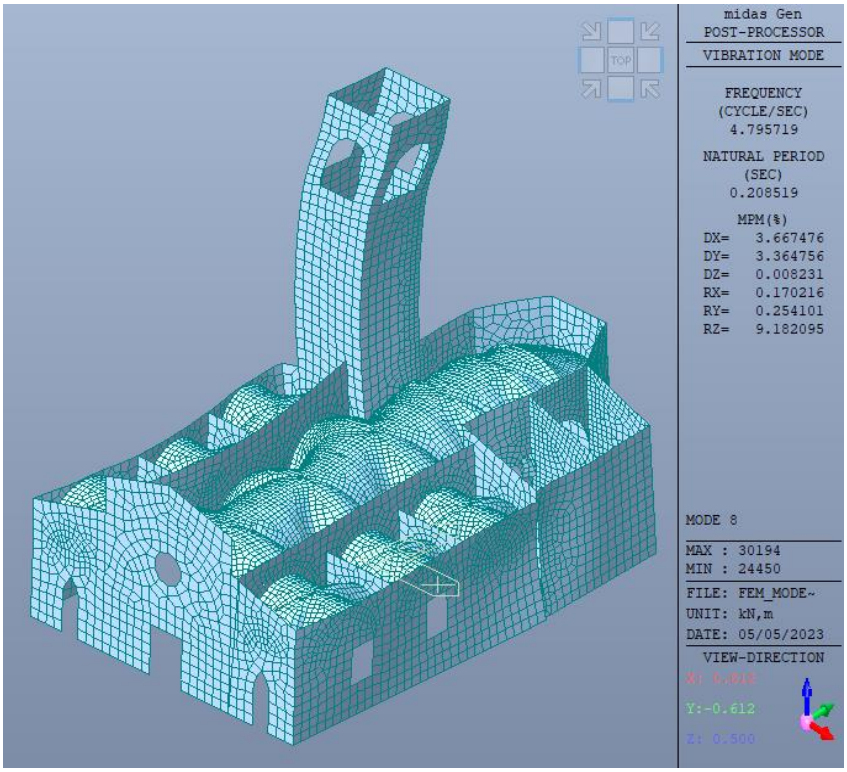


Figure 4-15. Eight Mode of Vibration. Extracted from Midas Gen.

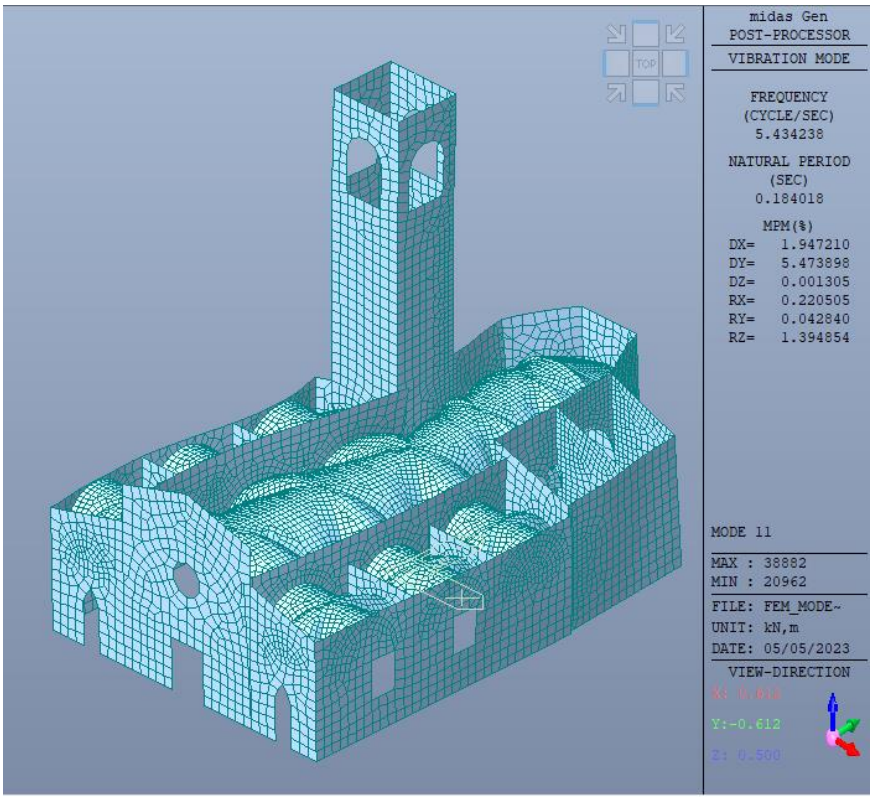


Figure 4-16. Eleventh Mode of Vibration. Extracted from Midas Gen.

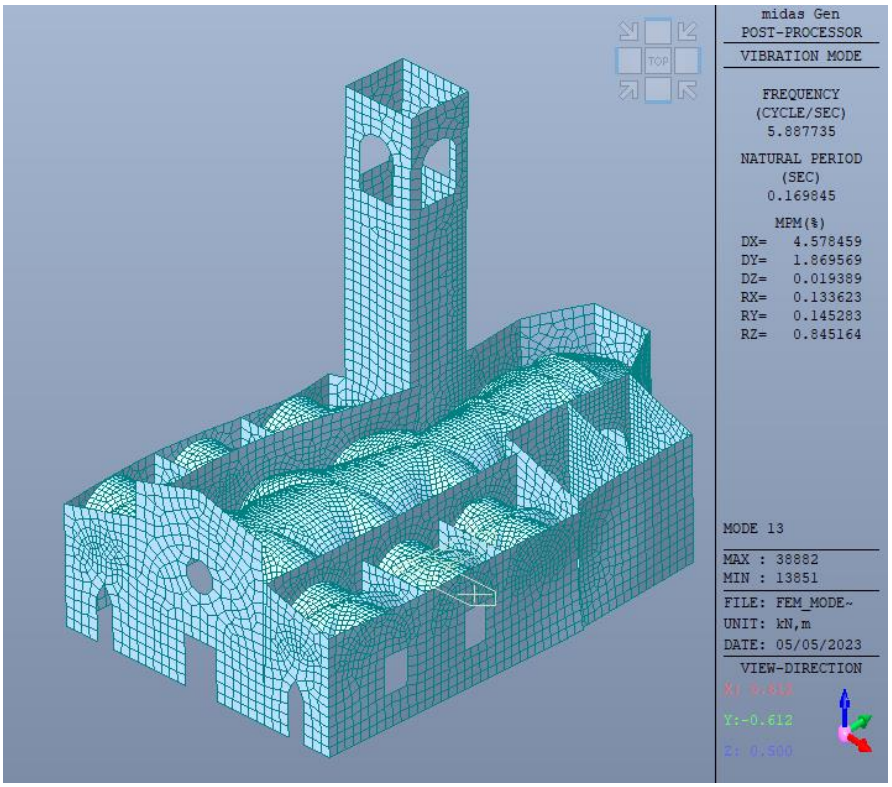


Figure 4-17. Thirteenth Mode of Vibration. Extracted from Midas Gen.

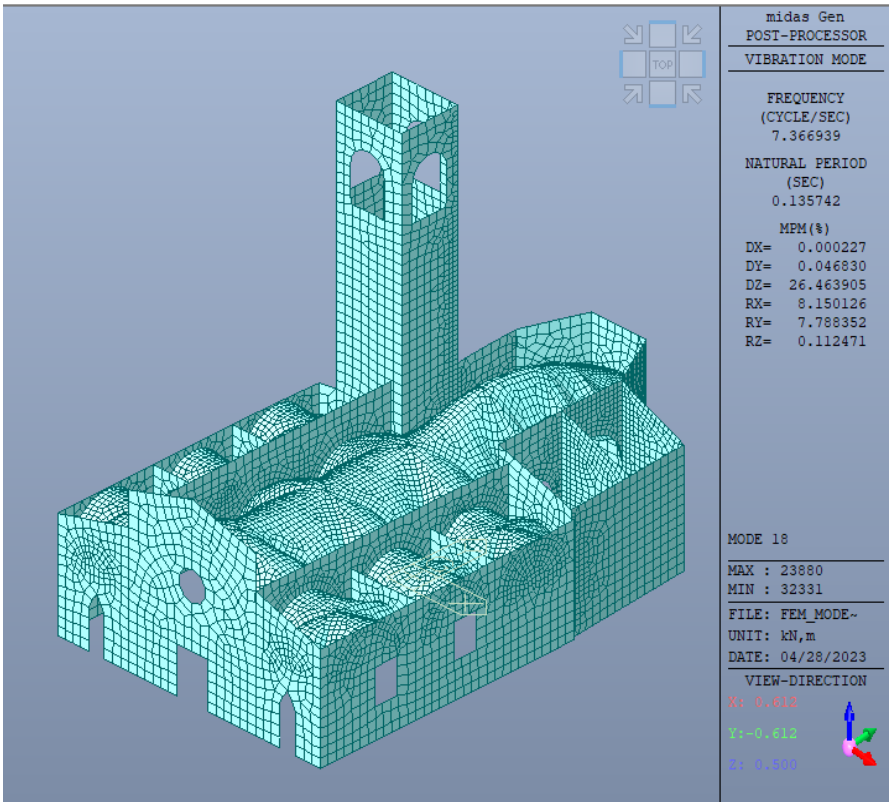


Figure 4-18. Eighteenth Mode of vibration. Extracted from Midas Gen.

Once the vibration modes were obtained the subsequent phase involved conducting an analysis of the deformation condition of the church under the ultimate limit state. This examination aimed to assess the structural response and potential deformations that may arise due to various loading conditions, including seismic forces. By evaluating the structural behaviour within the ultimate limit state, the focus was placed on identifying the critical points where damage could occur, such as excessive deflection, cracking, or failure of structural components. The assessment aimed to ensure the integrity and safety of the church under severe loading conditions, enabling appropriate mitigation measures to be implemented if necessary.

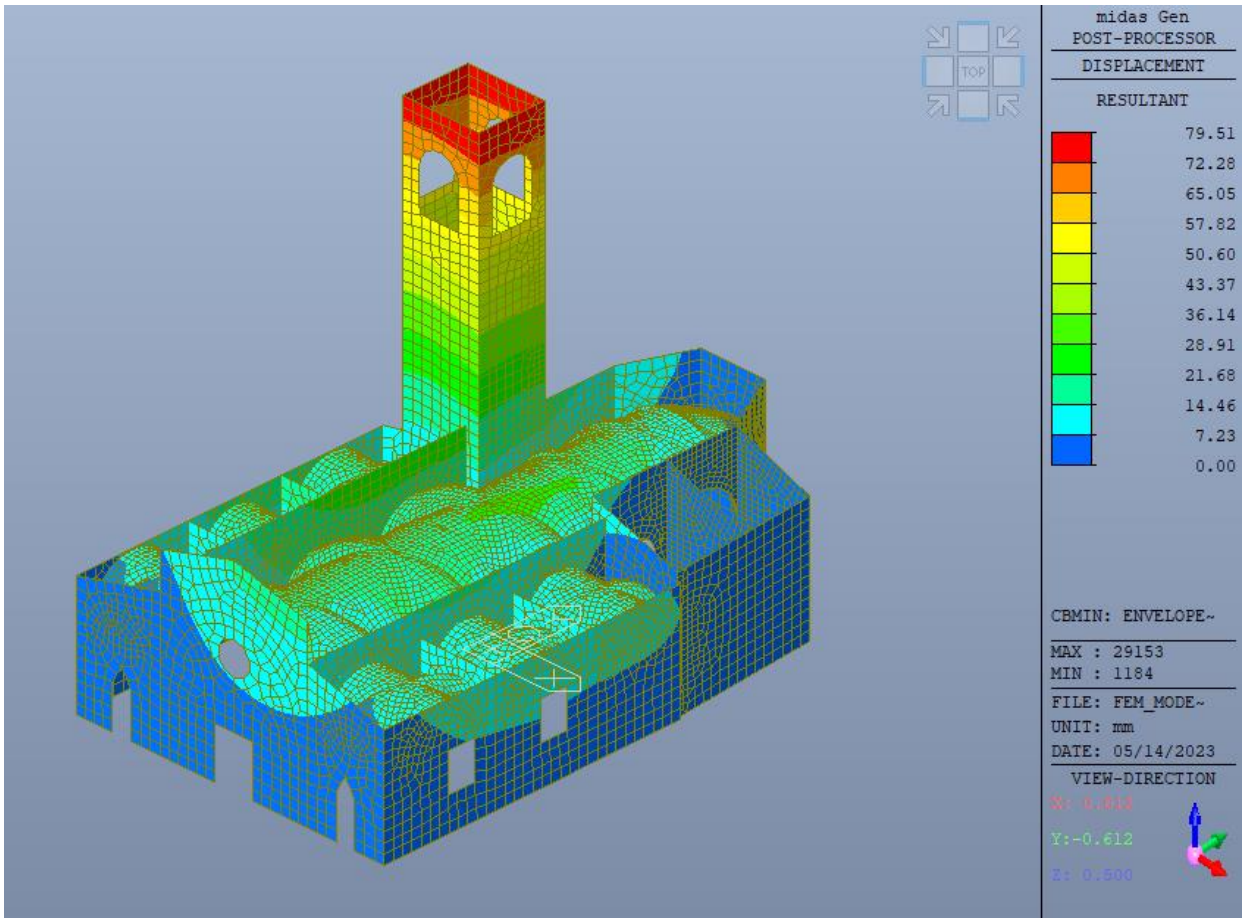


Figure 4-19. Resultant of the displacements Ultimate Limit State (SLU). Picture from Midas Gen.

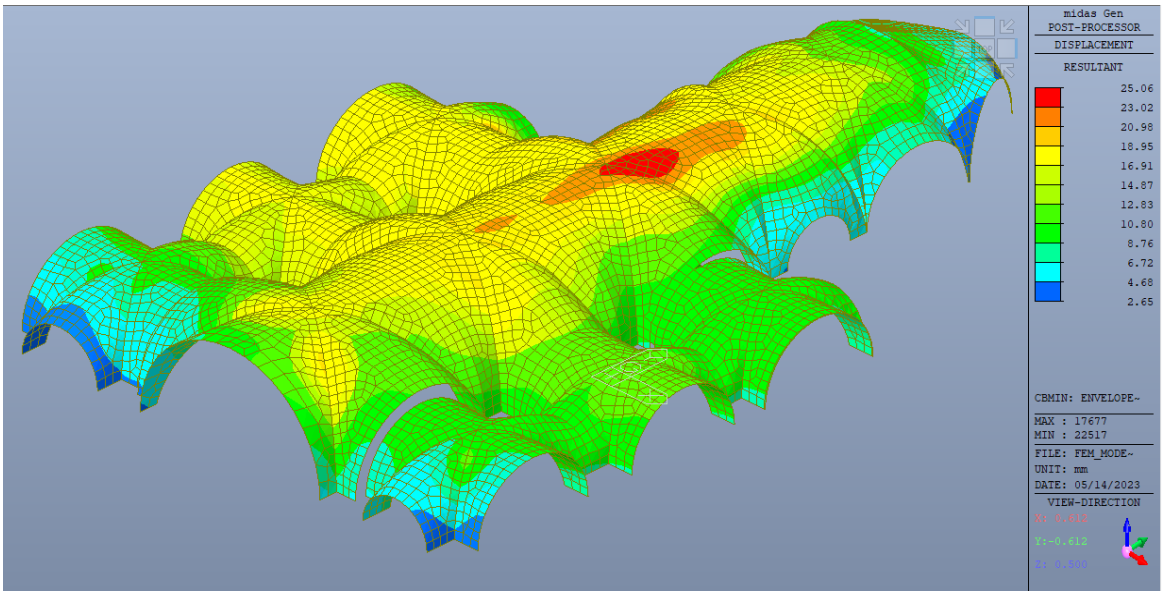


Figure 4-20. Resultant of the displacements Ultimate Limit State (SLU). Picture from Midas Gen.

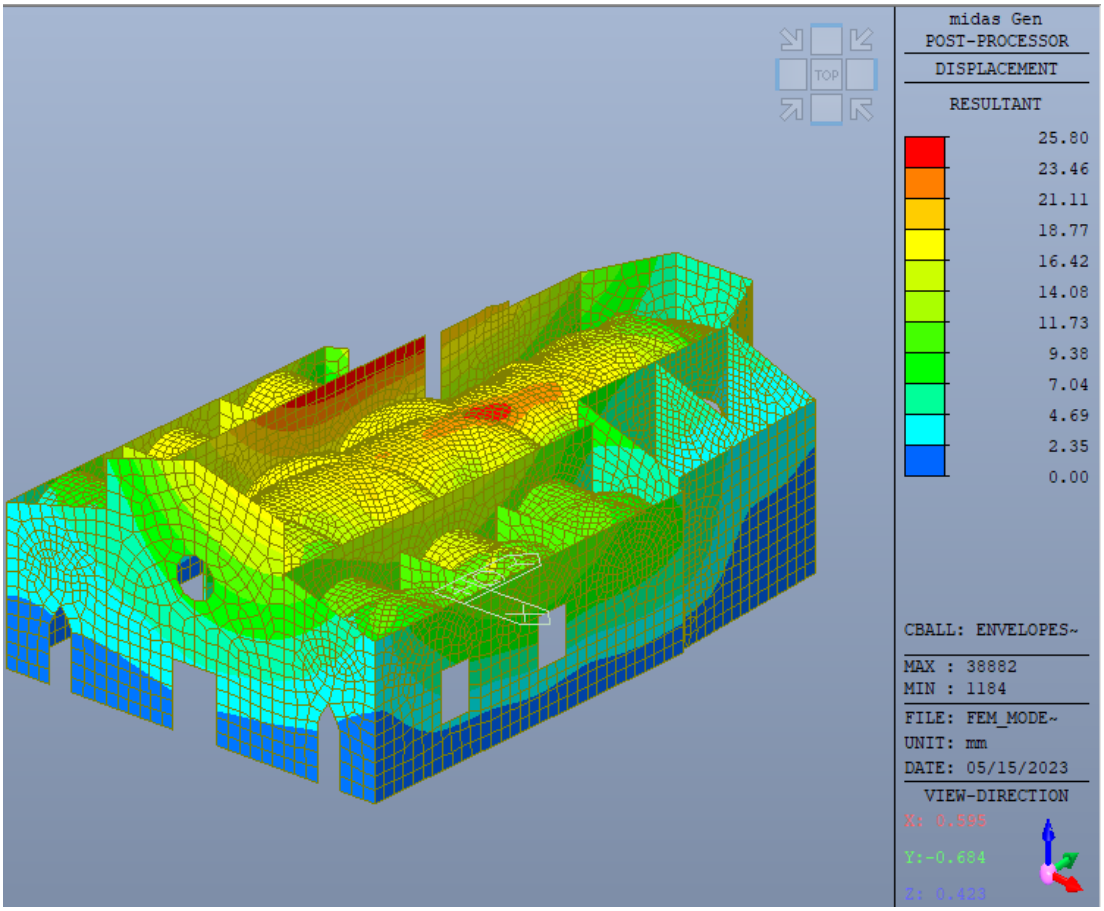


Figure 4-21. Resultant of the displacements Ultimate Limit State (SLU). Picture from Midas Gen.

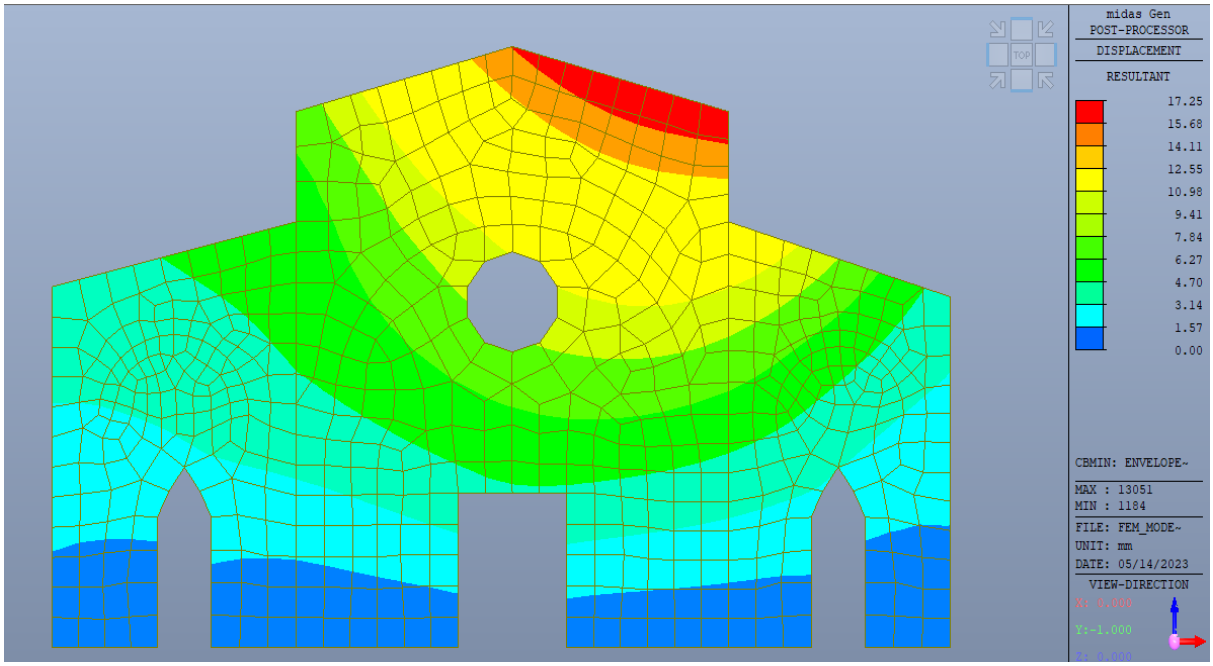


Figure 4-22. Resultant of the displacements Ultimate Limit State (SLU). Picture from Midas Gen.

From the Figure 4-19 it is possible to identify the value of the maximum displacement, which is at the tip of the bell tower, with a maximum value of 79.51mm, making a comparison with the Figure 4-3 which corresponds to the static case, there is a difference of 58.79 mm between both.

On the other hand, analysing the structure without considering the bell tower, it can be observed from the Figure 4-21 that the maximum displacement occurs in correspondence with the central walls, with a maximum value of 25.80 mm.

With regard to the vaults, the displacements can be seen in the Figure 4-20, with a value of 25.68 mm. Comparing this result with the displacement obtained in the serviceability limit state, there is a difference of 18.93 mm.

Finally, analyzing the, the displacements in the façade Figure 4-22 are equal to 17.25 mm (maximum at the top). Also in this instance, when comparing with the static case, there is a difference of 15.37 mm.

In summary, when the earthquake is introduced into the calculation model, larger displacements occur due to the higher seismic forces, the dynamic response of the structure, the nonlinear behaviour of materials, and the interaction between structural components. These factors collectively contribute to amplified displacements during a seismic event.

## 4.3 Verification of masonry walls.

The verification of masonry walls is conducted on the basis of the provisions of the Technical Standards for Construction of 2018 (NTC18). [19]

Two paragraphs of the above-mentioned regulation were used to carry out the corresponding verifications, paragraph 4.5.6.2 that is related with the statics, where the ultimate limit state will be verified and the paragraph 7.8.2.2 where in addition verifications to be carried out due to the Life-sustaining limit state (SLV).

The regulation specifies that the ultimate limit states to be verified are [12] :

- Bending for lateral loads (strength and stability out of plane).
- Axial and bending in the plane.
- Axial and bending out of plane.
- Shear for actions in the plane of the wall.
- Concentrated loads.
- Bending and shear of coupling beams.

The limit states that were then specified to be verified are the ultimate limit state and the life sustaining limit state. As far as the exercise limit state, known in the Italian standard as SLE, is concerned, it is not necessary to perform verifications on this state as long as the ultimate limit state is satisfactory. [12]

Due to the fact that the walls have different types of openings (doors and windows), they were divided into different sections called “fasce di piano” in Italian, that are those portions of masonry placed between two vertically overlapping openings and connecting the “maschio”. They are also called coupling beams as their behavior is similar to that of squat beams connecting masonry “maschio”. On the other hand, is called “maschio murario” to the portions of masonry that develop vertically with continuity from the foundations to the top.

Once the wall had been identified and divided into “maschi e fascie”, the stresses acting on it were determined. The result that was obtained from the calculation program, through the implementation of the finite element method are the compressive, tensile, and tangential stresses at each point of the mesh with which the walls are discretized.

So, to obtain the stress characteristics, it is necessary to integrate the stresses acting in the wall panels in the section of interest and compare these values with the resistance.[20]

This operation was performed in Midas Gen with a function called “Local Direction Force Sum” that provides internal forces on a selected plane in a plate element, it possible also to select the load cases and the load combination of interest. [21]

The walls considered for the verifications are the façade, the perimeter walls alongside the aisles, the walls adjacent to the nave and the walls of the presbytery. In order to give a better understanding of the division of the walls and the sectorization of the verifications, a guide plan is given by the Figure 4-23, where each wall is represented with a number.

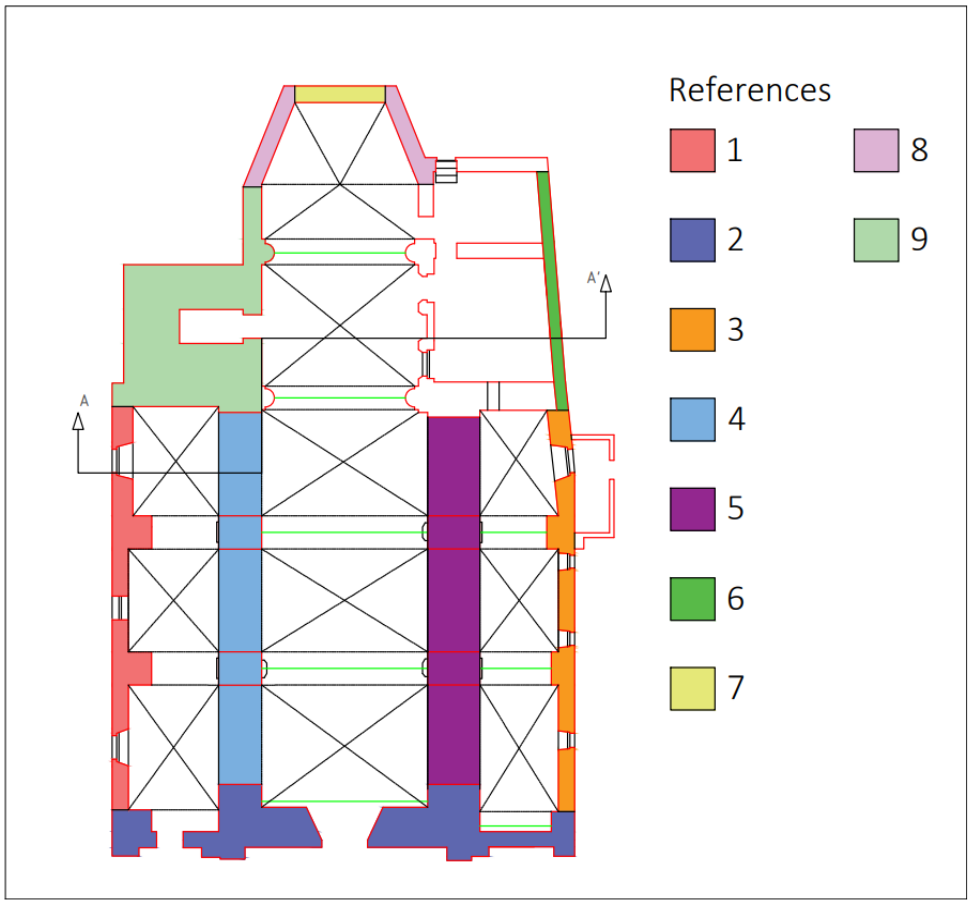


Figure 4-23. Walls under verification.

The above mentioned and described was applied for all verifications to be carried out on the walls.

### 4.3.1 Bending for lateral loads

To verify the bending for lateral loads a calculation sheet was made, which was made following the formula given by the regulation, which is as follows.

The reduced design unit resistance $f_{d,rid}$ referred to the structural element is assumed to be equal to (formulation 4.5.4 from the NTC2018):

$$f_{d,rid} = \phi f_d \tag{30}$$

Where :

$\Phi$ is the material strength reduction coefficient, it depends on the slenderness $\lambda$ and on the eccentricity coefficient m.

The first step, thus, was to determine the eccentricity. The eccentricities of the vertical loads on the masonry thickness are due to the total eccentricities of the vertical loads, execution tolerances and horizontal actions. They can be determined conventionally using the following criteria. [12]

1. Total eccentricity of vertical loads (equation 4.5.7 from the NTC2018):

$$e_{s1} = \frac{N_1 d_1}{N_1 + \sum N_2} \qquad e_{s2} = \frac{\sum N_2 d_2}{N_1 + \sum N_2} \tag{31}$$

Where:

- $e_{s1}$ is the eccentricity of the resultant of the loads transmitted by the walls of the upper floors with respect to the mean plane of the wall to be verified.
- $e_{s2}$ eccentricity of the support reactions of the floors above the verification section.
- $N_1$ load transmitted by the overlying wall assumed to be centered with respect to the wall.
- $N_2$ support reaction of floors above the wall to be verified.
- $d_1$ eccentricity of N1 with respect to the mean plane of the wall to be verified.
- $d_2$ eccentricity of N2 with respect to the mean plane of the wall to be verified.

It is important to consider that the eccentricities could be negative or positive. [12]

2. Eccentricity due to construction tolerances (equation 4.5.8 from the NTC2018):

Given the morphological and dimensional tolerances associated with masonry building construction technologies, it is necessary to consider an eccentricity $e_a$, that is equal to:

$$e_a = \frac{h}{200} \tag{32}$$

Where h is equal to the internal floor height.

3. Total eccentricity due to horizontal actions considered acting in the direction normal to the plane of the masonry (equation 4.5.9 from the NTC2018):

$$e_v = \frac{M_v}{N} \tag{33}$$

Where:

$M_v$ and $N$ are , respectively, the maximum bending moment due to horizontal actions and the normal stress in the relevant verification section.

The final value of the eccentricity to be considered is a result of the combination between the above calculated eccentricities. The combination to made is given by the following equation (equation 4.5.10 from the NTC2018).

$$e_1 = |e_s| + e_a$$
$$e_2 = \frac{e_1}{2} + |e_v| \tag{34}$$

The value of $e = e_1$ is adopted for the verification of walls in their end sections, while the value of $e = e_2$ is adopted for the verification of the section where the value of Mv

is maximum. The calculation eccentricity e may not, however, be assumed to be less than $e_a$.

In any case, where to result (equation 4.5.11 from the NTC2018):

$$e_1 \leq 0.33\,t \qquad e_2 \leq 0.33\,t \tag{35}$$

Once the eccentricities had been determined, once the eccentricities had been determined, the second step was to calculate the slenderness. It is known that second order effects can be controlled by the wall slenderness, it is defined as follows (equation 4.5.1 from the NTC2018):

$$\lambda = \frac{h_0}{t} \tag{36}$$

Where:

$h_0$ is the free length of wall deflection assessed according to edge constraint conditions.

t is the wall thickness.

The slenderness could not be higher than 20.

The free length of wall deflection is calculated according to the following equation (equation 4.5.5 from the NTC2018).

$$h_0 = \rho h \tag{37}$$

Where:

$\rho$ considers the effectiveness of the constraint provided by the orthogonal walls. It takes the value 1 for isolated wall, the value of 1 was the value chosen to perform the checks, which is already the worst situation.

$h$ is the internal floor height.

The last parameter to be calculated is the eccentricity coefficient, which is defined by the following relation (equation 4.5.6 from the NTC2018):

$$m = \frac{6e}{t} \tag{38}$$

Finally, with the slenderness and with the eccentricity coefficient Is possible to determine the reduction factor ϕ, the table 4.5.III of the Italian Standard was used. As will be seen below, in many cases the values of the slenderness and eccentricity coefficient did not correspond exactly to the values provided in the table, and in these cases a linear interpolation was necessary.

**Tab. 4.5.III** -*Valori del coefficiente Φ con l'ipotesi della articolazione (a cerniera)*

| Snellezza λ | Coefficiente di eccentricità m = 6 e/t | | | | |
|---|---|---|---|---|---|
| | 0 | 0,5 | 1,0 | 1,5 | 2,0 |
| 0 | 1,00 | 0,74 | 0,59 | 0,44 | 0,33 |
| 5 | 0,97 | 0,71 | 0,55 | 0,39 | 0,27 |
| 10 | 0,86 | 0,61 | 0,45 | 0,27 | 0,16 |
| 15 | 0,69 | 0,48 | 0,32 | 0,17 | |
| 20 | 0,53 | 0,36 | 0,23 | | |

Figure 4-24. Table 4.5.III extracted from the NTC2018.

The following are the calculations carried out to verify the various walls that form part of the structure.

At the time of the verification of the walls due to bending for lateral loads, from the formulations showed before it is possible to notice that two stresses are important: the normal force and the moment due to lateral loads. It may happen that the maxima are not found in the same load combination, for this reason it is necessary to analyze all load combinations, until the worst one is found.

Wall 1: This wall is related to the north walls, from the Figure 4-25 can be seen that the element was divided in seven different parts regarding the “fascia” and “maschio”, the stresses of each element were taken at the base. In order to minimize the number of tables inserted throughout the work, only the Table 4-3 and Table 4-2 were inserted which correspond to the “fascia” and “maschio” with higher stress values.

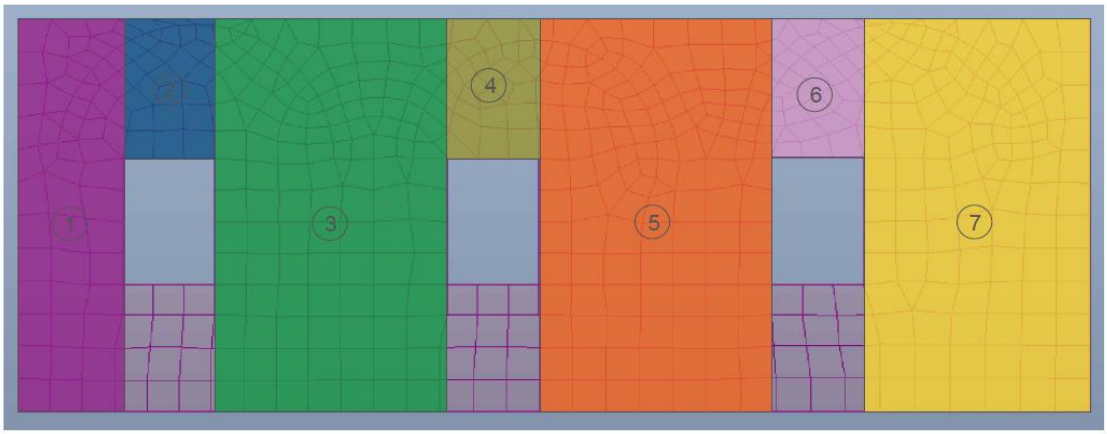


Figure 4-25. Wall N°1 - division. Image from Midas Gen.

| Combination 1 (N max) | | | |
|---|---|---|---|
| Load | N | -181 | kN |
| | Mv | 10 | kNm |
| | N1 | 0.00 | kN |
| | N2 | 0.00 | kN |
| Geometrical parameters | | | |
| | t | 0.7 | m |
| | l | 1.6 | m |
| | h | 2.6 | m |
| | d1 | 0 | m |
| | d2 | 0 | m |
| Eccentricity | | | |
| | es1 | 0.0000 | m |
| | es2 | 0.0000 | m |
| | ea | 0.0128 | m |
| | ev | -0.0570 | m |
| | e1 | 0.0128 | m |
| | e2 | 0.0634 | m |
| | e1/t | 0.0182 | Verify |
| | e2/t | 0.0905 | Verify |
| | e | 0.0128 | m |
| | e | 0.0634 | m |
| Verification | ρ | 1 | |
| | h0 | 2.55 | m |
| | λ | 3.643 | m |
| | λ<20 | Verifica | |
| | m | 0.109 | m |
| | Φ | 0.970 | |
| | FC | 1.2 | |
| | γM | 3 | |
| | fk | 1500 | kN/m2 |
| | fd | 417 | kN/m2 |
| | fd,rid | 404 | kN/m2 |
| | σ | -158 | kN/m2 |
| | σ/fd,rid | 39% | Verify |

| Combination 2 (Mv max) | | | |
|---|---|---|---|
| Load | N | -166 | kN |
| | Mv | 17 | kNm |
| | N1 | 0.00 | kN |
| | N2 | 0.00 | kN |
| Geometrical parameters | | | |
| | t | 0.7 | m |
| | l | 1.6 | m |
| | h | 2.6 | m |
| | d1 | 0 | m |
| | d2 | 0 | m |
| Eccentricity | | | |
| | es1 | 0.0000 | m |
| | es2 | 0.0000 | m |
| | ea | 0.0128 | m |
| | ev | -0.1010 | m |
| | e1 | 0.0128 | m |
| | e2 | 0.1074 | m |
| | e1/t | 0.0182 | Verify |
| | e2/t | 0.1534 | Verify |
| | e | 0.0128 | m |
| | e | 0.1074 | m |
| Verification | ρ | 1 | |
| | h0 | 2.55 | m |
| | λ | 3.643 | m |
| | λ<20 | Verifica | |
| | m | 0.921 | m |
| | Φ | 0.710 | |
| | FC | 1.2 | |
| | γM | 3 | |
| | fk | 1500 | kN/m2 |
| | fd | 417 | kN/m2 |
| | fd,rid | 296 | kN/m2 |
| | σ | -146 | kN/m2 |
| | σ/fd,rid | 49% | Verify |

Table 4-2. Verification of the section 2 of the wall 1.

| Combination 1 (N max) | | | |
|---|---|---|---|
| Load | N | -604 | kN |
| | Mv | -38 | kNm |
| | N1 | 0.00 | kN |
| | N2 | 0.00 | kN |
| Geometrical parameters | | | |
| | t | 0.7 | m |
| | l | 3.5 | m |
| | h | 7.2 | m |
| | d1 | 0 | m |
| | d2 | 0 | m |
| Eccentricity | | | |
| | es1 | 0.0000 | m |
| | es2 | 0.0000 | m |
| | ea | 0.0360 | m |
| | ev | 0.0624 | m |
| | e1 | 0.0360 | m |
| | e2 | 0.0804 | m |
| | e1/t | 0.0514 | Verify |
| | e2/t | 0.1149 | Verify |
| | e | 0.0360 | m |
| | e | 0.0804 | m |
| Verification | ρ | 1 | |
| | h0 | 7.2 | m |
| | λ | 10.286 | m |
| | λ<20 | Verifica | |
| | m | 0.309 | m |
| | Φ | 0.700 | |
| | FC | 1.2 | |
| | γM | 3 | |
| | fk | 1500 | kN/m2 |
| | fd | 417 | kN/m2 |
| | fd,rid | 292 | kN/m2 |
| | σ | -244 | kN/m2 |
| | σ/fd,rid | 84% | Verify |

| Combination 2 (Mv max) | | | |
|---|---|---|---|
| Load | N | -604 | kN |
| | Mv | -38 | kNm |
| | N1 | 0.00 | kN |
| | N2 | 0.00 | kN |
| Geometrical parameters | | | |
| | t | 0.7 | m |
| | l | 3.5 | m |
| | h | 7.2 | m |
| | d1 | 0 | m |
| | d2 | 0 | m |
| Eccentricity | | | |
| | es1 | 0.0000 | m |
| | es2 | 0.0000 | m |
| | ea | 0.0360 | m |
| | ev | 0.0624 | m |
| | e1 | 0.0360 | m |
| | e2 | 0.0804 | m |
| | e1/t | 0.0514 | Verify |
| | e2/t | 0.1149 | Verify |
| | e | 0.0360 | m |
| | e | 0.0804 | m |
| Verification | ρ | 1 | |
| | h0 | 7.2 | m |
| | λ | 10.286 | m |
| | λ<20 | Verifica | |
| | m | 0.700 | m |
| | Φ | 0.610 | |
| | FC | 1.2 | |
| | γM | 3 | |
| | fk | 1500 | kN/m2 |
| | fd | 417 | kN/m2 |
| | fd,rid | 254 | kN/m2 |
| | σ | -244 | kN/m2 |
| | σ/fd,rid | 96% | Verify |

Table 4-3. Verification of the section 5 of the wall 1.

From the results obtained, it is possible to conclude that the sections verify.

Wall 2: This wall is related to the façade walls. From the Figure 4-26 can be seen that the main wall was divided into nine different parts, also considering the lateral walls. Also in this case, the stresses were taken at the base of each divided element. The tables Table 4-5 and Table 4-4 correspond to the two most requested sections.

From the verifications carried out, it can be observed that in the case of section 4, which is defined as "maschio", it is requested at 84% of its resistant capacity, therefore it verifies. In the case of section 8, which is defined as "fascia", it is requested at 45% of its resistant capacity.

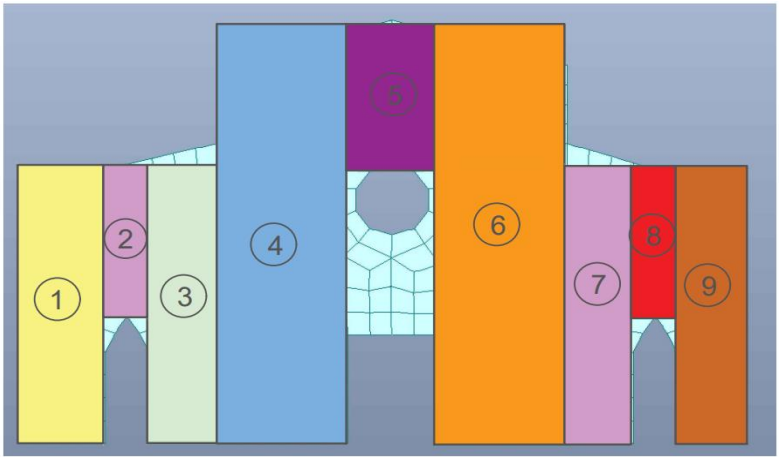


Figure 4-26. Wall N°2 - division. Image from Midas Gen.

| Combination 1 (N max) | | | |
|---|---|---|---|
| Load | N | -410 | kN |
| | Mv | -1 | kNm |
| | N1 | 0.00 | kN |
| | N2 | 0.00 | kN |
| Geometrical parameters | | | |
| | t | 1.7 | m |
| | l | 1.3 | m |
| | h | 4.2 | m |
| | d1 | 0 | m |
| | d2 | 0 | m |
| Eccentricity | es1 | 0.0000 | m |
| | es2 | 0.0000 | m |
| | ea | 0.0208 | m |
| | ev | 0.0026 | m |
| | e1 | 0.0208 | m |
| | e2 | 0.0129 | m |
| | e1/t | 0.0122 | Verify |
| | e2/t | 0.0076 | Verify |
| | e | 0.0208 | m |
| | e | 0.0129 | m |
| Verification | ρ | 1 | |
| | h0 | 4.15 | m |
| | λ | 2.441 | m |
| | λ<20 | Verifica | |
| | m | 0.073 | m |
| | Φ | 0.970 | |
| | FC | 1.2 | |
| | γM | 3 | |
| | fk | 1500 | kN/m2 |
| | fd | 417 | kN/m2 |
| | fd,rid | 404 | kN/m2 |
| | σ | -182 | kN/m2 |
| | σ/fd,rid | 45% | Verify |

| Combination 2 (Mv max) | | | |
|---|---|---|---|
| Load | N | -404 | kN |
| | Mv | -7 | kNm |
| | N1 | 0.00 | kN |
| | N2 | 0.00 | kN |
| Geometrical parameters | | | |
| | t | 1.7 | m |
| | l | 1.3 | m |
| | h | 4.2 | m |
| | d1 | 0 | m |
| | d2 | 0 | m |
| Eccentricity | es1 | 0.0000 | m |
| | es2 | 0.0000 | m |
| | ea | 0.0208 | m |
| | ev | 0.0168 | m |
| | e1 | 0.0208 | m |
| | e2 | 0.0272 | m |
| | e1/t | 0.0122 | Verify |
| | e2/t | 0.0160 | Verify |
| | e | 0.0208 | m |
| | e | 0.0272 | m |
| Verification | ρ | 1 | |
| | h0 | 4.15 | m |
| | λ | 2.441 | m |
| | λ<20 | Verifica | |
| | m | 0.096 | m |
| | Φ | 0.970 | |
| | FC | 1.2 | |
| | γM | 3 | |
| | fk | 1500 | kN/m2 |
| | fd | 417 | kN/m2 |
| | fd,rid | 404 | kN/m2 |
| | σ | -179 | kN/m2 |
| | σ/fd,rid | 44% | Verify |

Table 4-4. Verification of the section 8 of the wall 2.

| Combination 1 (N max) | | | |
|---|---|---|---|
| Load | N | -1772 | kN |
| | Mv | -2 | kNm |
| | N1 | 0.00 | kN |
| | N2 | 0.00 | kN |
| Geometrical parameters | | | |
| | t | 1.7 | m |
| | l | 3.5 | m |
| | h | 10.7 | m |
| | d1 | 0 | m |
| | d2 | 0 | m |
| Eccentricity | | | |
| | es1 | 0.0000 | m |
| | es2 | 0.0000 | m |
| | ea | 0.0535 | m |
| | ev | 0.0010 | m |
| | e1 | 0.0535 | m |
| | e2 | 0.0277 | m |
| | e1/t | 0.0315 | Verify |
| | e2/t | 0.0163 | Verify |
| | e | 0.0535 | m |
| | e | 0.0277 | m |
| Verification | ρ | 1 | |
| | h0 | 10.7 | m |
| | λ | 6.294 | m |
| | λ<20 | Verifica | |
| | m | 0.189 | m |
| | Φ | 0.860 | |
| | FC | 1.2 | |
| | γM | 3 | |
| | fk | 1500 | kN/m2 |
| | fd | 417 | kN/m2 |
| | fd,rid | 358 | kN/m2 |
| | σ | -302 | kN/m2 |
| | σ/fd,rid | 84% | Verify |

| Combination 2 (N max) | | | |
|---|---|---|---|
| Load | N | -1756 | kN |
| | Mv | -31 | kNm |
| | N1 | 0.00 | kN |
| | N2 | 0.00 | kN |
| Geometrical parameters | | | |
| | t | 1.7 | m |
| | l | 3.5 | m |
| | h | 10.7 | m |
| | d1 | 0 | m |
| | d2 | 0 | m |
| Eccentricity | | | |
| | es1 | 0.0000 | m |
| | es2 | 0.0000 | m |
| | ea | 0.0535 | m |
| | ev | 0.0178 | m |
| | e1 | 0.0535 | m |
| | e2 | 0.0445 | m |
| | e1/t | 0.0315 | Verify |
| | e2/t | 0.0262 | Verify |
| | e | 0.0535 | m |
| | e | 0.0445 | m |
| Verification | ρ | 1 | |
| | h0 | 10.7 | m |
| | λ | 6.294 | m |
| | λ<20 | Verifica | |
| | m | 0.157 | m |
| | Φ | 0.860 | |
| | FC | 1.2 | |
| | γM | 3 | |
| | fk | 1500 | kN/m2 |
| | fd | 417 | kN/m2 |
| | fd,rid | 358 | kN/m2 |
| | σ | -299 | kN/m2 |
| | σ/fd,rid | 84% | Verify |

Table 4-5 Verification of the section 4 of the wall 2.

Wall 3: This wall is releated to the south walls, from the Figure 4-27 can be seen that the element was divided in five different parts regarding the “fascia” and “maschio”.

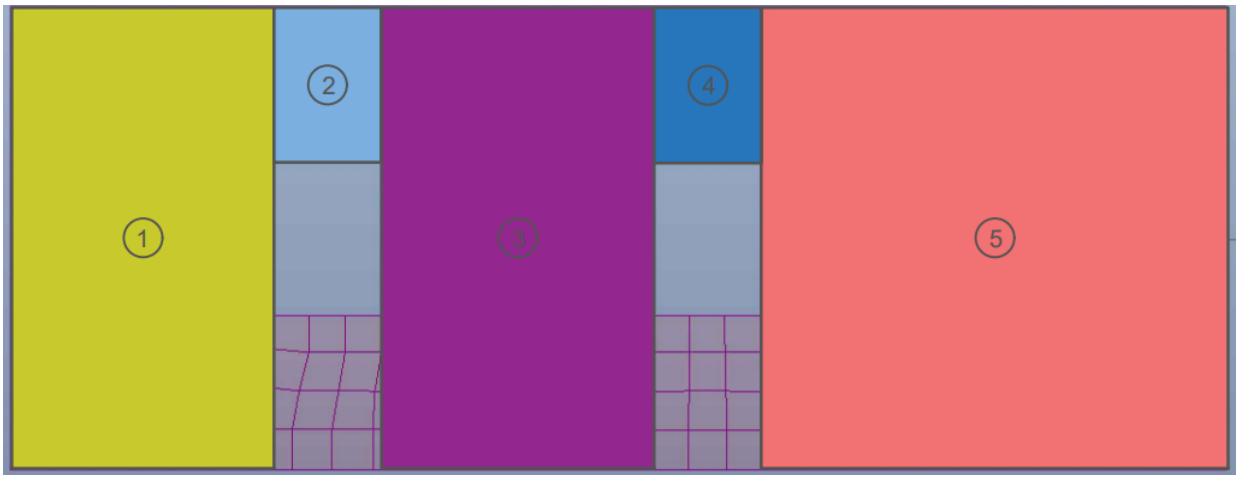


Figure 4-27. Wall N°3 - division. Image from Midas Gen.

The verification tables for this wall are presented below.

| Combination 1 (N max) | | | |
|---|---|---|---|
| Load | N | -295 | kN |
| | Mv | -57 | kNm |
| | N1 | 0.00 | kN |
| | N2 | 0.00 | kN |
| Geometrical parameters | | | |
| | t | 0.7 | m |
| | l | 1.8 | m |
| | h | 7.2 | m |
| | d1 | 0 | m |
| | d2 | 0 | m |
| Eccentricity | | | |
| | es1 | 0.0000 | m |
| | es2 | 0.0000 | m |
| | ea | 0.0360 | m |
| | ev | 0.1939 | m |
| | e1 | 0.0360 | m |
| | e2 | 0.2119 | m |
| | e1/t | 0.0514 | Verify |
| | e2/t | 0.3027 | Verify |
| | e | 0.0360 | m |
| | e | 0.2119 | m |
| Verification | | | |
| | ρ | 1 | |
| | h0 | 7.2 | m |
| | λ | 10.286 | m |
| | λ<20 | Verifica | |
| | m | 0.309 | m |
| | Φ | 0.610 | |
| | FC | 1.2 | |
| | γM | 3 | |
| | fk | 1500 | kN/m2 |
| | fd | 417 | kN/m2 |
| | fd,rid | 254 | kN/m2 |
| | σ | -237 | kN/m2 |
| | σ/fd,rid | 93% | Verify |

| Combination 2 (Mv max) | | | |
|---|---|---|---|
| Load | N | -291 | kN |
| | Mv | -58 | kNm |
| | N1 | 0.00 | kN |
| | N2 | 0.00 | kN |
| Geometrical parameters | | | |
| | t | 0.7 | m |
| | l | 1.8 | m |
| | h | 7.2 | m |
| | d1 | 0 | m |
| | d2 | 0 | m |
| Eccentricity | | | |
| | es1 | 0.0000 | m |
| | es2 | 0.0000 | m |
| | ea | 0.0360 | m |
| | ev | 0.2001 | m |
| | e1 | 0.0360 | m |
| | e2 | 0.2181 | m |
| | e1/t | 0.0514 | Verify |
| | e2/t | 0.3115 | Verify |
| | e | 0.0360 | m |
| | e | 0.2181 | m |
| Verification | | | |
| | ρ | 1 | |
| | h0 | 7.2 | m |
| | λ | 10.286 | m |
| | λ<20 | Verifica | |
| | m | 0.309 | m |
| | Φ | 0.610 | |
| | FC | 1.2 | |
| | γM | 3 | |
| | fk | 1500 | kN/m2 |
| | fd | 417 | kN/m2 |
| | fd,rid | 254 | kN/m2 |
| | σ | -234 | kN/m2 |
| | σ/fd,rid | 92% | Verify |

Table 4-6. Verification of the section 3 of the wall 3.

| Combination 1 (N max) | | | |
|---|---|---|---|
| Load | N | -101 | kN |
| | Mv | 5 | kNm |
| | N1 | 0.00 | kN |
| | N2 | 0.00 | kN |
| Geometrical parameters | | | |
| | t | 0.7 | m |
| | l | 1.6 | m |
| | h | 2.4 | m |
| | d1 | 0 | m |
| | d2 | 0 | m |
| Eccentricity | | | |
| | es1 | 0.0000 | m |
| | es2 | 0.0000 | m |
| | ea | 0.0120 | m |
| | ev | -0.0539 | m |
| | e1 | 0.0120 | m |
| | e2 | 0.0599 | m |
| | e1/t | 0.0171 | Verify |
| | e2/t | 0.0856 | Verify |
| | e | 0.0120 | m |
| | e | 0.0599 | m |
| Verification | | | |
| | ρ | 1 | |
| | h0 | 2.4 | m |
| | λ | 3.429 | m |
| | λ<20 | Verifica | |
| | m | 0.103 | m |
| | Φ | 0.970 | |
| | FC | 1.2 | |
| | γM | 3 | |
| | fk | 1500 | kN/m2 |
| | fd | 417 | kN/m2 |
| | fd,rid | 404 | kN/m2 |
| | σ | -88 | kN/m2 |
| | σ/fd,rid | 22% | Verify |

| Combination 2 (Mv max) | | | |
|---|---|---|---|
| Load | N | -92 | kN |
| | Mv | 9 | kNm |
| | N1 | 0.00 | kN |
| | N2 | 0.00 | kN |
| Geometrical parameters | | | |
| | t | 0.7 | m |
| | l | 1.6 | m |
| | h | 2.4 | m |
| | d1 | 0 | m |
| | d2 | 0 | m |
| Eccentricity | | | |
| | es1 | 0.0000 | m |
| | es2 | 0.0000 | m |
| | ea | 0.0120 | m |
| | ev | -0.1011 | m |
| | e1 | 0.0120 | m |
| | e2 | 0.1071 | m |
| | e1/t | 0.0171 | Verify |
| | e2/t | 0.1531 | Verify |
| | e | 0.0120 | m |
| | e | 0.1071 | m |
| Verification | | | |
| | ρ | 1 | |
| | h0 | 2.4 | m |
| | λ | 3.429 | m |
| | λ<20 | Verifica | |
| | m | 0.103 | m |
| | Φ | 0.970 | |
| | FC | 1.2 | |
| | γM | 3 | |
| | fk | 1500 | kN/m2 |
| | fd | 417 | kN/m2 |
| | fd,rid | 404 | kN/m2 |
| | σ | -80 | kN/m2 |
| | σ/fd,rid | 20% | Verify |

Table 4-7. Verification of the section 4 of the wall 3.

Wall 4: This is the wall on the left side of the central corridor of the structure. It is particularly influenced by the load of the vaults. The element was divided into 7 different sections (Figure 4-28). It is important to mention that these walls are made

of a material with better mechanical characteristics, for this reason the resistance is higher.

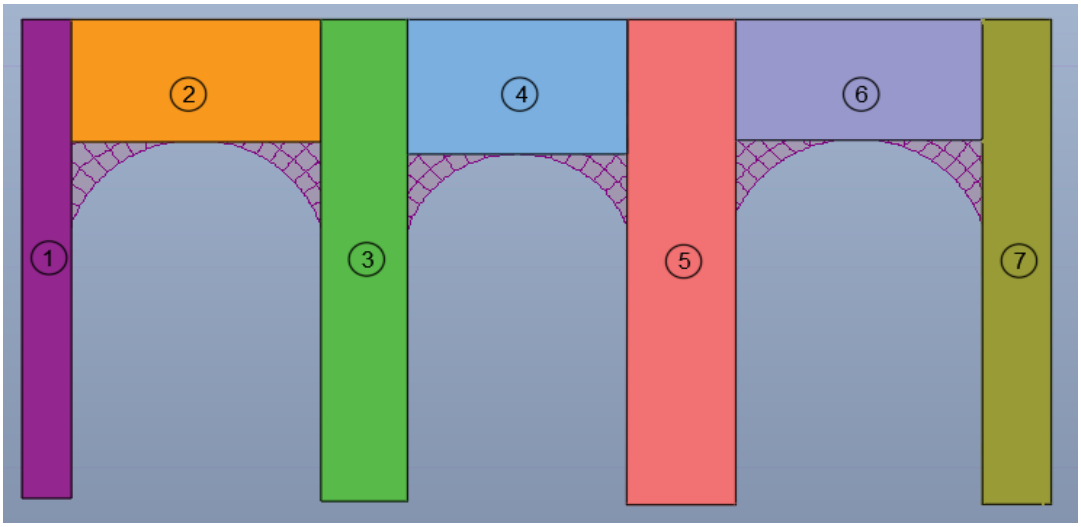


Figure 4-28. Wall N°4 - division. Image from Midas Gen.

| Combination 1 (N max) | | | |
|---|---|---|---|
| Load | N | -1689 | kN |
| | Mv | -2 | kNm |
| | N1 | 0.00 | kN |
| | N2 | 0.00 | kN |
| Geometrical parameters | | | |
| | t | 1.9 | m |
| | l | 1.4 | m |
| | h | 9.3 | m |
| | d1 | 0 | m |
| | d2 | 0 | m |
| Eccentricity | es1 | 0.0000 | m |
| | es2 | 0.0000 | m |
| | ea | 0.0465 | m |
| | ev | 0.0014 | m |
| | e1 | 0.0465 | m |
| | e2 | 0.0246 | m |
| | e1/t | 0.0251 | Verify |
| | e2/t | 0.0133 | Verify |
| | e | 0.0465 | m |
| | e | 0.0246 | m |
| Verification | ρ | 1 | |
| | h0 | 9.3 | m |
| | λ | 5.027 | m |
| | λ<20 | Verifica | |
| | m | 0.151 | m |
| | Φ | 0.710 | |
| | FC | 1.2 | |
| | γM | 3 | |
| | fk | 3450 | kN/m2 |
| | fd | 958 | kN/m2 |
| | fd,rid | 680 | kN/m2 |
| | σ | -647 | kN/m2 |
| | σ/fd,rid | 95% | Verify |

| Combination 2 (Mv max) | | | |
|---|---|---|---|
| Load | N | -1590 | kN |
| | Mv | -27 | kNm |
| | N1 | 0.00 | kN |
| | N2 | 0.00 | kN |
| Geometrical parameters | | | |
| | t | 1.9 | m |
| | l | 1.4 | m |
| | h | 9.3 | m |
| | d1 | 0 | m |
| | d2 | 0 | m |
| Eccentricity | es1 | 0.0000 | m |
| | es2 | 0.0000 | m |
| | ea | 0.0465 | m |
| | ev | 0.0172 | m |
| | e1 | 0.0465 | m |
| | e2 | 0.0405 | m |
| | e1/t | 0.0251 | Verify |
| | e2/t | 0.0219 | Verify |
| | e | 0.0465 | m |
| | e | 0.0405 | m |
| Verification | ρ | 1 | |
| | h0 | 9.3 | m |
| | λ | 5.027 | m |
| | λ<20 | Verifica | |
| | m | 0.131 | m |
| | Φ | 0.710 | |
| | FC | 1.2 | |
| | γM | 3 | |
| | fk | 3450 | kN/m2 |
| | fd | 958 | kN/m2 |
| | fd,rid | 680 | kN/m2 |
| | σ | -610 | kN/m2 |
| | σ/fd,rid | 90% | Verify |

Table 4-8. Verification of the section 3 of the wall 4.

| Combination 1 (N max) | | | |
|---|---|---|---|
| Load | N | -302 | kN |
| | Mv | 33 | kNm |
| | N1 | 0.00 | kN |
| | N2 | 0.00 | kN |
| Geometrical parameters | | | |
| | t | 1.9 | m |
| | l | 1.1 | m |
| | h | 2.5 | m |
| | d1 | 0 | m |
| | d2 | 0 | m |
| Eccentricity | | | |
| | es1 | 0.0000 | m |
| | es2 | 0.0000 | m |
| | ea | 0.0125 | m |
| | ev | -0.1091 | m |
| | e1 | 0.0125 | m |
| | e2 | 0.1153 | m |
| | e1/t | 0.0068 | Verify |
| | e2/t | 0.0623 | Verify |
| | e | 0.0125 | m |
| | e | 0.1153 | m |
| Verification | ρ | 1 | |
| | h0 | 2.5 | m |
| | λ | 1.351 | m |
| | λ<20 | Verifica | |
| | m | 0.041 | m |
| | Φ | 0.970 | |
| | FC | 1.2 | |
| | γM | 3 | |
| | fk | 3450 | kN/m2 |
| | fd | 958 | kN/m2 |
| | fd,rid | 930 | kN/m2 |
| | σ | -149 | kN/m2 |
| | σ/fd,rid | 16% | Verify |

| Combination 2 (Mv max) | | | |
|---|---|---|---|
| Load | N | -266 | kN |
| | Mv | 68 | kNm |
| | N1 | 0.00 | kN |
| | N2 | 0.00 | kN |
| Geometrical parameters | | | |
| | t | 1.9 | m |
| | l | 1.1 | m |
| | h | 2.5 | m |
| | d1 | 0 | m |
| | d2 | 0 | m |
| Eccentricity | | | |
| | es1 | 0.0000 | m |
| | es2 | 0.0000 | m |
| | ea | 0.0125 | m |
| | ev | -0.2544 | m |
| | e1 | 0.0125 | m |
| | e2 | 0.2606 | m |
| | e1/t | 0.0068 | Verify |
| | e2/t | 0.1409 | Verify |
| | e | 0.0125 | m |
| | e | 0.2606 | m |
| Verification | ρ | 1 | |
| | h0 | 2.5 | m |
| | λ | 1.351 | m |
| | λ<20 | Verifica | |
| | m | 0.041 | m |
| | Φ | 0.970 | |
| | FC | 1.2 | |
| | γM | 3 | |
| | fk | 3450 | kN/m2 |
| | fd | 958 | kN/m2 |
| | fd,rid | 930 | kN/m2 |
| | σ | -131 | kN/m2 |
| | σ/fd,rid | 14% | Verify |

Table 4-9. Verification of the section 4 of the wall 4.

As can be seen from the table Table 4-9, in the case of this wall the "fascia" is not so much in higher demand than in the case of the "maschio".

Wall 5: This is the wall on the right side of the central corridor of the structure and has the same characteristics as those mentioned for wall 4. In this case the element was also divided into 7 parts. Of which the verifications carried out for the most requested sections are presented.

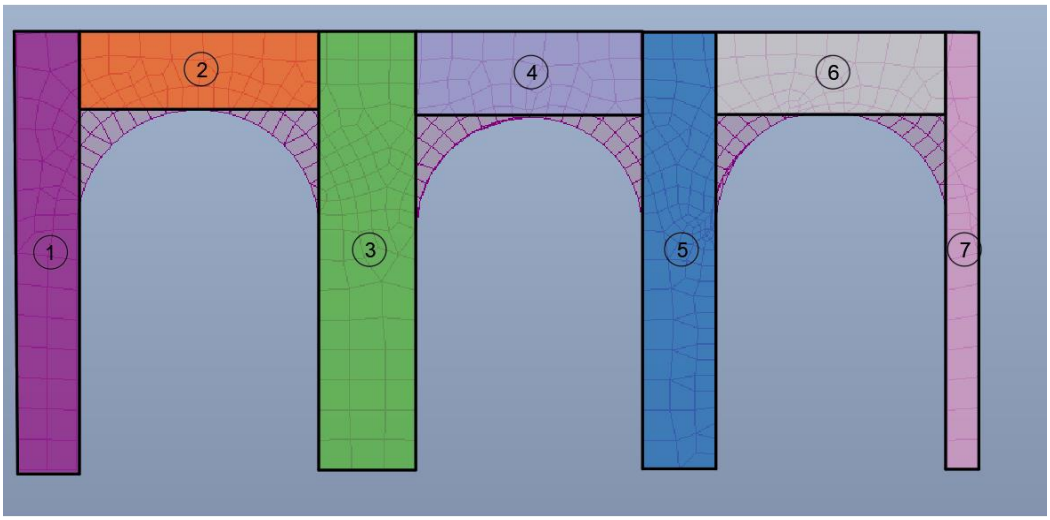


Figure 4-29. Wall N°5 - division. Image from Midas Gen.

| Combination 1 (N max) | | | |
|---|---|---|---|
| Load | N | -1650 | kN |
| | Mv | -5 | kNm |
| | N1 | 0.00 | kN |
| | N2 | 0.00 | kN |
| Geometrical parameters | | | |
| | t | 2.25 | m |
| | l | 1.2 | m |
| | h | 9.3 | m |
| | d1 | 0 | m |
| | d2 | 0 | m |
| Eccentricity | | | |
| | es1 | 0.0000 | m |
| | es2 | 0.0000 | m |
| | ea | 0.0465 | m |
| | ev | 0.0031 | m |
| | e1 | 0.0465 | m |
| | e2 | 0.0263 | m |
| | e1/t | 0.0207 | Verify |
| | e2/t | 0.0117 | Verify |
| | e | 0.0465 | m |
| | e | 0.0263 | m |
| Verification | ρ | 1 | |
| | h0 | 9.3 | m |
| | λ | 4.133 | m |
| | λ<20 | Verifica | |
| | m | 0.124 | m |
| | Φ | 0.710 | |
| | FC | 1.2 | |
| | γM | 3 | |
| | fk | 3450 | kN/m2 |
| | fd | 958 | kN/m2 |
| | fd,rid | 680 | kN/m2 |
| | σ | -621 | kN/m2 |
| | σ/fd,rid | 91% | Verify |

| Combination 2 (Mv max) | | | |
|---|---|---|---|
| Load | N | -1430 | kN |
| | Mv | -9 | kNm |
| | N1 | 0.00 | kN |
| | N2 | 0.00 | kN |
| Geometrical parameters | | | |
| | t | 2.25 | m |
| | l | 1.2 | m |
| | h | 9.3 | m |
| | d1 | 0 | m |
| | d2 | 0 | m |
| Eccentricity | | | |
| | es1 | 0.0000 | m |
| | es2 | 0.0000 | m |
| | ea | 0.0465 | m |
| | ev | 0.0062 | m |
| | e1 | 0.0465 | m |
| | e2 | 0.0295 | m |
| | e1/t | 0.0207 | Verify |
| | e2/t | 0.0131 | Verify |
| | e | 0.0465 | m |
| | e | 0.0295 | m |
| Verification | ρ | 1 | |
| | h0 | 9.3 | m |
| | λ | 4.133 | m |
| | λ<20 | Verifica | |
| | m | 0.079 | m |
| | Φ | 0.710 | |
| | FC | 1.2 | |
| | γM | 3 | |
| | fk | 3450 | kN/m2 |
| | fd | 958 | kN/m2 |
| | fd,rid | 680 | kN/m2 |
| | σ | -539 | kN/m2 |
| | σ/fd,rid | 79% | Verify |

Table 4-10. Verification of the section 7 of the wall 5.

| Combination 1 (N max) | | | |
|---|---|---|---|
| Load | N | -450 | kN |
| | Mv | -6 | kNm |
| | N1 | 0.00 | kN |
| | N2 | 0.00 | kN |
| Geometrical parameters | | | |
| | t | 2.25 | m |
| | l | 0.5 | m |
| | h | 2.5 | m |
| | d1 | 0 | m |
| | d2 | 0 | m |
| Eccentricity | | | |
| | es1 | 0.0000 | m |
| | es2 | 0.0000 | m |
| | ea | 0.0125 | m |
| | ev | 0.0131 | m |
| | e1 | 0.0125 | m |
| | e2 | 0.0194 | m |
| | e1/t | 0.0056 | Verify |
| | e2/t | 0.0086 | Verify |
| | e | 0.0125 | m |
| | e | 0.0194 | m |
| Verification | | | |
| | ρ | 1 | |
| | h0 | 2.5 | m |
| | λ | 1.111 | m |
| | λ<20 | Verifica | |
| | m | 0.033 | m |
| | Φ | 0.710 | |
| | FC | 1.2 | |
| | γM | 3 | |
| | fk | 3450 | kN/m2 |
| | fd | 958 | kN/m2 |
| | fd,rid | 680 | kN/m2 |
| | σ | -444 | kN/m2 |
| | σ/fd,rid | 65% | Verify |

| Combination 2 (Mv max) | | | |
|---|---|---|---|
| Load | N | -150 | kN |
| | Mv | 6 | kNm |
| | N1 | 0.00 | kN |
| | N2 | 0.00 | kN |
| Geometrical parameters | | | |
| | t | 2.25 | m |
| | l | 0.5 | m |
| | h | 2.5 | m |
| | d1 | 0 | m |
| | d2 | 0 | m |
| Eccentricity | | | |
| | es1 | 0.0000 | m |
| | es2 | 0.0000 | m |
| | ea | 0.0125 | m |
| | ev | -0.0403 | m |
| | e1 | 0.0125 | m |
| | e2 | 0.0466 | m |
| | e1/t | 0.0056 | Verify |
| | e2/t | 0.0207 | Verify |
| | e | 0.0125 | m |
| | e | 0.0466 | m |
| Verification | | | |
| | ρ | 1 | |
| | h0 | 2.5 | m |
| | λ | 1.111 | m |
| | λ<20 | Verifica | |
| | m | 0.124 | m |
| | Φ | 0.600 | |
| | FC | 1.2 | |
| | γM | 3 | |
| | fk | 3450 | kN/m2 |
| | fd | 958 | kN/m2 |
| | fd,rid | 575 | kN/m2 |
| | σ | -148 | kN/m2 |
| | σ/fd,rid | 26% | Verify |

Table 4-11. Verification of the section 4 of the wall 5.

Wall 6: This wall is located on the south façade of the church, and because it has no openings, it was divided into three different sections along its height. The most requested section is the one at the base. The following is the verification of section 1.

| Combination 1 (N max) | | | |
|---|---|---|---|
| Load | N | -977 | kN |
| | Mv | 185 | kNm |
| | N1 | 0.00 | kN |
| | N2 | 0.00 | kN |
| Geometrical parameters | | | |
| | t | 0.5 | m |
| | l | 9.0 | m |
| | h | 7.5 | m |
| | d1 | 0 | m |
| | d2 | 0 | m |
| Eccentricity | | | |
| | es1 | 0.0000 | m |
| | es2 | 0.0000 | m |
| | ea | 0.0375 | m |
| | ev | -0.1888 | m |
| | e1 | 0.0375 | m |
| | e2 | 0.2076 | m |
| | e1/t | 0.0750 | Verify |
| | e2/t | 0.4152 | No Verify |
| | e | 0.0375 | m |
| | e | 0.2076 | m |
| Verification | | | |
| | ρ | 1 | |
| | h0 | 7.5 | m |
| | λ | 15.000 | m |
| | λ<20 | Verifica | |
| | m | 0.450 | m |
| | Φ | 0.501 | |
| | FC | 1.2 | |
| | γM | 3 | |
| | fk | 1500 | kN/m2 |
| | fd | 500 | kN/m2 |
| | fd,rid | 251 | kN/m2 |
| | σ | -217 | kN/m2 |
| | σ/fd,rid | 87% | Verify |

| Combination 2 (Mv max) | | | |
|---|---|---|---|
| Load | N | -970 | kN |
| | Mv | 190 | kNm |
| | N1 | 0.00 | kN |
| | N2 | 0.00 | kN |
| Geometrical parameters | | | |
| | t | 0.5 | m |
| | l | 9.0 | m |
| | h | 7.5 | m |
| | d1 | 0 | m |
| | d2 | 0 | m |
| Eccentricity | | | |
| | es1 | 0.0000 | m |
| | es2 | 0.0000 | m |
| | ea | 0.0375 | m |
| | ev | -0.1954 | m |
| | e1 | 0.0375 | m |
| | e2 | 0.2142 | m |
| | e1/t | 0.0750 | Verify |
| | e2/t | 0.4284 | No Verify |
| | e | 0.0375 | m |
| | e | 0.2142 | m |
| Verification | | | |
| | ρ | 1 | |
| | h0 | 7.5 | m |
| | λ | 15.000 | m |
| | λ<20 | Verifica | |
| | m | 0.450 | m |
| | Φ | 0.501 | |
| | FC | 1.2 | |
| | γM | 3 | |
| | fk | 1500 | kN/m2 |
| | fd | 500 | kN/m2 |
| | fd,rid | 251 | kN/m2 |
| | σ | -216 | kN/m2 |
| | σ/fd,rid | 86% | Verify |

Table 4-12. Verification of the section 1 of the wall 6.

Wall 7: This wall represents the central wall of the presbytery, which corresponds to the east façade of the church. It can be seen from the Figure 4-30 that it was divided into three parts, due to the presence of an opening. As in the other cases, the results of the most requested sections are presented in the calculation tables.

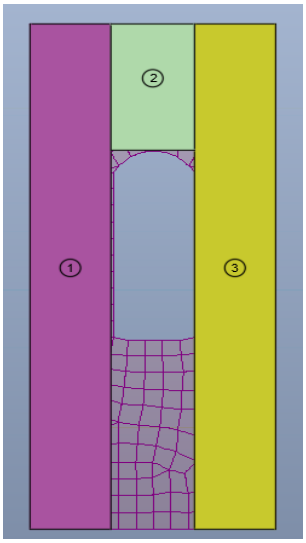


Figure 4-30. Wall N°7 - division. Image from Midas Gen.

| Combination 1 (N max) | | | |
|---|---|---|---|
| Load | N | -207 | kN |
| | Mv | -11 | kNm |
| | N1 | 0.00 | kN |
| | N2 | 0.00 | kN |
| Geometrical parameters | | | |
| | t | 0.7 | m |
| | l | 1.1 | m |
| | h | 9.3 | m |
| | d1 | 0 | m |
| | d2 | 0 | m |
| Eccentricity | | | |
| | es1 | 0.0000 | m |
| | es2 | 0.0000 | m |
| | ea | 0.0465 | m |
| | ev | 0.0540 | m |
| | e1 | 0.0465 | m |
| | e2 | 0.0772 | m |
| | e1/t | 0.0664 | Verify |
| | e2/t | 0.1103 | Verify |
| | e | 0.0465 | m |
| | e | 0.0772 | m |
| Verification | | | |
| | ρ | 1 | |
| | h0 | 9.3 | m |
| | λ | 13.286 | m |
| | λ<20 | Verifica | |
| | m | 0.399 | m |
| | Φ | 0.770 | |
| | FC | 1.2 | |
| | γM | 3 | |
| | fk | 1500 | kN/m2 |
| | fd | 417 | kN/m2 |
| | fd,rid | 321 | kN/m2 |
| | σ | -259 | kN/m2 |
| | σ/fd,rid | 81% | Verify |

| Combination 2 (Mv max) | | | |
|---|---|---|---|
| Load | N | -198 | kN |
| | Mv | -12 | kNm |
| | N1 | 0.00 | kN |
| | N2 | 0.00 | kN |
| Geometrical parameters | | | |
| | t | 0.7 | m |
| | l | 1.1 | m |
| | h | 9.3 | m |
| | d1 | 0 | m |
| | d2 | 0 | m |
| Eccentricity | | | |
| | es1 | 0.0000 | m |
| | es2 | 0.0000 | m |
| | ea | 0.0465 | m |
| | ev | 0.0617 | m |
| | e1 | 0.0465 | m |
| | e2 | 0.0850 | m |
| | e1/t | 0.0664 | Verify |
| | e2/t | 0.1214 | Verify |
| | e | 0.0465 | m |
| | e | 0.0850 | m |
| Verification | | | |
| | ρ | 1 | |
| | h0 | 9.3 | m |
| | λ | 13.286 | m |
| | λ<20 | Verifica | |
| | m | 0.399 | m |
| | Φ | 0.770 | |
| | FC | 1.2 | |
| | γM | 3 | |
| | fk | 1500 | kN/m2 |
| | fd | 417 | kN/m2 |
| | fd,rid | 321 | kN/m2 |
| | σ | -249 | kN/m2 |
| | σ/fd,rid | 77% | Verify |

Figure 4-31. Verification of the section 3 of the wall 7.

| Combination 1 (N max) | | | |
|---|---|---|---|
| Load | N | -44 | kN |
| | Mv | 5 | kNm |
| | N1 | 0.00 | kN |
| | N2 | 0.00 | kN |
| Geometrical parameters | | | |
| | t | 0.7 | m |
| | l | 1.0 | m |
| | h | 3.0 | m |
| | d1 | 0 | m |
| | d2 | 0 | m |
| Eccentricity | | | |
| | es1 | 0.0000 | m |
| | es2 | 0.0000 | m |
| | ea | 0.0150 | m |
| | ev | -0.1208 | m |
| | e1 | 0.0150 | m |
| | e2 | 0.1283 | m |
| | e1/t | 0.0214 | Verify |
| | e2/t | 0.1833 | Verify |
| | e | 0.0150 | m |
| | e | 0.1283 | m |
| Verification | | | |
| | ρ | 1 | |
| | h0 | 3 | m |
| | λ | 4.286 | m |
| | λ<20 | Verifica | |
| | m | 0.129 | m |
| | Φ | 0.750 | |
| | FC | 1.2 | |
| | γM | 3 | |
| | fk | 1500 | kN/m2 |
| | fd | 417 | kN/m2 |
| | fd,rid | 313 | kN/m2 |
| | σ | -62 | kN/m2 |
| | σ/fd,rid | 20% | Verify |

| Combination 2 (Mv max) | | | |
|---|---|---|---|
| Load | N | -30 | kN |
| | Mv | -7 | kNm |
| | N1 | 0.00 | kN |
| | N2 | 0.00 | kN |
| Geometrical parameters | | | |
| | t | 0.7 | m |
| | l | 1.0 | m |
| | h | 3.0 | m |
| | d1 | 0 | m |
| | d2 | 0 | m |
| Eccentricity | | | |
| | es1 | 0.0000 | m |
| | es2 | 0.0000 | m |
| | ea | 0.0150 | m |
| | ev | 0.2465 | m |
| | e1 | 0.0150 | m |
| | e2 | 0.2540 | m |
| | e1/t | 0.0214 | Verify |
| | e2/t | 0.3629 | No Verify |
| | e | 0.0150 | m |
| | e | 0.2540 | m |
| Verification | | | |
| | ρ | 1 | |
| | h0 | 3 | m |
| | λ | 4.286 | m |
| | λ<20 | Verifica | |
| | m | 0.129 | m |
| | Φ | 0.750 | |
| | FC | 1.2 | |
| | γM | 3 | |
| | fk | 1500 | kN/m2 |
| | fd | 417 | kN/m2 |
| | fd,rid | 313 | kN/m2 |
| | σ | -43 | kN/m2 |
| | σ/fd,rid | 14% | Verify |

Figure 4-32. Verification of the section 2 of the wall 7.

Wall 8: this wall corresponds to the lateral part of the presbytery, the number of divisions considered were the same as for wall 7, as the geometry of both walls is very close to each other. The results are as follows:

| Combination 1 (N max) | | | |
|---|---|---|---|
| Load | N | -235 | kN |
| | Mv | -14 | kNm |
| | N1 | 0.00 | kN |
| | N2 | 0.00 | kN |
| Geometrical parameters | | | |
| | t | 0.7 | m |
| | l | 1.2 | m |
| | h | 9.3 | m |
| | d1 | 0 | m |
| | d2 | 0 | m |
| Eccentricity | | | |
| | es1 | 0.0000 | m |
| | es2 | 0.0000 | m |
| | ea | 0.0465 | m |
| | ev | 0.0590 | m |
| | e1 | 0.0465 | m |
| | e2 | 0.0822 | m |
| | e1/t | 0.0664 | Verify |
| | e2/t | 0.1174 | Verify |
| | e | 0.0465 | m |
| | e | 0.0822 | m |
| Verification | ρ | 1 | |
| | h0 | 9.3 | m |
| | λ | 13.286 | m |
| | λ<20 | Verifica | |
| | m | 0.399 | m |
| | Φ | 0.500 | |
| | FC | 1.2 | |
| | γM | 3 | |
| | fk | 1500 | kN/m2 |
| | fd | 417 | kN/m2 |
| | fd,rid | 208 | kN/m2 |
| | σ | -271 | kN/m2 |
| | σ/fd,rid | 130% | No verify |

| Combination 2 (Mv max) | | | |
|---|---|---|---|
| Load | N | -235 | kN |
| | Mv | -15 | kNm |
| | N1 | 0.00 | kN |
| | N2 | 0.00 | kN |
| Geometrical parameters | | | |
| | t | 0.7 | m |
| | l | 1.2 | m |
| | h | 9.3 | m |
| | d1 | 0 | m |
| | d2 | 0 | m |
| Eccentricity | | | |
| | es1 | 0.0000 | m |
| | es2 | 0.0000 | m |
| | ea | 0.0465 | m |
| | ev | 0.0646 | m |
| | e1 | 0.0465 | m |
| | e2 | 0.0879 | m |
| | e1/t | 0.0664 | Verify |
| | e2/t | 0.1255 | Verify |
| | e | 0.0465 | m |
| | e | 0.0879 | m |
| Verification | ρ | 1 | |
| | h0 | 9.3 | m |
| | λ | 13.286 | m |
| | λ<20 | Verifica | |
| | m | 0.399 | m |
| | Φ | 0.500 | |
| | FC | 1.2 | |
| | γM | 3 | |
| | fk | 1500 | kN/m2 |
| | fd | 417 | kN/m2 |
| | fd,rid | 208 | kN/m2 |
| | σ | -271 | kN/m2 |
| | σ/fd,rid | 130% | No verify |

Table 4-13. Verification of the section 3 of the wall 8.

| Combination 1 (N max) | | | |
|---|---|---|---|
| Load | N | -134 | kN |
| | Mv | -25 | kNm |
| | N1 | 0.00 | kN |
| | N2 | 0.00 | kN |
| Geometrical parameters | | | |
| | t | 0.7 | m |
| | l | 0.4 | m |
| | h | 2.4 | m |
| | d1 | 0 | m |
| | d2 | 0 | m |
| Eccentricity | | | |
| | es1 | 0.0000 | m |
| | es2 | 0.0000 | m |
| | ea | 0.0120 | m |
| | ev | 0.1857 | m |
| | e1 | 0.0120 | m |
| | e2 | 0.1917 | m |
| | e1/t | 0.0171 | Verify |
| | e2/t | 0.2739 | Verify |
| | e | 0.0120 | m |
| | e | 0.1917 | m |
| Verification | ρ | 1 | |
| | h0 | 2.4 | m |
| | λ | 3.429 | m |
| | λ<20 | Verifica | |
| | m | 0.103 | m |
| | Φ | 0.960 | |
| | FC | 1.2 | |
| | γM | 3 | |
| | fk | 1500 | kN/m2 |
| | fd | 417 | kN/m2 |
| | fd,rid | 400 | kN/m2 |
| | σ | -467 | kN/m2 |
| | σ/fd,rid | 117% | No verify |

| Combination 2 (Mv max) | | | |
|---|---|---|---|
| Load | N | -130 | kN |
| | Mv | -26 | kNm |
| | N1 | 0.00 | kN |
| | N2 | 0.00 | kN |
| Geometrical parameters | | | |
| | t | 0.7 | m |
| | l | 0.4 | m |
| | h | 2.4 | m |
| | d1 | 0 | m |
| | d2 | 0 | m |
| Eccentricity | | | |
| | es1 | 0.0000 | m |
| | es2 | 0.0000 | m |
| | ea | 0.0120 | m |
| | ev | 0.1971 | m |
| | e1 | 0.0120 | m |
| | e2 | 0.2031 | m |
| | e1/t | 0.0171 | Verify |
| | e2/t | 0.2902 | Verify |
| | e | 0.0120 | m |
| | e | 0.2031 | m |
| Verification | ρ | 1 | |
| | h0 | 2.4 | m |
| | λ | 3.429 | m |
| | λ<20 | Verifica | |
| | m | 0.103 | m |
| | Φ | 0.960 | |
| | FC | 1.2 | |
| | γM | 3 | |
| | fk | 1500 | kN/m2 |
| | fd | 417 | kN/m2 |
| | fd,rid | 400 | kN/m2 |
| | σ | -454 | kN/m2 |
| | σ/fd,rid | 114% | No verify |

Table 4-14. Verification of the section 2 of the wall 8.

From the Table 4-13 and Table 4-14 it can be seen that both sections do not check. As far as section 3 is concerned, which is defined as "maschio", the condition of maximum moment and maximum normal stress are given together, this section does not verify by 30%. On the other hand, as for section 2, which is defined as "fascia", it does not verify by 16%, in this case, the combination of maximum moment and maximum normal stress occur in different combinations.

Wall 9: This category of wall corresponds to the bell tower wall, unlike the other walls, this one has a considerable height, therefore for its analysis it was divided into different segments along its height. From the Figure 4-33, it can be seen that in the upper part in correspondence with the opening, the same reasoning was carried out as for the other sections.

In the verifications of the various sections, it was found that the first 2 sections (up to 6m from the structure) do not pass verification. Then from the 3rd section onwards, the verifications are successful. This may be due to the great height of this structure, with a greater concentration of stresses in the lower part, which are responsible for governing the construction.

The Table 4-15 and Table 4-16 show the results obtained in the first 6 meters of the wall, then the Table 4-17 Table 4-16shows the results obtained from 6 meters onwards, where it can be seen that from this height onwards it verifies.

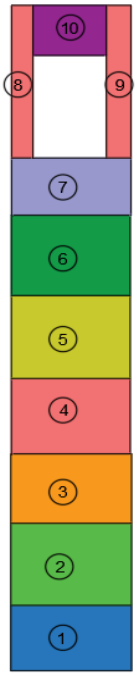


Figure 4-33. Wall N°9 - division. Image from Midas Gen.

| Combination 1 (N max) | | | |
|---|---|---|---|
| Load | N | -5782 | kN |
| | Mv | 420 | kNm |
| | N1 | 0.00 | kN |
| | N2 | 0.00 | kN |
| Geometrical parameters | | | |
| | t | 1.9 | m |
| | l | 5.2 | m |
| | h | 3.0 | m |
| | d1 | 0 | m |
| | d2 | 0 | m |
| Eccentricity | | | |
| | es1 | 0.0000 | m |
| | es2 | 0.0000 | m |
| | ea | 0.0150 | m |
| | ev | -0.0726 | m |
| | e1 | 0.0150 | m |
| | e2 | 0.0801 | m |
| | e1/t | 0.0079 | Verify |
| | e2/t | 0.0421 | Verify |
| | e | 0.015000 | m |
| | e | 0.0801 | m |
| Verification | | | |
| | ρ | 1 | |
| | h0 | 3 | m |
| | λ | 1.579 | m |
| | λ<20 | Verifica | |
| | m | 0.047 | m |
| | Φ | 0.970 | |
| | FC | 1.2 | |
| | γM | 3 | |
| | fk | 1500 | kN/m2 |
| | fd | 417 | kN/m2 |
| | fd,rid | 404 | kN/m2 |
| | σ | -591 | kN/m2 |
| | σ/fd,rid | 1.46 | No verify |

| Combination 2 (Mv max) | | | |
|---|---|---|---|
| Load | N | -5624 | kN |
| | Mv | 722 | kNm |
| | N1 | 0.00 | kN |
| | N2 | 0.00 | kN |
| Geometrical parameters | | | |
| | t | 1.9 | m |
| | l | 5.2 | m |
| | h | 3.0 | m |
| | d1 | 0 | m |
| | d2 | 0 | m |
| Eccentricity | | | |
| | es1 | 0.0000 | m |
| | es2 | 0.0000 | m |
| | ea | 0.0150 | m |
| | ev | -0.1283 | m |
| | e1 | 0.0150 | m |
| | e2 | 0.1358 | m |
| | e1/t | 0.0079 | Verify |
| | e2/t | 0.0715 | Verify |
| | e | 0.0150 | m |
| | e | 0.1358 | m |
| Verification | | | |
| | ρ | 1 | |
| | h0 | 3 | m |
| | λ | 1.579 | m |
| | λ<20 | Verifica | |
| | m | 0.429 | m |
| | Φ | 0.970 | |
| | FC | 1.2 | |
| | γM | 3 | |
| | fk | 1500 | kN/m2 |
| | fd | 417 | kN/m2 |
| | fd,rid | 404 | kN/m2 |
| | σ | -575 | kN/m2 |
| | σ/fd,rid | 1.42 | No verify |

Table 4-15. Verification of the section 1 of the wall 9.

| Combination 1 (N max) | | | |
|---|---|---|---|
| Load | N | -5009 | kN |
| | Mv | 80 | kNm |
| | N1 | 0.00 | kN |
| | N2 | 0.00 | kN |
| Geometrical parameters | | | |
| | t | 1.9 | m |
| | l | 5.9 | m |
| | h | 3.0 | m |
| | d1 | 0 | m |
| | d2 | 0 | m |
| Eccentricity | | | |
| | es1 | 0.0000 | m |
| | es2 | 0.0000 | m |
| | ea | 0.0150 | m |
| | ev | -0.0160 | m |
| | e1 | 0.0150 | m |
| | e2 | 0.0235 | m |
| | e1/t | 0.0079 | Verify |
| | e2/t | 0.0124 | Verify |
| | e | 0.015000 | m |
| | e | 0.0235 | m |
| Verification | | | |
| | ρ | 1 | |
| | h0 | 3 | m |
| | λ | 1.579 | m |
| | λ<20 | Verifica | |
| | m | 0.047 | m |
| | Φ | 0.970 | |
| | FC | 1.2 | |
| | γM | 3 | |
| | fk | 1500 | kN/m2 |
| | fd | 417 | kN/m2 |
| | fd,rid | 404 | kN/m2 |
| | σ | -447 | kN/m2 |
| | σ/fd,rid | 111% | No verify |

| Combination 2 (Mv max) | | | |
|---|---|---|---|
| Load | N | -3579 | kN |
| | Mv | 261 | kNm |
| | N1 | 0.00 | kN |
| | N2 | 0.00 | kN |
| Geometrical parameters | | | |
| | t | 1.9 | m |
| | l | 5.9 | m |
| | h | 3.0 | m |
| | d1 | 0 | m |
| | d2 | 0 | m |
| Eccentricity | | | |
| | es1 | 0.0000 | m |
| | es2 | 0.0000 | m |
| | ea | 0.0150 | m |
| | ev | -0.0731 | m |
| | e1 | 0.0150 | m |
| | e2 | 0.0806 | m |
| | e1/t | 0.0079 | Verify |
| | e2/t | 0.0424 | Verify |
| | e | 0.0150 | m |
| | e | 0.0806 | m |
| Verification | | | |
| | ρ | 1 | |
| | h0 | 3 | m |
| | λ | 1.579 | m |
| | λ<20 | Verifica | |
| | m | 0.254 | m |
| | Φ | 0.970 | |
| | FC | 1.2 | |
| | γM | 3 | |
| | fk | 1500 | kN/m2 |
| | fd | 417 | kN/m2 |
| | fd,rid | 404 | kN/m2 |
| | σ | -319 | kN/m2 |
| | σ/fd,rid | 79% | Verify |

Table 4-16. Verification of the section 2 of the wall 9.

| Combination 1 (N max) | | | |
|---|---|---|---|
| Load | N | -4689 | kN |
| | Mv | 139 | kNm |
| | N1 | 0.00 | kN |
| | N2 | 0.00 | kN |
| Geometrical parameters | | | |
| | t | 1.9 | m |
| | l | 6.0 | m |
| | h | 3.0 | m |
| | d1 | 0 | m |
| | d2 | 0 | m |
| Eccentricity | | | |
| | es1 | 0.0000 | m |
| | es2 | 0.0000 | m |
| | ea | 0.0150 | m |
| | ev | -0.0296 | m |
| | e1 | 0.0150 | m |
| | e2 | 0.0371 | m |
| | e1/t | 0.0079 | Verify |
| | e2/t | 0.0195 | Verify |
| | e | 0.015000 | m |
| | e | 0.0371 | m |
| Verification | ρ | 1 | |
| | h0 | 3 | m |
| | λ | 1.579 | m |
| | λ<20 | Verifica | |
| | m | 0.047 | m |
| | Φ | 0.970 | |
| | FC | 1.2 | |
| | γM | 3 | |
| | fk | 1500 | kN/m2 |
| | fd | 500 | kN/m2 |
| | fd,rid | 485 | kN/m2 |
| | σ | -411 | kN/m2 |
| | σ/fd,rid | 85% | Verify |

| Combination 2 (Mv max) | | | |
|---|---|---|---|
| Load | N | -4689 | kN |
| | Mv | 139 | kNm |
| | N1 | 0.00 | kN |
| | N2 | 0.00 | kN |
| Geometrical parameters | | | |
| | t | 1.9 | m |
| | l | 6.0 | m |
| | h | 3.0 | m |
| | d1 | 0 | m |
| | d2 | 0 | m |
| Eccentricity | | | |
| | es1 | 0.0000 | m |
| | es2 | 0.0000 | m |
| | ea | 0.0150 | m |
| | ev | -0.0296 | m |
| | e1 | 0.0150 | m |
| | e2 | 0.0371 | m |
| | e1/t | 0.0079 | Verify |
| | e2/t | 0.0195 | Verify |
| | e | 0.0150 | m |
| | e | 0.0371 | m |
| Verification | ρ | 1 | |
| | h0 | 3 | m |
| | λ | 1.579 | m |
| | λ<20 | Verifica | |
| | m | 0.047 | m |
| | Φ | 0.980 | |
| | FC | 1.2 | |
| | γM | 3 | |
| | fk | 1500 | kN/m2 |
| | fd | 500 | kN/m2 |
| | fd,rid | 490 | kN/m2 |
| | σ | -411 | kN/m2 |
| | σ/fd,rid | 84% | Verify |

Table 4-17. Verification of the section 3 of the wall 9.

In conclusion, after carried out the verifications of the walls given, is possible to find criticisms in 2 elements that have been analysed, the side walls that delimit the presbytery and the walls of the bell tower side, these walls do not satisfy the verifications carried out.

For this reason, some kind of intervention must be carried out on them, since due to the loads defined as static they do not check.

### 4.3.2 Axial and bending in plane

The “axial and bending in plane” is a stress composed of compression and bending, i.e. generated by an axial compressive force and a bending moment. [22]

The Italian regulation, in paragraph 7.8.2.2.1, states that “The axial and bending” of a section of a structural element is performed by comparing the design acting moment with the ultimate resistant moment calculated by assuming the masonry not reacting to tension and a propriate non-linear compression distribution. In the case of a

rectangular section and rectangular compression diagram with a resistance value of 0.85 $f_d$". [12]

The formula for the calculation of the resistant moment of the structure is as follows ( equation 7.8.2 of NTC2018):

$$M_u = \left(l^2\, t\, \frac{\sigma_0}{2}\right)\left(1 - \frac{\sigma_0}{0.85\, f_d}\right) \tag{39}$$

Where:

$M_u$ is the moment of collapse by pressure bending.

$l$ is the length of the wall.

$t$ is the thickness of the wall.

$\sigma_0$ is the mean normal stress (coincident with $\sigma_{med}$), referred to the total area of the section calculated as $\sigma_0 = \frac{N}{lt}$ where N is the axial force. If N is a compressive force it is assumed with a positive sign, instead if N is of traction the moment of collapse is considered equal to zero. $f_d$ is the design compressive strength of the masonry equal to $\frac{f_m}{\gamma_M\, FC}$, where $f_m$ is the average compressive strength calculated in the section 2.2, $FC$ is the confidence factor which as determined in section 2.1 takes a value equal to 1.2. Finally, $\gamma_M$ is extracted from the table 4.5.II of the Italian regulation, this coefficient depends on the type of mortar used and the execution class adopted, because there are many uncertainties in the building under analysis, the worst value of 3 was adopted for this coefficient. [12]

To accelerate the work and make it more organised, at this stage it was decided to perform the in-plane, shear and out-of-plane pressure bending verification in the same spreadsheet. To provide more organisation in the document, the calculation tables will be presented at the end of the explanation of all the verifications to be carried out, carrying out the verification of all the load combinations.

### 4.3.3 Shear

The "Circolare del 21 gennaio 2019" in paragraph C.8.7.1.3.1.1 states that two families of masonry are distinguished for shear assessment, both for "maschio" and

“fascia”. In the first place, there are regular-textured masonry, for which cracking can be stepped. In second place, irregularly textured masonry, with diagonal tensile cracking governed by the parameter $\tau_0$ (average shear strength in the absence of normal stress).

The equation for the calculation of the resistant shear of the structure is as follows ( equation 8.7.1.16 of Circolare del 21 gennaio 2019). It is important to note that this formula is derived from defining a Mohr's circle, because diagonal cracking of a wall occurs when the principal tensile stress in the central part is equal to the tensile strength of the masonry.

$$V_t = l\,t\,\frac{1.5\,\tau_{0d}}{b}\,\sqrt{1+\frac{\sigma_0}{1.5\,\tau_{0d}}} = l\,t\,\frac{f_{td}}{b}\,\sqrt{1+\frac{\sigma_0}{f_{td}}} \tag{40}$$

Where:

$l, t$ and $\sigma_0$ are the above-mentioned parameters.

$f_{td}$ and $\tau_{0d}$ are the calculation values of the diagonal crack tensile strength and of the corresponding reference shear strength of the masonry.

$b$ is a corrective coefficient related to the distribution of stresses on the section. Its value depends on the slenderness of the wall, is assumed to be h/l (with h being the height of the panel) and must necessarily be between 1 and 1.5.

Shear strength values must be compared with the acting values.

### 4.3.4 Axial and bending out of the plane

The regulation, in paragraph 7.8.2.2.3 states that for this verification reference can be made to the formula used for the verification in the plane. In this case the equation to be used is the equation 38, but the wall thickness is what was previously considered the length and vice versa.

As mentioned before, the verification of the three mechanisms was carried out in one table, all load combinations were analysed. The names of the walls are the same as in the Figure 4-23 and the division of the structural elements into "fascie" and "maschi" is the same as in Section 4.3.1.

At the same time, in order not to make the document too extensive, what was decided to do, as in section 4.3.1, is not to include all the verifications carried out, but rather to make known those sections that are most critical.

Wall 1:

In the initial phase, for each of the mechanisms to be verified, the necessary parameters are determined. Once the parameters were obtained, we proceeded to verify the various sections. The Table 4-19 refers to section 1 of this wall, which can be seen that for various load combinations it does not verify. The verification that was not mainly passed is the shear.

| ***Bending in the plane*** | | | |
|---|---|---|---|
| **Geometrical parameters** | l | 1.73 | m |
| | t | 0.7 | m |
| | | | |
| **Mechanical parameters** | $f_m$ | 1500 | kN/m2 |
| | $\gamma_m$ | 2 | - |
| | FC | 1.2 | - |
| | $f_d$ | 625 | kN/m2 |

| ***Shear*** | | | |
|---|---|---|---|
| **Geometrical parameters** | l | 1.73 | m |
| | t | 0.7 | m |
| | h | 7.2 | m |
| | b | 1.5 | |
| **Mechanical parameters** | $\tau_0$ | 25 | kN/m2 |
| | $f_{td}$ | 15.625 | kN/m2 |
| | $\gamma_m$ | 2 | - |
| | FC | 1.2 | - |

| ***Bending out of the plane*** | | | |
|---|---|---|---|
| **Geometrical parameters** | l | 0.7 | m |
| | t | 1.73 | m |
| **Mechanical parameters** | $f_m$ | 1500 | kN/m2 |
| | $\gamma_m$ | 2 | - |
| | FC | 1.2 | - |
| | $f_d$ | 625 | kN/m2 |

Table 4-18. Parameters for the verification of the Wall 1.

| Combination | BENDING IN THE PLANE | | | | | | SHEAR | | | | BENDING OUT OF THE PLANE | | | | |
|---|---|---|---|---|---|---|---|---|---|---|---|---|---|---|---|
| | N | $\sigma_0$ | $M_{Ed}$ | $M_{Rd}$ | MEd/MRd | Verification | $V_{Ed}$ | $V_{Rd}$ | VEd/VRd | Verification | $\sigma_0$ | $M_{Ed}$ | $M_{Rd}$ | MEd/MRd | Verification |
| | kN | kN/m2 | kNm | kNm | - | - | kN | kN | - | - | kN/m2 | kNm | kNm | - | - |
| Seismic_1 | 105 | 86 | 74 | 76 | 98% | Verify | 51 | 32 | 2 | No verify | 86 | 9 | 31 | 30% | Verify |
| Seismic_2 | 104 | 86 | 74 | 76 | 98% | Verify | 51 | 32 | 2 | No verify | 86 | 9 | 31 | 30% | Verify |
| Seismic_3 | 76 | 63 | 60 | 58 | 104% | No verify | 10 | 28 | 0 | Verify | 63 | 8 | 23 | 33% | Verify |
| Seismic_4 | 76 | 63 | 60 | 58 | 104% | No verify | 10 | 28 | 0 | Verify | 63 | 8 | 23 | 33% | Verify |
| Seismic_5 | 702 | 580 | -7 | -55 | 13% | Verify | -49 | 78 | -1 | Verify | 580 | -5 | -22 | 24% | Verify |
| Seismic_6 | 702 | 580 | -7 | -55 | 13% | Verify | -49 | 78 | -1 | Verify | 580 | -5 | -22 | 24% | Verify |
| Seismic_7 | 882 | 728 | -21 | -283 | 8% | Verify | -90 | 87 | -1 | No verify | 728 | -7 | -115 | 6% | Verify |
| Seismic_8 | 882 | 729 | -21 | -283 | 8% | Verify | -90 | 87 | -1 | No verify | 729 | -7 | -115 | 6% | Verify |
| Seismic_9 | 32 | 27 | 62 | 27 | 233% | No verify | 63 | 21 | 3 | No verify | 27 | 6 | 11 | 54% | Verify |
| Seismic_10 | 209 | 173 | 38 | 122 | 31% | Verify | 34 | 44 | 1 | Verify | 173 | 1 | 49 | 3% | Verify |
| Seismic_11 | 210 | 173 | 38 | 122 | 31% | Verify | 34 | 44 | 1 | Verify | 173 | 1 | 49 | 3% | Verify |
| Seismic_12 | 32 | 27 | 62 | 27 | 233% | No verify | 63 | 21 | 3 | No verify | 27 | 6 | 11 | 54% | Verify |
| Seismic_13 | 810 | 669 | -9 | -182 | 5% | Verify | -102 | 83 | -1 | No verify | 669 | -4 | -74 | 5% | Verify |
| Seismic_14 | 568 | 469 | 15 | 57 | 26% | Verify | -72 | 70 | -1 | No verify | 469 | 1 | 23 | 4% | Verify |
| Seismic_15 | 568 | 469 | 15 | 57 | 26% | Verify | -72 | 70 | -1 | No verify | 469 | 1 | 23 | 4% | Verify |
| Seismic_16 | 810 | 669 | -9 | -182 | 5% | Verify | -102 | 84 | -1 | No verify | 669 | -4 | -74 | 5% | Verify |
| Seismic_17 | 178 | 147 | 46 | 111 | 41% | Verify | 16 | 41 | 0 | Verify | 147 | 4 | 45 | 9% | Verify |
| Seismic_18 | 420 | 346 | 21 | 126 | 17% | Verify | -14 | 61 | 0 | Verify | 346 | 0 | 51 | -1% | Verify |
| Seismic_19 | 358 | 296 | 31 | 137 | 23% | Verify | -25 | 56 | 0 | Verify | 296 | 3 | 56 | 5% | Verify |
| Seismic_20 | 600 | 495 | 7 | 35 | 20% | Verify | -55 | 72 | -1 | Verify | 495 | -2 | 14 | -13% | Verify |
| Seismic_21 | 420 | 347 | 21 | 126 | 17% | Verify | -14 | 61 | 0 | Verify | 347 | 0 | 51 | -1% | Verify |
| Seismic_22 | 358 | 296 | 31 | 137 | 23% | Verify | -25 | 56 | 0 | Verify | 296 | 3 | 56 | 5% | Verify |
| Seismic_23 | 178 | 147 | 46 | 111 | 41% | Verify | 16 | 41 | 0 | Verify | 147 | 4 | 45 | 9% | Verify |
| Seismic_24 | 600 | 496 | 7 | 35 | 20% | Verify | -55 | 72 | -1 | Verify | 496 | -2 | 14 | -13% | Verify |
| SLU1_1 | 486 | 402 | 33 | 103 | 32% | Verify | -21 | 65 | 0 | Verify | 402 | 2 | 42 | 6% | Verify |
| SLU1_2 | 614 | 507 | 43 | 24 | 175% | No verify | -42 | 73 | -1 | Verify | 507 | -2 | 10 | -19% | Verify |
| SLU2_1 | 507 | 419 | 37 | 93 | 40% | Verify | -19 | 67 | 0 | Verify | 419 | 1 | 38 | 4% | Verify |
| SLU2_2 | 519 | 429 | 34 | 87 | 39% | Verify | -27 | 67 | 0 | Verify | 429 | 1 | 35 | 3% | Verify |
| SLU3_1 | 485 | 400 | 32 | 103 | 31% | Verify | -21 | 65 | 0 | Verify | 400 | 3 | 42 | 6% | Verify |
| SLU3_2 | 612 | 506 | 42 | 25 | 165% | No verify | -42 | 73 | -1 | Verify | 506 | -2 | 10 | -16% | Verify |
| SLU4_1 | 506 | 418 | 37 | 93 | 39% | Verify | -19 | 66 | 0 | Verify | 418 | 2 | 38 | 4% | Verify |
| SLU4_2 | 518 | 428 | 34 | 87 | 38% | Verify | -27 | 67 | 0 | Verify | 428 | 1 | 35 | 4% | Verify |
| SLU5_1 | 464 | 383 | 30 | 112 | 27% | Verify | -20 | 64 | 0 | Verify | 383 | 3 | 45 | 7% | Verify |
| SLU5_2 | 676 | 558 | 46 | -30 | -155% | No verify | -56 | 76 | -1 | Verify | 558 | -4 | -12 | 32% | Verify |
| SLU6_1 | 499 | 412 | 37 | 97 | 38% | Verify | -17 | 66 | 0 | Verify | 412 | 2 | 39 | 4% | Verify |
| SLU6_2 | 519 | 428 | 32 | 87 | 37% | Verify | -31 | 67 | 0 | Verify | 428 | 1 | 35 | 4% | Verify |
| SLU7 | 389 | 321 | 26 | 133 | 20% | Verify | -19 | 59 | 0 | Verify | 321 | 1 | 54 | 2% | Verify |
| SLU8_1 | 370 | 305 | 25 | 136 | 18% | Verify | -15 | 57 | 0 | Verify | 305 | 2 | 55 | 4% | Verify |
| SLU8_2 | 497 | 411 | 35 | 98 | 35% | Verify | -37 | 66 | -1 | Verify | 411 | -2 | 40 | -6% | Verify |
| SLU9_1 | 391 | 323 | 29 | 133 | 22% | Verify | -13 | 59 | 0 | Verify | 323 | 1 | 54 | 2% | Verify |
| SLU9_2 | 403 | 333 | 26 | 130 | 20% | Verify | -21 | 60 | 0 | Verify | 333 | 1 | 53 | 2% | Verify |
| SLU10_1 | 368 | 304 | 24 | 136 | 18% | Verify | -15 | 57 | 0 | Verify | 304 | 2 | 55 | 4% | Verify |
| SLU10_2 | 496 | 409 | 34 | 98 | 35% | Verify | -37 | 66 | -1 | Verify | 409 | -2 | 40 | -5% | Verify |
| SLU11_1 | 389 | 321 | 29 | 133 | 22% | Verify | -13 | 59 | 0 | Verify | 321 | 1 | 54 | 2% | Verify |
| SLU11_2 | 401 | 331 | 26 | 131 | 20% | Verify | -21 | 59 | 0 | Verify | 331 | 1 | 53 | 2% | Verify |
| SLU12_1 | 347 | 287 | 22 | 138 | 16% | Verify | -14 | 55 | 0 | Verify | 287 | 3 | 56 | 5% | Verify |
| SLU12_2 | 560 | 462 | 38 | 63 | 61% | Verify | -50 | 70 | -1 | Verify | 462 | -4 | 25 | -16% | Verify |
| SLU13_1 | 382 | 315 | 29 | 134 | 22% | Verify | -12 | 58 | 0 | Verify | 315 | 1 | 54 | 2% | Verify |
| SLU13_2 | 402 | 332 | 24 | 130 | 19% | Verify | -25 | 60 | 0 | Verify | 332 | 1 | 53 | 2% | Verify |
| SLU14 | 506 | 417 | 34 | 94 | 37% | Verify | -25 | 66 | 0 | Verify | 417 | 1 | 38 | 4% | Verify |

Table 4-19. Verification of section 1 - Wall 1 in Ultimate limit state (SLU) and in Life sustaining state (SLV).

Wall 2: In this case, the verified section was section 3, where it can be observed that predominantly, the most critical mechanism is the shear mechanism, not satisfying many verifications.

| *Bending in the plane* | | | |
|---|---|---|---|
| **Geometrical parameters** | l | 1.8 | m |
| | t | 1.7 | m |
| | | | |
| **Mechanical parameters** | $f_m$ | 1500 | kN/m2 |
| | $\gamma_m$ | 2 | - |
| | FC | 1.2 | - |
| | $f_d$ | 625 | kN/m2 |

| *Shear* | | | |
|---|---|---|---|
| **Geometrical parameters** | l | 1.8 | m |
| | t | 1.7 | m |
| | h | 7.2 | m |
| | b | 1.5 | |
| **Mechanical parameters** | $\tau_0$ | 25 | kN/m2 |
| | $f_{td}$ | 15.625 | kN/m2 |
| | $\gamma_m$ | 2 | - |
| | FC | 1.2 | - |

| *Bending out of the plane* | | | |
|---|---|---|---|
| **Geometrical parameters** | l | 1.7 | m |
| | t | 1.8 | m |
| **Mechanical parameters** | $f_m$ | 1500 | kN/m2 |
| | $\gamma_m$ | 2 | - |
| | FC | 1.2 | - |
| | $f_d$ | 625 | kN/m2 |

Table 4-20. Parameters for the verification of the Wall 2.

| | BENDING IN THE PLANE | | | | | | SHEAR | | | | BENDING OUT OF THE PLANE | | | | |
|---|---|---|---|---|---|---|---|---|---|---|---|---|---|---|---|
| Combination | N | $\sigma_0$ | $M_{Ed}$ | $M_{Rd}$ | MEd/MRd | Verification | $V_{Ed}$ | $V_{Rd}$ | VEd/VRd | Verification | $\sigma_0$ | $M_{Ed}$ | $M_{Rd}$ | MEd/MRd | Verification |
| | kN | kN/m2 | kNm | kNm | - | - | kN | kN | - | - | kN/m2 | kNm | kNm | - | - |
| **Seismic_1** | **172** | **56** | **263** | **139** | **190%** | **No verify** | **377** | **68** | **551%** | **No verify** | **56** | **40** | **131** | **30%** | **Verify** |
| **Seismic_2** | **173** | **57** | **262** | **139** | **188%** | **No verify** | **376** | **69** | **549%** | **No verify** | **57** | **39** | **132** | **30%** | **Verify** |
| **Seismic_3** | **479** | **157** | **236** | **304** | **77%** | **Verify** | **290** | **106** | **274%** | **No verify** | **157** | **25** | **287** | **9%** | **Verify** |
| **Seismic_4** | **481** | **157** | **235** | **305** | **77%** | **Verify** | **290** | **106** | **273%** | **No verify** | **157** | **25** | **288** | **9%** | **Verify** |
| Seismic_5 | 957 | 313 | -133 | 354 | -38% | Verify | -100 | 146 | -68% | Verify | 313 | -21 | 335 | -6% | Verify |
| Seismic_6 | 958 | 313 | -134 | 354 | -38% | Verify | -100 | 146 | -69% | Verify | 313 | -21 | 334 | -6% | Verify |
| **Seismic_7** | **1264** | **413** | **-160** | **253** | **-63%** | **Verify** | **-186** | **167** | **-112%** | **No verify** | **413** | **-36** | **239** | **-15%** | **Verify** |
| **Seismic_8** | **1265** | **413** | **-161** | **252** | **-64%** | **Verify** | **-187** | **167** | **-112%** | **No verify** | **413** | **-36** | **238** | **-15%** | **Verify** |
| **Seismic_9** | **89** | **29** | **156** | **75** | **207%** | **No verify** | **311** | **54** | **578%** | **No verify** | **29** | **35** | **71** | **49%** | **Verify** |
| **Seismic_10** | **324** | **106** | **37** | **233** | **16%** | **Verify** | **168** | **89** | **189%** | **No verify** | **106** | **17** | **220** | **8%** | **Verify** |
| **Seismic_11** | **325** | **106** | **37** | **234** | **16%** | **Verify** | **167** | **89** | **188%** | **No verify** | **106** | **17** | **221** | **8%** | **Verify** |
| **Seismic_12** | **90** | **29** | **155** | **76** | **204%** | **No verify** | **310** | **54** | **574%** | **No verify** | **29** | **35** | **72** | **49%** | **Verify** |
| Seismic_13 | 1348 | 440 | -54 | 207 | -26% | Verify | -120 | 172 | -70% | Verify | 440 | -31 | 196 | -16% | Verify |
| Seismic_14 | 1114 | 364 | 65 | 316 | 21% | Verify | 22 | 157 | 14% | Verify | 364 | -13 | 298 | -4% | Verify |
| Seismic_15 | 1112 | 364 | 65 | 316 | 21% | Verify | 23 | 157 | 14% | Verify | 364 | -13 | 299 | -4% | Verify |
| Seismic_16 | 1349 | 441 | -54 | 207 | -26% | Verify | -121 | 172 | -70% | Verify | 441 | -32 | 195 | -16% | Verify |
| **Seismic_17** | **446** | **146** | **125** | **291** | **43%** | **Verify** | **211** | **102** | **206%** | **No verify** | **146** | **18** | **275** | **7%** | **Verify** |
| Seismic_18 | 681 | 223 | 6 | 356 | 2% | Verify | 68 | 124 | 55% | Verify | 223 | 0 | 336 | 0% | Verify |
| Seismic_19 | 753 | 246 | 98 | 364 | 27% | Verify | 124 | 130 | 95% | Verify | 246 | 4 | 344 | 1% | Verify |
| Seismic_20 | 988 | 323 | -21 | 349 | -6% | Verify | -19 | 148 | -13% | Verify | 323 | -15 | 329 | -4% | Verify |
| Seismic_21 | 685 | 224 | 4 | 357 | 1% | Verify | 66 | 125 | 53% | Verify | 224 | 0 | 337 | 0% | Verify |
| Seismic_22 | 757 | 247 | 96 | 364 | 26% | Verify | 122 | 131 | 93% | Verify | 247 | 4 | 344 | 1% | Verify |
| **Seismic_23** | **449** | **147** | **123** | **293** | **42%** | **Verify** | **209** | **103** | **203%** | **No verify** | **147** | **18** | **276** | **7%** | **Verify** |
| Seismic_24 | 992 | 324 | -23 | 348 | -7% | Verify | -21 | 149 | -14% | Verify | 324 | -15 | 329 | -4% | Verify |

| | | | | | | | | | | | | | | | |
|---|---|---|---|---|---|---|---|---|---|---|---|---|---|---|---|
| SLU1_1 | 949 | 310 | 63 | 355 | 18% | Verify | 123 | 146 | 85% | Verify | 310 | 3 | 336 | 1% | Verify |
| SLU1_2 | 960 | 314 | 80 | 354 | 23% | Verify | 137 | 146 | 94% | Verify | 314 | 7 | 334 | 2% | Verify |
| SLU2_1 | 941 | 308 | 68 | 357 | 19% | Verify | 124 | 145 | 85% | Verify | 308 | 3 | 337 | 1% | Verify |
| SLU2_2 | 966 | 316 | 65 | 353 | 18% | Verify | 130 | 147 | 89% | Verify | 316 | 3 | 333 | 1% | Verify |
| SLU3_1 | 944 | 309 | 62 | 356 | 17% | Verify | 122 | 145 | 84% | Verify | 309 | 3 | 336 | 1% | Verify |
| SLU3_2 | 955 | 312 | 79 | 355 | 22% | Verify | 136 | 146 | 93% | Verify | 312 | 7 | 335 | 2% | Verify |
| SLU4_1 | 936 | 306 | 67 | 357 | 19% | Verify | 123 | 145 | 85% | Verify | 306 | 3 | 337 | 1% | Verify |
| SLU4_2 | 961 | 314 | 64 | 354 | 18% | Verify | 129 | 146 | 88% | Verify | 314 | 3 | 334 | 1% | Verify |
| SLU5_1 | 932 | 305 | 60 | 358 | 17% | Verify | 118 | 144 | 82% | Verify | 305 | 2 | 338 | 1% | Verify |
| SLU5_2 | 951 | 311 | 89 | 355 | 25% | Verify | 141 | 146 | 97% | Verify | 311 | 9 | 336 | 3% | Verify |
| SLU6_1 | 919 | 300 | 68 | 360 | 19% | Verify | 119 | 143 | 83% | Verify | 300 | 3 | 340 | 1% | Verify |
| SLU6_2 | 961 | 314 | 64 | 354 | 18% | Verify | 130 | 146 | 88% | Verify | 314 | 3 | 334 | 1% | Verify |
| SLU7 | 719 | 235 | 51 | 361 | 14% | Verify | 95 | 128 | 74% | Verify | 235 | 2 | 341 | 1% | Verify |
| SLU8_1 | 734 | 240 | 47 | 362 | 13% | Verify | 95 | 129 | 74% | Verify | 240 | 2 | 342 | 1% | Verify |
| SLU8_2 | 745 | 243 | 65 | 363 | 18% | Verify | 109 | 130 | 84% | Verify | 243 | 7 | 343 | 2% | Verify |
| SLU9_1 | 725 | 237 | 53 | 362 | 15% | Verify | 95 | 128 | 74% | Verify | 237 | 3 | 341 | 1% | Verify |
| SLU9_2 | 751 | 245 | 50 | 364 | 14% | Verify | 102 | 130 | 78% | Verify | 245 | 3 | 343 | 1% | Verify |
| SLU10_1 | 729 | 238 | 46 | 362 | 13% | Verify | 94 | 128 | 73% | Verify | 238 | 2 | 342 | 1% | Verify |
| SLU10_2 | 740 | 242 | 64 | 363 | 18% | Verify | 108 | 129 | 83% | Verify | 242 | 6 | 343 | 2% | Verify |
| SLU11_1 | 720 | 235 | 52 | 361 | 14% | Verify | 94 | 128 | 74% | Verify | 235 | 2 | 341 | 1% | Verify |
| SLU11_2 | 746 | 244 | 49 | 363 | 13% | Verify | 101 | 130 | 78% | Verify | 244 | 2 | 343 | 1% | Verify |
| SLU12_1 | 717 | 234 | 44 | 361 | 12% | Verify | 90 | 127 | 70% | Verify | 234 | 2 | 341 | 0% | Verify |
| SLU12_2 | 735 | 240 | 73 | 362 | 20% | Verify | 113 | 129 | 87% | Verify | 240 | 9 | 342 | 3% | Verify |
| SLU13_1 | 703 | 230 | 53 | 359 | 15% | Verify | 90 | 126 | 72% | Verify | 230 | 2 | 339 | 1% | Verify |
| SLU13_2 | 745 | 243 | 48 | 363 | 13% | Verify | 101 | 130 | 78% | Verify | 243 | 2 | 343 | 1% | Verify |
| SLU14 | 934 | 305 | 66 | 358 | 19% | Verify | 124 | 144 | 85% | Verify | 305 | 2 | 338 | 1% | Verify |

Table 4-21. Verification of section 3 - Wall 2 in Ultimate limit state (SLU) and in Life sustaining state (SLV).

Wall 3: The main problem with this wall lies in the fascia, which is under severe seismic stress, it can be noticed in the Table 4-23.

| ***Bending in the plane*** | | | |
|---|---|---|---|
| **Geometrical parameters** | l | 1.63 | m |
| | t | 0.7 | m |
| | | | |
| **Mechanical parameters** | $f_m$ | 1500 | kN/m2 |
| | $\gamma_m$ | 2 | - |
| | FC | 1.2 | - |
| | $f_d$ | 625 | kN/m2 |

| ***Shear*** | | | |
|---|---|---|---|
| **Geometrical parameters** | l | 1.63 | m |
| | t | 0.7 | m |
| | h | 3 | m |
| | b | 1.5 | |
| **Mechanical parameters** | $\tau_0$ | 25 | kN/m2 |
| | $f_{td}$ | 15.625 | kN/m2 |
| | $\gamma_m$ | 2 | - |
| | FC | 1.2 | - |

| ***Bending out of the plane*** | | | |
|---|---|---|---|
| **Geometrical parameters** | l | 0.7 | m |
| | t | 1.63 | m |
| **Mechanical parameters** | $f_m$ | 1500 | kN/m2 |
| | $\gamma_m$ | 2 | - |
| | FC | 1.2 | - |
| | $f_d$ | 625 | kN/m2 |

Table 4-22. Parameters for the verification of the Wall 3.

| | BENDING IN THE PLANE | | | | | | SHEAR | | | | BENDING OUT OF THE PLANE | | | | |
|---|---|---|---|---|---|---|---|---|---|---|---|---|---|---|---|
| Combination | N | $\sigma_0$ | $M_{Ed}$ | $M_{Rd}$ | MEd/MRd | Verification | $V_{Ed}$ | $V_{Rd}$ | VEd/VRd | Verification | $\sigma_0$ | $M_{Ed}$ | $M_{Rd}$ | MEd/MRd | Verification |
| | kN | kN/m2 | kNm | kNm | - | - | kN | kN | - | - | kN/m2 | kNm | kNm | - | - |
| **Seismic_1** | **33** | **29** | **18** | **25** | **72%** | **Verify** | **45** | **20** | **227%** | **No verify** | **29** | **3** | **11** | **24%** | **Verify** |
| **Seismic_2** | **33** | **29** | **18** | **25** | **72%** | **Verify** | **45** | **20** | **227%** | **No verify** | **29** | **3** | **11** | **24%** | **Verify** |
| **Seismic_3** | **43** | **37** | **-2** | **32** | **-5%** | **Verify** | **26** | **22** | **120%** | **No verify** | **37** | **1** | **14** | **10%** | **Verify** |
| **Seismic_4** | **43** | **37** | **-2** | **32** | **-6%** | **Verify** | **26** | **22** | **120%** | **No verify** | **37** | **1** | **14** | **10%** | **Verify** |
| **Seismic_5** | **76** | **66** | **-58** | **54** | **-106%** | **No verify** | **-17** | **27** | **-61%** | **Verify** | **66** | **-6** | **23** | **-24%** | **Verify** |
| **Seismic_6** | **76** | **67** | **-58** | **54** | **-106%** | **No verify** | **-17** | **27** | **-62%** | **Verify** | **67** | **-6** | **23** | **-24%** | **Verify** |
| **Seismic_7** | **86** | **75** | **-78** | **60** | **-129%** | **No verify** | **-36** | **29** | **-126%** | **No verify** | **75** | **-7** | **26** | **-26%** | **Verify** |
| **Seismic_8** | **86** | **75** | **-78** | **60** | **-129%** | **No verify** | **-36** | **29** | **-126%** | **No verify** | **75** | **-7** | **26** | **-26%** | **Verify** |
| **Seismic_9** | **36** | **32** | **15** | **28** | **54%** | **Verify** | **46** | **21** | **222%** | **No verify** | **32** | **1** | **12** | **10%** | **Verify** |
| **Seismic_10** | **49** | **43** | **-8** | **37** | **-21%** | **Verify** | **27** | **23** | **119%** | **No verify** | **43** | **-1** | **16** | **-8%** | **Verify** |
| **Seismic_11** | **49** | **43** | **-8** | **37** | **-21%** | **Verify** | **27** | **23** | **119%** | **No verify** | **43** | **-1** | **16** | **-8%** | **Verify** |
| **Seismic_12** | **37** | **32** | **15** | **28** | **54%** | **Verify** | **46** | **21** | **222%** | **No verify** | **32** | **1** | **12** | **10%** | **Verify** |
| **Seismic_13** | **82** | **72** | **-74** | **58** | **-129%** | **No verify** | **-37** | **28** | **-130%** | **No verify** | **72** | **-5** | **25** | **-22%** | **Verify** |
| **Seismic_14** | **69** | **61** | **-52** | **50** | **-104%** | **No verify** | **-18** | **26** | **-69%** | **Verify** | **61** | **-3** | **21** | **-14%** | **Verify** |
| **Seismic_15** | **69** | **60** | **-52** | **50** | **-103%** | **No verify** | **-18** | **26** | **-69%** | **Verify** | **60** | **-3** | **21** | **-14%** | **Verify** |
| **Seismic_16** | **82** | **72** | **-74** | **58** | **-129%** | **No verify** | **-37** | **28** | **-131%** | **No verify** | **72** | **-5** | **25** | **-22%** | **Verify** |
| **Seismic_17** | **48** | **42** | **-8** | **36** | **-23%** | **Verify** | **24** | **23** | **104%** | **No verify** | **42** | **0** | **15** | **-2%** | **Verify** |
| Seismic_18 | 61 | 53 | -31 | 45 | -69% | Verify | 5 | 25 | 20% | Verify | 53 | -3 | 19 | -14% | Verify |
| Seismic_19 | 58 | 50 | -28 | 42 | -66% | Verify | 5 | 24 | 18% | Verify | 50 | -2 | 18 | -8% | Verify |
| **Seismic_20** | **70** | **62** | **-51** | **51** | **-100%** | **No verify** | **-14** | **26** | **-53%** | **Verify** | **62** | **-4** | **22** | **-18%** | **Verify** |
| Seismic_21 | 61 | 53 | -31 | 45 | -70% | Verify | 5 | 25 | 20% | Verify | 53 | -3 | 19 | -14% | Verify |
| Seismic_22 | 58 | 51 | -28 | 43 | -67% | Verify | 4 | 24 | 18% | Verify | 51 | -2 | 18 | -8% | Verify |
| **Seismic_23** | **48** | **42** | **-8** | **36** | **-23%** | **Verify** | **24** | **23** | **103%** | **No verify** | **42** | **0** | **15** | **-2%** | **Verify** |
| **Seismic_24** | **71** | **62** | **-51** | **51** | **-101%** | **No verify** | **-14** | **26** | **-54%** | **Verify** | **62** | **-4** | **22** | **-18%** | **Verify** |
| SLU1_1 | 86 | 76 | -42 | 60 | -70% | Verify | 12 | 29 | 41% | Verify | 76 | -4 | 26 | -14% | Verify |
| **SLU1_2** | **100** | **88** | **-70** | **68** | **-103%** | **No verify** | **-14** | **31** | **-47%** | **Verify** | **88** | **0** | **29** | **-1%** | **Verify** |
| SLU2_1 | 89 | 78 | -47 | 62 | -76% | Verify | 8 | 29 | 27% | Verify | 78 | -3 | 27 | -12% | Verify |
| SLU2_2 | 87 | 76 | -42 | 61 | -69% | Verify | 13 | 29 | 46% | Verify | 76 | -3 | 26 | -13% | Verify |
| SLU3_1 | 89 | 78 | -45 | 62 | -72% | Verify | 12 | 29 | 43% | Verify | 78 | -3 | 27 | -12% | Verify |
| **SLU3_2** | **103** | **90** | **-72** | **69** | **-104%** | **No verify** | **-14** | **31** | **-44%** | **Verify** | **90** | **0** | **30** | **1%** | **Verify** |
| SLU4_1 | 92 | 81 | -50 | 64 | -78% | Verify | 8 | 30 | 29% | Verify | 81 | -3 | 27 | -10% | Verify |
| SLU4_2 | 90 | 78 | -44 | 62 | -71% | Verify | 14 | 29 | 48% | Verify | 78 | -3 | 27 | -11% | Verify |
| SLU5_1 | 81 | 71 | -39 | 57 | -68% | Verify | 10 | 28 | 37% | Verify | 71 | -3 | 25 | -13% | Verify |
| **SLU5_2** | **104** | **91** | **-85** | **70** | **-121%** | **No verify** | **-33** | **31** | **-106%** | **No verify** | **91** | **2** | **30** | **8%** | **Verify** |
| SLU6_1 | 86 | 76 | -48 | 60 | -79% | Verify | 4 | 29 | 13% | Verify | 76 | -3 | 26 | -10% | Verify |
| SLU6_2 | 82 | 72 | -38 | 58 | -66% | Verify | 13 | 28 | 46% | Verify | 72 | -3 | 25 | -12% | Verify |
| SLU7 | 59 | 52 | -30 | 44 | -68% | Verify | 5 | 25 | 19% | Verify | 52 | -2 | 19 | -11% | Verify |
| SLU8_1 | 69 | 60 | -33 | 50 | -67% | Verify | 10 | 26 | 39% | Verify | 60 | -3 | 21 | -14% | Verify |
| **SLU8_2** | **82** | **72** | **-61** | **58** | **-105%** | **No verify** | **-16** | **28** | **-56%** | **Verify** | **72** | **0** | **25** | **2%** | **Verify** |
| SLU9_1 | 72 | 63 | -38 | 52 | -75% | Verify | 6 | 27 | 24% | Verify | 63 | -3 | 22 | -12% | Verify |
| SLU9_2 | 69 | 61 | -33 | 50 | -66% | Verify | 12 | 26 | 45% | Verify | 61 | -3 | 21 | -13% | Verify |
| SLU10_1 | 71 | 63 | -36 | 51 | -69% | Verify | 11 | 27 | 41% | Verify | 63 | -2 | 22 | -11% | Verify |
| **SLU10_2** | **85** | **74** | **-63** | **59** | **-106%** | **No verify** | **-15** | **29** | **-53%** | **Verify** | **74** | **1** | **26** | **4%** | **Verify** |
| SLU11_1 | 74 | 65 | -41 | 53 | -77% | Verify | 7 | 27 | 26% | Verify | 65 | -2 | 23 | -9% | Verify |
| SLU11_2 | 72 | 63 | -35 | 52 | -68% | Verify | 12 | 27 | 47% | Verify | 63 | -2 | 22 | -10% | Verify |
| SLU12_1 | 63 | 56 | -30 | 46 | -65% | Verify | 9 | 25 | 35% | Verify | 56 | -3 | 20 | -13% | Verify |
| **SLU12_2** | **86** | **75** | **-76** | **60** | **-127%** | **No verify** | **-34** | **29** | **-120%** | **No verify** | **75** | **3** | **26** | **12%** | **Verify** |
| SLU13_1 | 69 | 60 | -39 | 50 | -78% | Verify | 2 | 26 | 9% | Verify | 60 | -2 | 21 | -9% | Verify |
| SLU13_2 | 64 | 56 | -29 | 47 | -63% | Verify | 11 | 25 | 45% | Verify | 56 | -2 | 20 | -12% | Verify |
| SLU14 | 77 | 67 | -39 | 55 | -70% | Verify | 6 | 27 | 22% | Verify | 67 | -3 | 24 | -12% | Verify |

Table 4-23. Verification of section 2 - Wall 3 in Ultimate limit state (SLU) and in Life sustaining state (SLV).

Wall 4:

Due to the material with which this wall was made, the mechanical characteristics and the resistance is higher, for this reason the section is fully verified.

| *Bending in the plane* | | | |
|---|---|---|---|
| **Geometrical parameters** | l | 3.62 | m |
| | t | 1.85 | m |
| | | | |
| **Mechanical parameters** | $f_m$ | 3450 | kN/m2 |
| | $\gamma_m$ | 2 | - |
| | FC | 1.2 | - |
| | $f_d$ | 1437.5 | kN/m2 |

| *Shear* | | | |
|---|---|---|---|
| **Geometrical parameters** | l | 3.62 | m |
| | t | 1.85 | m |
| | h | 3 | m |
| | b | 1 | |
| **Mechanical parameters** | $\tau_0$ | 90 | kN/m2 |
| | $f_{td}$ | 56.25 | kN/m2 |
| | $\gamma_m$ | 2 | - |
| | FC | 1.2 | - |

| *Bending out of the plane* | | | |
|---|---|---|---|
| **Geometrical parameters** | l | 1.85 | m |
| | t | 3.62 | m |
| **Mechanical parameters** | $f_m$ | 3450 | kN/m2 |
| | $\gamma_m$ | 2 | - |
| | FC | 1.2 | - |
| | $f_d$ | 1437.5 | kN/m2 |

Table 4-24. Parameters for the verification of the Wall 4.

| | BENDING IN THE PLANE | | | | | | SHEAR | | | | BENDING OUT OF THE PLANE | | | | |
|---|---|---|---|---|---|---|---|---|---|---|---|---|---|---|---|
| Combination | N | $\sigma_0$ | $M_{Ed}$ | $M_{Rd}$ | MEd/MRd | Verification | $V_{Ed}$ | $V_{Rd}$ | VEd/VRd | Verification | $\sigma_0$ | $M_{Ed}$ | $M_{Rd}$ | MEd/MRd | Verification |
| | kN | kN/m2 | kNm | kNm | - | - | kN | kN | - | - | kN/m2 | kNm | kNm | - | - |
| Seismic_1 | 450 | 243 | 100 | 180 | 55% | Verify | 110 | 160 | 68% | Verify | 243 | 13 | 333 | 4% | Verify |
| Seismic_2 | 450 | 243 | 100 | 180 | 55% | Verify | 110 | 160 | 68% | Verify | 243 | 13 | 333 | 4% | Verify |
| Seismic_3 | 547 | 296 | 36 | 207 | 17% | Verify | 36 | 174 | 21% | Verify | 296 | 8 | 384 | 2% | Verify |
| Seismic_4 | 547 | 296 | 35 | 207 | 17% | Verify | 36 | 174 | 21% | Verify | 296 | 8 | 384 | 2% | Verify |
| Seismic_5 | 633 | 342 | 9 | 228 | 4% | Verify | 3 | 185 | 1% | Verify | 342 | -7 | 422 | -2% | Verify |
| Seismic_6 | 634 | 342 | 9 | 228 | 4% | Verify | 3 | 185 | 1% | Verify | 342 | -7 | 422 | -2% | Verify |
| Seismic_7 | 731 | 395 | -55 | 247 | -22% | Verify | -71 | 197 | -36% | Verify | 395 | -13 | 457 | -3% | Verify |
| Seismic_8 | 731 | 395 | -55 | 247 | -22% | Verify | -71 | 197 | -36% | Verify | 395 | -13 | 458 | -3% | Verify |
| Seismic_9 | 412 | 223 | 143 | 168 | 85% | Verify | 154 | 154 | 100% | Verify | 223 | 12 | 312 | 4% | Verify |
| Seismic_10 | 456 | 246 | 116 | 182 | 64% | Verify | 126 | 161 | 79% | Verify | 246 | 6 | 336 | 2% | Verify |
| Seismic_11 | 456 | 246 | 116 | 182 | 64% | Verify | 126 | 161 | 78% | Verify | 246 | 6 | 337 | 2% | Verify |
| Seismic_12 | 401 | 217 | 143 | 165 | 87% | Verify | 145 | 149 | 97% | Verify | 217 | 12 | 305 | 4% | Verify |
| Seismic_13 | 780 | 422 | -98 | 255 | -38% | Verify | -120 | 202 | -59% | Verify | 422 | -12 | 473 | -2% | Verify |
| Seismic_14 | 725 | 392 | -71 | 246 | -29% | Verify | -88 | 196 | -45% | Verify | 392 | -5 | 456 | -1% | Verify |
| Seismic_15 | 725 | 392 | -71 | 246 | -29% | Verify | -88 | 196 | -45% | Verify | 392 | -5 | 456 | -1% | Verify |
| Seismic_16 | 780 | 422 | -98 | 256 | -38% | Verify | -120 | 202 | -59% | Verify | 422 | -12 | 473 | -2% | Verify |
| Seismic_17 | 514 | 278 | 68 | 199 | 34% | Verify | 72 | 169 | 43% | Verify | 278 | 6 | 367 | 2% | Verify |
| Seismic_18 | 569 | 308 | 41 | 213 | 19% | Verify | 40 | 176 | 23% | Verify | 308 | 0 | 394 | 0% | Verify |
| Seismic_19 | 612 | 331 | 4 | 223 | 2% | Verify | -2 | 182 | -1% | Verify | 331 | 1 | 413 | 0% | Verify |
| Seismic_20 | 667 | 360 | -23 | 235 | -10% | Verify | -34 | 189 | -18% | Verify | 360 | -5 | 435 | -1% | Verify |
| Seismic_21 | 569 | 308 | 41 | 213 | 19% | Verify | 40 | 176 | 23% | Verify | 308 | 0 | 394 | 0% | Verify |
| Seismic_22 | 612 | 331 | 4 | 223 | 2% | Verify | -2 | 182 | -1% | Verify | 331 | 1 | 413 | 0% | Verify |
| Seismic_23 | 514 | 278 | 68 | 199 | 34% | Verify | 72 | 169 | 43% | Verify | 278 | 6 | 368 | 2% | Verify |
| Seismic_24 | 667 | 360 | -24 | 235 | -10% | Verify | -34 | 189 | -18% | Verify | 360 | -5 | 435 | -1% | Verify |
| SLU1_1 | 764 | 413 | 39 | 253 | 15% | Verify | 37 | 200 | 19% | Verify | 413 | 0 | 468 | 0% | Verify |
| SLU1_2 | 801 | 433 | 19 | 259 | 7% | Verify | 14 | 205 | 7% | Verify | 433 | 4 | 478 | 1% | Verify |
| SLU2_1 | 789 | 427 | 23 | 257 | 9% | Verify | 18 | 203 | 9% | Verify | 427 | 2 | 475 | 0% | Verify |
| SLU2_2 | 750 | 406 | 49 | 251 | 20% | Verify | 50 | 199 | 25% | Verify | 406 | 0 | 464 | 0% | Verify |
| SLU3_1 | 759 | 410 | 39 | 252 | 16% | Verify | 38 | 200 | 19% | Verify | 410 | 0 | 466 | 0% | Verify |
| SLU3_2 | 796 | 430 | 20 | 258 | 8% | Verify | 15 | 204 | 7% | Verify | 430 | 4 | 477 | 1% | Verify |
| SLU4_1 | 785 | 424 | 23 | 256 | 9% | Verify | 18 | 203 | 9% | Verify | 424 | 1 | 474 | 0% | Verify |
| SLU4_2 | 746 | 403 | 50 | 250 | 20% | Verify | 50 | 198 | 25% | Verify | 403 | 0 | 462 | 0% | Verify |
| SLU5_1 | 760 | 411 | 35 | 252 | 14% | Verify | 33 | 200 | 16% | Verify | 411 | 0 | 467 | 0% | Verify |
| SLU5_2 | 821 | 444 | 3 | 261 | 1% | Verify | -5 | 207 | -3% | Verify | 444 | 6 | 484 | 1% | Verify |
| SLU6_1 | 802 | 433 | 9 | 259 | 3% | Verify | 0 | 205 | 0% | Verify | 433 | 2 | 479 | 0% | Verify |
| SLU6_2 | 737 | 398 | 52 | 248 | 21% | Verify | 54 | 197 | 27% | Verify | 398 | -1 | 459 | 0% | Verify |
| SLU7 | 590 | 319 | 22 | 218 | 10% | Verify | 19 | 179 | 11% | Verify | 319 | 0 | 404 | 0% | Verify |
| SLU8_1 | 587 | 317 | 32 | 217 | 15% | Verify | 32 | 179 | 18% | Verify | 317 | 0 | 402 | 0% | Verify |
| SLU8_2 | 624 | 337 | 13 | 226 | 6% | Verify | 9 | 183 | 5% | Verify | 337 | 4 | 418 | 1% | Verify |
| SLU9_1 | 612 | 331 | 16 | 223 | 7% | Verify | 12 | 182 | 7% | Verify | 331 | 1 | 413 | 0% | Verify |
| SLU9_2 | 573 | 310 | 42 | 214 | 20% | Verify | 44 | 177 | 25% | Verify | 310 | 0 | 396 | 0% | Verify |
| SLU10_1 | 582 | 315 | 33 | 216 | 15% | Verify | 32 | 178 | 18% | Verify | 315 | 0 | 400 | 0% | Verify |
| SLU10_2 | 619 | 335 | 13 | 225 | 6% | Verify | 9 | 183 | 5% | Verify | 335 | 4 | 416 | 1% | Verify |
| SLU11_1 | 607 | 328 | 17 | 222 | 7% | Verify | 13 | 181 | 7% | Verify | 328 | 1 | 411 | 0% | Verify |
| SLU11_2 | 569 | 307 | 43 | 213 | 20% | Verify | 44 | 176 | 25% | Verify | 307 | -1 | 394 | 0% | Verify |
| SLU12_1 | 583 | 315 | 29 | 216 | 13% | Verify | 27 | 178 | 15% | Verify | 315 | 0 | 400 | 0% | Verify |
| SLU12_2 | 644 | 348 | -4 | 230 | -2% | Verify | -11 | 186 | -6% | Verify | 348 | 6 | 426 | 1% | Verify |
| SLU13_1 | 625 | 338 | 2 | 226 | 1% | Verify | -5 | 184 | -3% | Verify | 338 | 2 | 418 | 0% | Verify |
| SLU13_2 | 560 | 303 | 46 | 211 | 22% | Verify | 48 | 175 | 27% | Verify | 303 | -1 | 390 | 0% | Verify |
| SLU14 | 768 | 415 | 29 | 253 | 11% | Verify | 25 | 201 | 12% | Verify | 415 | 1 | 469 | 0% | Verify |

Table 4-25. Verification of section 1 - Wall 4 in Ultimate limit state (SLU) and in Life sustaining state (SLV).

Wall 5: This section is also completely verified.

| *Bending in the plane* | | | |
|---|---|---|---|
| **Geometrical parameters** | l | 0.8 | m |
| | t | 2.25 | m |

| | | | |
|---|---|---|---|
| **Mechanical parameters** | $f_m$ | 3450 | kN/m2 |
| | $\gamma_m$ | 2 | - |
| | FC | 1.2 | - |
| | $f_d$ | 1437.5 | kN/m2 |

| *Shear* | | | |
|---|---|---|---|
| **Geometrical parameters** | l | 0.8 | m |
| | t | 2.25 | m |
| | h | 9.3 | m |
| | b | 1.5 | |
| **Mechanical parameters** | $\tau_0$ | 90 | kN/m2 |
| | $f_{td}$ | 56.25 | kN/m2 |
| | $\gamma_m$ | 2 | - |
| | FC | 1.2 | - |

| *Bending out of the plane* | | | |
|---|---|---|---|
| **Geometrical parameters** | l | 1.85 | m |
| | t | 0.8 | m |
| **Mechanical parameters** | $f_m$ | 3450 | kN/m2 |
| | $\gamma_m$ | 2 | - |
| | FC | 1.2 | - |
| | $f_d$ | 1437.5 | kN/m2 |

Table 4-26. Parameters for the verification of the Wall 5.

| | BENDING IN THE PLANE | | | | | | SHEAR | | | | BENDING OUT OF THE PLANE | | | | |
|---|---|---|---|---|---|---|---|---|---|---|---|---|---|---|---|
| Combination | N | $\sigma_0$ | $M_{Ed}$ | $M_{Rd}$ | MEd/MRd | Verification | $V_{Ed}$ | $V_{Rd}$ | VEd/VRd | Verification | $\sigma_0$ | $M_{Ed}$ | $M_{Rd}$ | MEd/MRd | Verification |
| | kN | kN/m2 | kNm | kNm | - | - | kN | kN | - | - | kN/m2 | kNm | kNm | - | - |
| Seismic_1 | 450 | 250 | 100 | 143 | 70% | Verify | 110 | 157 | 70% | Verify | 304 | 13 | 313 | 4% | Verify |
| Seismic_2 | 450 | 250 | 100 | 143 | 70% | Verify | 110 | 158 | 70% | Verify | 304 | 13 | 313 | 4% | Verify |
| Seismic_3 | 547 | 304 | 36 | 164 | 22% | Verify | 36 | 171 | 21% | Verify | 370 | 8 | 353 | 2% | Verify |
| Seismic_4 | 547 | 304 | 35 | 164 | 22% | Verify | 36 | 171 | 21% | Verify | 370 | 8 | 353 | 2% | Verify |
| Seismic_5 | 633 | 352 | 9 | 180 | 5% | Verify | 3 | 182 | 1% | Verify | 428 | -7 | 381 | -2% | Verify |
| Seismic_6 | 634 | 352 | 9 | 180 | 5% | Verify | 3 | 182 | 1% | Verify | 428 | -7 | 381 | -2% | Verify |
| Seismic_7 | 731 | 406 | -55 | 195 | -28% | Verify | -71 | 194 | -37% | Verify | 494 | -13 | 403 | -3% | Verify |
| Seismic_8 | 731 | 406 | -55 | 195 | -28% | Verify | -71 | 194 | -37% | Verify | 494 | -13 | 403 | -3% | Verify |
| Seismic_9 | 400 | 222 | 131 | 131 | 100% | Verify | 148 | 150 | 98% | Verify | 271 | 12 | 288 | 4% | Verify |
| Seismic_10 | 456 | 253 | 116 | 144 | 80% | Verify | 126 | 158 | 80% | Verify | 308 | 6 | 315 | 2% | Verify |
| Seismic_11 | 456 | 253 | 116 | 144 | 80% | Verify | 126 | 158 | 80% | Verify | 308 | 6 | 315 | 2% | Verify |
| Seismic_12 | 401 | 223 | 127 | 131 | 97% | Verify | 139 | 150 | 92% | Verify | 271 | 12 | 288 | 4% | Verify |
| Seismic_13 | 780 | 434 | -98 | 201 | -49% | Verify | -120 | 199 | -60% | Verify | 527 | -12 | 410 | -3% | Verify |
| Seismic_14 | 725 | 403 | -71 | 194 | -37% | Verify | -88 | 193 | -46% | Verify | 490 | -5 | 402 | -1% | Verify |
| Seismic_15 | 725 | 403 | -71 | 194 | -37% | Verify | -88 | 193 | -46% | Verify | 490 | -5 | 402 | -1% | Verify |
| Seismic_16 | 780 | 434 | -98 | 201 | -49% | Verify | -120 | 199 | -60% | Verify | 527 | -12 | 410 | -3% | Verify |
| Seismic_17 | 514 | 286 | 68 | 158 | 43% | Verify | 72 | 166 | 43% | Verify | 347 | 6 | 340 | 2% | Verify |
| Seismic_18 | 569 | 316 | 41 | 169 | 24% | Verify | 40 | 174 | 23% | Verify | 385 | 0 | 361 | 0% | Verify |
| Seismic_19 | 612 | 340 | 4 | 177 | 2% | Verify | -2 | 179 | -1% | Verify | 413 | 1 | 374 | 0% | Verify |
| Seismic_20 | 667 | 370 | -23 | 186 | -13% | Verify | -34 | 186 | -18% | Verify | 450 | -5 | 389 | -1% | Verify |
| Seismic_21 | 569 | 316 | 41 | 169 | 24% | Verify | 40 | 174 | 23% | Verify | 385 | 0 | 361 | 0% | Verify |
| Seismic_22 | 612 | 340 | 4 | 177 | 2% | Verify | -2 | 179 | -1% | Verify | 413 | 1 | 374 | 0% | Verify |
| Seismic_23 | 514 | 286 | 68 | 158 | 43% | Verify | 72 | 166 | 43% | Verify | 348 | 6 | 340 | 2% | Verify |
| Seismic_24 | 667 | 370 | -24 | 186 | -13% | Verify | -34 | 186 | -18% | Verify | 451 | -5 | 389 | -1% | Verify |

| | | | | | | | | | | | | | | | |
|---|---|---|---|---|---|---|---|---|---|---|---|---|---|---|---|
| SLU1_1 | 764 | 424 | 39 | 199 | 20% | Verify | 37 | 197 | 19% | Verify | 516 | 0 | 408 | 0% | Verify |
| SLU1_2 | 801 | 445 | 19 | 204 | 9% | Verify | 14 | 201 | 7% | Verify | 541 | 4 | 413 | 1% | Verify |
| SLU2_1 | 789 | 438 | 23 | 202 | 11% | Verify | 18 | 200 | 9% | Verify | 533 | 2 | 411 | 0% | Verify |
| SLU2_2 | 750 | 417 | 49 | 198 | 25% | Verify | 50 | 196 | 25% | Verify | 507 | 0 | 406 | 0% | Verify |
| SLU3_1 | 759 | 422 | 39 | 199 | 20% | Verify | 38 | 197 | 19% | Verify | 513 | 0 | 407 | 0% | Verify |
| SLU3_2 | 796 | 442 | 20 | 203 | 10% | Verify | 15 | 201 | 7% | Verify | 538 | 4 | 412 | 1% | Verify |
| SLU4_1 | 785 | 436 | 23 | 202 | 12% | Verify | 18 | 200 | 9% | Verify | 530 | 1 | 411 | 0% | Verify |
| SLU4_2 | 746 | 414 | 50 | 197 | 25% | Verify | 50 | 195 | 26% | Verify | 504 | 0 | 405 | 0% | Verify |
| SLU5_1 | 760 | 422 | 35 | 199 | 18% | Verify | 33 | 197 | 17% | Verify | 513 | 0 | 408 | 0% | Verify |
| SLU5_2 | 821 | 456 | 3 | 206 | 1% | Verify | -5 | 204 | -3% | Verify | 555 | 6 | 415 | 1% | Verify |
| SLU6_1 | 802 | 445 | 9 | 204 | 4% | Verify | 0 | 202 | 0% | Verify | 542 | 2 | 413 | 1% | Verify |
| SLU6_2 | 737 | 410 | 52 | 196 | 27% | Verify | 54 | 194 | 28% | Verify | 498 | -1 | 404 | 0% | Verify |
| SLU7 | 590 | 328 | 22 | 173 | 13% | Verify | 19 | 176 | 11% | Verify | 399 | 0 | 368 | 0% | Verify |
| SLU8_1 | 587 | 326 | 32 | 172 | 19% | Verify | 32 | 176 | 18% | Verify | 396 | 0 | 367 | 0% | Verify |
| SLU8_2 | 624 | 347 | 13 | 179 | 7% | Verify | 9 | 181 | 5% | Verify | 421 | 4 | 378 | 1% | Verify |
| SLU9_1 | 612 | 340 | 16 | 177 | 9% | Verify | 12 | 179 | 7% | Verify | 413 | 1 | 374 | 0% | Verify |
| SLU9_2 | 573 | 318 | 42 | 170 | 25% | Verify | 44 | 174 | 25% | Verify | 387 | 0 | 362 | 0% | Verify |
| SLU10_1 | 582 | 323 | 33 | 171 | 19% | Verify | 32 | 175 | 18% | Verify | 393 | 0 | 365 | 0% | Verify |
| SLU10_2 | 619 | 344 | 13 | 178 | 7% | Verify | 9 | 180 | 5% | Verify | 418 | 4 | 377 | 1% | Verify |
| SLU11_1 | 607 | 337 | 17 | 176 | 9% | Verify | 13 | 179 | 7% | Verify | 410 | 1 | 373 | 0% | Verify |
| SLU11_2 | 569 | 316 | 43 | 169 | 25% | Verify | 44 | 174 | 26% | Verify | 384 | -1 | 361 | 0% | Verify |
| SLU12_1 | 583 | 324 | 29 | 171 | 17% | Verify | 27 | 175 | 15% | Verify | 394 | 0 | 365 | 0% | Verify |
| SLU12_2 | 644 | 358 | -4 | 182 | -2% | Verify | -11 | 183 | -6% | Verify | 435 | 6 | 384 | 2% | Verify |
| SLU13_1 | 625 | 347 | 2 | 179 | 1% | Verify | -5 | 181 | -3% | Verify | 422 | 2 | 378 | 1% | Verify |
| SLU13_2 | 560 | 311 | 46 | 167 | 27% | Verify | 48 | 172 | 28% | Verify | 378 | -1 | 358 | 0% | Verify |
| SLU14 | 768 | 426 | 29 | 200 | 14% | Verify | 25 | 198 | 13% | Verify | 519 | 1 | 409 | 0% | Verify |

Table 4-27. Verification of section 1 - Wall 5 in Ultimate limit state (SLU) and in Life sustaining state (SLV).

Wall 6: As can be seen from the Table 4-29 the section does not check mainly in shear.

| ***Bending in the plane*** | | | |
|---|---|---|---|
| **Geometrical parameters** | l | 9 | m |
| | t | 0.5 | m |
| | | | |
| **Mechanical parameters** | $f_m$ | 1500 | kN/m2 |
| | $\gamma_m$ | 2 | - |
| | FC | 1.2 | - |
| | $f_d$ | 625 | kN/m2 |

| ***Shear*** | | | |
|---|---|---|---|
| **Geometrical parameters** | l | 9 | m |
| | t | 0.5 | m |
| | h | 7.2 | m |
| | b | 1.5 | |
| **Mechanical parameters** | $\tau_0$ | 25 | kN/m2 |
| | $f_{td}$ | 15.625 | kN/m2 |
| | $\gamma_m$ | 2 | - |
| | FC | 1.2 | - |

| ***Bending out of the plane*** | | | |
|---|---|---|---|
| **Geometrical parameters** | l | 0.5 | m |
| | t | 9 | m |
| **Mechanical parameters** | $f_m$ | 1500 | kN/m2 |
| | $\gamma_m$ | 2 | - |
| | FC | 1.2 | - |
| | $f_d$ | 625 | kN/m2 |

Table 4-28. Parameters for the verification of the Wall 6.

| Combination | BENDING IN THE PLANE | | | | | | SHEAR | | | | BENDING OUT OF THE PLANE | | | | |
|---|---|---|---|---|---|---|---|---|---|---|---|---|---|---|---|
| | N | $\sigma_0$ | $M_{Ed}$ | $M_{Rd}$ | MEd/MRd | Verification | $V_{Ed}$ | $V_{Rd}$ | VEd/VRd | Verification | $\sigma_0$ | $M_{Ed}$ | $M_{Rd}$ | MEd/MRd | Verification |
| | kN | kN/m2 | kNm | kNm | - | - | kN | kN | - | - | kN/m2 | kNm | kNm | - | - |
| **Seismic_1** | **263** | **58** | **541** | **1053** | **51%** | **Verify** | **109** | **102** | **106%** | **No verify** | **58** | **7** | **58** | **13%** | **Verify** |
| **Seismic_2** | **265** | **59** | **537** | **1060** | **51%** | **Verify** | **108** | **102** | **105%** | **No verify** | **59** | **7** | **59** | **12%** | **Verify** |
| Seismic_3 | 441 | 98 | 243 | 1619 | 15% | Verify | -35 | 126 | -28% | Verify | 98 | 1 | 90 | 1% | Verify |
| Seismic_4 | 443 | 98 | 239 | 1624 | 15% | Verify | -36 | 127 | -29% | Verify | 98 | 1 | 90 | 1% | Verify |
| Seismic_5 | 949 | 211 | -576 | 2575 | -22% | Verify | -39 | 178 | -22% | Verify | 211 | -30 | 143 | -21% | Verify |
| Seismic_6 | 951 | 211 | -580 | 2577 | -23% | Verify | -40 | 179 | -22% | Verify | 211 | -30 | 143 | -21% | Verify |
| Seismic_7 | 1127 | 250 | -873 | 2681 | -33% | Verify | -183 | 193 | -95% | Verify | 250 | -36 | 149 | -24% | Verify |
| Seismic_8 | 1129 | 251 | -878 | 2681 | -33% | Verify | -184 | 194 | -95% | Verify | 251 | -36 | 149 | -24% | Verify |
| **Seismic_9** | **295** | **66** | **498** | **1163** | **43%** | **Verify** | **225** | **107** | **210%** | **No verify** | **66** | **2** | **65** | **2%** | **Verify** |
| **Seismic_10** | **501** | **111** | **163** | **1781** | **9%** | **Verify** | **181** | **134** | **135%** | **No verify** | **111** | **-10** | **99** | **-10%** | **Verify** |
| **Seismic_11** | **503** | **112** | **159** | **1786** | **9%** | **Verify** | **180** | **134** | **134%** | **No verify** | **112** | **-10** | **99** | **-10%** | **Verify** |
| **Seismic_12** | **297** | **66** | **494** | **1170** | **42%** | **Verify** | **224** | **107** | **209%** | **No verify** | **66** | **1** | **65** | **2%** | **Verify** |
| **Seismic_13** | **1095** | **243** | **-830** | **2670** | **-31%** | **Verify** | **-299** | **191** | **-157%** | **No verify** | **243** | **-30** | **148** | **-20%** | **Verify** |
| **Seismic_14** | **891** | **198** | **-500** | **2515** | **-20%** | **Verify** | **-256** | **173** | **-148%** | **No verify** | **198** | **-19** | **140** | **-14%** | **Verify** |
| **Seismic_15** | **889** | **198** | **-495** | **2513** | **-20%** | **Verify** | **-255** | **173** | **-147%** | **No verify** | **198** | **-19** | **140** | **-14%** | **Verify** |
| **Seismic_16** | **1097** | **244** | **-835** | **2671** | **-31%** | **Verify** | **-300** | **191** | **-157%** | **No verify** | **244** | **-30** | **148** | **-21%** | **Verify** |
| Seismic_17 | 501 | 111 | 155 | 1781 | 9% | Verify | 58 | 134 | 43% | Verify | 111 | -6 | 99 | -6% | Verify |
| Seismic_18 | 706 | 157 | -180 | 2239 | -8% | Verify | 14 | 156 | 9% | Verify | 157 | -17 | 124 | -13% | Verify |
| Seismic_19 | 679 | 151 | -143 | 2187 | -7% | Verify | -86 | 153 | -56% | Verify | 151 | -12 | 122 | -10% | Verify |
| Seismic_20 | 885 | 197 | -478 | 2508 | -19% | Verify | -130 | 173 | -75% | Verify | 197 | -23 | 139 | -16% | Verify |
| Seismic_21 | 713 | 158 | -194 | 2251 | -9% | Verify | 11 | 156 | 7% | Verify | 158 | -17 | 125 | -14% | Verify |
| Seismic_22 | 685 | 152 | -157 | 2200 | -7% | Verify | -89 | 154 | -58% | Verify | 152 | -12 | 122 | -10% | Verify |
| Seismic_23 | 507 | 113 | 141 | 1798 | 8% | Verify | 55 | 134 | 41% | Verify | 113 | -6 | 100 | -6% | Verify |
| Seismic_24 | 891 | 198 | -492 | 2515 | -20% | Verify | -133 | 173 | -77% | Verify | 198 | -23 | 140 | -17% | Verify |
| SLU1_1 | 969 | 215 | -327 | 2593 | -13% | Verify | -44 | 180 | -25% | Verify | 215 | -20 | 144 | -14% | Verify |
| **SLU1_2** | **302** | **67** | **1470** | **1188** | **124%** | **No verify** | **-272** | **108** | **-252%** | **No verify** | **67** | **1** | **66** | **2%** | **Verify** |
| SLU2_1 | 959 | 213 | -283 | 2584 | -11% | Verify | -58 | 179 | -32% | Verify | 213 | -20 | 144 | -14% | Verify |
| SLU2_2 | 952 | 212 | -259 | 2578 | -10% | Verify | -40 | 179 | -23% | Verify | 212 | -21 | 143 | -15% | Verify |
| SLU3_1 | 963 | 214 | -316 | 2588 | -12% | Verify | -44 | 180 | -25% | Verify | 214 | -20 | 144 | -14% | Verify |
| **SLU3_2** | **296** | **66** | **1482** | **1167** | **127%** | **No verify** | **-272** | **107** | **-255%** | **No verify** | **66** | **2** | **65** | **3%** | **Verify** |
| SLU4_1 | 952 | 212 | -271 | 2578 | -11% | Verify | -58 | 179 | -33% | Verify | 212 | -20 | 143 | -14% | Verify |
| SLU4_2 | 946 | 210 | -248 | 2572 | -10% | Verify | -41 | 178 | -23% | Verify | 210 | -20 | 143 | -14% | Verify |
| SLU5_1 | 950 | 211 | -331 | 2576 | -13% | Verify | -40 | 179 | -22% | Verify | 211 | -19 | 143 | -13% | Verify |
| **SLU5_2** | **162** | **36** | **2665** | **678** | **393%** | **No verify** | **-420** | **85** | **-493%** | **No verify** | **36** | **17** | **38** | **44%** | **Verify** |
| SLU6_1 | 933 | 207 | -257 | 2560 | -10% | Verify | -63 | 177 | -35% | Verify | 207 | -19 | 142 | -13% | Verify |
| SLU6_2 | 921 | 205 | -217 | 2548 | -9% | Verify | -34 | 176 | -19% | Verify | 205 | -20 | 142 | -14% | Verify |
| SLU7 | 696 | 155 | -168 | 2220 | -8% | Verify | -38 | 155 | -24% | Verify | 155 | -14 | 123 | -12% | Verify |
| SLU8_1 | 760 | 169 | -277 | 2333 | -12% | Verify | -33 | 161 | -20% | Verify | 169 | -16 | 130 | -12% | Verify |
| **SLU8_2** | **93** | **21** | **1521** | **404** | **377%** | **No verify** | **-261** | **72** | **-365%** | **No verify** | **21** | **5** | **22** | **24%** | **Verify** |
| SLU9_1 | 750 | 167 | -233 | 2316 | -10% | Verify | -47 | 160 | -29% | Verify | 167 | -16 | 129 | -12% | Verify |
| SLU9_2 | 743 | 165 | -209 | 2304 | -9% | Verify | -29 | 159 | -18% | Verify | 165 | -17 | 128 | -13% | Verify |
| SLU10_1 | 754 | 168 | -265 | 2323 | -11% | Verify | -33 | 160 | -21% | Verify | 168 | -15 | 129 | -12% | Verify |
| **SLU10_2** | **87** | **19** | **1533** | **378** | **405%** | **No verify** | **-261** | **70** | **-372%** | **No verify** | **19** | **6** | **21** | **29%** | **Verify** |
| SLU11_1 | 744 | 165 | -221 | 2306 | -10% | Verify | -47 | 159 | -29% | Verify | 165 | -15 | 128 | -12% | Verify |
| SLU11_2 | 737 | 164 | -197 | 2294 | -9% | Verify | -29 | 159 | -19% | Verify | 164 | -16 | 127 | -13% | Verify |
| SLU12_1 | 741 | 165 | -280 | 2301 | -12% | Verify | -29 | 159 | -18% | Verify | 165 | -15 | 128 | -12% | Verify |
| **SLU12_2** | **370** | **82** | **2716** | **1408** | **193%** | **No verify** | **-408** | **117** | **-348%** | **No verify** | **82** | **21** | **78** | **27%** | **Verify** |
| SLU13_1 | 724 | 161 | -206 | 2271 | -9% | Verify | -51 | 158 | -33% | Verify | 161 | -14 | 126 | -11% | Verify |
| SLU13_2 | 712 | 158 | -167 | 2251 | -7% | Verify | -22 | 156 | -14% | Verify | 158 | -16 | 125 | -13% | Verify |
| SLU14 | 905 | 201 | -219 | 2530 | -9% | Verify | -49 | 175 | -28% | Verify | 201 | -19 | 141 | -13% | Verify |

Table 4-29. Verification of section 1 - Wall 6 in Ultimate limit state (SLU) and in Life sustaining state (SLV).

Wall 7: Also, in this section can be noticed that the shear verification is the most critical.

| ***Bending in the plane*** | | | |
|---|---|---|---|
| **Geometrical parameters** | l | 1.14 | m |
| | t | 0.7 | m |

| | | | |
|---|---|---|---|
| **Mechanical parameters** | $f_m$ | 1500 | kN/m2 |
| | $\gamma_m$ | 2 | - |
| | FC | 1.2 | - |
| | $f_d$ | 625 | kN/m2 |

| *Shear* | | | |
|---|---|---|---|
| **Geometrical parameters** | l | 0.8 | m |
| | t | 0.7 | m |
| | h | 9.3 | m |
| | b | 1.5 | |
| **Mechanical parameters** | $\tau_0$ | 25 | kN/m2 |
| | $f_{td}$ | 15.625 | kN/m2 |
| | $\gamma_m$ | 2 | - |
| | FC | 1.2 | - |

| *Bending out of the plane* | | | |
|---|---|---|---|
| **Geometrical parameters** | l | 0.7 | m |
| | t | 0.8 | m |
| **Mechanical parameters** | $f_m$ | 1500 | kN/m2 |
| | $\gamma_m$ | 2 | - |
| | FC | 1.2 | - |
| | $f_d$ | 625 | kN/m2 |

Table 4-30. Parameters for the verification of the Wall 7.

| | BENDING IN THE PLANE | | | | | | SHEAR | | | | BENDING OUT OF THE PLANE | | | | |
|---|---|---|---|---|---|---|---|---|---|---|---|---|---|---|---|
| Combination | N | $\sigma_0$ | $M_{Ed}$ | $M_{Rd}$ | MEd/MRd | Verification | $V_{Ed}$ | $V_{Rd}$ | VEd/VRd | Verification | $\sigma_0$ | $M_{Ed}$ | $M_{Rd}$ | MEd/MRd | Verification |
| | kN | kN/m2 | kNm | kNm | - | - | kN | kN | - | - | kN/m2 | kNm | kNm | - | - |
| **Seismic_1** | **59** | **74** | **24** | **29** | **83%** | **Verify** | **40** | **14** | **286%** | **No verify** | **106** | **2** | **17** | **14%** | **Verify** |
| **Seismic_2** | **60** | **75** | **24** | **29** | **82%** | **Verify** | **40** | **14** | **283%** | **No verify** | **107** | **2** | **17** | **14%** | **Verify** |
| **Seismic_3** | **126** | **158** | **19** | **50** | **38%** | **Verify** | **31** | **19** | **157%** | **No verify** | **225** | **2** | **25** | **6%** | **Verify** |
| **Seismic_4** | **126** | **158** | **19** | **51** | **37%** | **Verify** | **30** | **19** | **155%** | **No verify** | **226** | **1** | **25** | **6%** | **Verify** |
| **Seismic_5** | **166** | **208** | **-14** | **58** | **-24%** | **Verify** | **-41** | **22** | **-186%** | **No verify** | **297** | **1** | **26** | **3%** | **Verify** |
| **Seismic_6** | **167** | **209** | **-14** | **58** | **-24%** | **Verify** | **-41** | **22** | **-187%** | **No verify** | **298** | **1** | **26** | **3%** | **Verify** |
| **Seismic_7** | **233** | **292** | **-19** | **60** | **-31%** | **Verify** | **-51** | **26** | **-196%** | **No verify** | **415** | **0** | **18** | **0%** | **Verify** |
| **Seismic_8** | **233** | **292** | **-19** | **60** | **-32%** | **Verify** | **-51** | **26** | **-197%** | **No verify** | **416** | **0** | **18** | **0%** | **Verify** |
| **Seismic_9** | **19** | **24** | **17** | **10** | **161%** | **No verify** | **23** | **9** | **247%** | **No verify** | **34** | **3** | **6** | **43%** | **Verify** |
| Seismic_10 | 51 | 64 | 6 | 26 | 21% | Verify | -1 | 13 | -11% | Verify | 92 | 2 | 15 | 15% | Verify |
| Seismic_11 | 52 | 65 | 5 | 26 | 21% | Verify | -2 | 13 | -14% | Verify | 92 | 2 | 15 | 15% | Verify |
| **Seismic_12** | **20** | **25** | **17** | **11** | **156%** | **No verify** | **23** | **9** | **240%** | **No verify** | **35** | **3** | **6** | **42%** | **Verify** |
| **Seismic_13** | **273** | **342** | **-12** | **55** | **-21%** | **Verify** | **-33** | **28** | **-120%** | **No verify** | **487** | **0** | **8** | **-5%** | **Verify** |
| Seismic_14 | 241 | 302 | 0 | 59 | -1% | Verify | -10 | 26 | -36% | Verify | 431 | 0 | 16 | 0% | Verify |
| Seismic_15 | 241 | 302 | 0 | 59 | 0% | Verify | -9 | 26 | -35% | Verify | 430 | 0 | 16 | 0% | Verify |
| **Seismic_16** | **273** | **343** | **-12** | **55** | **-21%** | **Verify** | **-34** | **28** | **-121%** | **No verify** | **488** | **0** | **8** | **-5%** | **Verify** |
| Seismic_17 | 96 | 121 | 11 | 42 | 26% | Verify | 12 | 17 | 71% | Verify | 172 | 2 | 23 | 8% | Verify |
| Seismic_18 | 128 | 161 | 0 | 51 | -1% | Verify | -12 | 20 | -62% | Verify | 229 | 1 | 26 | 5% | Verify |
| Seismic_19 | 163 | 204 | 6 | 57 | 10% | Verify | 3 | 22 | 12% | Verify | 290 | 1 | 26 | 4% | Verify |
| Seismic_20 | 195 | 244 | -5 | 60 | -9% | Verify | -22 | 24 | -92% | Verify | 348 | 1 | 24 | 3% | Verify |
| Seismic_21 | 130 | 163 | -1 | 51 | -2% | Verify | -13 | 20 | -68% | Verify | 232 | 1 | 26 | 5% | Verify |
| Seismic_22 | 164 | 206 | 5 | 57 | 9% | Verify | 1 | 22 | 6% | Verify | 294 | 1 | 26 | 4% | Verify |
| Seismic_23 | 98 | 123 | 11 | 43 | 25% | Verify | 11 | 17 | 63% | Verify | 175 | 2 | 23 | 8% | Verify |
| Seismic_24 | 196 | 246 | -6 | 60 | -10% | Verify | -23 | 24 | -97% | Verify | 351 | 0 | 23 | 2% | Verify |
| SLU1_1 | 204 | 256 | 7 | 60 | 11% | Verify | -2 | 24 | -8% | Verify | 364 | 2 | 22 | 8% | Verify |
| **SLU1_2** | **353** | **443** | **-335** | **34** | **-999%** | **No verify** | **-891** | **32** | **-2821%** | **No verify** | **631** | **12** | **-23** | **-52%** | **Verify** |
| SLU2_1 | 204 | 256 | 4 | 60 | 7% | Verify | -9 | 24 | -36% | Verify | 365 | 2 | 22 | 7% | Verify |
| SLU2_2 | 194 | 243 | 3 | 60 | 5% | Verify | -9 | 24 | -36% | Verify | 346 | 2 | 24 | 9% | Verify |
| SLU3_1 | 204 | 255 | 7 | 60 | 11% | Verify | -2 | 24 | -6% | Verify | 364 | 2 | 22 | 8% | Verify |
| **SLU3_2** | **354** | **443** | **-335** | **33** | **-1002%** | **No verify** | **-891** | **32** | **-2819%** | **No verify** | **632** | **12** | **-23** | **-51%** | **Verify** |
| SLU4_1 | 204 | 256 | 4 | 60 | 7% | Verify | -8 | 24 | -35% | Verify | 365 | 1 | 22 | 6% | Verify |
| SLU4_2 | 193 | 242 | 3 | 60 | 5% | Verify | -8 | 24 | -35% | Verify | 345 | 2 | 24 | 9% | Verify |
| SLU5_1 | 202 | 254 | 8 | 60 | 14% | Verify | 4 | 24 | 15% | Verify | 361 | 2 | 23 | 7% | Verify |
| **SLU5_2** | **727** | **911** | **-560** | **-296** | **189%** | **No verify** | **-1479** | **45** | **-3292%** | **No verify** | **1298** | **19** | **-367** | **-5%** | **Verify** |
| SLU6_1 | 203 | 254 | 4 | 60 | 7% | Verify | -8 | 24 | -32% | Verify | 363 | 1 | 23 | 5% | Verify |
| SLU6_2 | 185 | 232 | 3 | 59 | 4% | Verify | -8 | 23 | -32% | Verify | 330 | 2 | 24 | 9% | Verify |
| SLU7 | 146 | 183 | 3 | 55 | 5% | Verify | -5 | 21 | -26% | Verify | 261 | 1 | 26 | 4% | Verify |
| SLU8_1 | 160 | 201 | 6 | 57 | 10% | Verify | 0 | 22 | -1% | Verify | 286 | 1 | 26 | 6% | Verify |
| **SLU8_2** | **397** | **498** | **-336** | **14** | **-2361%** | **No verify** | **-890** | **33** | **-2661%** | **No verify** | **710** | **12** | **-47** | **-25%** | **Verify** |
| SLU9_1 | 161 | 201 | 3 | 57 | 6% | Verify | -7 | 22 | -33% | Verify | 287 | 1 | 26 | 5% | Verify |
| SLU9_2 | 150 | 188 | 2 | 55 | 4% | Verify | -7 | 21 | -33% | Verify | 267 | 2 | 26 | 7% | Verify |
| SLU10_1 | 160 | 200 | 6 | 57 | 10% | Verify | 0 | 22 | 0% | Verify | 286 | 1 | 26 | 5% | Verify |
| **SLU10_2** | **398** | **498** | **-335** | **14** | **-2379%** | **No verify** | **-889** | **33** | **-2659%** | **No verify** | **710** | **12** | **-47** | **-25%** | **Verify** |
| SLU11_1 | 160 | 201 | 3 | 57 | 6% | Verify | -7 | 22 | -31% | Verify | 286 | 1 | 26 | 4% | Verify |
| SLU11_2 | 150 | 187 | 2 | 55 | 4% | Verify | -7 | 21 | -32% | Verify | 267 | 2 | 26 | 6% | Verify |
| SLU12_1 | 158 | 199 | 8 | 57 | 14% | Verify | 5 | 22 | 25% | Verify | 283 | 1 | 26 | 5% | Verify |
| **SLU12_2** | **771** | **966** | **-561** | **-359** | **156%** | **No verify** | **-1477** | **46** | **-3195%** | **No verify** | **1376** | **18** | **-429** | **-4%** | **Verify** |
| SLU13_1 | 159 | 199 | 3 | 57 | 6% | Verify | -6 | 22 | -28% | Verify | 284 | 1 | 26 | 3% | Verify |
| SLU13_2 | 141 | 177 | 2 | 54 | 3% | Verify | -6 | 20 | -29% | Verify | 252 | 2 | 26 | 7% | Verify |
| SLU14 | 190 | 238 | 3 | 60 | 6% | Verify | -7 | 24 | -30% | Verify | 340 | 2 | 24 | 6% | Verify |

Table 4-31. Verification of section 1 - Wall 7 in Ultimate limit state (SLU) and in Life sustaining state (SLV).

Wall 8:

| *Bending in the plane* | | | |
|---|---|---|---|
| **Geometrical parameters** | l | 1.3 | m |
| | t | 0.7 | m |
| | | | |
| **Mechanical parameters** | $f_m$ | 1500 | kN/m2 |
| | $\gamma_m$ | 2 | - |
| | FC | 1.2 | - |
| | $f_d$ | 625 | kN/m2 |

| *Shear* | | | |
|---|---|---|---|
| **Geometrical parameters** | l | 1.3 | m |
| | t | 0.7 | m |
| | h | 9.3 | m |
| | b | 1.5 | |
| **Mechanical parameters** | $\tau_0$ | 25 | kN/m2 |
| | $f_{td}$ | 15.625 | kN/m2 |
| | $\gamma_m$ | 2 | - |
| | FC | 1.2 | - |

| *Bending out of the plane* | | | |
|---|---|---|---|
| **Geometrical parameters** | l | 0.7 | m |
| | t | 1.3 | m |
| **Mechanical parameters** | $f_m$ | 1500 | kN/m2 |
| | $\gamma_m$ | 2 | - |
| | FC | 1.2 | - |
| | $f_d$ | 625 | kN/m2 |

Table 4-32. Parameters for the verification of the Wall 8.

| | BENDING IN THE PLANE | | | | | | SHEAR | | | | BENDING OUT OF THE PLANE | | | | |
|---|---|---|---|---|---|---|---|---|---|---|---|---|---|---|---|
| Combination | N | $\sigma_0$ | $M_{Ed}$ | $M_{Rd}$ | MEd/MRd | Verification | $V_{Ed}$ | $V_{Rd}$ | VEd/VRd | Verification | $\sigma_0$ | $M_{Ed}$ | $M_{Rd}$ | MEd/MRd | Verification |
| | kN | kN/m2 | kNm | kNm | - | - | kN | kN | - | - | kN/m2 | kNm | kNm | - | - |
| **Seismic_1** | **93** | **102** | **44** | **49** | **91%** | **Verify** | **59** | **26** | **226%** | **No verify** | **102** | **0** | **26** | **2%** | **Verify** |
| **Seismic_2** | **93** | **102** | **44** | **49** | **90%** | **Verify** | **59** | **26** | **225%** | **No verify** | **102** | **0** | **26** | **1%** | **Verify** |
| Seismic_3 | 188 | 206 | 32 | 75 | 42% | Verify | 20 | 36 | 56% | Verify | 206 | 0 | 40 | -1% | Verify |
| Seismic_4 | 188 | 207 | 31 | 75 | 42% | Verify | 20 | 36 | 55% | Verify | 207 | 0 | 40 | -1% | Verify |
| Seismic_5 | 221 | 243 | 28 | 78 | 36% | Verify | -12 | 39 | -31% | Verify | 243 | -4 | 42 | -8% | Verify |
| Seismic_6 | 221 | 243 | 28 | 78 | 36% | Verify | -12 | 39 | -32% | Verify | 243 | -4 | 42 | -8% | Verify |
| **Seismic_7** | **316** | **347** | **15** | **71** | **21%** | **Verify** | **-51** | **46** | **-111%** | **No verify** | **347** | **-4** | **38** | **-11%** | **Verify** |
| **Seismic_8** | **317** | **348** | **15** | **71** | **21%** | **Verify** | **-51** | **46** | **-111%** | **No verify** | **348** | **-4** | **38** | **-11%** | **Verify** |
| **Seismic_9** | **27** | **29** | **53** | **16** | **325%** | **No verify** | **79** | **16** | **493%** | **No verify** | **29** | **0** | **9** | **-2%** | **Verify** |
| **Seismic_10** | **65** | **72** | **48** | **37** | **132%** | **No verify** | **58** | **22** | **259%** | **No verify** | **72** | **-1** | **20** | **-7%** | **Verify** |
| **Seismic_11** | **66** | **72** | **48** | **37** | **131%** | **No verify** | **58** | **22** | **257%** | **No verify** | **72** | **-1** | **20** | **-7%** | **Verify** |
| **Seismic_12** | **27** | **30** | **53** | **17** | **320%** | **No verify** | **79** | **16** | **489%** | **No verify** | **30** | **0** | **9** | **-3%** | **Verify** |
| **Seismic_13** | **382** | **420** | **6** | **52** | **12%** | **Verify** | **-71** | **50** | **-142%** | **No verify** | **420** | **-4** | **28** | **-13%** | **Verify** |
| **Seismic_14** | **344** | **378** | **11** | **64** | **17%** | **Verify** | **-50** | **48** | **-106%** | **No verify** | **378** | **-2** | **35** | **-7%** | **Verify** |
| **Seismic_15** | **344** | **378** | **11** | **65** | **17%** | **Verify** | **-50** | **48** | **-105%** | **No verify** | **378** | **-2** | **35** | **-7%** | **Verify** |
| **Seismic_16** | **383** | **420** | **6** | **52** | **12%** | **Verify** | **-71** | **50** | **-143%** | **No verify** | **420** | **-4** | **28** | **-13%** | **Verify** |
| **Seismic_17** | **137** | **151** | **39** | **64** | **60%** | **Verify** | **34** | **31** | **111%** | **No verify** | **151** | **-1** | **34** | **-3%** | **Verify** |
| Seismic_18 | 176 | 193 | 34 | 73 | 46% | Verify | 13 | 35 | 38% | Verify | 193 | -2 | 39 | -5% | Verify |
| Seismic_19 | 232 | 255 | 26 | 78 | 33% | Verify | -4 | 39 | -11% | Verify | 255 | -2 | 42 | -4% | Verify |
| Seismic_20 | 271 | 298 | 21 | 77 | 27% | Verify | -26 | 42 | -60% | Verify | 298 | -3 | 42 | -7% | Verify |
| Seismic_21 | 177 | 194 | 33 | 73 | 46% | Verify | 12 | 35 | 35% | Verify | 194 | -2 | 39 | -6% | Verify |
| Seismic_22 | 234 | 257 | 26 | 78 | 33% | Verify | -5 | 40 | -14% | Verify | 257 | -2 | 42 | -4% | Verify |
| **Seismic_23** | **138** | **152** | **38** | **64** | **60%** | **Verify** | **33** | **31** | **108%** | **No verify** | **152** | **-1** | **35** | **-3%** | **Verify** |
| Seismic_24 | 272 | 299 | 21 | 77 | 27% | Verify | -27 | 43 | -62% | Verify | 299 | -3 | 42 | -7% | Verify |
| SLU1_1 | 285 | 313 | 43 | 76 | 57% | Verify | 7 | 43 | 17% | Verify | 313 | -3 | 41 | -8% | Verify |
| **SLU1_2** | **288** | **317** | **60** | **76** | **80%** | **Verify** | **100** | **44** | **229%** | **No verify** | **317** | **15** | **41** | **37%** | **Verify** |
| SLU2_1 | 283 | 311 | 44 | 76 | 58% | Verify | 14 | 43 | 33% | Verify | 311 | -2 | 41 | -6% | Verify |
| SLU2_2 | 294 | 323 | 41 | 75 | 55% | Verify | 5 | 44 | 12% | Verify | 323 | -3 | 40 | -8% | Verify |
| SLU3_1 | 290 | 319 | 43 | 75 | 58% | Verify | 8 | 44 | 18% | Verify | 319 | -3 | 41 | -8% | Verify |
| **SLU3_2** | **294** | **323** | **61** | **75** | **81%** | **Verify** | **301** | **44** | **683%** | **No verify** | **323** | **15** | **40** | **37%** | **Verify** |
| SLU4_1 | 288 | 317 | 45 | 76 | 59% | Verify | 15 | 44 | 34% | Verify | 317 | -2 | 41 | -6% | Verify |
| SLU4_2 | 299 | 329 | 42 | 74 | 56% | Verify | 6 | 45 | 13% | Verify | 329 | -3 | 40 | -8% | Verify |
| SLU5_1 | 275 | 302 | 41 | 77 | 53% | Verify | 3 | 43 | 6% | Verify | 302 | -3 | 42 | -8% | Verify |
| **SLU5_2** | **281** | **308** | **70** | **77** | **91%** | **Verify** | **492** | **43** | **1139%** | **No verify** | **308** | **27** | **41** | **66%** | **Verify** |
| SLU6_1 | 272 | 298 | 43 | 77 | 56% | Verify | 15 | 42 | 34% | Verify | 298 | -2 | 42 | -5% | Verify |
| SLU6_2 | 290 | 318 | 38 | 75 | 50% | Verify | -1 | 44 | -1% | Verify | 318 | -3 | 41 | -8% | Verify |
| SLU7 | 205 | 225 | 30 | 77 | 39% | Verify | 4 | 37 | 11% | Verify | 225 | -2 | 41 | -5% | Verify |
| SLU8_1 | 223 | 246 | 34 | 78 | 44% | Verify | 6 | 39 | 15% | Verify | 246 | -3 | 42 | -6% | Verify |
| **SLU8_2** | **227** | **249** | **51** | **78** | **66%** | **Verify** | **49** | **39** | **126%** | **No verify** | **249** | **16** | **42** | **37%** | **Verify** |
| SLU9_1 | 221 | 243 | 36 | 78 | 46% | Verify | 13 | 39 | 34% | Verify | 243 | -2 | 42 | -5% | Verify |
| SLU9_2 | 232 | 255 | 32 | 78 | 41% | Verify | 4 | 39 | 10% | Verify | 255 | -3 | 42 | -6% | Verify |
| SLU10_1 | 229 | 251 | 35 | 78 | 44% | Verify | 7 | 39 | 17% | Verify | 251 | -3 | 42 | -6% | Verify |
| **SLU10_2** | **232** | **255** | **52** | **78** | **66%** | **Verify** | **300** | **39** | **760%** | **No verify** | **255** | **16** | **42** | **37%** | **Verify** |
| SLU11_1 | 227 | 249 | 36 | 78 | 46% | Verify | 14 | 39 | 35% | Verify | 249 | -2 | 42 | -4% | Verify |
| SLU11_2 | 238 | 261 | 33 | 79 | 42% | Verify | 5 | 40 | 12% | Verify | 261 | -2 | 42 | -6% | Verify |
| SLU12_1 | 214 | 235 | 32 | 77 | 41% | Verify | 2 | 38 | 4% | Verify | 235 | -3 | 42 | -7% | Verify |
| **SLU12_2** | **219** | **241** | **61** | **78** | **78%** | **Verify** | **49** | **38** | **128%** | **No verify** | **241** | **28** | **42** | **66%** | **Verify** |
| SLU13_1 | 210 | 231 | 34 | 77 | 44% | Verify | 13 | 38 | 35% | Verify | 231 | -2 | 42 | -4% | Verify |
| SLU13_2 | 228 | 251 | 29 | 78 | 37% | Verify | -2 | 39 | -5% | Verify | 251 | -3 | 42 | -6% | Verify |
| SLU14 | 266 | 292 | 39 | 78 | 50% | Verify | 5 | 42 | 12% | Verify | 292 | -2 | 42 | -6% | Verify |

Table 4-33. Verification of section 1 - Wall 8 in Ultimate limit state (SLU) and in Life sustaining state (SLV).

Wall 9: this section is related to the bell tower, as before the most critical section of this part of the structure was chosen. From the results obtained it can be seen that the wall does not verify, the verification that is least satisfied is the one related to the shear.

| ***Bending in the plane*** | | | |
|---|---|---|---|
| **Geometrical parameters** | l | 5 | m |
| | t | 1.9 | m |
| | | | |
| **Mechanical parameters** | $f_m$ | 2000 | kN/m2 |
| | $\gamma_m$ | 2 | - |
| | FC | 1.2 | - |
| | $f_d$ | 833.333 | kN/m2 |

| ***Shear*** | | | |
|---|---|---|---|
| **Geometrical parameters** | l | 5 | m |
| | t | 1.9 | m |
| | h | 7.2 | m |
| | b | 1.5 | |
| **Mechanical parameters** | $\tau_0$ | 45 | kN/m2 |
| | $f_{td}$ | 28.125 | kN/m2 |
| | $\gamma_m$ | 2 | - |
| | FC | 1.2 | - |

| ***Bending out of the plane*** | | | |
|---|---|---|---|
| **Geometrical parameters** | l | 1.9 | m |
| | t | 5 | m |
| **Mechanical parameters** | $f_m$ | 2000 | kN/m2 |
| | $\gamma_m$ | 2 | - |
| | FC | 1.2 | - |
| | $f_d$ | 833.333 | kN/m2 |

Table 4-34. Parameters for the verification of the Wall 9.

| Combination | N | $\sigma_0$ | $M_{Ed}$ | $M_{Rd}$ | MEd/MRd | Verification | $V_{Ed}$ | $V_{Rd}$ | VEd/VRd | Verification | $\sigma_0$ | $M_{Ed}$ | $M_{Rd}$ | MEd/MRd | Verification |
|---|---|---|---|---|---|---|---|---|---|---|---|---|---|---|---|
| | kN | kN/m2 | kNm | kNm | - | - | kN | kN | - | - | kN/m2 | kNm | kNm | - | - |
| **Seismic_1** | **1374** | **145** | **5228** | **2733** | **191%** | **No verify** | **1128** | **441** | **256%** | **No verify** | **145** | **74** | **1039** | **7%** | **Verify** |
| **Seismic_2** | **1465** | **154** | **5223** | **2866** | **182%** | **No verify** | **1122** | **454** | **247%** | **No verify** | **154** | **72** | **1089** | **7%** | **Verify** |
| **Seismic_3** | **2942** | **310** | **3756** | **4139** | **91%** | **Verify** | **738** | **617** | **120%** | **No verify** | **310** | **22** | **1573** | **1%** | **Verify** |
| **Seismic_4** | **3033** | **319** | **3751** | **4165** | **90%** | **Verify** | **732** | **626** | **117%** | **No verify** | **319** | **20** | **1583** | **1%** | **Verify** |
| **Seismic_5** | **4408** | **464** | **-3589** | **3801** | **-94%** | **Verify** | **-927** | **745** | **-124%** | **No verify** | **464** | **-171** | **1445** | **-12%** | **Verify** |
| **Seismic_6** | **4500** | **474** | **-3594** | **3727** | **-96%** | **Verify** | **-932** | **752** | **-124%** | **No verify** | **474** | **-173** | **1416** | **-12%** | **Verify** |
| **Seismic_7** | **5976** | **629** | **-5061** | **1672** | **-303%** | **No verify** | **-1317** | **861** | **-153%** | **No verify** | **629** | **-223** | **635** | **-35%** | **Verify** |
| **Seismic_8** | **6068** | **639** | **-5066** | **1491** | **-340%** | **No verify** | **-1322** | **867** | **-152%** | **No verify** | **639** | **-225** | **567** | **-40%** | **Verify** |
| **Seismic_9** | **606** | **64** | **3859** | **1379** | **280%** | **No verify** | **864** | **322** | **268%** | **No verify** | **64** | **49** | **524** | **9%** | **Verify** |
| Seismic_10 | 1516 | 160 | 1214 | 2937 | 41% | Verify | 247 | 460 | 54% | Verify | 160 | -24 | 1116 | -2% | Verify |
| Seismic_11 | 1608 | 169 | 1209 | 3060 | 40% | Verify | 242 | 472 | 51% | Verify | 169 | -26 | 1163 | -2% | Verify |
| **Seismic_12** | **698** | **73** | **3854** | **1564** | **246%** | **No verify** | **858** | **339** | **254%** | **No verify** | **73** | **48** | **594** | **8%** | **Verify** |
| **Seismic_13** | **6743** | **710** | **-3693** | **-36** | **10304%** | **No verify** | **-1053** | **912** | **-115%** | **No verify** | **710** | **-198** | **-14** | **1457%** | **No verify** |
| Seismic_14 | 5925 | 624 | -1052 | 1770 | -59% | Verify | -442 | 858 | -52% | Verify | 624 | -126 | 673 | -19% | Verify |
| Seismic_15 | 5833 | 614 | -1047 | 1942 | -54% | Verify | -436 | 851 | -51% | Verify | 614 | -125 | 738 | -17% | Verify |
| **Seismic_16** | **6835** | **719** | **-3697** | **-269** | **1373%** | **No verify** | **-1058** | **918** | **-115%** | **No verify** | **719** | **-200** | **-102** | **195%** | **No verify** |
| Seismic_17 | 2329 | 245 | 2148 | 3807 | 56% | Verify | 415 | 555 | 75% | Verify | 245 | -10 | 1447 | -1% | Verify |
| Seismic_18 | 3239 | 341 | -498 | 4200 | -12% | Verify | -201 | 645 | -31% | Verify | 341 | -83 | 1596 | -5% | Verify |
| Seismic_19 | 3897 | 410 | 676 | 4101 | 16% | Verify | 25 | 703 | 4% | Verify | 410 | -62 | 1558 | -4% | Verify |
| Seismic_20 | 4807 | 506 | -1969 | 3433 | -57% | Verify | -591 | 776 | -76% | Verify | 506 | -136 | 1304 | -10% | Verify |
| Seismic_21 | 3545 | 373 | -514 | 4194 | -12% | Verify | -219 | 673 | -33% | Verify | 373 | -89 | 1594 | -6% | Verify |
| Seismic_22 | 4203 | 442 | 659 | 3945 | 17% | Verify | 7 | 729 | 1% | Verify | 442 | -67 | 1499 | -4% | Verify |
| Seismic_23 | 2634 | 277 | 2131 | 4008 | 53% | Verify | 397 | 587 | 68% | Verify | 277 | -15 | 1523 | -1% | Verify |
| Seismic_24 | 5113 | 538 | -1986 | 3070 | -65% | Verify | -609 | 799 | -76% | Verify | 538 | -141 | 1167 | -12% | Verify |

| | | | | | | | | | | | | | | | |
|---|---|---|---|---|---|---|---|---|---|---|---|---|---|---|---|
| SLU1_1 | 4894 | 515 | -144 | 3337 | -4% | Verify | -188 | 783 | -24% | Verify | 515 | -95 | 1268 | -7% | Verify |
| **SLU1_2** | **5025** | **529** | **2001** | **3181** | **63%** | **Verify** | **1144** | **793** | **144%** | **No verify** | **529** | **153** | **1209** | **13%** | **Verify** |
| SLU2_1 | 5025 | 529 | 191 | 3181 | 6% | Verify | -111 | 793 | -14% | Verify | 529 | -98 | 1209 | -8% | Verify |
| SLU2_2 | 4761 | 501 | 33 | 3481 | 1% | Verify | -109 | 773 | -14% | Verify | 501 | -100 | 1323 | -8% | Verify |
| SLU3_1 | 4905 | 516 | -168 | 3324 | -5% | Verify | -200 | 784 | -26% | Verify | 516 | -96 | 1263 | -8% | Verify |
| **SLU3_2** | **5037** | **530** | **1977** | **3167** | **62%** | **Verify** | **1133** | **794** | **143%** | **No verify** | **530** | **152** | **1203** | **13%** | **Verify** |
| SLU4_1 | 5036 | 530 | 167 | 3167 | 5% | Verify | -123 | 794 | -15% | Verify | 530 | -99 | 1204 | -8% | Verify |
| SLU4_2 | 4772 | 502 | 9 | 3469 | 0% | Verify | -121 | 774 | -16% | Verify | 502 | -101 | 1318 | -8% | Verify |
| SLU5_1 | 4873 | 513 | -330 | 3360 | -10% | Verify | -254 | 781 | -33% | Verify | 513 | -92 | 1277 | -7% | Verify |
| **SLU5_2** | **5092** | **536** | **3246** | **3097** | **105%** | **No verify** | **1967** | **798** | **247%** | **No verify** | **536** | **321** | **1177** | **27%** | **Verify** |
| SLU6_1 | 5092 | 536 | 230 | 3097 | 7% | Verify | -126 | 798 | -16% | Verify | 536 | -97 | 1177 | -8% | Verify |
| SLU6_2 | 4652 | 490 | -34 | 3590 | -1% | Verify | -123 | 764 | -16% | Verify | 490 | -101 | 1364 | -7% | Verify |
| SLU7 | 3721 | 392 | 81 | 4159 | 2% | Verify | -97 | 688 | -14% | Verify | 392 | -75 | 1580 | -5% | Verify |
| SLU8_1 | 3778 | 398 | -169 | 4142 | -4% | Verify | -159 | 693 | -23% | Verify | 398 | -72 | 1574 | -5% | Verify |
| **SLU8_2** | **3909** | **411** | **1977** | **4096** | **48%** | **Verify** | **1173** | **704** | **167%** | **No verify** | **411** | **176** | **1556** | **11%** | **Verify** |
| SLU9_1 | 3909 | 411 | 167 | 4096 | 4% | Verify | -82 | 704 | -12% | Verify | 411 | -75 | 1556 | -5% | Verify |
| SLU9_2 | 3645 | 384 | 9 | 4177 | 0% | Verify | -80 | 682 | -12% | Verify | 384 | -77 | 1587 | -5% | Verify |
| SLU10_1 | 3789 | 399 | -193 | 4139 | -5% | Verify | -171 | 694 | -25% | Verify | 399 | -73 | 1573 | -5% | Verify |
| **SLU10_2** | **3920** | **413** | **1953** | **4091** | **48%** | **Verify** | **1162** | **705** | **165%** | **No verify** | **413** | **175** | **1555** | **11%** | **Verify** |
| SLU11_1 | 3920 | 413 | 143 | 4091 | 3% | Verify | -94 | 705 | -13% | Verify | 413 | -76 | 1555 | -5% | Verify |
| SLU11_2 | 3656 | 385 | -15 | 4174 | 0% | Verify | -92 | 683 | -13% | Verify | 385 | -79 | 1586 | -5% | Verify |
| SLU12_1 | 3757 | 395 | -354 | 4149 | -9% | Verify | -225 | 691 | -33% | Verify | 395 | -70 | 1576 | -4% | Verify |
| **SLU12_2** | **3976** | **419** | **3222** | **4067** | **79%** | **Verify** | **1996** | **710** | **281%** | **No verify** | **419** | **344** | **1545** | **22%** | **Verify** |
| SLU13_1 | 3976 | 419 | 205 | 4067 | 5% | Verify | -96 | 710 | -14% | Verify | 419 | -75 | 1545 | -5% | Verify |
| SLU13_2 | 3536 | 372 | -58 | 4195 | -1% | Verify | -94 | 672 | -14% | Verify | 372 | -78 | 1594 | -5% | Verify |
| SLU14 | 4837 | 509 | 105 | 3400 | 3% | Verify | -126 | 779 | -16% | Verify | 509 | -98 | 1292 | -8% | Verify |

Table 4-35. Verification of section 1 - Wall 9 in Ultimate limit state (SLU) and in Life sustaining state (SLV).

To conclude, as foreseen in this chapter, verifications of the walls that make up the church were carried out. Applying all the corresponding verifications , it can be said that the predominant failure is due to the shear that occurs in the walls, which is strongly linked to the mechanical resistance.

The most stressed and worst conditioned walls are the bell tower, both from a dynamic and static point of view, as they do not pass the shear verification and do not pass the bending for lateral loads verification.

The bell tower, in turn, besides being the element that is dynamically and statically in the worst state, also presents considerable displacements in both cases. For the purposes of the model of calculation this can be explained by the fact that, the different floors of the bell tower, distributed along its height, were not considered as rigid planes, since after several inspections carried out on the site, they are in a state that does not allow us to consider them as structural.

## 4.4 Vault verification

The statics of masonry arches is treated scientifically only from the end of the 18th century with the studies of Coulomb. The concept of the pressure curve and its method for a minimal thrust was developed by Mèry in the latter half of the 19th century. [23]

In general, a 'exact' calculation of the masonry arch is extremely difficult, if not impossible, because the material laws are not precisely known and it is difficult to consider the effects of settlements, cracks, load patterns etc.

For the verification of the vaults in masonry, in a static configuration, the calculation program used was Arco. The "safe theorem" of the plastic analysis method, often known as the "lower bound" or "equilibrium" theorem, serves as the basis for the program.

The "safe theorem" can be stated as follow: "a masonry arch is safe if a line of thrust, in equilibrium with external loads and lying wholly within the thickness, can be found and the corresponding stresses are sufficiently low." [24]

The software uses the Mèry method (1840), which states that the static verification of the arch requires the determination of the pressure curve to check that this curve is contained in the central core of inertia of the segments. If this condition is verified, the arch will be fully compressed, without any tensile stress zone.

Mèry demonstrated that for a symmetrically loaded and constrained arch, the static regime could be determined using an equilibrium polygon with forced passage for two points the upper middle third of the section in the correct horizontal action key and the lower middle third in the section at the ends (Figure 4-34. The springers represent the weakest zone of this structure which, when subjected to uniformly distributed load, reveals any cracks in this zone, together with the key point. [25] In this way, knowing the external loads, it was possible to obtain the course of the pressure curve.

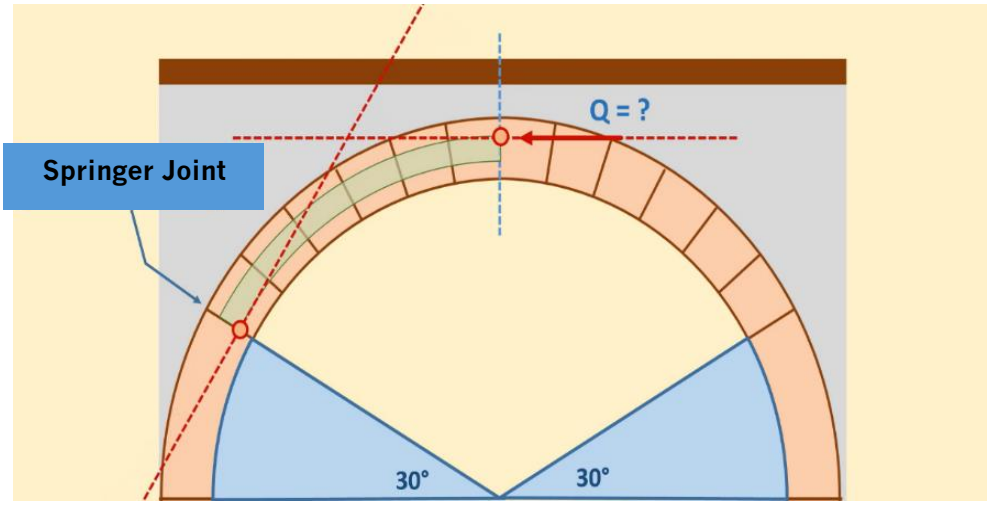


Figure 4-34.

Since the arc is symmetrically loaded, the study can be limited to half of it, applying the transmitted force of the remaining part to the key section (Figure 4-35.

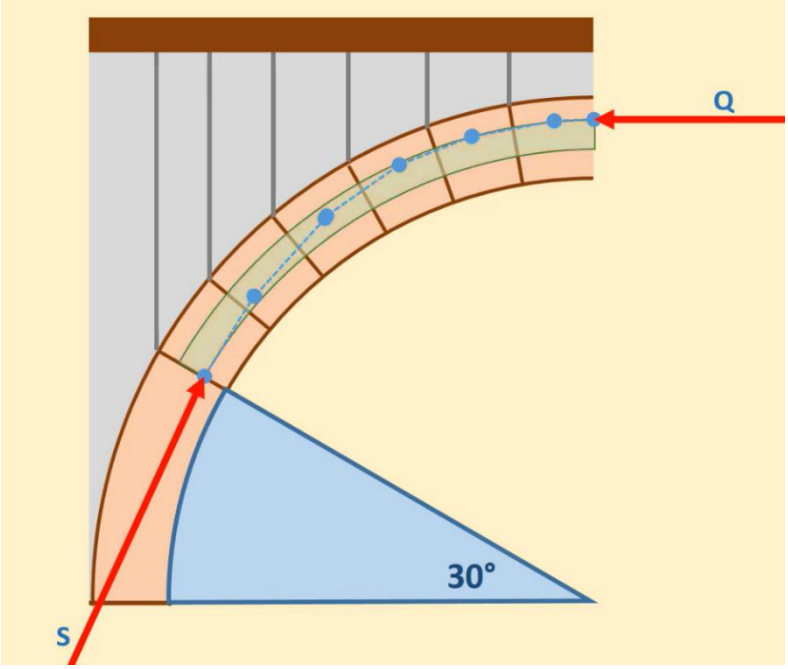


Figure 4-35.

In order to draw the pressure curve, the reaction Q and the thrust of the arch named as S need to be determined. Knowing the weights of the individual arch segments and the weight of the superstructure bearing on each segment, it is possible to determine the resultant of the applied vertical load (Figure 4-36.

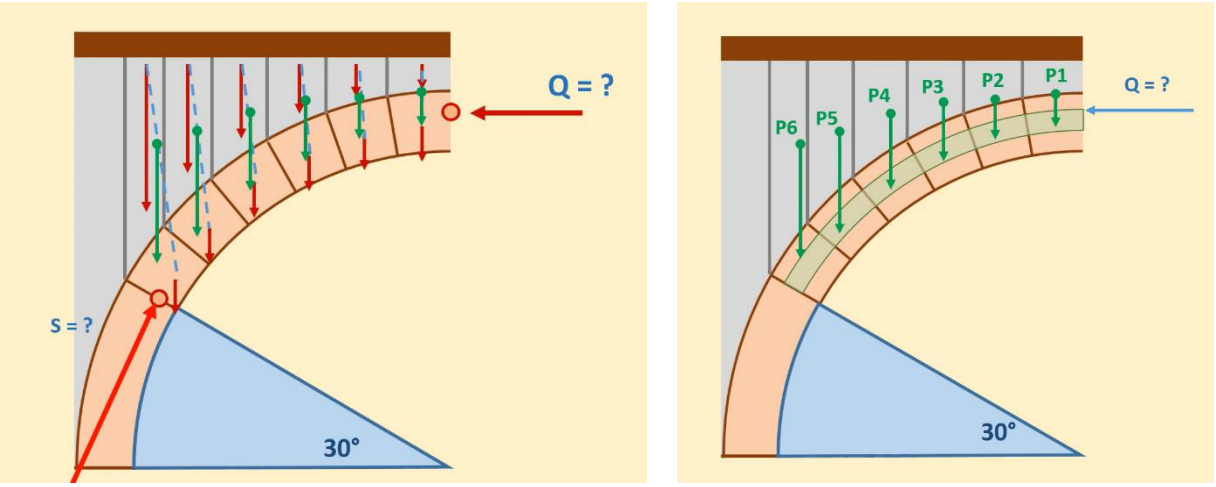


Figure 4-36.

This resultant can be determined using the point-tail method to determine the position of the resultant of the weight forces by choosing an arbitrary pole P and drawing the vertex-joints of each vector from pole to vector. Using the straight lines

from pole P, the line of action of the resultant and the thrust of the arc can be determined. By drawing the lines of action of each weight force from p1 to pn and drawing the lines from the pole p to the vertices of the vectors until they meet the lines of action of the weight forces, one will obtain a line through which the line of action of the resultant can be determined. Once the line of action of the resultant is known, it is possible to determine the line of action of the thrust S, by imposing the passage of this line to the lower middle third in the section at the springers and for the intersection of the line of action of the resultant is the line of action of the reaction in key Q (Figure 4-37.Figure 4-39.)

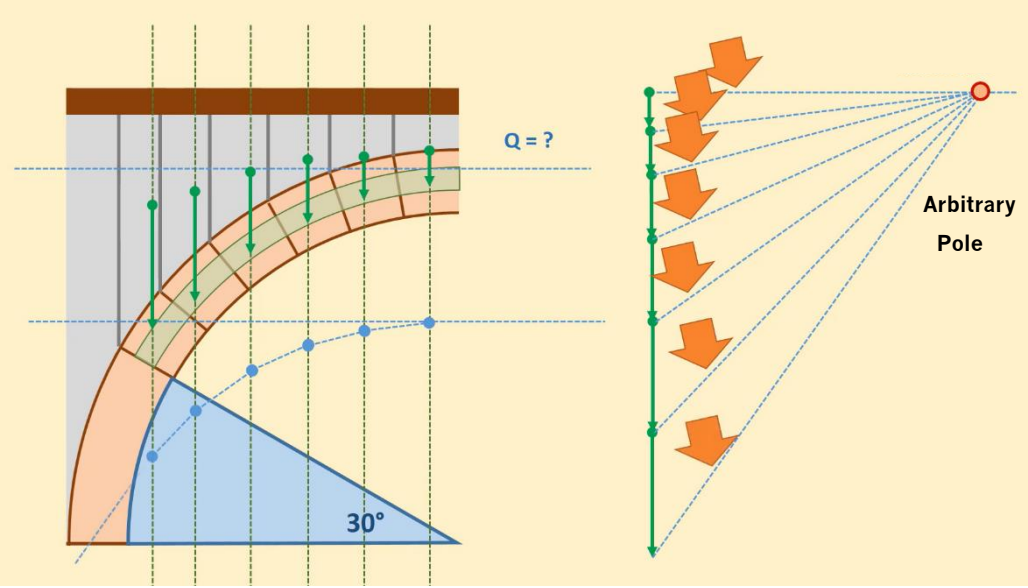


Figure 4-37.

Given the reactions of all the forces, the modulus of each force can be determined graphically. At this point it is possible to identify the pressure curve using the pole P' which is identified by the line of action of the force Q and the thrust S, by drawing the straight lines joining the pole P with the vectors of the weight forces it is possible to obtain the pressure curve, if this curve is contained in the central core of inertia of the arc then the arc will result to be entirely compressed (Figure 4-39.).

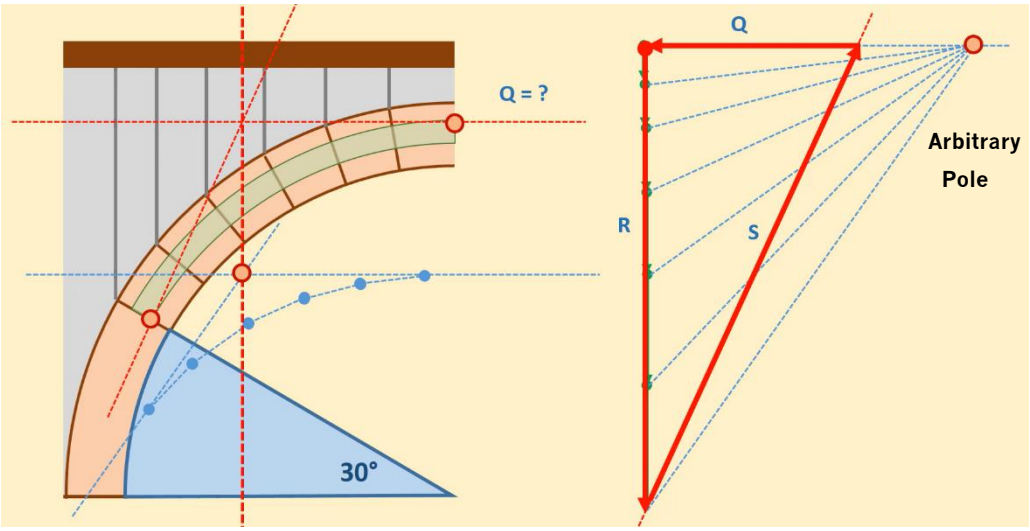


Figure 4-38

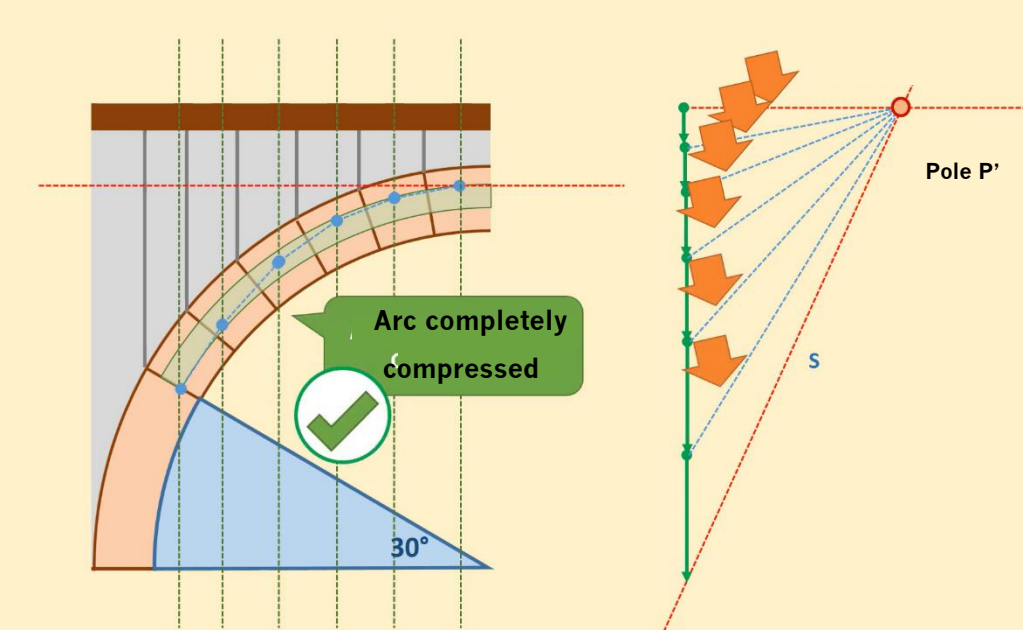


Figure 4-39.

Once the method used by the software was understood, the implementation of it was started. The software's interface is user-friendly and intuitive, allowing the user to set the language in which the program is to be operated, Italian or English.

First of all, the geometry of the problem must be set, where various parameters such as length, thickness and the layers above the dome are required, as well as other parameters. Regarding the definition of the densities, since the dead load effect is

favourable as it tends to centre the thrust line, a partial factor value 0.9 was applied to the material densities. [26]

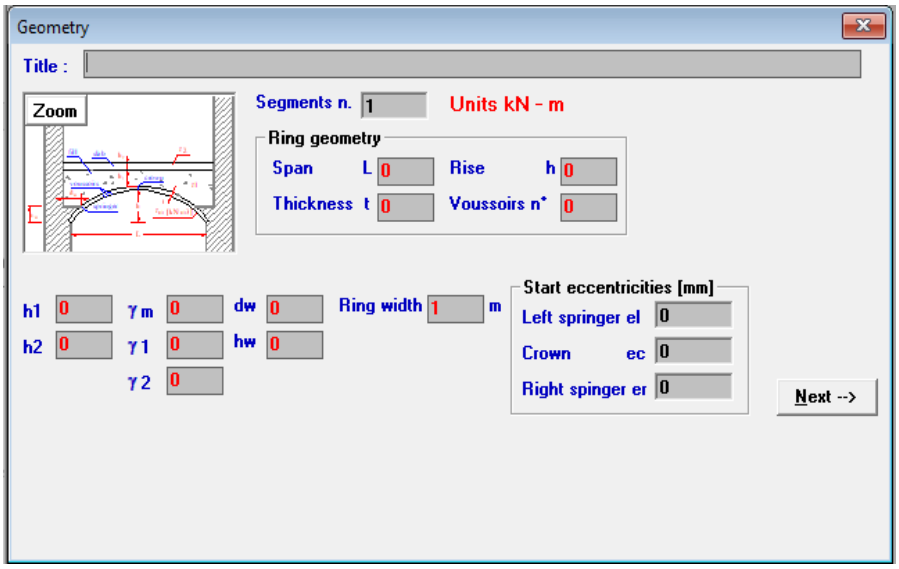


Figure 4-40. Definition of the geometry in Arco Software.

Once the geometry has been defined, the program plots it in a format very similar to AutoCAD. Then, it is necessary to define if there is any type of live load (q) in the vaults, in which the value and the start and end position must be specified. In the case of the overload a partial factor of 2.0 was adopted to allow also for uncertainties in the arch geometry.

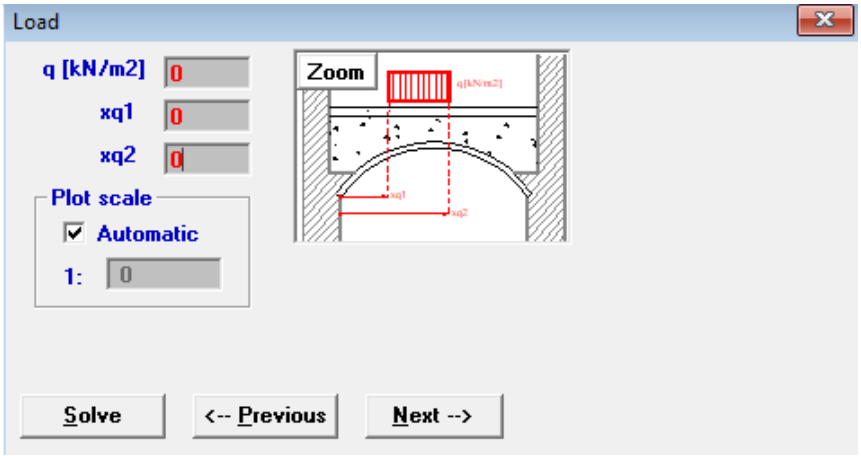


Figure 4-41. Definition of the Load in Arco Software.

Then, the solve options must be set, once done that the solution is obtained. The trust-line is drawn in blue, the diagrams of the maximum stresses in each section at extrados (green curve) and intrados (magenta curve). Maximum stresses are calculated according to the classical elastic theory for no-tension materials, that is:

$$\sigma_{max} = \frac{2N}{3u} \tag{41}$$

being N the compression axial force per ring unit width and u the distance of the trust-line from the compressed edge. If the trust-line lies outside the ring thickness, no equilibrium is possible without tension, and stresses are calculated as if the section were wholly reactive:

$$\sigma_{max} = \frac{N}{t} \pm \frac{6N_e}{t^2} \tag{42}$$

It is important to mention that in order to be on the side of security, backfill is taken into account as a mere vertical surcharge, ignoring the horizontal passive pressures which can be mobilized when the arch sways into the backfill. [26]

To get a more realistic representation of what the vaults are and how to divide them, it was decided to divide them into three different sections, obtaining arches with different diameters. In turn, based on the results previously analysed, it was decided to take the geometry of the most required vault.

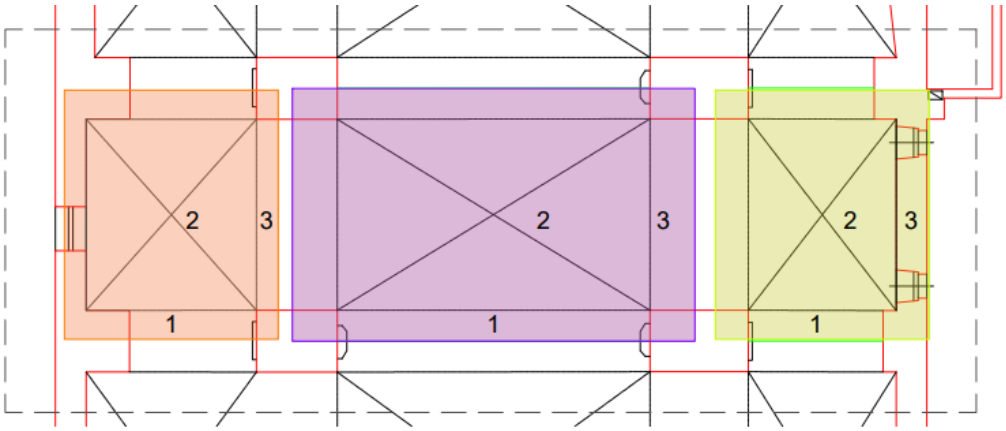


Figure 4-42. Division of the vaults in different segments.

As can be seen in the Figure 4-42, the vaults has been divided in 3 different segments, the first segment indicated with the number 1 corresponds to the first ach, the segment 2 corresponds to the diagonal of the vault, and finally the segment 3 corresponds to the transversal arch.

The following are the diagrams of the different vaults, and the results obtained with the use of the software. Starting with the analysis of the central vault, the results are as follows.

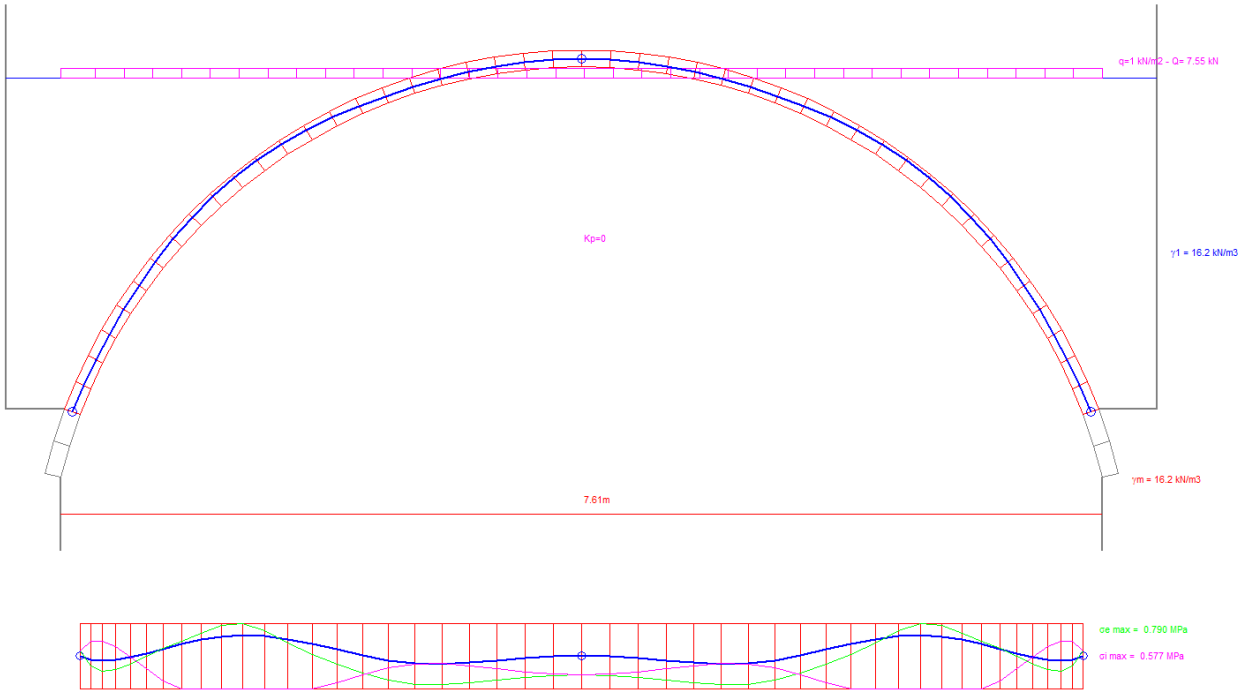


Figure 4-43. Pressure line of the Central Vault- Centred distributed load - Section 1.

The Figure 4-43 represents the pressure line obtained for the section 1 related to the central vault, as can be seen two results are displayed, first the maximum stresses at the intrados (magenta line) and at the extrados (magenta line). Regarding the pressure at the intrados, it can be noticed that the results are positive ($\sigma_i = 0.57\ \text{MPa}$) number which represents that the stresses are of compression.

The program also allows for a detailed report on each of the sections into which the arch was divided. It provides for each one the tension at the intrados, extrados, and the percentage of compression. Also, the reactions at spring (making a distinction between the right and the left side) and at the walls are determined. In addition, the software supplies the tie thrust that needs to be applied.

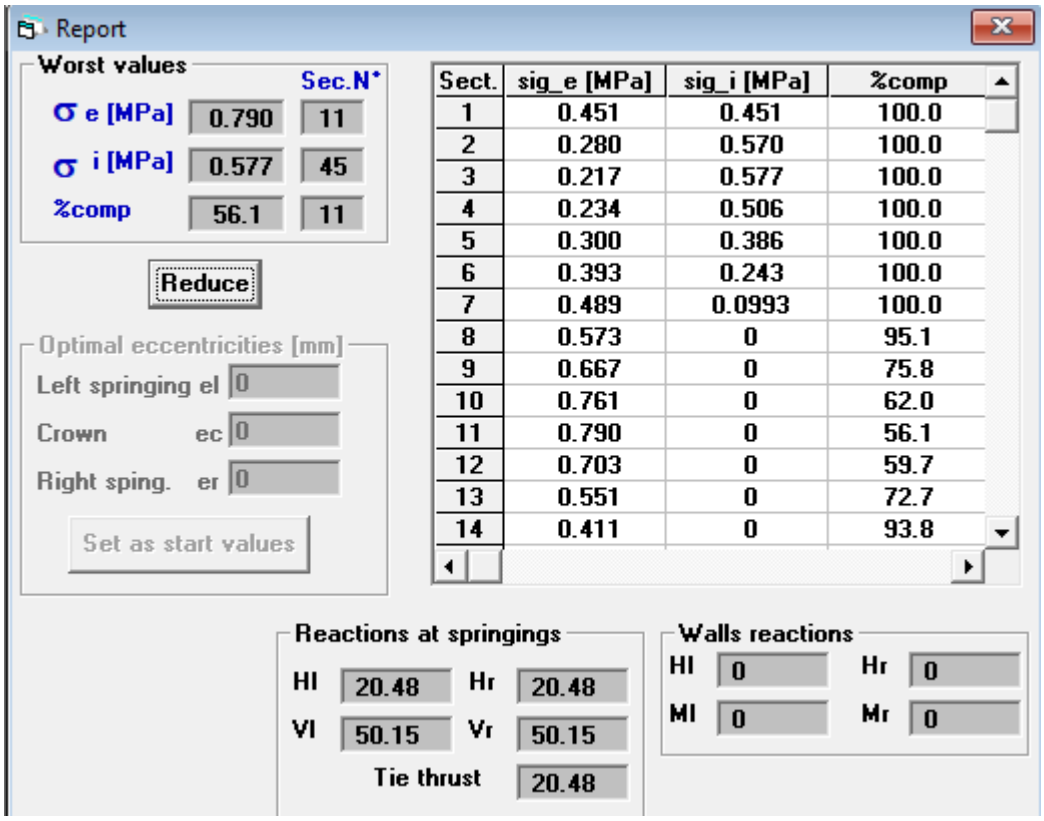


Figure 4-44. Report of the section 1 related to the Central Vault.

From the Figure 4-44 it can be seen that section 11 experiences the maximum compression stress. Analyzing the situation in which the distributed load is not centered, it is located in a lateral side, the result obtained is described by the Figure 4-45, where it can be noticed that $\sigma_e 12.9\ \text{MPa}$, while $\sigma_i = -0.633\ \text{MPa}$.

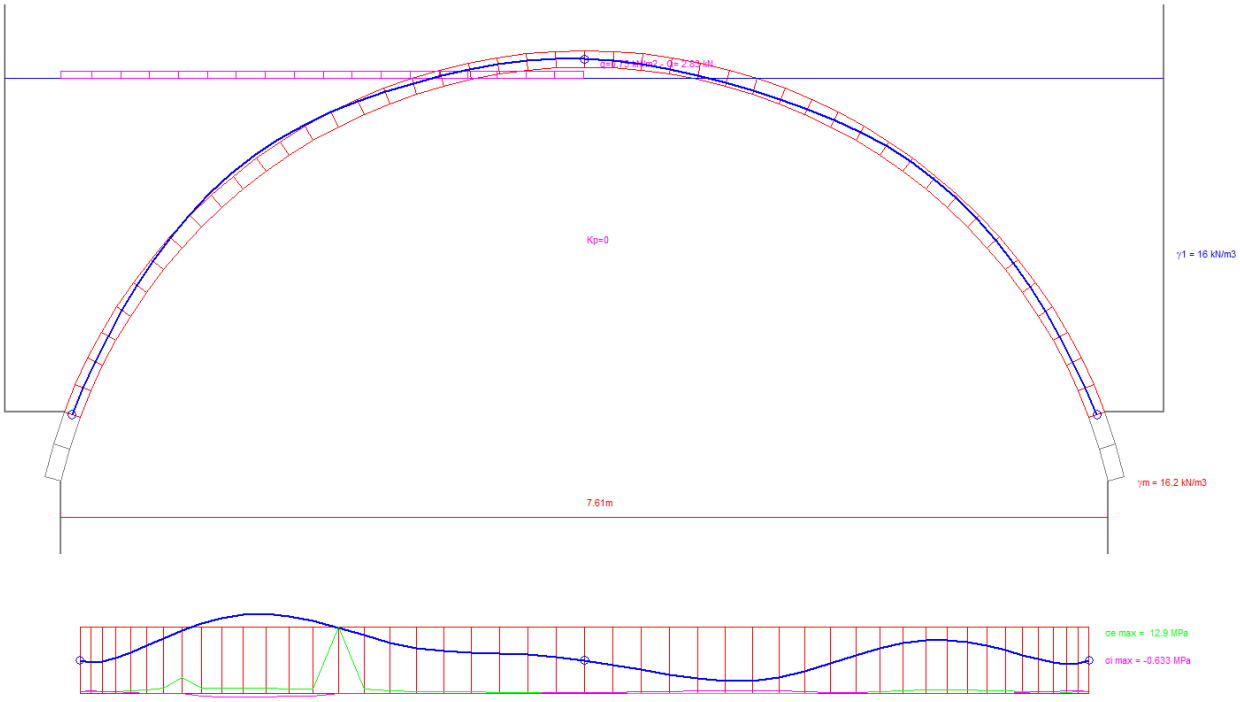


Figure 4-45 · Pressure line of the Central Vault· Asymmetrical Lateral distributed load · Section 1.

The same procedure conducted previously was executed on the remaining sections of the vaults under examination. The subsequent section presents the outcomes obtained for the left and right vaults.

Continuing with the vault of the left-hand side, the examined portion was Section 2, which corresponds to the diagonal of the vault. This particular section holds the highest dimensions, making it the most critical segment of analysis. From the Figure 4-46, it can be noticed that for this condition on load, the vault is in equilibrium, as not traction stresses are present, whit values of stresses at the intrados and extrados of $\sigma_e = -1.01\ \text{MPa}\ \ \text{MPa and}\ \sigma_i = 10.8\text{MPa}$ .

Also, evaluating the case in which the distributed load is not symmetrical (Figure 4-47)it is possible to notice that the vault is not under equilibrium, with values of $\sigma_e = -1.39\ \ \text{MPa and}\ \sigma_i = 10.8\ \text{MPa}$.

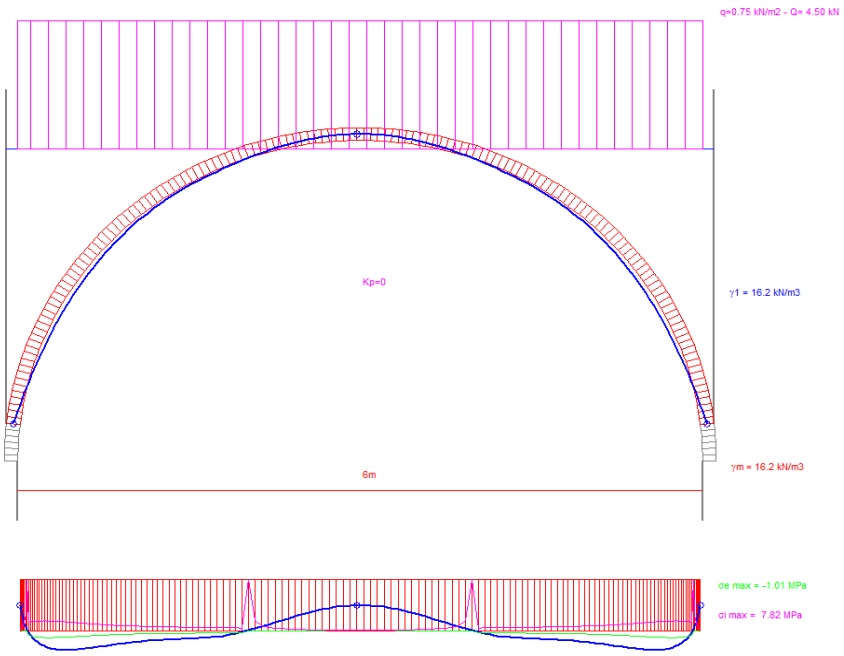


Figure 4-46. Pressure line of the Left Lateral Vault· Centred distributed load · Section 2.

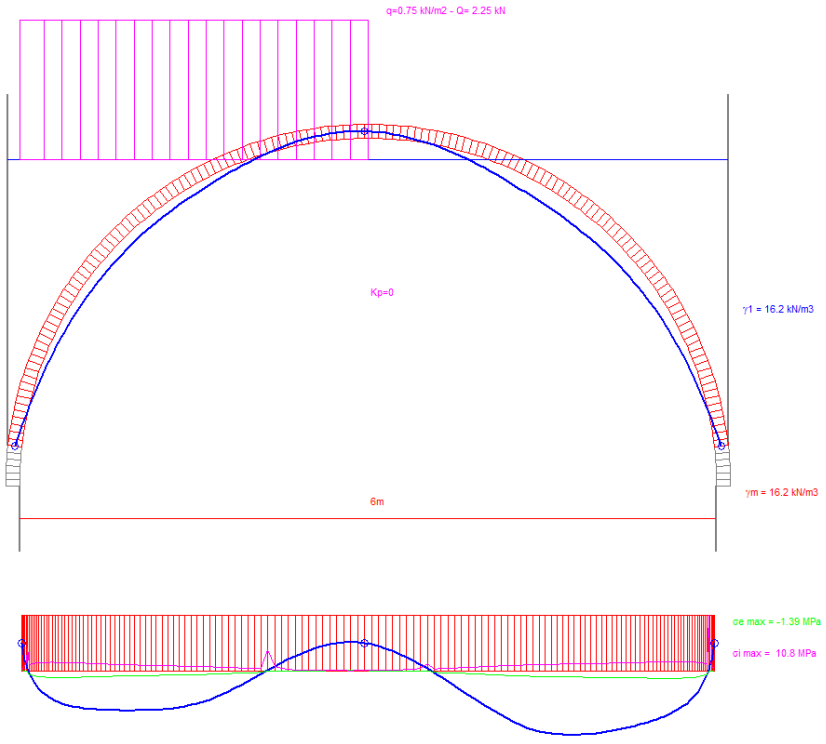


Figure 4-47. Pressure line of the Left Lateral Vault· Asymmetrical load · Section 2.

Finally, the results obtained for the case of the right-side vault are detailed. The same considerations were assumed as for the previous cases, the structure was divided into

the same number of sections and the analysis of the influence of a non-symmetrical load was considered.

In the case of section 2, which represents the diagonal of the vault, it can be observed that for the symmetric load it is not in equilibrium (Figure 4-48), with values of tension for the intrados and extrados equal to $\sigma_e = -0.695$ MPa and $\sigma_i = -4.55$MPa.

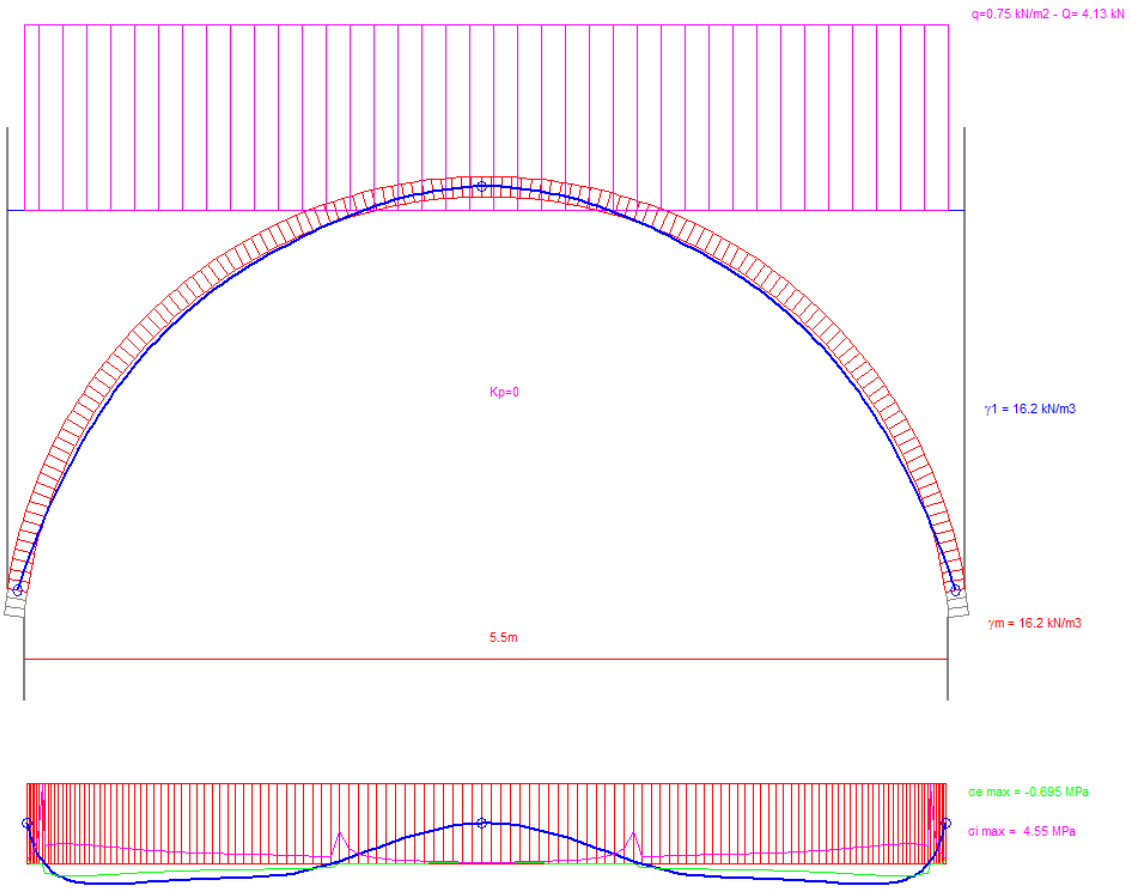


Figure 4-48. Pressure line of the Lateral Right Vault – Condition of centred distributed load - Section 2.

In the case of asymmetric loading, the condition of non-equilibrium is repeated with values equal to $\sigma_e = -0.695$ MPa and $\sigma_i = -4.55$MPa.. This can be observed in Figure 4-49.

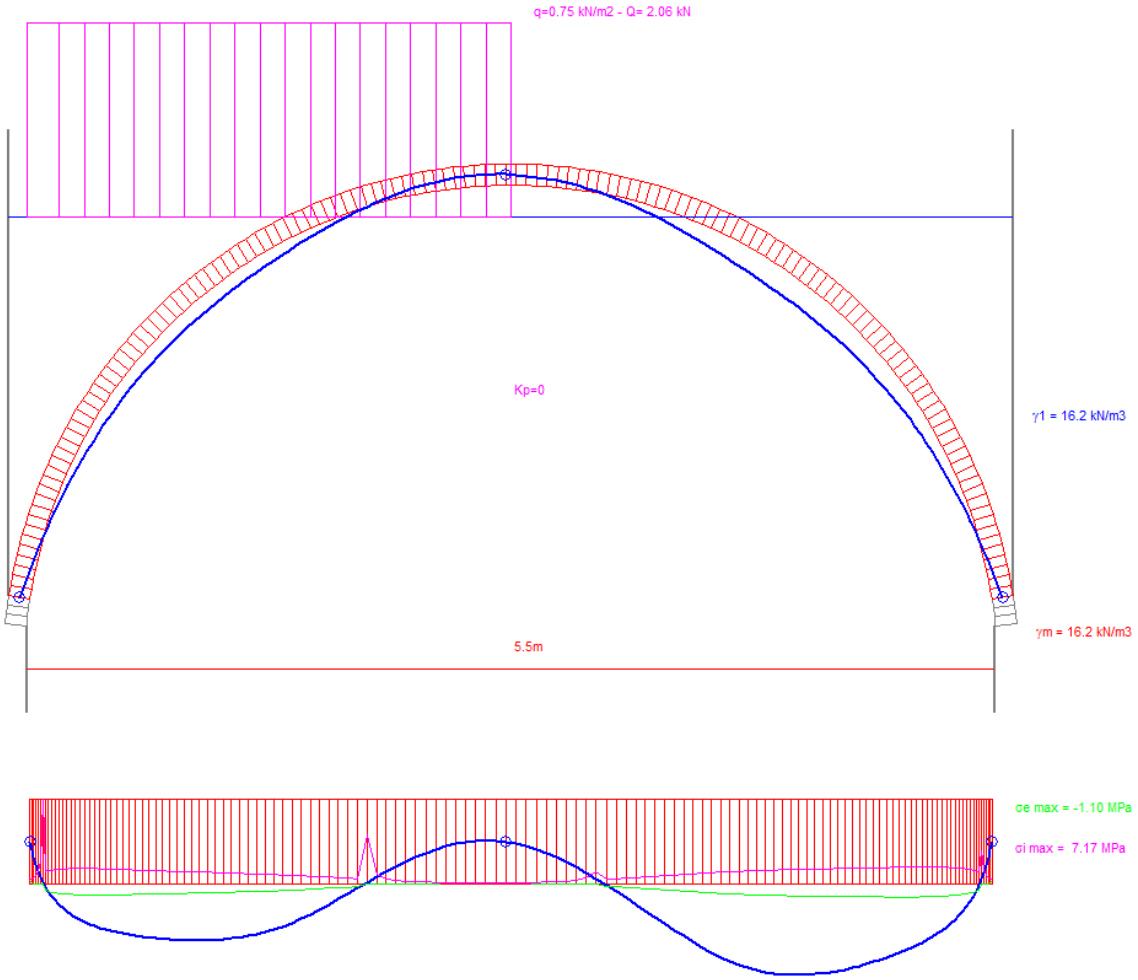


Figure 4-49. Pressure line of the Lateral Right Vault – Condition of asymmetrical load - Section 2.

The Table 4-36 represents a summary of the analyzed vaults with the results obtained. From this table it can be seen that of all the sections analyzed, considering both load positions, whether symmetrical or non-symmetrical, the section always has an internal tensile stress.

Furthermore, it can be observed that the compressive stresses are high, surpassing the allowable limits for the masonry's resistance capacity. For this reason, some action should be taken to solve this problem.

It is important to mention that during the modeling process in this software, several iterations were performed to optimize the geometry and achieve the best results. Multiple attempts were made to refine the analysis and obtain the most accurate outcomes.

| Position | | Symetrical Load | | Non Symmetrical load | |
|---|---|---|---|---|---|
| | | $\sigma_e$ | $\sigma_i$ | $\sigma_e$ | $\sigma_i$ |
| Vault | Division | [MPa] | [MPa] | [MPa] | [MPa] |
| Central | 1 | 0.79 | 0.577 | 12.9 | -0.633 |
| | 2 | 4.57 | -1.87 | 8.21 | -2.34 |
| | 3 | -0.826 | 5.52 | -0.7282 | 0.25 |
| Right Lateral | 1 | -0.254 | 1.44 | -0.267 | 2.74 |
| | 2 | -0.695 | 4.55 | -1.1 | 7.17 |
| | 3 | -0.745 | 4 | -0.329 | 7.86 |
| Left Lateral | 1 | -0.14 | 2.14 | -0.327 | 0.479 |
| | 2 | -1.01 | 7.82 | -1.39 | 10.8 |
| | 3 | 0.291 | 0.6 | -0.396 | 1.2 |

Table 4-36. Results of the vault verification.

After applying this graphical method to perform the verification of the vaults some weaknesses can be seen. The first is based on the fact that it is a graphical method, which is approximate. The second is that the method presents a restriction which is the boundary condition, not in all cases the boundary condition between the vaults and the walls is simply supported. For this reason, in many cases it may be that the structural element passes the verification through this method, but then when it is inspected it shows cracks.

# 5

# Local analysis

In the “Norme Tecniche per le Costruzioni 2018” it is indicated that in masonry constructions subject to seismic action, particularly in buildings, local mechanisms and overall mechanisms can occur. Local mechanisms affect individual masonry panels or larger portions of the building and are favored by the absence or poor effectiveness of connections between walls and horizons and at masonry intersections. The safety of the construction must be assessed against both types of mechanism.

For the seismic analysis of local mechanisms, the methods of limit analysis of the equilibrium of masonry structures can be used, considering, albeit in an approximate form, the compressive strength of the masonry , the quality of the connection between the masonry walls, and the presence of chains and tie rods. With such methods, it is possible to assess the seismic capacity in terms of resistance or in terms of displacement.

## 5.1 Calculation Method

Out-of-plane failure mechanism analysis are developed with limit analysis, basing on kinematic approach which consists in the evaluation of horizontal action that activate the specific mechanism considered basing on the geometry and the constraints of the wall.

### 5.1.1 Linear Kinematic Analysis

Out-of-plane failures on walls are usually caused by actions perpendicular to wall's plane. Current regulations suggest checking in and out-of-plane failures with limit analysis, with kinematic approach, which consists in the evaluation of horizontal action that activate the specific mechanism considered basing on the geometry and the constraints of the wall. In the kinematic analysis it is considered that masonry is composed by rigid bodies. The aim of this analysis is to evaluate the limit equilibrium conditions of these rigid bodies. [27]

For each failure mechanism considered the analysis requires the following steps:

– the structure is commuted into a kinematic chain finding on the masonry one or more rigid bodies which are allowed to mutually rotate.

– evaluation of the multiplier of horizontal loads $\alpha_0$which entails the activation of the mechanism.

– evaluation, with non-linear kinematic analysis, of the evolution of the multiplier of horizontal loads $\alpha$ at the increasing of the displacement $d_k$ of a control point of the kinematic chain, usually the centre of mass, till the annulment of the horizontal force due to seismic action.

– conversion of the curve into capacity curve, or in spectral acceleration $a^*$ and spectral displacement $d^*$, with evaluation of the ultimate displacement due to the mechanism (ultimate limit state).

– safety checks, performed controlling compatibility of displacements and/or resistance.

The following assumptions are made for the application of the method:

- masonry tension resistance is null
- rigid bodies can't mutually slide.

- masonry has an infinite compression resistance

With linear kinematic analysis it's possible to find, after a virtual rotation $\vartheta_K$is assigned to the generic rigid body k, the displacements function of the assigned rotation and of the geometry of the structure. The load multiplier $\alpha_0$ is obtained applying the virtual work principle, written in term of displacements, imposing that the total work of external forces is equal to the total work of internal forces, as follows:

$$\alpha_0 = \frac{\sum_{k=1}^{n} P_k \delta_{Py,k} - \sum_{k=1}^{m} F_k \delta_{F,k} + L_i}{\sum_{k=1}^{n} (P_k + Q_k) \delta_{PQx,k}} \tag{43}$$

where:

- n is the number of all weight forces applied to the different blocks of the kinematic chain.
- m is the number of external forces, taken independent of the seismic action, applied to the different blocks.
- $P_k$ is the result of the weight forces applied to the k-th block (weight of the block, applied in its center of gravity, added to the other weights carried).
- $Q_k$ it is the result of the weight forces not on the k-th block but whose mass generates a horizontal seismic force on it, as it is not effectively transmitted to other parts of the building.
- Fk is the generic external force applied to one of the blocks; these forces can favor the activation of the mechanism (for example, thrust of times) or hinder it (for example, contrast arcs, that is, the forces of attraction that develop in the presence of parts of the construction not involved in the mechanism).
- $\delta_{py,k}$ is the vertical virtual displacement of the center of gravity of the forces of own weight and Pk flows, acting on the k-th block, assumed positive if upward.
- $\delta_{F,k}$ is the virtual displacement of the point of application of the external force Fk, projected in the direction of the same (positive or negative sign depending on whether it favors or contrasts the mechanism).
- $\delta_{PQ,k}$ is the virtual horizontal displacement of the center of gravity of the horizontal forces α (Pk + Qk) acting on the k-th block, assuming as positive the one of the seismic action that activates the mechanism.

- Li is the total work of possible internal forces (lengthening of a chain, sliding with friction in the presence of clenching between the blocks of the mechanism, due to translational or torsional motions, deformation in the plane of floors connected or not rigid).

In the case of linear kinematic analysis, the checks to be carried out are distinguished at the quota at which the kinematics is being evaluated, making a distinction between the ground quota and at elevated quota. If the check concerns an isolated element, or a section of the construction however substantially placed on the ground, the security check is executed if the spectral acceleration $a_0^*$ that starts the mechanism, compared with the acceleration to the ground, respects the following inequality:

For a Damage Limit State.

At quota zero:

$$a_{g,SLD} \geq \frac{a_g \cdot S}{q_{SLD}} \tag{44}$$

At elevated quota:

$$a_{z,SLD} \geq a_z(z) \tag{45}$$

Where:

$$a_z(z)=\sqrt{\sum_k (a_{z,k}(z))^2} \qquad a_{z,k}(z)=S_e(T_k,\xi_k)\gamma_k\psi_k\sqrt{1+0.0004\xi_k^2} \tag{46}$$

For a Life-sustaining Limit State.

At quota zero:

$$a_{g,SLV} \geq \frac{a_g \cdot S}{q_{SLV}} \tag{47}$$

At elevated quota:

$$a_{z,SLV} \geq \frac{a_z(z)}{q_{SLV}} \tag{48}$$

### 5.1.2 Nonlinear kinematic analysis

The evolution of kinematic is followed by analytical - numerical, considering a sequence of finished virtual rotations and revising varied geometry of the system: fixed a finished rotation $\vartheta_K$, we can establish the multiplier $\alpha$ corresponding to it, as well as done in the example of the starting configuration of the system, but considering of the variation of geometry.

By means of trigonometric relations, supposing that the actions remain unvaried, is possible to obtain the expressions for the arms of the acting forces depending on the rotation $\vartheta_K$ that the structure makes, and to follow the variations of the coefficient $\alpha$ until his annulment.

Growing the angle of rotation, there's a decrease of the arm of the vertical forces in relation to the cylindrical hinge (for some values of $\vartheta_K$ the point of application of some forces comes out of the thread of wall on which we find the rotation pole and, in these cases, the moment produced by these forces, that become unstable, will be negative, contributing to the decrease of the resistant moment) and an increase of the horizontal arm forces: It follows a reduction of the stabilizing moment, that in a certain form is annulled, and an increase of the overturning moment. Corresponding, a decrease of the coefficient $\alpha$, that will be cancelled in that form in which the resistant moment is null.

It's possible to define the angle $\vartheta_{K_0}$ (to which correspond the displacement $d_{k0}$ of the considered control point) that characterize the configuration why there's the annulment of the multiplier $\alpha$, and to say of the stabilizing moment Ms.

The security check of the local mechanisms towards the Limit State of life safety consists in the comparison between the ultimate displacement capacity $d_u$* of the local mechanism and the request of displacement obtained by the displacement spectrum in correspondence with the secant period $T_{SLV}$. [27]

At quota zero:

$$d_u^* \geq S_{De}(T_{SLV}) \tag{49}$$

At elevated quota:

$$d_u^* \geq S_{ez}(T_{SLV},\xi,z)\frac{T_{SLV}^2}{4\pi^2} \tag{50}$$

Where:

$$S_{ez}(T_{SLV},\xi,z)=1.1\xi^{-0.5}\eta(\xi)a_{z,k}(z) \tag{51}$$

## 5.2 Analysis of the mechanisms

For the verification of these mechanisms the software used was PRO_CineM which enables the automatic analysis of local kinematics.

As input to the software the geometry of the wall, the materials of which the walls are composed, and the roofs must be defined. As far as the material is concerned, it is possible to choose between the different types of masonry provided by the "NTC2018". At the same time, it is likewise possible to set the various openings, such as doors and windows, as well as the damping walls. The seismic parameters and the level of knowledge of the building are also to be entered.

Of importance, it is to be noted that the various mechanisms that the software is able to analyze are the following:

-Simple overturning kinematics of a single-story monolithic wall.

-Simple overturning kinematics of a monolithic multiple-story wall.

-Single-plane and multi-plane diagonal wedge overturning.

-Vertical deflection of single-story and multi-story monolithic wall.

-Horizontal deflection of confined and unconfined monolithic wall.

-Overturning the tympanum.

Once all inputs have been defined, the analysis is carried out. The various walls that were verified are presented in the next sections.

### 5.2.1 Façade

In the evaluation of this wall, the influence of the vaults, which exert weight on the wall, was considered. The influence of the walls of the main nave, which act as bond walls, was also considered. In turn, when defining these walls, it is important to define an angle of inclination, in this case because the quality of the masonry is very poor it was decided to opt for an angle of 30 degrees.

At the same time, the presence of the roof covering, which is made of wood, was also taken into consideration. The closure of this roof generates a tympanum, which will be an object of possible vulnerability in the construction.

The Figure 5-1 represents the 3D model done in the software, where it is possible to see the adhesion walls that are in the lateral sides. On the other hand, the Figure 5-2 represents a front view of the wall from can be seen the openings (main door and window) and it is also possible to see the roofs that directly influence this wall.

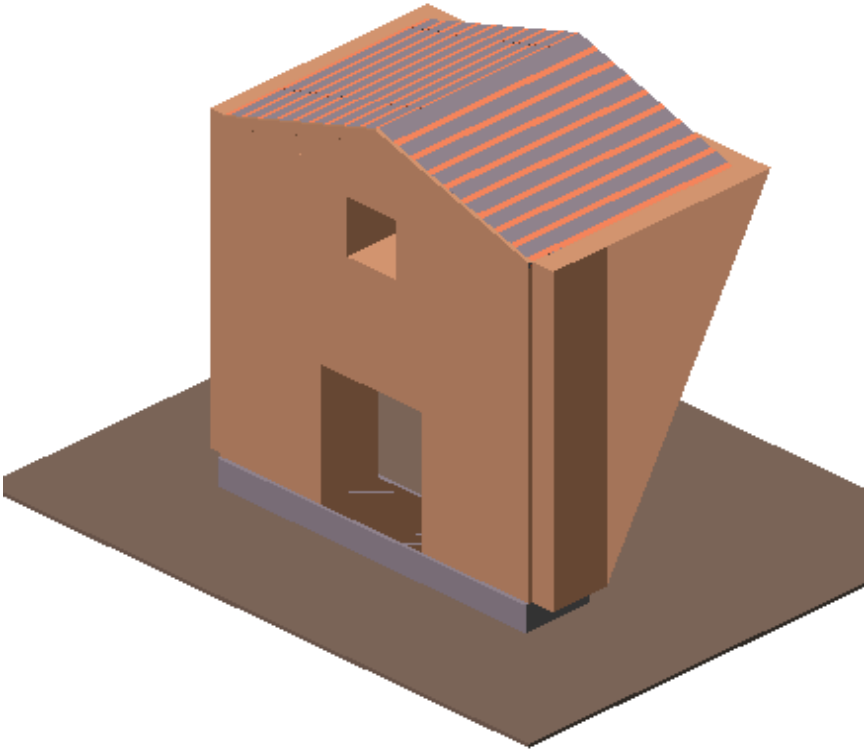

Figure 5-1. 3D model of the wall obtained from PRO_CINEm.

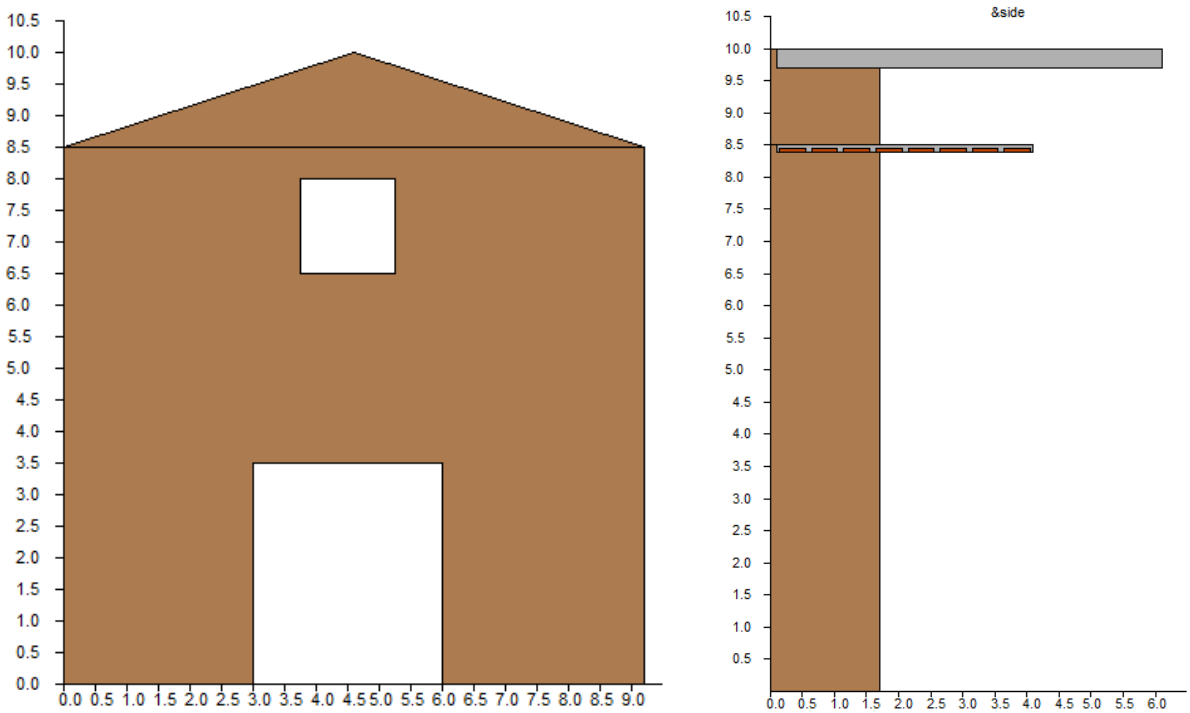


Figure 5-2. Front view and a section of the wall obtained from PRO_CINEm.

The verified mechanisms are as listed further below:

<u>Kinematic N° 1: Overturning of the tympanum</u>

-Activation fee of the kinematic mechanism: 8.50 [m]

-First mode of vibration normalized to 1 at the top of the building $y_{(z)}$: 1.000 [-]

-Overturning Moment $M_{rib}$: 177.276 [kN*m]

-Stabilizing moment $M_{st}$: 249.566 [kN*m]

-Horizontal load collapse multiplier $\alpha_0$ : 1.408 [-]

-Spectral acceleration of kinematic activation $a_0$*: 1.083 [g]

-Mass participating in the kinematic M*: 30.494 [kN]

-Participating mass fraction of the structure e*: 0.963 [-]

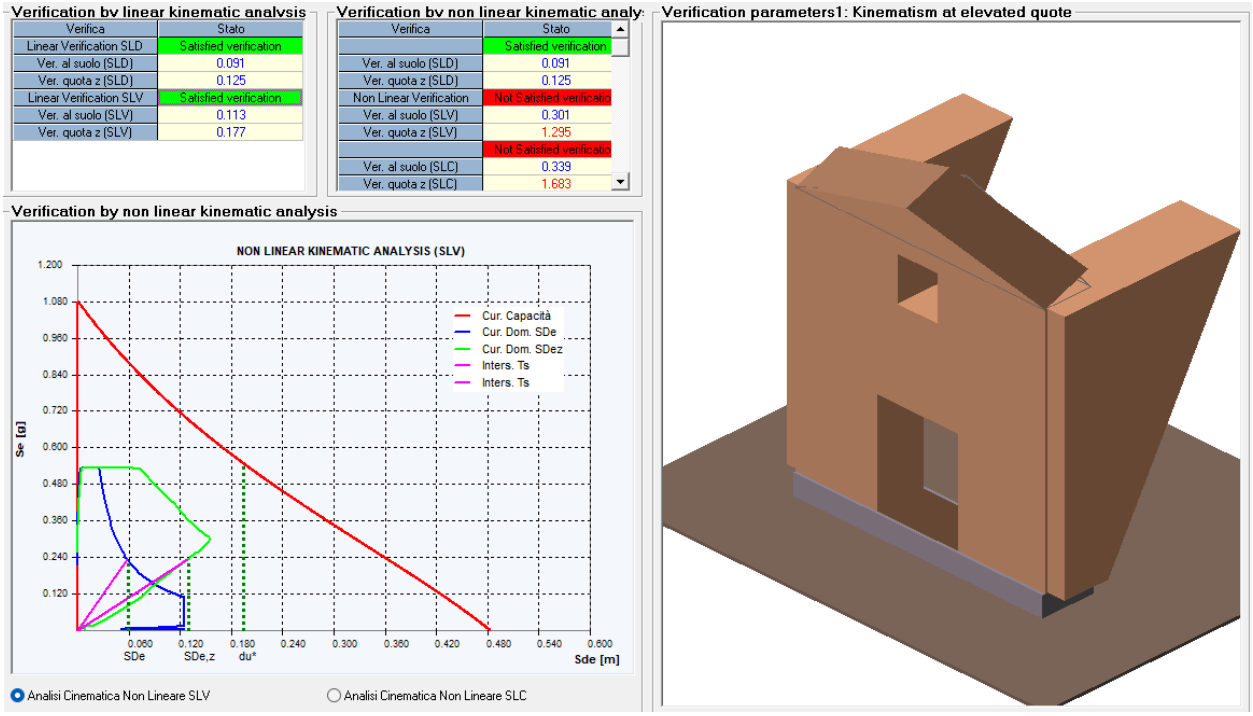


Figure 5-3. Results obtained from PRO_CINEm for the Overturning of the tympanum.

The results obtained through the use of the software are as follows:

| Linear Kinematic Analysis SLD | | |
|---|---|---|
| | At zero level | In elevation |
| $a_{g,SLD}$ (g) | 0.055 | |
| $a_{g,SLD}$ S)/$q_{,SLD}$ (g) | 0.099 | - |
| $a_z(z)_{,SLD}$ (g) | - | 0.135 |
| Verification factor | 0.091 | 0.125 |
| Result verification | Verify | Verify |

| Linear Kinematic Analysis SLV | | |
|---|---|---|
| | At zero level | In elevation |
| $a_{g,SLV}$ (g) | 0.137 | |
| $a_{g,SLV}$ S)/$q_{,SLV}$ (g) | 0.123 | - |
| $a_z(z)_{,SLV}$ (g) | - | 0.192 |
| Verification factor | 0.114 | 0.177 |
| Result verification | Verify | Verify |

Table 5-1- Results of the Linear Kinematic Analysis for the Damage Limit and Life Sustaining Limit state.

| Non - Linear Kinematic Analysis SLD | | |
|---|---|---|
| | At zero level | In elevation |
| $a_{g,SLD}$ (g) | 0.055 | |
| $a_{g,SLD}$ S)/$q_{,SLD}$ (g) | 0.099 | - |
| $a_z(z)_{,SLD}$ (g) | - | 0.135 |
| Verification factor | 0.091 | 0.125 |
| Result verification | Verify | Verify |

| Non - Linear Kinematic Analysis SLV | | |
|---|---|---|
| | At zero level | In elevation |
| $T_s$ (sec) | 0.999 | |
| $d_u$* (m) | 0.193 | |
| $d_{SLV,z}$ (m) | 0.058 | |
| $d_{SLV,e}$ (m) | | 0.250 |
| Verification factor | 0.301 | 1.295 |
| Result verification | Verify | Not Verify |

| Non - Linear Kinematic Analysis SLC | | |
|---|---|---|
| | At zero level | In elevation |
| $T_s$ (sec) | 1.307 | |
| $d_u$* (m) | 0.29 | |
| $d_{SLC,z}$ (m) | 0.098 | |
| $d_{SLC,e}$ (m) | | 0.488 |
| Verification factor | 0.338 | 1.683 |
| Result verification | Verify | Not Verify |

Table 5-2. Results of the Non- Linear Kinematic Analysis for the Damage Limit, Life Sustaining and Collapse Limit state.

From the Table 5-1 it can be seen that in the case of linear kinematic analysis, the comparison is made in terms of acceleration, i.e. in terms of the acceleration that activates the mechanism vs. the maximum acceleration of the site, either at zero level or at a given ground level. In the case of linear kinematics, the checks are satisfied.

In contrast, in Table 5-2 it can be seen that for the Life sustaining and Collapse limit state, the verifications are carried out in terms of displacement, comparing the displacement requested by the mechanism vs. the displacement that the structure is able to withstand, in this case it can be seen that the verifications are not satisfied.

Kinematic N° 2: Overturning Single Wall with involvement of one of the orthogonal walls at zero:

-Activation fee of the kinematic mechanism: 0.00 [m]

-First mode of vibration normalized to 1 at the top of the building $y_{(z)}$: 0.000 [-]

-Overturning Moment $M_{rib}$: 22572.640 [kN*m]

-Stabilizing moment $M_{st}$: 4596.248 [kN*m]

-Horizontal load collapse multiplier $\alpha_0$ : 0.204 [-]

-Spectral acceleration of kinematic activation $a_0$*: 0.148 [g]

-Mass participating in the kinematic M*: 410.300 [kN]

-Participating mass fraction of the structure e*: 1.016 [-]

The results obtained through the use of the software are as follows:

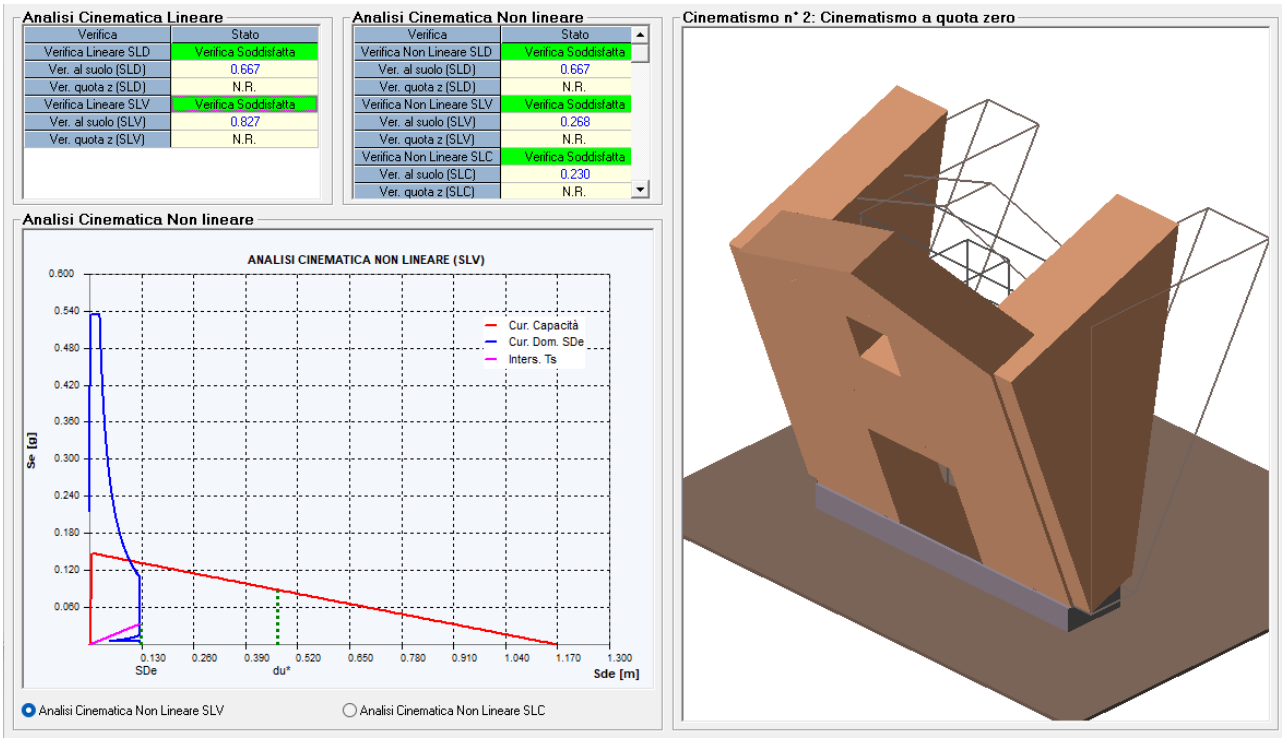


Figure 5-4. Results obtained from PRO_CINEm for the Overturning Single Wall.

| Linear Kinematic Analysis SLD | | |
|---|---|---|
| | At zero level | In elevation |
| $a_{g,SLD}$ (g) | 0.055 | |
| $a_{g,SLD}$ S)/$q_{,SLD}$ (g) | 0.099 | - |
| $a_z(z)_{,SLD}$ (g) | - | NR |
| Verification factor | 0.669 | NR |
| Result verification | Verify | NR |

| Linear Kinematic Analysis SLV | | |
|---|---|---|
| | At zero level | In elevation |
| $a_{g,SLV}$ (g) | 0.137 | |
| $a_{g,SLV}$ S)/$q_{,SLV}$ (g) | 0.123 | - |
| $a_z(z)_{,SLV}$ (g) | - | NR |
| Verification factor | 0.831 | NR |
| Result verification | Verify | NR |

Table 5-3. Results of the Linear Kinematic Analysis for the Damage Limit and Life Sustaining Limit state.

| Non - Linear Kinematic Analysis SLD | | |
|---|---|---|
| | At zero level | In elevation |
| $a_{g,SLD}$ (g) | 0.055 | |
| $a_{g,SLD}$ S)/$q_{,SLD}$ (g) | 0.099 | - |
| $a_z(z)_{,SLD}$ (g) | - | 0.135 |
| Verification factor | 0.669 | 0.912 |
| Result verification | Verify | Verify |

| Non - Linear Kinematic Analysis SLV | | |
|---|---|---|
| | At zero level | In elevation |
| $T_s$ (sec) | 3.866 | |
| $d_u$* (m) | 0.467 | |
| $d_{SLV,z}$ (m) | 0.125 | |
| $d_{SLV,e}$ (m) | | NR |
| Verification factor | 0.268 | NR |
| Result verification | Verify | NR |

| Non - Linear Kinematic Analysis SLC | | |
|---|---|---|
| | At zero level | In elevation |
| $T_s$ (sec) | 5.385 | |
| $d_u$* (m) | 0.7 | |
| $d_{SLC,z}$ (m) | 0.161 | |
| $d_{SLC,e}$ (m) | | NR |
| Verification factor | 0.230 | NR |
| Result verification | Verify | NR |

Table 5-4. Results of the Non- Linear Kinematic Analysis for the Damage Limit, Life Sustaining and Collapse Limit state.

From the tables Table 5-3 and Table 5-4 representing the linear and non-linear kinematic analysis, it can be remarked that the verifications are satisfied in both cases, due to the fact that the verification factors are lower than one. Therefore, this mechanism cannot be activated in the current construction conditions.

Kinematic N° 3: Flexible horizontal ejection at high altitude

-Activation fee of the kinematic mechanism: 0.00 [m]

-First mode of vibration normalized to 1 at the top of the building $y_{(z)}$: 0.812 [-]

-Overturning Moment $M_{rib}$: 917.233 [kN*m]

-Stabilizing moment $M_{st}$: 494.438 [kN*m]

-Horizontal load collapse multiplier $\alpha_0$ : 0.539 [-]

-Spectral acceleration of kinematic activation $a_0$*: 0.405 [g]

-Mass participating in the kinematic M*: 27.898 [kN]

-Participating mass fraction of the structure e*: 0.985 [-]

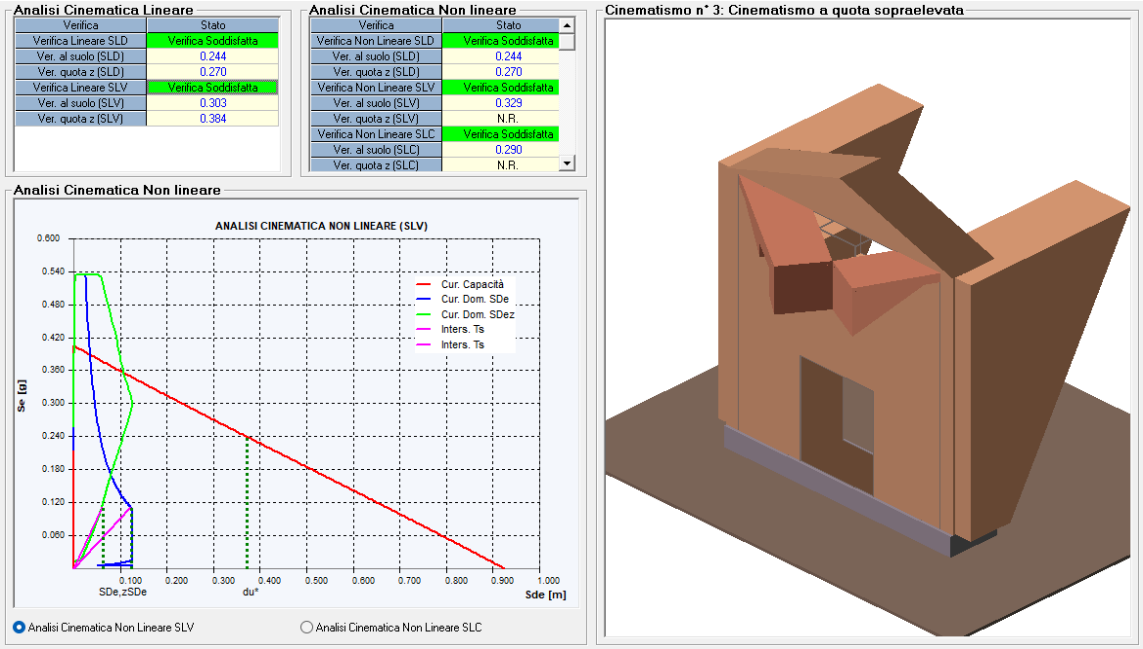


Figure 5-5. Results obtained from PRO_CINEm for Flexible horizontal ejection at high altitude.

The results obtained through the use of the software are as follows:

| Linear Kinematic Analysis SLD | | |
|---|---|---|
| | At zero level | In elevation |
| $a_{g,SLD}$ (g) | 0.055 | |
| $a_{g,SLD}$ S)/$q_{,SLD}$ (g) | 0.099 | - |
| $a_z(z)_{,SLD}$ (g) | - | 0.11 |
| Verification factor | 0.244 | 0.272 |
| Result verification | Verify | Verify |

| Linear Kinematic Analysis SLV | | |
|---|---|---|
| | At zero level | In elevation |
| $a_{g,SLV}$ (g) | 0.137 | |
| $a_{g,SLV}$ S)/$q_{,SLV}$ (g) | 0.123 | - |
| $a_z(z)_{,SLV}$ (g) | - | 0.156 |
| Verification factor | 0.304 | 0.385 |
| Result verification | Verify | Verify |

Table 5-5. Results of the Linear Kinematic Analysis for the Damage Limit and Life Sustaining Limit state.

| Non - Linear Kinematic Analysis SLD | | |
|---|---|---|
| | At zero level | In elevation |
| $a_{g,SLD}$ (g) | 0.055 | |
| $a_{g,SLD}$ S)/$q_{,SLD}$ (g) | 0.099 | - |
| $a_z(z)_{,SLD}$ (g) | - | 0.11 |
| Verification factor | 0.244 | 0.272 |
| Result verification | Verify | Verify |

| Non - Linear Kinematic Analysis SLV | | |
|---|---|---|
| | At zero level | In elevation |
| $T_s$ (sec) | 2.093 | |
| $d_u$* (m) | 0.371 | |
| $d_{SLV,z}$ (m) | 0.122 | |
| $d_{SLV,e}$ (m) | | NR |
| Verification factor | 0.329 | NR |
| Result verification | Verify | NR |

| Non - Linear Kinematic Analysis SLC | | |
|---|---|---|
| | At zero level | In elevation |
| $T_s$ (sec) | 2.909 | |
| $d_u$* (m) | 0.556 | |
| $d_{SLC,z}$ (m) | 0.161 | |
| $d_{SLC,e}$ (m) | | NR |
| Verification factor | 0.290 | NR |
| Result verification | Verify | NR |

Table 5-6. Results of the Non- Linear Kinematic Analysis for the Damage Limit, Life Sustaining and Collapse Limit state.

Like the previous mechanism, the verifications are satisfied in both cases, due to the fact that the verification factors are lower than one. Therefore, this mechanism cannot be activated in the current construction conditions. This can be observed in the Table 5-5 and Table 5-6.

The same model was run, but with an earthquake at 30%, in which case the mechanism overturning of the tympanum in the nonlinear analysis in Life sustaining limit state and in collapse limit state at elevated quota verifies. The result is that all the verifications are satisfied.

### 5.2.2 North Façade

In the evaluation of this wall, the influence of the vaults, which exert weight on the wall, was considered. The influence of the façade wall and the wall adjacent to the bell tower were taken into consideration, which act as bond walls. In turn, when defining these walls, it is important to define an angle of inclination, in this case because the quality of the masonry is very poor it was decided to opt for an angle of 30 degrees.

At the same time, the presence of the roof covering, which is made of wood, was also taken into consideration, in this case the cover type is a cover with flap. In addition to considering the influence of the side walls, the presence of the chains located in the left aisle was also considered. It is worth mentioning that the exact mechanical parameters of the chains are not known, the lowest mechanical parameters were chosen in order to be on the safe side.

The Figure 5-6 represents the 3D model done in the software, where it is possible to see the adhesion walls that are in the lateral sides. On the other hand, the Figure 5-7 represents a front view of the wall from can be seen the openings and it is also possible to see the roofs that directly influence this wall and the chains.

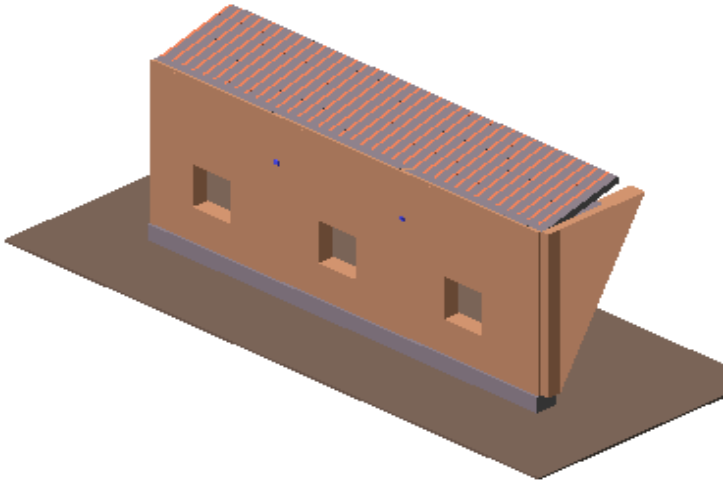

Figure 5-6. 3D model of the wall obtained from PRO_CINEm.

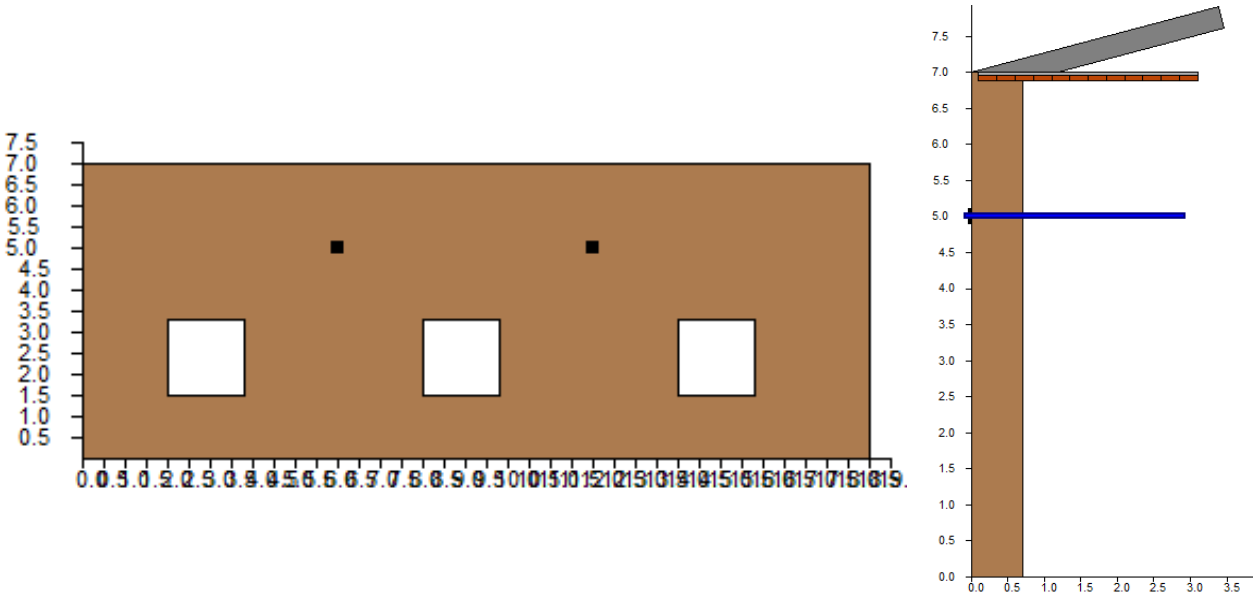

Figure 5-7. Front view and a section of the wall obtained from PRO_CINEm.

In this case, only one mechanism was verified, the Overturning Single Wall.

Kinematic N° 1: Overturning of a Single wall.

-Activation fee of the kinematic mechanism: 0.00 [m]

-First mode of vibration normalized to 1 at the top of the building $y_{(z)}$: 0.000 [-]

-Overturning Moment $M_{rib}$: 12730.210 [kN*m]

-Stabilizing moment $M_{st}$: 2169.492 [kN*m]

·Horizontal load collapse multiplier $\alpha_0$ : 0.170 [-]

·Spectral acceleration of kinematic activation $a_0$*: 0.144 [g]

·Mass participating in the kinematic M*: 288.330 [kN]

·Participating mass fraction of the structure e*: 0.989 [-]

The results obtained through the use of the software are as follows:

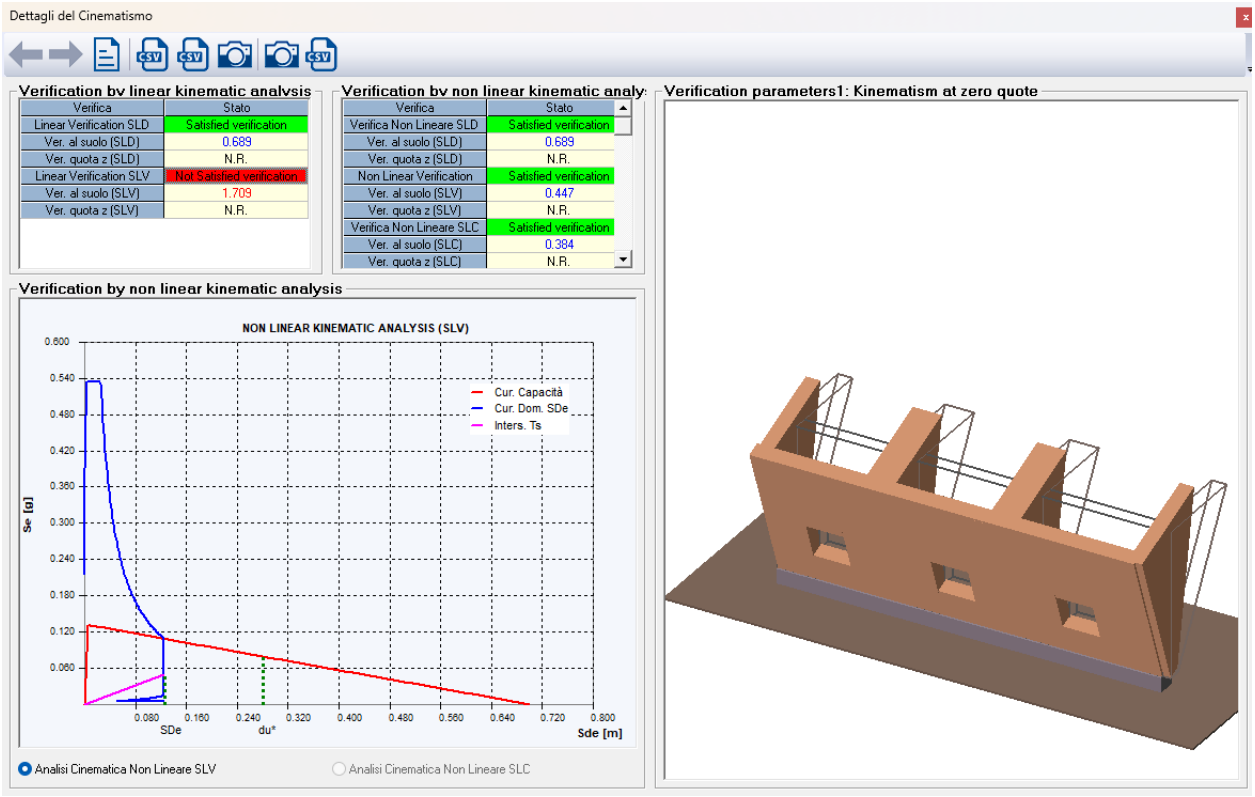


Figure 5-8. Results obtained from “Overturning of a single wall”.

| Linear Kinematic Analysis SLD | | |
|---|---|---|
| | At zero level | In elevation |
| $a_{g,SLD}$ (g) | 0.055 | |
| $a_{g,SLD}$ S)/$q_{,SLD}$ (g) | 0.099 | - |
| $a_z(z)_{,SLD}$ (g) | - | N.R |
| Verification factor | 0.688 | N.R |
| Result verification | Verify | N-R |

| Linear Kinematic Analysis SLV | | |
|---|---|---|
| | At zero level | In elevation |
| $a_{g,SLV}$ (g) | 0.137 | |
| $a_{g,SLV}$ S)/$q_{,SLV}$ (g) | 0.246 | - |
| $a_z(z)_{,SLV}$ (g) | - | N.R |
| Verification factor | 1.708 | N.R |
| Result verification | No Verify | N-R |

Table 5-7. Results of the Linear Kinematic Analysis for the Damage Limit and Life Sustaining Limit state.

| Non - Linear Kinematic Analysis SLD | | |
|---|---|---|
| | At zero level | In elevation |
| $a_{g,SLD}$ (g) | 0.055 | |
| $a_{g,SLD}$ S)/$q_{,SLD}$ (g) | 0.099 | - |
| $a_z(z)_{,SLD}$ (g) | - | N.R |
| Verification factor | 0.688 | N.R |
| Result verification | Verify | N-R |

| Non - Linear Kinematic Analysis SLV | | |
|---|---|---|
| | At zero level | In elevation |
| $T_s$ (sec) | 3.167 | |
| $d_u$* (m) | 0.28 | |
| $d_{SLV,z}$ (m) | 0.125 | |
| $d_{SLV,e}$ (m) | | N.R |
| Verification factor | 0.446 | N.R |
| Result verification | Verify | N-R |

| Non - Linear Kinematic Analysis SLC | | |
|---|---|---|
| | At zero level | In elevation |
| $T_s$ (sec) | 4.412 | |
| $d_u$* (m) | 0.42 | |
| $d_{SLC,z}$ (m) | 0.161 | |
| $d_{SLC,e}$ (m) | | N.R |
| Verification factor | 0.383 | N.R |
| Result verification | Verify | N-R |

Table 5-8. Results of the Non- Linear Kinematic Analysis for the Damage Limit, Life Sustaining and Collapse Limit state.

In this case, it can be observed from the Table 5-7 that in the context of the linear kinematic analysis for a state of Life sustaining limit state at zero level, the mechanism does not verify, since the verification factor is greater than one. This means that the acceleration that is presented is greater than the one that activates the mechanism, therefore it is activated in this state.

The model was also run considering an earthquake of 30%, as in the previous model. In this case the checks are satisfied in all cases, satisfying the case of the linear kinematic analysis for a state of Life sustaining limit state at zero level.

### 5.2.3 Bell Tower

In the evaluation of this wall, the different wooden ceilings inside the bell tower were considered. These ceilings have an influence on the wall because their weight is transferred on it. At the same time, an equivalent roof was considered at the top. The influence of the orthogonal walls was considered, always in order to be on the side of safety, the quality of the material considered was low and as a consequence the angle of inclination was taken as 30 degrees.

The Figure 5-9 represents the 3D model done in the software, where it is possible to see the adhesion walls that are in the lateral sides. On the other hand, the Figure 5-10 represents a front view of the wall from can be seen the opening at the top part. It is also possible to see the roofs that directly influence this wall. It is important to mention that the precise location of these different wooden planks is not perfectly known, but it was decided to adopt an approximation.

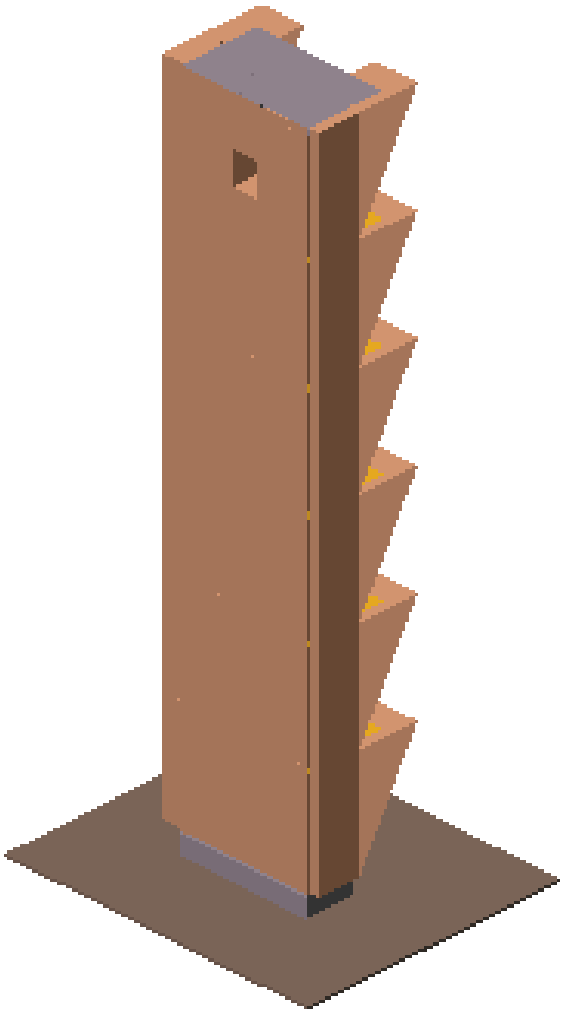

Figure 5-9. 3D model of the wall obtained from PRO_CINEm.

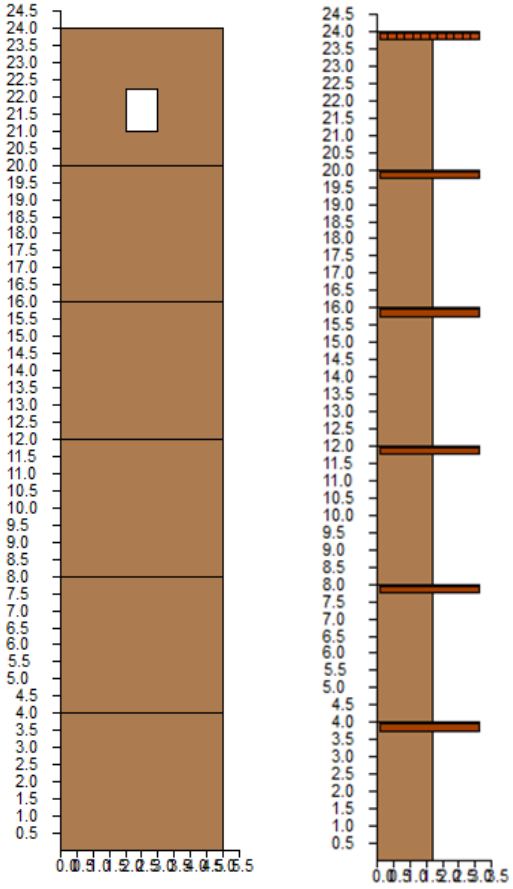

Figure 5-10. Front view and a section of the wall obtained from PRO_CINEm.

The verified mechanisms are as listed further below

Kinematic N° 1: Overturning Single Wall with involvement of one of the orthogonal walls at high altitude.

In the first instance, this mechanism was evaluated at the top of the bell tower.

-Activation fee of the kinematic mechanism: 20.00 [m]

-First mode of vibration normalized to 1 at the top of the building $y_{(z)}$: 0.833 [-]

-Overturning Moment $M_{rib}$: 2145.650 [kN*m]

-Stabilizing moment $M_{st}$: 998.460 [kN*m]

-Horizontal load collapse multiplier $\alpha_0$ : 0.465 [-]

-Spectral acceleration of kinematic activation $a_0$*: 0.401 [g]

-Mass participating in the kinematic M*: 92.181 [kN]

-Participating mass fraction of the structure e*: 0.966 [-]

The results obtained through the use of the software are as follows:

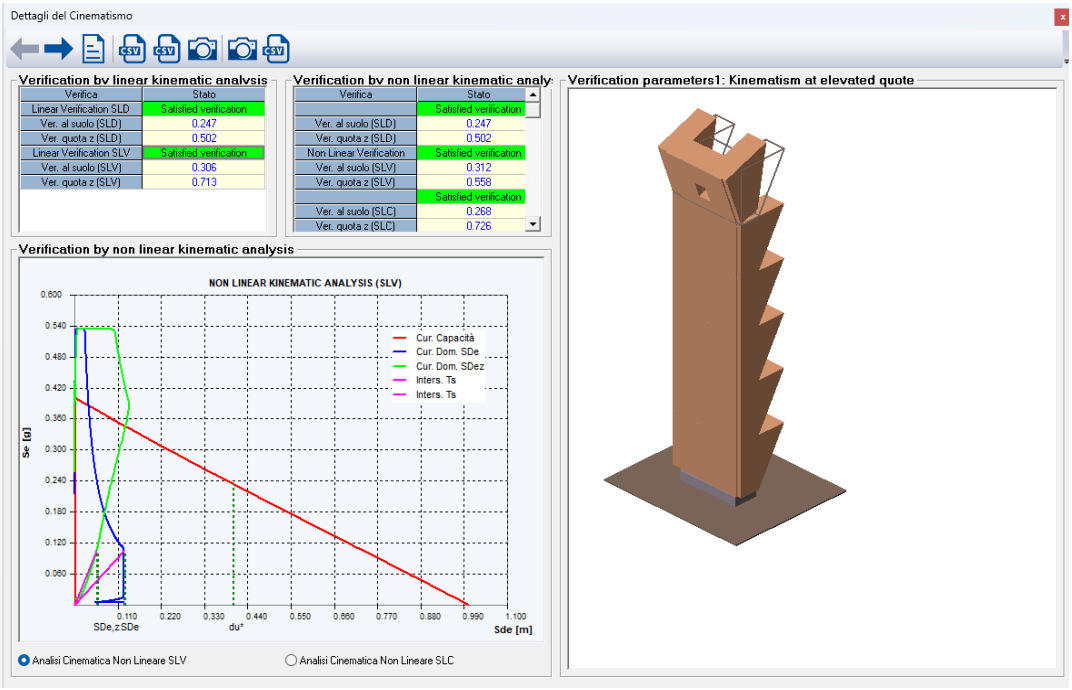


Figure 5-11. Results obtained from PRO_CINEm for the Overturning single wall.

| Linear Kinematic Analysis SLD | | |
|---|---|---|
| | At zero level | In elevation |
| $a_{g,SLD}$ (g) | 0.055 | |
| $a_{g,SLD}$ S)/$q_{,SLD}$ (g) | 0.099 | - |
| $a_z(z)_{,SLD}$ (g) | - | 0.135 |
| Verification factor | 0.247 | 0.337 |
| Result verification | Verify | Verify |

| Linear Kinematic Analysis SLV | | |
|---|---|---|
| | At zero level | In elevation |
| $a_{g,SLV}$ (g) | 0.137 | |
| $a_{g,SLV}$ S)/$q_{,SLV}$ (g) | 0.123 | - |
| $a_z(z)_{,SLV}$ (g) | - | 0.286 |
| Verification factor | 0.307 | 0.713 |
| Result verification | Verify | Verify |

Table 5-9. Results of the Linear Kinematic Analysis for the Damage Limit and Life Sustaining Limit state.

| Non - Linear Kinematic Analysis SLD | | |
|---|---|---|
| | At zero level | In elevation |
| $a_{g,SLD}$ (g) | 0.055 | |
| $a_{g,SLD}$ S)/$q_{,SLD}$ (g) | 0.099 | - |
| $a_z(z)_{,SLD}$ (g) | - | 0.201 |
| Verification factor | 0.247 | 0.501 |
| Result verification | Verify | Verify |

| Non - Linear Kinematic Analysis SLV | | |
|---|---|---|
| | At zero level | In elevation |
| $T_s$ (sec) | 2.02 | |
| $d_u$* (m) | 0.401 | |
| $d_{SLV,z}$ (m) | 0.125 | |
| $d_{SLV,e}$ (m) | | 0.224 |
| Verification factor | 0.312 | 0.559 |
| Result verification | Verify | Verify |

| Non - Linear Kinematic Analysis SLC | | |
|---|---|---|
| | At zero level | In elevation |
| $T_s$ (sec) | 3.069 | |
| $d_u$* (m) | 0.601 | |
| $d_{SLC,z}$ (m) | 0.161 | |
| $d_{SLC,e}$ (m) | | 0.224 |
| Verification factor | 0.268 | 0.726 |
| Result verification | Verify | Verify |

Table 5-10. Results of the Non- Linear Kinematic Analysis for the Damage Limit, Life Sustaining and Collapse Limit state.

From the Table 5-9 and Table 5-10 it can be seen that at a height of 20 m this mechanism is verified for both linear and non-linear kinematic analysis and for all the limit states.

Kinematic N° 2: Overturning Single Wall with involvement of one of the orthogonal walls at high altitude.

-Activation fee of the kinematic mechanism: 16.00 [m]

-First mode of vibration normalized to 1 at the top of the building $y_{(z)}$: 0.667 [-]

-Overturning Moment $M_{rib}$: 8078.974 [kN*m]

-Stabilizing moment $M_{st}$: 1424.285 [kN*m]

-Horizontal load collapse multiplier $\alpha_0$ : 0.176 [-]

-Spectral acceleration of kinematic activation $a_0$*: 0.182 [g]

-Mass participating in the kinematic M*: 157.181 [kN]

-Participating mass fraction of the structure e*: 0.809 [-]

The results obtained through the use of the software are as follows:

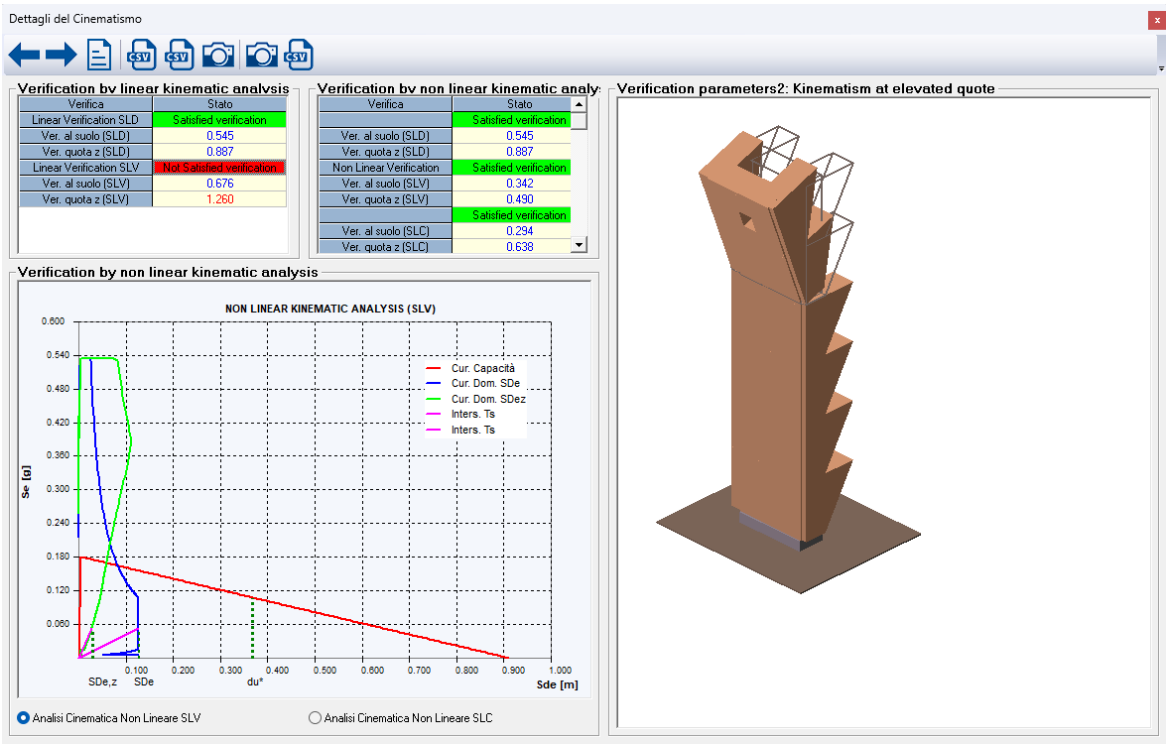


Figure 5-12. Results obtained from PRO_CINEm for the Overturning single wall.

The tables obtained are presented below.

| Linear Kinematic Analysis SLD | | |
|---|---|---|
| | At zero level | In elevation |
| $a_{g,SLD}$ (g) | 0.055 | |
| $a_{g,SLD}$ S)/$q_{,SLD}$ (g) | 0.099 | - |
| $a_z(z)_{,SLD}$ (g) | - | 0.161 |
| Verification factor | 0.544 | 0.885 |
| Result verification | Verify | Verify |

| Linear Kinematic Analysis SLV | | |
|---|---|---|
| | At zero level | In elevation |
| $a_{g,SLV}$ (g) | 0.137 | |
| $a_{g,SLV}$ S)/$q_{,SLV}$ (g) | 0.123 | - |
| $a_z(z)_{,SLV}$ (g) | - | 0.229 |
| Verification factor | 0.676 | 1.258 |
| Result verification | Verify | No Verify |

Table 5-11. Results of the Linear Kinematic Analysis for the Damage Limit and Life Sustaining Limit state.

| Non - Linear Kinematic Analysis SLD | | |
|---|---|---|
| | At zero level | In elevation |
| $a_{g,SLD}$ (g) | 0.055 | |
| $a_{g,SLD}$ S)/$q_{,SLD}$ (g) | 0.099 | - |
| $a_z(z)_{,SLD}$ (g) | - | 0.161 |
| Verification factor | 0.544 | 0.885 |
| Result verification | Verify | Verify |

| Non - Linear Kinematic Analysis SLV | | |
|---|---|---|
| | At zero level | In elevation |
| $T_s$ (sec) | 3.093 | |
| $d_u$* (m) | 0.365 | |
| $d_{SLV,z}$ (m) | 0.125 | |
| $d_{SLV,e}$ (m) | | 0.179 |
| Verification factor | 0.342 | 0.490 |
| Result verification | Verify | Verify |

| Non - Linear Kinematic Analysis SLC | | |
|---|---|---|
| | At zero level | In elevation |
| $T_s$ (sec) | 3.069 | |
| $d_u$* (m) | 0.365 | |
| $d_{SLC,z}$ (m) | 0.125 | |
| $d_{SLC,e}$ (m) | | 0.179 |
| Verification factor | 0.342 | 0.490 |
| Result verification | Verify | Verify |

Table 5-12. Results of the Non- Linear Kinematic Analysis for the Damage Limit, Life Sustaining and Collapse Limit state.

As can be observed in Table 5-11 for the case of linear analysis in the state of Limit state for safeguarding life, the verification is not satisfied, with the verification factor exceeding 1. In the case of nonlinear analysis, the verifications are indeed satisfied. It is important to mention that beyond this threshold, as the altitude decreases, the verifications are no longer satisfied, with the situation becoming increasingly critical.

Proceeding to examine an alternative form of local mechanism that may arise.

Kinematic N° 3: Flexible horizontal ejection at high altitude.

-Activation fee of the kinematic mechanism: 0.00 [m]

-First mode of vibration normalized to 1 at the top of the building $y_{(z)}$: 0.100 [-]

-Overturning Moment $M_{rib}$: 200.543 [kN*m]

-Stabilizing moment $M_{st}$: 1025.772 [kN*m]

-Horizontal load collapse multiplier $\alpha_0$ : 5.115 [-]

-Spectral acceleration of kinematic activation $a_0$*: 4.303 [g]

-Mass participating in the kinematic M*: 14.093 [kN]

-Participating mass fraction of the structure e*: 0.991 [-]

By employing the software, the obtained results were as follows

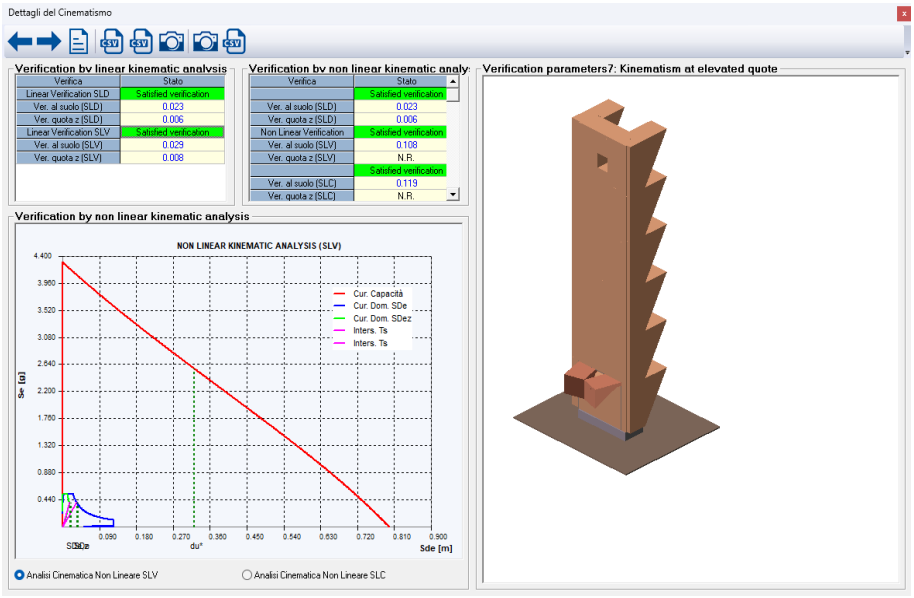


Figure 5-13. Results obtained from PRO_CINEm for Flexible horizontal ejection at high altitude.

Presented below are the obtained tables.

| Linear Kinematic Analysis SLD | | |
|---|---|---|
| | At zero level | In elevation |
| $a_{g,SLD}$ (g) | 0.055 | |
| $a_{g,SLD}$ S)/$q_{,SLD}$ (g) | 0.099 | - |
| $a_z(z)_{,SLD}$ (g) | - | 0.024 |
| Verification factor | 0.023 | 0.006 |
| Result verification | Verify | Verify |

| Linear Kinematic Analysis SLV | | |
|---|---|---|
| | At zero level | In elevation |
| $a_{g,SLV}$ (g) | 0.137 | |
| $a_{g,SLV}$ S)/$q_{,SLV}$ (g) | 0.123 | - |
| $a_z(z)_{,SLV}$ (g) | - | 0.034 |
| Verification factor | 0.029 | 0.008 |
| Result verification | Verify | Verify |

Table 5-13. Results of the Linear Kinematic Analysis for the Damage Limit and Life Sustaining Limit state.

| Non - Linear Kinematic Analysis SLD | | |
|---|---|---|
| | At zero level | In elevation |
| $a_{g,SLD}$ (g) | 0.055 | |
| $a_{g,SLD}$ S)/$q_{,SLD}$ (g) | 0.099 | - |
| $a_z(z)_{,SLD}$ (g) | - | 0.024 |
| Verification factor | 0.023 | 0.006 |
| Result verification | Verify | Verify |

| Non - Linear Kinematic Analysis SLV | | |
|---|---|---|
| | At zero level | In elevation |
| $T_s$ (sec) | 0.529 | |
| $d_u$* (m) | 0.319 | |
| $d_{SLV,z}$ (m) | 0.034 | |
| $d_{SLV,e}$ (m) | | NR |
| Verification factor | 0.107 | NR |
| Result verification | Verify | NR |

| Non - Linear Kinematic Analysis SLC | | |
|---|---|---|
| | At zero level | In elevation |
| $T_s$ (sec) | 0.808 | |
| $d_u$* (m) | 0.478 | |
| $d_{SLC,z}$ (m) | 0.057 | |
| $d_{SLC,e}$ (m) | | NR |
| Verification factor | 0.119 | NR |
| Result verification | Verify | NR |

Table 5-14. Results of the Non- Linear Kinematic Analysis for the Damage Limit, Life Sustaining and Collapse Limit state.

As observed in both cases, whether in linear or nonlinear analysis, the verifications are satisfied for all considered limit states. The same mechanism was evaluated at different altitudes, and the verifications were consistently satisfied.

It is of utmost importance to emphasize that, like the preceding cases, the identical model was employed, considering a seismic event of 30%. Nonetheless, unlike the instances where the verifications proved to be satisfactory, in this specific case, pertaining to the “overturning of a single wall”', the verification factor surpasses 1, leading to the dissatisfaction of the verification.

In conclusion, it can be established that for the analysed structural components, under a 100% seismic event, the construction exhibits issues concerning the activation of local mechanisms. However, when considering a 30% seismic event, the main façade satisfies the verifications, while the north façade also meets the

requirements. On the other hand, the bell tower proves to be a critical element as it does not satisfy the verifications under a 30% seismic event.

After evaluating the local collapse mechanisms, measures must be implemented to strengthen the structure and mitigate identified risks to ensure long-term safety and stability.

# 6

# Reinforcement techniques

This last chapter addresses the topic of structural strengthening interventions in structural components that do not meet design requirements or fail to adequately verify the applied loads. In many cases, existing structures may exhibit deficiencies in their load-carrying capacity or resistance to specific forces, compromising their integrity and safety. In response to this issue, various techniques and solutions for structural reinforcement have been developed with the aim of strengthening and improving the performance of these elements.

## 6.1 Reinforcement of walls

Within the critical structural elements that require reinforcement, walls stand out as a fundamental priority. In this context, the most crucial verification to consider is their shear capacity. Ensuring the resistance of walls to shear forces is indispensable for ensuring the stability and safety of any structure against lateral loads such as earthquakes or strong winds. Therefore, it is essential to carry out a comprehensive analysis and propose improvements in the methods of verification and reinforcement of walls, with the aim of strengthening their shear resistance and, consequently, enhancing the quality and durability of constructions.

In the present section, the available wall reinforcement techniques in the market, notably those of Italian origin, will be discussed within the theoretical framework. A comprehensive evaluation of the advantages and disadvantages associated with each technique will be presented, leading to a conclusive assessment of the most suitable approach for the analyzed construction. The primary reinforcements for masonry walls are as follows:

### 6.1.1 Reinforced plaster (or reinforced mortar) with welded mesh.

The technique involves the construction of two concrete slabs on both faces of the masonry, reinforced with metal mesh and connected to the masonry itself through transverse bars. The consolidation is effective only if the concrete slabs are constructed on both sides and the necessary connections (injected bars) are properly installed.

For the consolidation to be effective, it must be applied on both sides of the wall, and the two concrete slabs should be properly connected with transverse connectors (at least 4 per square meter). Plating the walls with reinforced plaster is a measure that can be employed when the walls are severely damaged or inconsistent, and for limited sections of the wall heavily loaded with vertical loads (thus not related to seismic actions).

The mesh used must be made of stainless steel (as indicated in Paragraph C8.7.4.1 of the NTC18), properly overlapped at interruptions to ensure continuity, and effectively anchored to the connectors passing through the thickness of the wall. In the Figure 6-1,

a detailed depiction of the previously specified aspects can be observed. The correct and incorrect ways of implementing this intervention.

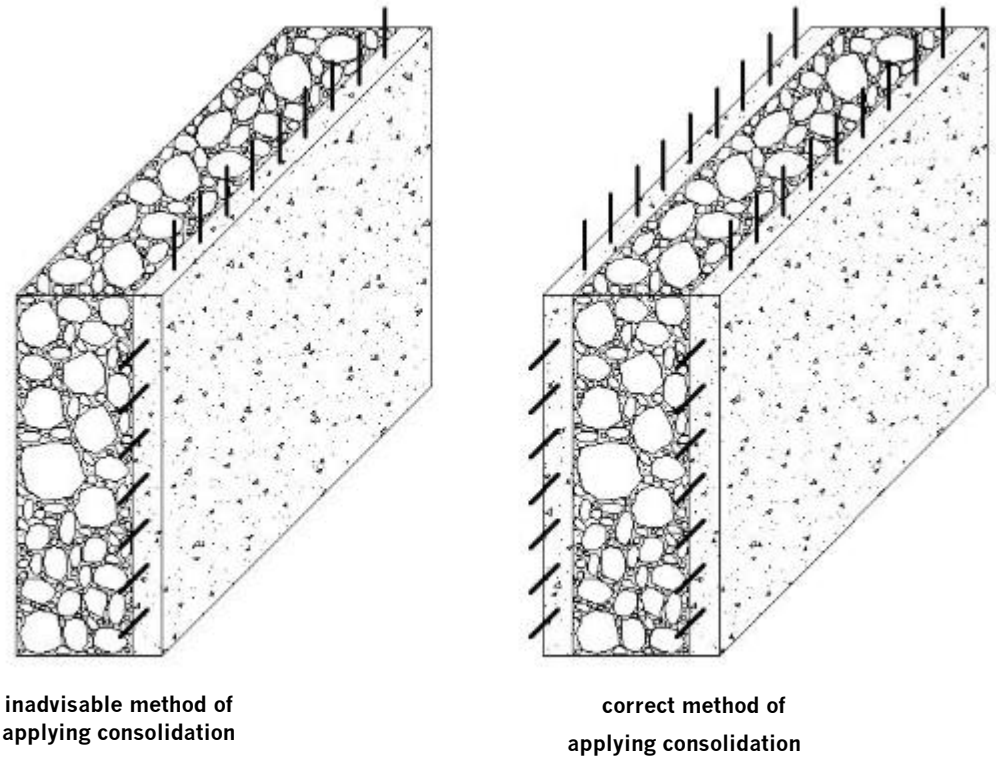


Figure 6-1. Correct and incorrect way to apply the reinforcement, image extracted from internet.

It is strongly discouraged if there is a need to reinforce large portions of a building due to the significant increase in stiffness and resulting mass which can lead to foundation problems, such as exceeding the bearing capacity of the soil and settlements, due to the excessive load resulting from the reinforcement. The reinforcement system, necessarily, cannot have a thickness less than 5 cm per wall facade (approximately ranging from 5 to 7 cm). This translates into an increase of at least 250 kg per square meter of wall.

As a result of this, within the "Directive of the President of the Council of Ministers for the assessment and reduction of seismic risk to cultural heritage", issued on October 12, 2007, and subsequent amendments, the intervention of wall consolidation with reinforced plaster using electro-welded mesh is defined as "invasive and inconsistent with conservation principles." In addition, the reinforcement system is not reversible. [28]

Based on the reasons, which can be summarized as the significant increase in stiffness and mass, the lack of chemical-physical compatibility with the masonry, and

the non-reversibility, it can be concluded that this type of intervention is not recommended for the analysed construction.

### 6.1.2 Composite Reinforced Mortar

The CRM reinforced plaster is created by using a preformed composite mesh embedded in a structural mortar and applied to the surface of the masonry element to be reinforced. In this system, the composite mesh is capable of absorbing tensile forces, while the structural mortar helps absorb compressive forces. The transfer of forces between the substrate and the reinforcement mesh is also ensured by the presence of connectors, which provide structural collaboration between the masonry element and the reinforced plaster.

The thickness of CRM reinforcement systems typically ranges from 3 to 5 cm, excluding the levelling of the substrate. For this reason, it is commonly referred to as high-thickness reinforcement.

CRM (Composite Reinforced Mortar) reinforcement systems typically consist of preformed meshes made by impregnating alkali-resistant fibres, such as glass, carbon, basalt, or aramid, in a single production phase. The meshes serve to increase tensile strength and confine the elements being reinforced. Preformed corner angles made of fiberglass, carbon fibre, basalt, or aramid, using the same materials and manufacturing process as the meshes, are employed to achieve structural continuity at the corners.

Fully or partially preformed connection elements made of alkali-resistant fiberglass, carbon fibber, basalt, or aramid, using the same materials, are utilized to ensure the connection between the reinforced plaster and the masonry element, as well as with the reinforcement installed on the opposite face, where applicable. Cement-based or lime-based mortars with guaranteed structural performance are employed. Chemical anchors are used to bond the connectors together or to anchor them into the masonry substrate.

The meshes, corner angles, and composite connection elements that make up CRM reinforcement systems are manufactured using long continuous fibers of glass, carbon, basalt, or aramid, embedded in a thermosetting polymer matrix.

Like reinforced concrete, it is necessary for the reinforcement to be applied on both sides of the masonry surface, and these two sides should be interconnected through elements that are compatible in terms of material with the used mesh.

In this case as well, due to the increased thickness (although less than in the case of reinforced concrete), there is an increase in the stiffness and mass of the wall, which could lead to similar foundational issues such as exceeding the load-bearing capacity and settlements.

The CRM reinforcement technique is applicable to all types of masonry, including stone, brick, or block masonry, with a preference for multi-leaf or loosely connected sack walls that are at high risk of disintegration during seismic events. Unlike traditional reinforced concrete, which involves the use of cementitious mortars combined with welded wire meshes, the use of CRM system offers the advantage of employing lime-based plasters. Lime plasters have a lower elastic modulus, higher breathability, and better chemical-physical compatibility, making them more suitable for use in protected buildings.

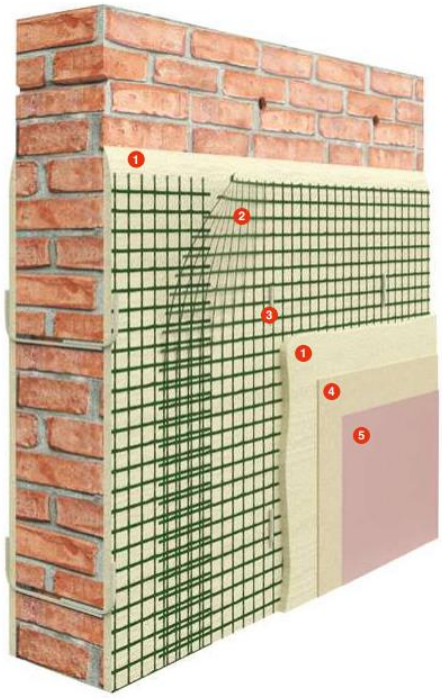


Figure 6-2. Composite reinforced mortar, image extracted from internet.

In summary, the CRM method would be a suitable option for the analysed church due to its ability to enhance structural strength, compatibility with protected buildings,

and potential for reversibility in the consolidation process. Additionally, the fact that most of the walls in the church to be reinforced are composed of random stone masonry, sometimes with voids within the same wall, makes the CRM option particularly well-suited. [29]

### 6.1.3 Fiber Reinforced Cementitious Matrix

Fiber reinforced Cementitious Matrix are obtained by using grids made of high-strength steel wires, aramid, basalt, carbon, PBO, and glass. These grids are combined with specific inorganic matrices designed for reinforcement, such as lime-based or cement-based chemical binders, which are formulated to ensure adhesion to the substrate. In the case of FRCM applied on both sides of the masonry, connectors are not necessary as the grids bond directly to the substrate. The application is preferable when it is symmetrically applied to both surfaces of the structure. However, in exceptional cases, it can also be applied from only one side. In the case of sack walls or walls with disconnected leaves, it is mandatory for the reinforcement to be present on both faces and for passing connectors to be installed. This ensures structural continuity and proper load transfer between the two leaves of the wall, providing enhanced stability and resistance to seismic forces.

Typically, when a single grid is used, the thickness of the system ranges from 5 to 15 mm, excluding the level of the substrate. For this reason, it is commonly referred to as a low-thickness reinforcement. In the case of multiple grids, the thickness increases but is usually limited to around 30 mm.

The high strength-to-weight ratio of FRCM systems allows them to resist tensile forces without significantly increasing the mass or altering the stiffness of the structure. FRCM reinforcements generally exhibit good chemical and physical compatibility with the masonry substrate, and they are reversible.

The reinforcement system is strongly discouraged by manufacturers for use on heterogeneous masonry (such as mixed stonework and bricks) where the surface is not perfectly flat. In such cases, the thickness of the reinforcement may exceed the allowed limits in certain areas, compromising its effectiveness. Therefore, alternative reinforcement methods should be considered for such irregular masonry structures to ensure proper and reliable strengthening. [30]

Due to the strong recommendation against using this reinforcement technique for walls constructed with disordered masonry, despite its advantages, this method was discarded. The potential challenges posed by the irregular surface and varying thicknesses of the reinforcement in such masonry types outweighed the benefits. It is crucial to consider alternative reinforcement methods.

### 6.1.4 Fiber Reinforced Polymer

The FRP reinforcement system consists of an organic matrix reinforced with fiber fabric. This matrix serves to protect the fibers and acts as a means of transferring forces between the fibers and potentially between the fibers and the structural element to be reinforced (in cases where connectors are not present). The matrix enhances the load-bearing capacity of the fibers and helps distribute the applied forces throughout the reinforcement system, improving the overall strength and performance of the structure.

For masonry structures reinforced with FRP subjected to cyclic tensile and compressive stresses, such as those induced by seismic events, the bond between the masonry and FRP can significantly deteriorate over the lifespan of the structure. In such cases, it becomes necessary to incorporate reinforcement into the form of grooves or apply mechanical connection devices.

When applying FRP fabrics or laminates to masonry surfaces, it is important to consider the lack of breathability of composite materials. Therefore, reinforcement interventions using such materials should not typically cover extensive areas of the masonry in order to preserve adequate breathability of the system. It is crucial to strike a balance between providing reinforcement and maintaining the natural moisture exchange of the masonry, which is important for its long-term durability and preservation.

Reinforcement systems with FRP (Fiber Reinforced Polymers) present delamination resistance issues. In the reinforcement of masonry structures, the role of the bond between the masonry and the composite is of great importance, as failure due to loss of bond in the reinforcement is a brittle and undesirable mode of failure (CNR-DT 200/2013). In addition, in heterogeneous masonry, the same strip of fabric can be connected to different materials characterized by different interface properties. If the adhesive strength used for applying the reinforcement is higher than the strength of

the material to which the reinforcement is applied, the loss of bond between the composite and the masonry occurs through the decohesion of a superficial layer of the brick, stone block, or mortar. [31]

In summary, due to the potential delamination issues and the low mechanical strength of random rubble masonry, the use of FRP reinforcement is not chosen as a preferred reinforcement method in this type of historical construction. More suitable alternatives that are respectful of the integrity and authenticity of the structure should be considered.

### 6.1.5 Active Confinement of Masonry (CAM)

The main element of the CAM system is a metallic strip that, when closed upon itself and tensioned, creates hoops that provide active three-dimensional confinement. Additionally, these metallic strips form actual metal reinforcement, which, depending on their placement, contribute to both shear and flexural strength. They also exhibit good resistance to out-of-plane actions. Furthermore, when the mesh is spread throughout the masonry structure, it benefits from a box-like effect. The CAM system's metallic strip ensures high performance in compact dimensions (19x0.9 mm). Thanks to the pre-tensioning of the steel strips, the behaviour of the structure is improved even under static conditions.

The strips are closed upon themselves to form closed loops, and the system is consequently applied on both faces of the wall, without adding mass or stiffness. The formation of a three-dimensional lattice allows for a final condition of triaxial confinement, which provides increased compressive strength to the masonry volume through induced confinement. At the same time, the connections act as reinforcement and offer load-bearing capacity in tension. [32]

The pre-stressed steel ribbons function as tie rods, resisting both deformations and disconnections of the building elements. Specifically, as the straps create closed loops in both horizontal and vertical directions, the CAM ribbon replicates the reinforcement scheme with horizontal and vertical ties. [33]

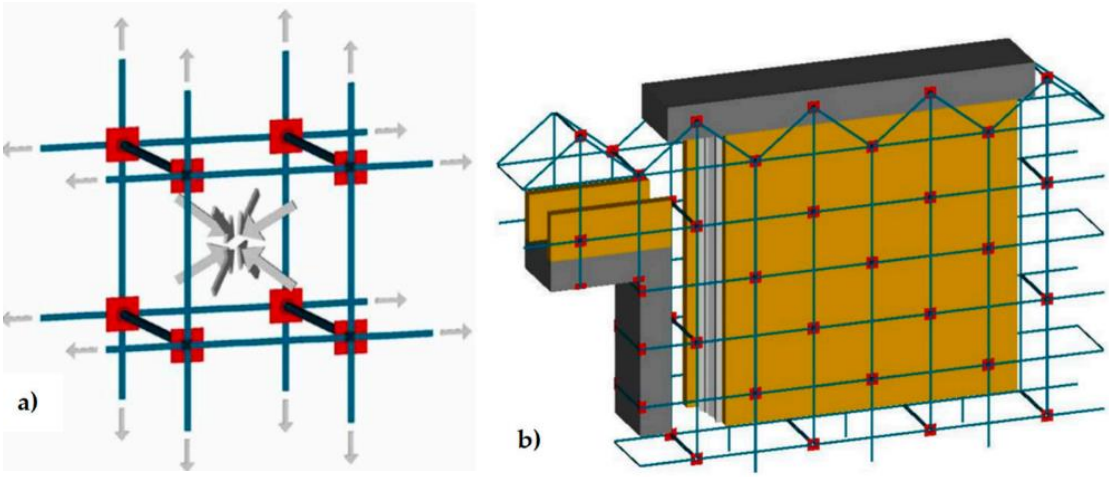


Figure 6-3. Figure a) The intended method for transferring stress from the ribbons of the rectangular arrangement to the confined masonry involves applying hydrostatic compression. Figure b) The connections between a double layer vertical wall.

The mechanism of brittle collapse due to displacement of stone elements in rubble masonry is the primary brittle mechanism to be avoided. The disintegration of the masonry can also affect only one of the double faces that constitute the rubble masonry. The disintegrating masonry typology has such poor characteristics that it can withstand minimal shaking, relying solely on the frictional resistance between the various stone elements. The ensemble of ribbons that traverse the thickness of the masonry and compose the widespread mesh of CAM creates a diatonic mechanical connection between the two faces that constitute the rubble masonry. They absorb the pushing action of the core, and the ensemble of the lattice under restraint provides a beneficial action against the displacement of components and helps promote good interaction between faces and core. The action exerted by the CAM diatonic system, in terms of containment force against thrust, is significantly superior to any other type of diatonic system, whether existing or artificially created, as it does not work based on adhesion (the diatonic system's capacity depends on the state of vertical stress) but rather through mechanical means (the CAM diatonic system's capacity is solely a function of the number of ribbons).[34]

The CAM system is also completely reversible, and being composed of only stainless-steel elements, it is 100% recyclable.

Utilizing the CAM method in an existing masonry structure provides multiple justifications. Firstly, it enhances the strength and stability of the structure, improving its load-bearing capacity. This method also offers complete reversibility, allowing for

easy removal or modification without damaging the original masonry. Additionally, the use of stainless-steel elements in the system ensures 100% recyclability, promoting environmentally friendly construction practices. By reinforcing the masonry, it preserves the building's structural integrity, prolonging its lifespan and avoiding extensive reconstruction. Moreover, the implementation of this method can be cost-effective, minimizing material waste and requiring less invasive construction procedures.

After analyzing all the information presented earlier, it can be concluded that two potential interventions to consider for the studied construction in the walls would be the implementation of composite reinforced mortar and active confinement of masonry (CAM). These interventions have been identified as effective solutions to address the structural challenges and enhance the overall performance and longevity of the construction.

In relation to the bell tower, a potential intervention to address its stability concerns in static conditions would involve the implementation of a steel structure with newly constructed solid wood floors. This approach entails utilizing a steel framework to provide support for the new wooden floors, thereby reinforcing the masonry of the bell tower, particularly with regards to horizontal load-bearing capabilities.

## 6.2 Vault reinforcement

As discussed in Chapter 4.4, the structural element "vaults" exhibit notable structural concerns. Tensile stresses exceeding the load-bearing capacity of the masonry, along with elevated compressive stresses, have been observed. Hence, an appropriate solution needs to be devised. The proposed reinforcement methodology involves the implementation of an external cladding system utilizing galvanized steel fibre strips and a geomesh composed of pure natural hydraulic lime. The objective is to restore structural continuity and integrity to the vaults.

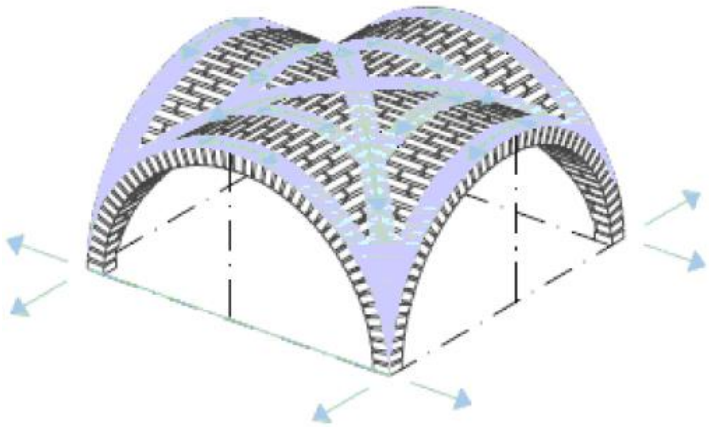

Figure 6-4. Scheme of how the reinforcement is applied.

To designing the reinforcement intervention, the software GeoForce One, developed by the renowned brand Kerakoll, was employed. Kerakoll is a leading company in the manufacture and supply of sustainable construction products. Known for their innovative and environmentally friendly solutions, Kerakoll offers a wide range of materials and systems for building construction and rehabilitation. [35]

Similarly, to the static verification of the vaults, in this case, the vault was divided into sections due to the limitation of modeling the entire structure. The same nomenclature was used as in the previous case to designate these sections, taking as a reference the Figure 4-42.

To assess the critical condition of the structure prior to the intervention, a structural analysis was conducted by modelling the structure both before and after the intervention. This involved defining two distinct scenarios: pre-opera (before the intervention) and post-opera (after the intervention).

The calculation model followed the subsequent steps. The initial step involved the precise definition of the masonry type employed. In the examined construction, the arches were constructed using solid brick masonry with lime mortar. Consequently, the mechanical properties of this specific material were adopted for the analysis. Additionally, it is possible to determine the level of knowledge applicable to the construction, as expounded upon in preceding chapters. In the present case, the LC2 (KL2) level was ascertained. As can be observed in the Figure 6-5.

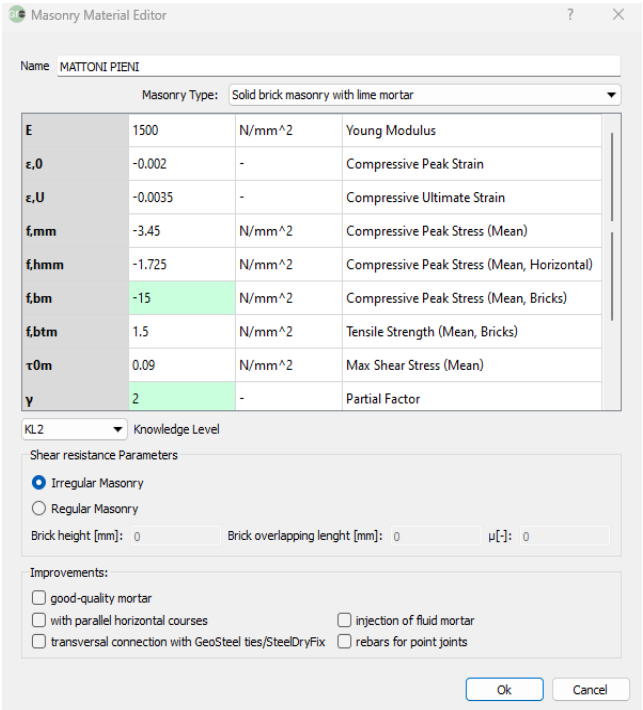


Figure 6-5. Material definitions. Image extracted from the GeoForce One.

Once the material characteristics were established, the subsequent phase entailed defining the geometric attributes of each arch element slated for analysis. The employed software facilitated this process by incorporating a dedicated module tailored specifically to handle such elements. Consequently, only pertinent geometric data were required to be inputted. Regarding the post-opera phase, which encompasses the reinforcement intervention, the introduction of GEOSTEEL steel fiber was incorporated into the arches.

Once the geometry and materials were defined, the next step involved conducting the analysis. The software performs a nonlinear static analysis, which results in a capacity curve depicting displacement versus load multiplier. This curve represents

the structural capacity to withstand the load and provides insight into the margin of safety.

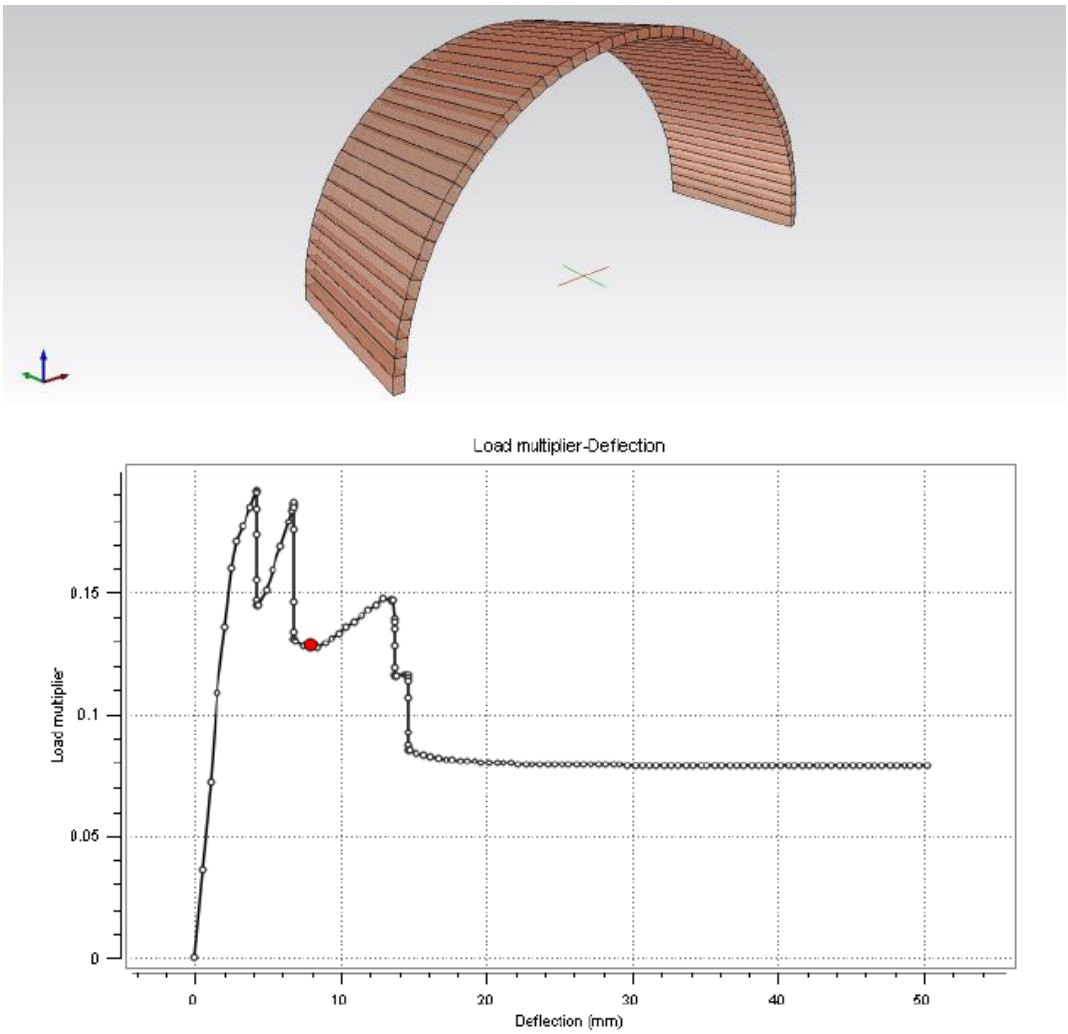


Figure 6-6. Pre opera of the central vault- Section 1. Image extracted from the GeoForce One.

The following are the results obtained for the central nave arch, which, due to its geometry, presents the highest criticalities. The width of the applied reinforcement in the central vault is 80 cm.

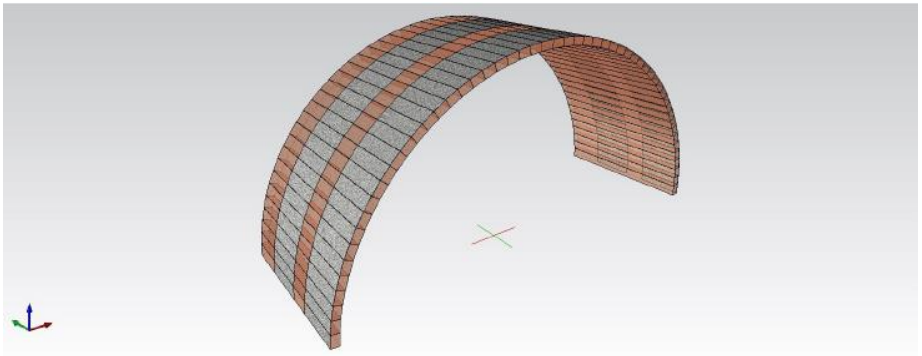

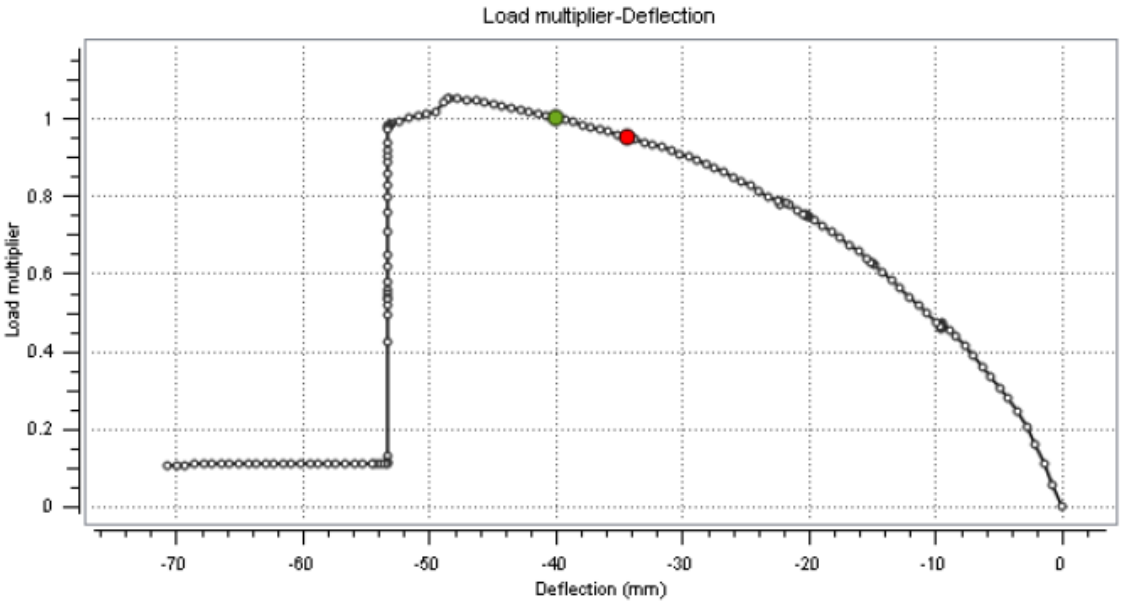


Figure 6-7. Post opera of the central vault – Section 1.

The Figure 6-6 illustrates the initial condition of the vault prior to reinforcement. The capacity curve demonstrates that the vault is incapable of sustaining the applied loads, as evidenced by the load multiplier being less than unity. However, following the implementation of reinforcement measures, it is notable that the load multiplier increases to unity, as depicted in Figure 6-7.

In the case of Section 2, which consists of the arch in the opposite direction, it can be observed that without intervention, the load multiplier is close to 0.7 (Figure 6-8). However, when reinforcement is applied, the load multiplier increases significantly, approaching a value of 1.6 (Figure 6-9).

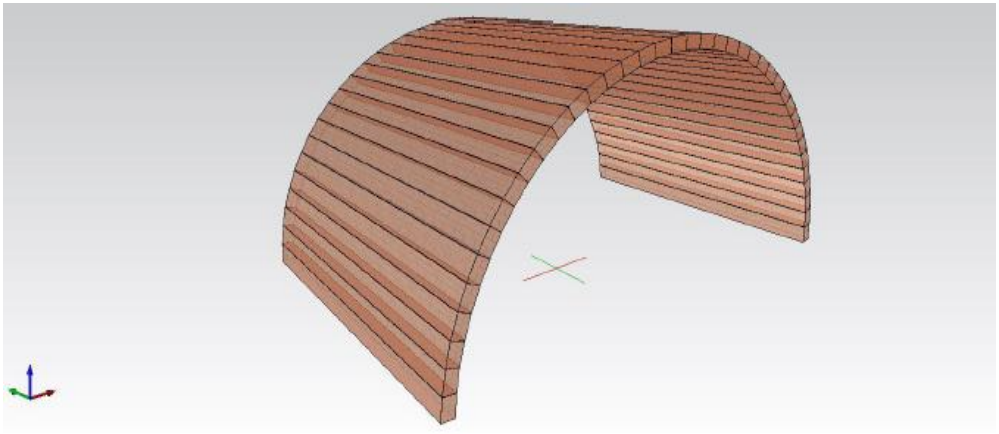

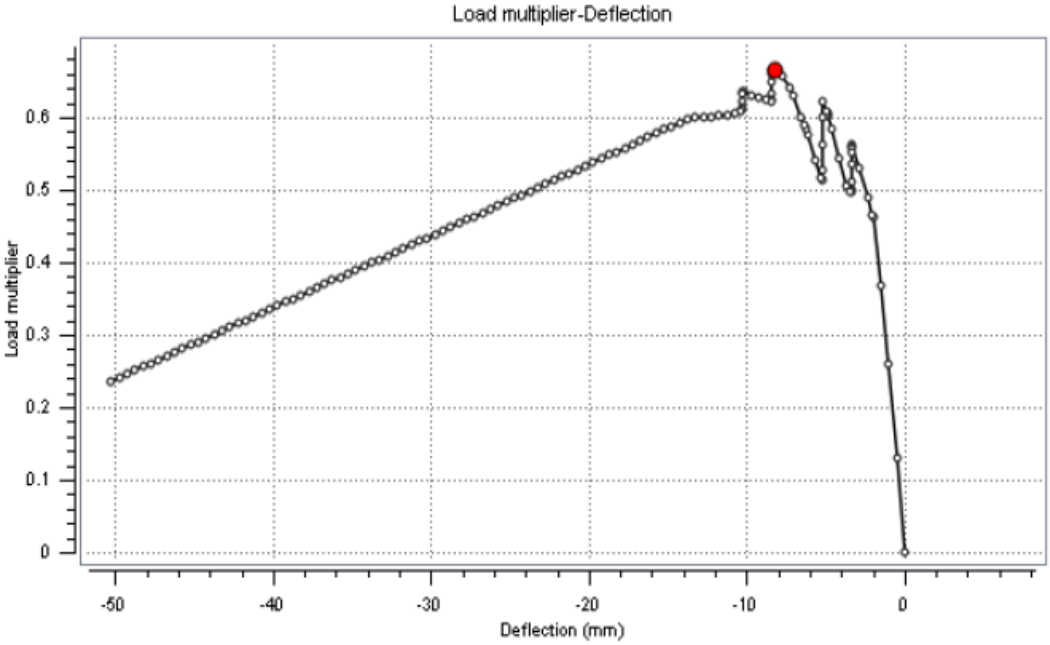


Figure 6-8. Pre opera of the central vault- Section 2.

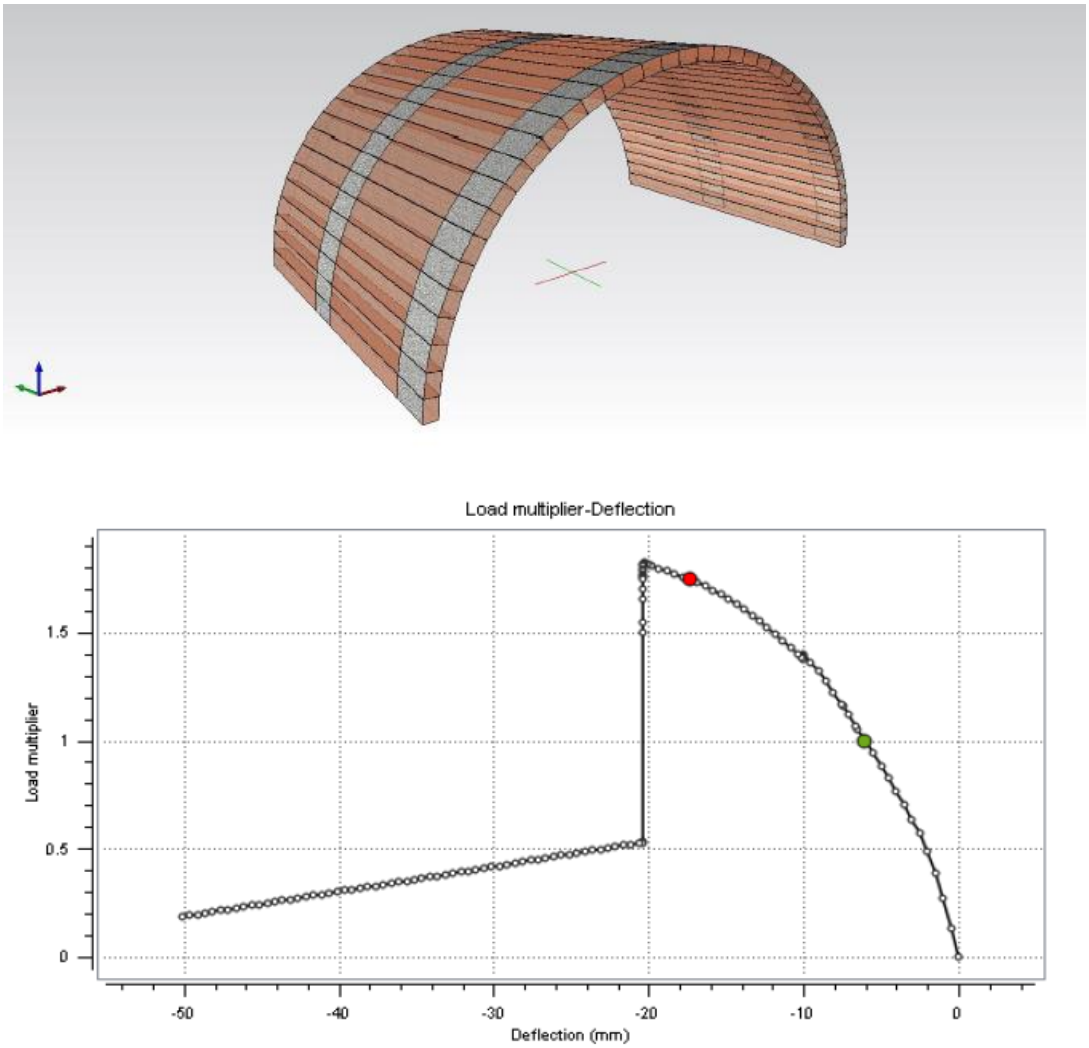


Figure 6-9. Post opera of the central vault – Section 2.

Lastly, analyzing the diagonal section, which represents the most critical part due to the length of the arch and the inability to apply reinforcements over an extensive area, the results obtained before the reinforcement application are very low, with a load multiplier of 0.03 (Figure 6-10). After the reinforcement is applied, this value increases, approaching 0.7 (Figure 6-11). It is noteworthy that it is not possible to achieve a load multiplier of unity for this section. However, it is important to consider that modeling inaccuracies were encountered in this specific section, resulting in less precise results.

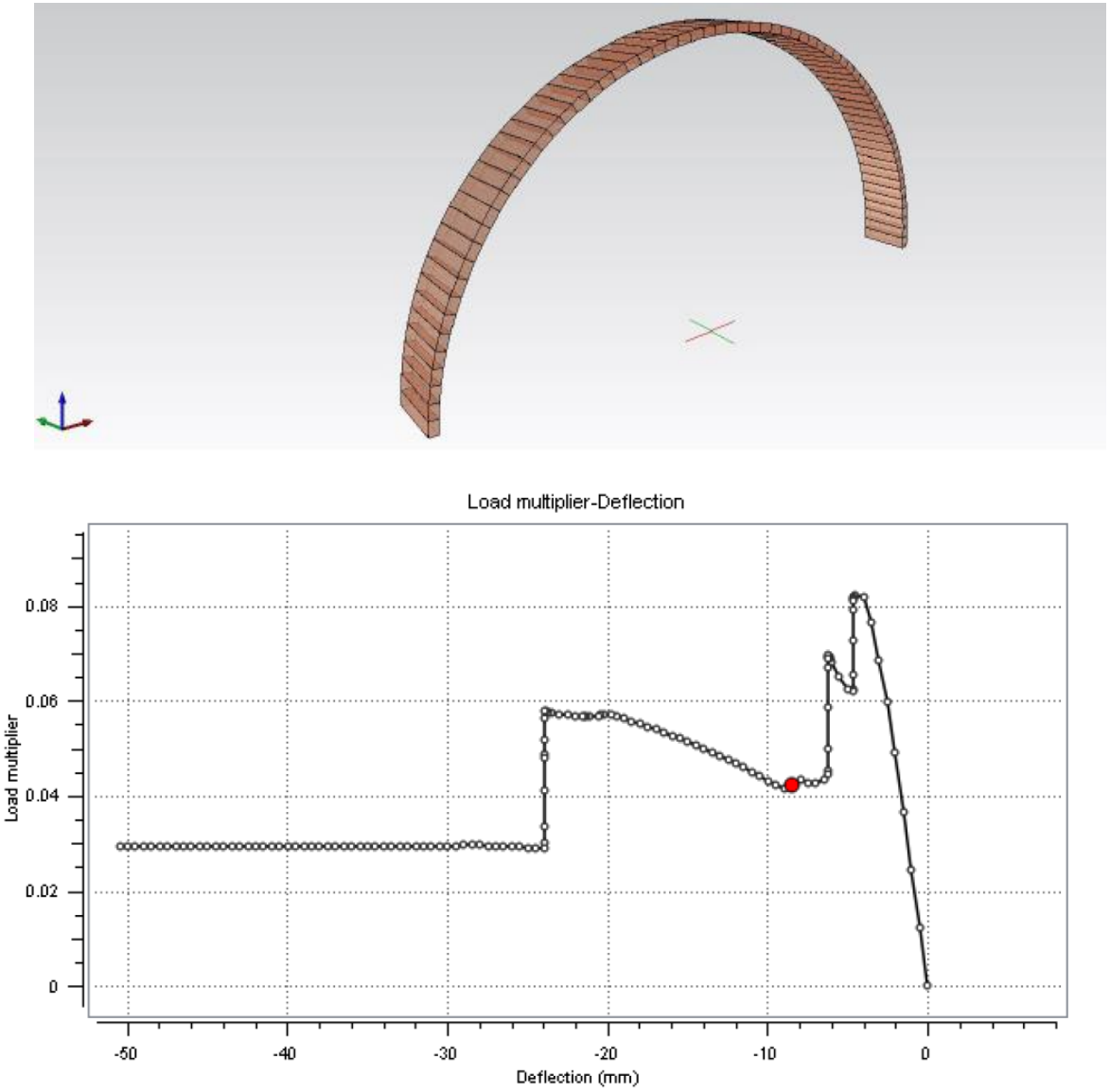


Figure 6-10. Pre opera of the central vault- Section 3.

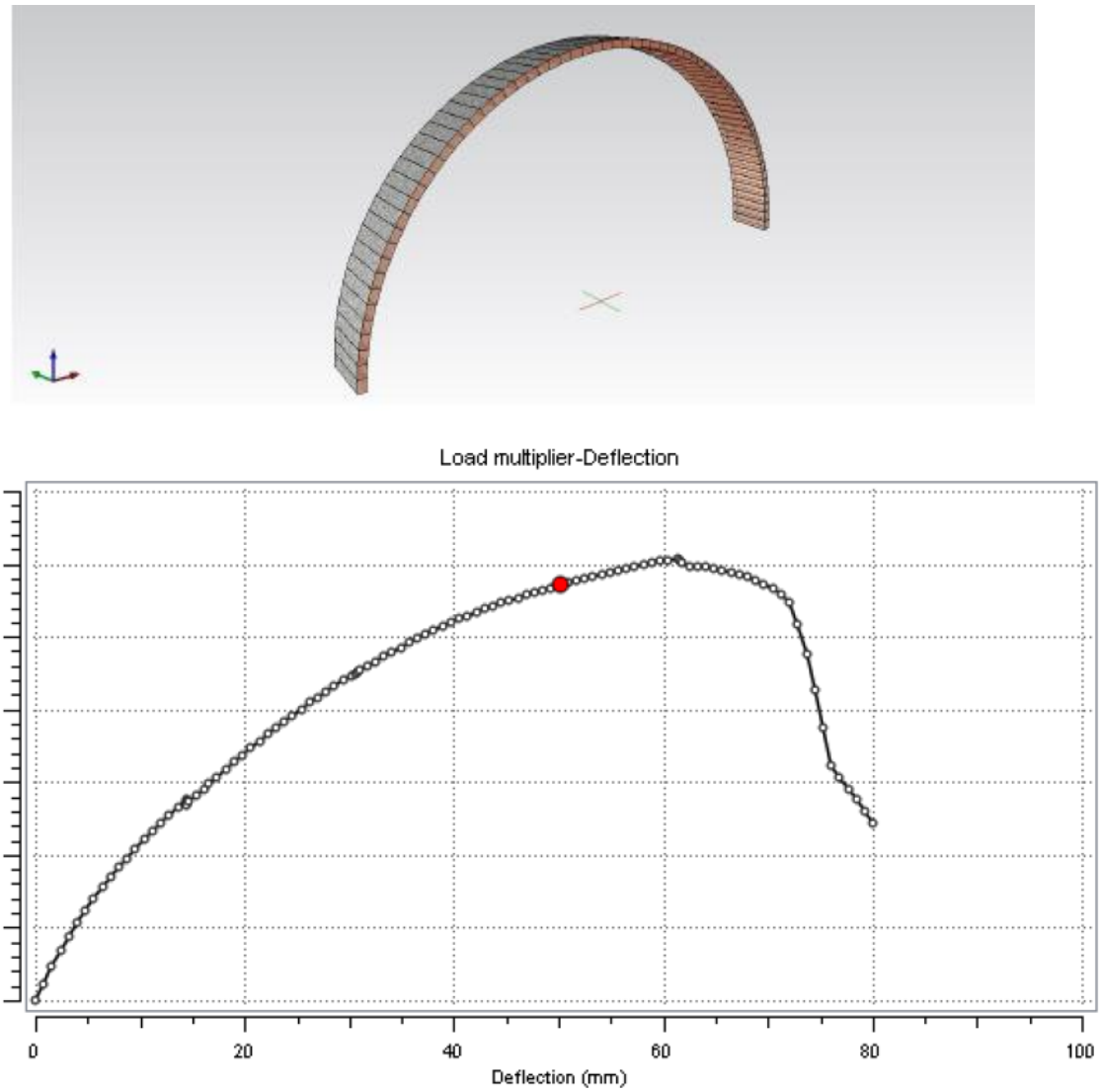


Figure 6-11. Post opera of the central vault – Section 3.

In order to avoid excessive length in this report, it is worth mentioning that the same analyses were conducted for the lateral vaults, employing a reinforcement thickness of 40 cm. Prior to reinforcement, the load multiplier for these vaults was below unity, albeit not as low as observed in the central vault. However, after the reinforcement was implemented, all cases demonstrated a load multiplier greater than unity. It is important to note that the most critical scenario in the lateral nave vaults is also observed in the diagonal section.

As can be seen in the Figure 6-12, various reinforcements were designed for the different vaults, where the width of these "metallic bands" increases according to the considered section. This design approach considers the varying structural demands of different sections of the vaults and ensures that the reinforcement is appropriately distributed to strengthen the specific areas that require additional support.

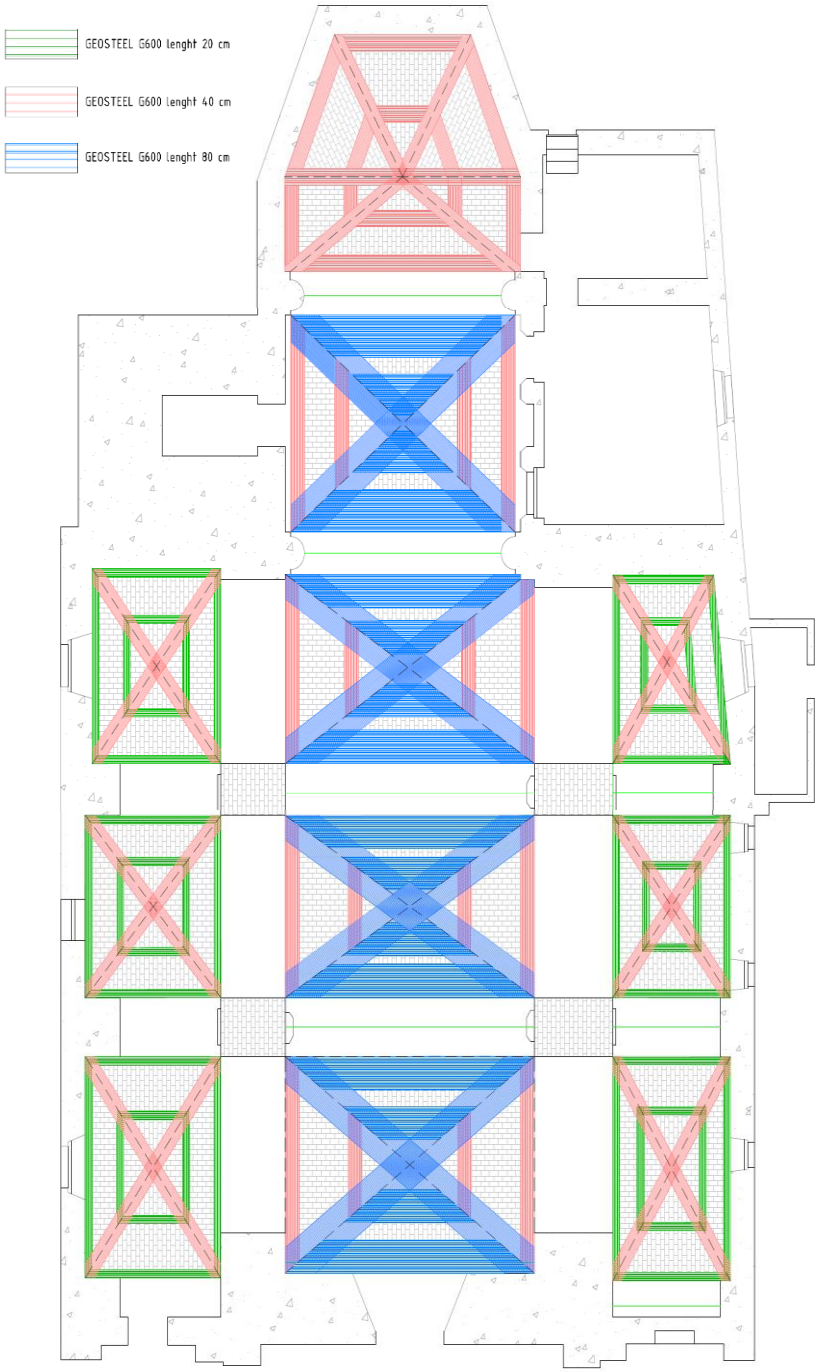


Figure 6-12. Vault's reinforcement.

# 7

# Conclusion

In conclusion, this study has focused on the structural analysis of Santo Stefano Church in Frassino. Through detailed information collection regarding the geometry and materials composing the construction, a comprehensive structural evaluation has been conducted.

By employing calculation programs and structural analysis, both static and dynamic studies have been performed. The obtained results have allowed for the verification of the capacity of the church's main structural elements, such as walls and vaults.

The findings revealed that these elements do not meet the seismic resistance requirements under seismic activity conditions. Considering this issue, the application of various reinforcement techniques suitable for enhancing the seismic capacity of the church has been explored.

This study highlights the significance of addressing the structural safety of historical buildings, particularly in areas prone to seismic activities. The findings serve as a solid foundation for future interventions and reinforcement measures aimed at preserving and safeguarding this valuable architectural heritage.

Moreover, it is strongly recommended that future research focuses on evaluating the proposed reinforcement techniques at a calculation level. Conducting a detailed analysis of the effectiveness and feasibility of these techniques to enhance the seismic capacity of Santo Stefano Church is imperative.

To conclude, this study has provided a comprehensive evaluation of the structural analysis of Santo Stefano Church in Frassino, identifying the need for improvements to enhance its seismic resistance. The conclusions emphasize the importance of ongoing research and the development of effective solutions to protect our valuable architectural heritage and ensure the safety of individuals using these historical buildings.

# 8 Bibliography

[1] Laura. Moro and Italia. Direzione generale per i beni architettonici e paesaggistici., *Linee guida per la valutazione e riduzione del rischio sismico del patrimonio culturale*. Gangemi, 2007.

[2] Giuseppe Genovese and Alberto Berloffa, "INTERVENTI DI RECUPERO E RISTRUTTURAZIONE DELLA CHIESA DI SANTO STEFANO RELAZIONE GEOLOGICA, GEOTECNICA E DI COMPATIBILITA' GEOMORFOLOGICA," 2021.

[3] Paolo Fissore, "CHIESA DI SANTO STEFANO IN FRASSINO - Cronologia storica," 2002.

[4] FRANCESCA PEZZELLA, "23 febbraio 1887, i tre terremoti che sconvolsero la Liguria." https://www.ingv.it/newsletter-ingv-n-03-2022-anno-xvi/23-febbraio-1887-i-tre-terremoti-che-sconvolsero-la-liguria (accessed May 30, 2023).

[5] "Valle Varaita - Wikipedia." https://it.wikipedia.org/wiki/Valle_Varaita (accessed May 30, 2023).

[6] "Prove Penetrometriche Dinamiche DPSH - Crestana." https://www.crestanasrls.com/indagini-geotecniche/prove-penetrometriche-dinamiche-dpsh/ (accessed May 30, 2023).

[7] "Cosa si intende per terreni granulari (o non coesivi)? -." https://geologobarbero.it/cosa-si-intende-per-terreni-granulari-o-non-coesivi/ (accessed May 30, 2023).

[8] "Unità litologica e modello geologico per le ntc18 | BGeo." https://www.bgeo.it/glossario/unita-litologica/ (accessed May 30, 2023).

[9] "Multi-Channel Analysis of Surface Waves Surveys | MASW | Vs30." https://olsonengineering.com/methods/geophysical-methods/seismic/multi-channel-analysis-of-surface-waves-masw/ (accessed May 31, 2023).

[10] "Seismic wave | Britannica." https://www.britannica.com/science/seismic-wave (accessed May 31, 2023).

[11] "MASW." https://www.geostru.eu/blog/2019/06/02/masw/?lang=es. (accessed May 31, 2023).

[12] Ministero delle Infrastrutture e dei Trasporti, Ministero dell'interno, and Dipartamento della Protezione Civile., "Norme Tecniche per le Costruzioni (NTC2018)," Jan. 2018.

[13] A. Sandoli, G. Brandonisio, L. Mazzocca, and B. Calderoni, "Assessment of seismic capacity of masonry churches according to Code indications: some remarks on a real case."

[14] Joel Gutiérrez Lozano, Virginia Vargas Tristán, Moisés Romero Rodríguez, José Manuel Plácido de la Cruz, Manuel de Jesús Aguirre Bortoni, and Hugo Tomás Silva Espinoza., "Periodos de retorno de lluvias torrenciales para el estado de Tamaulipas, México." Accessed: May 31, 2023. [Online]. Available: https://www.scielo.org.mx/scielo.php?script=sci_arttext&pid=S0188-46112011000300003

[15] "What is AutoCAD? - Definition from Techopedia." https://www.techopedia.com/definition/6080/autocad (accessed Jun. 01, 2023).

[16] "Eurocode 1: Actions on structures," 1991.

[17] "Assign Floor Loads." http://manual.midasuser.com/EN_Common/Gen/845/Start/05_Load/Assign_Floor_Loads.htm (accessed Apr. 28, 2023).

[18] "McLaskey research group." https://courses.cit.cornell.edu/mclaskey/vib/struct/Koppi/modesOfVibrations.html (accessed Apr. 27, 2023).

[19] "EN 1996-1-1: Eurocode 6: Design of masonry structures," 2005.

[20] "Strutture in muratura: analisi con metodo POR, PORflex, telaio equivalente." https://www.marcodepisapia.com/strutture-in-muratura-metodi-di-analisi/ (accessed Apr. 24, 2023).

[21] "Local Direction Force Sum." http://manual.midasuser.com/EN_Common/Gen/855/Start/07_Results/Local_Direction_Force_Sum.htm (accessed Apr. 26, 2023).

[22] “Pressoflessione - Wikipedia.” https://it.wikipedia.org/wiki/Pressoflessione (accessed Apr. 28, 2023).

[23] “Verifica statica dell’arco: metodo grafico di Mèry e curva delle pressioni.” https://www.marcodepisapia.com/verifica-statica-arco-metodo-grafico-mery/ (accessed Apr. 21, 2023).

[24] “Manual for users of Arco software. .” https://gelfi.unibs.it/software/Arco-ENG.pdf (accessed Apr. 21, 2023).

[25] “Reni dell’arco - Teknoring.” https://www.teknoring.com/wikitecnica/costruzioni/reni-dell-arco/ (accessed Apr. 21, 2023).

[26] P. Gelfi, “Role of Horizontal Backfill Passive Pressure on the Stability of Masonry Vaults,” *Bauinstandsetzen und Baudenkmalpflege 8. Jahrgang, Heft*, vol. 6, pp. 573–590, 2002.

[27] “PRO_CINEm Analisi Cinematica Lineare e Non Lineare sulla Muratura.”

[28] “EdificiInMuratura.it -.” https://www.edificiinmuratura.it/Pagina/92/l1-consolidamento-elevazione-intonaco-armato-immagini (accessed May 16, 2023).

[29] “La tecnica CRM - Composite Reinforced Mortar | Articoli | Ingenio.” https://www.ingenio-web.it/articoli/rinforzo-strutturale-la-tecnica-crm-composite-reinforced-mortar/ (accessed May 17, 2023).

[30] F. G. Carozzi and C. Poggi, “Mechanical properties and debonding strength of Fabric Reinforced Cementitious Matrix (FRCM) systems for masonry strengthening,” *Compos B Eng*, vol. 70, pp. 215–230, Mar. 2015, doi: 10.1016/J.COMPOSITESB.2014.10.056.

[31] “CNR-Advisory Committee on Technical Recommendations for Construction NATIONAL RESEARCH COUNCIL ADVISORY COMMITTEE ON TECHNICAL RECOMMENDATIONS FOR CONSTRUCTION Guide for the Design and Construction of Concrete Structures Reinforced with Fiber-Reinforced Polymer Bars,” 2006.

[32] A. Recupero and N. Spinella, “The Strengthening of Masonry Walls in Seismic-Prone Areas with the CAM System: Experimental and Numerical Results,” *Infrastructures 2020, Vol. 5, Page 108*, vol. 5, no. 12, p. 108, Dec. 2020, doi: 10.3390/INFRASTRUCTURES5120108.

[33] “The Active Confinement of Masonry (CAM) system: a) desired... | Download Scientific Diagram.” https://www.researchgate.net/figure/The-Active-Confinement-of-Masonry-CAM-system-a-desired-stress-transfer-scheme-from_fig1_332301309 (accessed May 17, 2023).

[34] I. Alessandro and V.-I. M. Leonori, “EDIL CAM Sistemi srl GUIDA INTRODUTTIVA AGLI INTERVENTI A MARCHIO CAM® SUI FABBRICATI IN MURATURA Tipologici e applicazioni.”

[35] Kerakoll, *Linee guida per il consolidamento, il rinforzo strutturale e la sicurezza sismica con nuove tecnologie green*. 2023.